

Distribution Agreement

In presenting this thesis or dissertation as a partial fulfillment of the requirements for an advanced degree from Emory University, I hereby grant Emory University and its agents the non-exclusive license to archive, make accessible, and display my thesis or dissertation in whole or in part in all forms of media, now or hereafter known, including display on the world wide web. I understand that I may select some access restrictions as part of the online submission of this thesis or dissertation. I retain all ownership rights to the copyright of the thesis or dissertation. I also retain the right to use in future works (such as articles or books) all or part of this thesis or dissertation.

Signature:

Bo Wei

Date

Practical Application and *In Situ* Kinetic Studies of
Dirhodium(II) Tetracarboxylate Catalyzed Carbene Reactions

By

Bo Wei

Doctor of Philosophy

Chemistry

Huw M. L. Davies, Ph.D.

Advisor

Simon Blakey, Ph.D.

Committee Member

Lanny S. Liebeskind, Ph.D.

Committee Member

Accepted:

Kimberly Jacob Arriola, Ph.D.

Dean of the James T. Laney School of Graduate Studies

Date

Practical Application and *In Situ* Kinetic Studies of
Dirhodium(II) Tetracarboxylate Catalyzed Carbene Reactions

By

Bo Wei

B.S., Nanjing University, 2017

Advisor: Huw M. L. Davies, Ph.D.

An abstract of

A dissertation submitted to the Faculty of the
James T. Laney School of Graduate Studies of Emory University
in partial fulfillment of the requirements for the degree of

Doctor of Philosophy

in Chemistry

2022

Abstract

Practical Application and *In Situ* Kinetic Studies of Dirhodium(II) Tetracarboxylate Catalyzed Carbene Reactions

By Bo Wei

Dirhodium(II) tetracarboxylates are versatile catalysts for the enantioselective reactions of donor/acceptor carbenes. The overarching goal of the work described in this thesis is to gain deeper kinetic understanding and broader practical application of dirhodium(II) catalyzed carbene chemistry. The first chapter is an overview of carbene chemistry, dirhodium(II) tetracarboxylate catalysts and recent advances in the field.

The second chapter investigates the kinetic profiles of Rh(II) catalyzed cyclopropanation under high catalyst turnover number (TON) conditions. A robust method was developed to achieve 100,000 catalyst TONs with consistently high yields and enantioselectivities in various cyclopropanation reactions. 4Å MS and dimethyl carbonate solvent were crucial for the high catalyst TONs reaction efficiency.

The third chapter further explores the practicality of Rh(II) catalyzed cyclopropanation by focusing on the flow system generation of diazo compound synthesis and their application in the cyclopropanation reaction. An upstream Cu(OAc)₂-H₂O/DMAP mixed silica column catalyzed the oxidation of hydrazones and was applied to generate diazo compounds under flow conditions. The crude diazo compounds were subsequently injected directly without extra purification into the downstream dirhodium(II)-catalyzed cyclopropanation reaction. Kinetic studies demonstrated that addition of HFIP in the downstream process is crucial to deliver the desired cyclopropanation products.

The fourth chapter shows the application of dirhodium(II)-catalyzed carbene chemistry in the synthesis of a wide variety of heterocycle-functionalized cyclopropanes by applying complementary methodologies. The cyclopropyl-based scaffolds are of pharmaceutical interest and hard to prepare by other methods. The novel method has been utilized in a large-scale synthesis of a key pharmaceutical intermediate.

The last chapter concentrated on the kinetic profiles of Rh(II) catalyzed C–H functionalization. The kinetic study gained a comprehensive understanding of the reaction progress at low catalyst loading. The study of the model C–H insertion of cyclohexane revealed the rate-determine step is carbene insertion instead of the carbene formation. The kinetic insights have driven rational optimization of the stoichiometry, carbene precursor structures and additives of the reaction. As a result, about 580,000 Rh(II) catalyst TONs have been achieved in the C–H insertion reaction with 1 mol % N,N'-dicyclohexylcarbodiimide (DCC) as additive.

Practical Application and *In Situ* Kinetic Studies of
Dirhodium(II) Tetracarboxylate Catalyzed Carbene Reactions

By

Bo Wei

B.S., Nanjing University, 2017

Advisor: Huw M. L. Davies, Ph.D.

A dissertation submitted to the Faculty of the
James T. Laney School of Graduate Studies of Emory University
in partial fulfillment of the requirements for the degree of
Doctor of Philosophy
in Chemistry
2022

Acknowledgements

The past five years have been very precious and meaningful to me. At the end of this stage, I would like to acknowledge the individuals who helped and supported me during my time at Emory.

First of all, I would like to sincerely thank my advisor, Professor Huw M. L. Davies. Before I started my graduate study, I had no idea how to be a good scientist. Huw has acted as an excellent role model. He is always supportive and has provided so many valuable suggestions as well as precious opportunities to me. His genuineness, humor and optimism make me feel less stress and more confident to overcome all the difficulties during the research progress. It is a great pleasure for me to study under his guidance. Huw also acted as an excellent leader in the NSF Center for Selective C–H Functionalization. I am impressed by his brilliant leadership, smart work strategy and wonderful presentation skills. Joining the Davies lab is one of the best decisions I have ever made, and the experience has benefited me a lot.

I would also like to thank my committee members, Professor Lanny S. Liebeskind and Professor Simon Blakey. I always get instructive insight and feedback from our annually milestone meeting. I've learned a lot from their classes, *Organic Spectroscopy* and *Physical Organic Chemistry*. They keep encouraging me to be a more critical thinker. I am still on a long way to be fully qualified, but I really appreciate the advice they gave to make me start moving.

NSF Center for Selective C–H Functionalization acted as an amazing platform for my professional growth. Taking the advantage of the center, I have collaborated and connected with numerous outstanding chemists outside of Emory. Especially, I would like to thank my collaborators from the Blackmond group, AbbVie, the Jones group, and the Stahl group. It is great opportunity to

work with experts from different areas as a team. The experience taught me how to work creatively and collaborate effectively in a team. It is an exceptional preparation for my future career development.

Dr. Bing Wang and Dr. Shaoxiong Wu in the NMR Center helped me on my data collection and analysis. Also, working as a service instructor under their supervision is highly valuable experience for me.

The life in the Davies group is full of memories. I want to thank everyone I've met in the lab. They are both great co-workers and wonderful friends: Dr. Wenbin Liu introduced the lab to me when I was doing my rotation. She was so hardworking, organized, and detailed. Her work style encouraged me to do more and do better in my own research. Dr. Benjamin Wertz, Dr. Robert W. Kubiak II and Dr. Zachary J. Garlets worked next to me after I joined the lab. They are caring and nice mentors that taught me experiment techniques and chemistry knowledge. Patricia Lin, Dr. Sydney M. Wilkerson-Hill, Sam Mckinnon and Jack C. Sharland collaborated with me in my first project, which set a great start point for all my five year research. Thanks for all their effort to accelerate our project progress. Jack further collaborated on two projects with me, and I have learned a lot from his great problem-solving ability and negotiation skill. Dr. Janakiram Vaitla worked in our lab for a very short period, but he provided so many great advice for both my life and research. I was very impressed by his great work efficiency and wish him and his sweet family all the best. Aaron Bosse and Ingrid Wilt shared many useful information and tips when I am looking for jobs. I appreciate all their generous help and suggestions. Dr. Bowen Zhang, Dr. Jiantao Fu, Maizie Lee and Yannick T. Boni and I always went to seminars, gym, and dinner together and had so many interesting conversations and discussions about chemistry and other topics. The time

with them was always full of fun. Yannick and I joined the lab at the same time and supported each other to go through many struggling conditions together. He is my best friend in the lab, and it is lucky to have him in this journey. I wish him success in medical school. To the rest of the Davies group, Dr. Xun Yang, Dr. Zhi Ren, Douglas Kavaguti, Carolyn Ma, Fahad Alduayji, Anna Cai, Kuo Zhang, Ziyi Chen, Kristin Shimabukuro, Will Tracy, Terrence-Thang H. Nguyen, Yujie Luo, Josh Sailer, Brockton Keen, and Yasir Naeem, it has been a great pleasure working with them, and I wish them all the best.

Many thanks should also go to all the friends I met in Emory. I would like to express my special thanks to Xiangning Xue, Yuan Zhao, Shihua Wang, Ardica Kamalanathan, Philip Zhu, Yuxin Duan, Yunlong Zhang, Sa Suo, Qinyi Lu and Youngsun Kim. During the five years, their cheering and accompanying have made my time much easier and happier. The chats, trips, and parties we had together are memorable. I am grateful for having them as friends in my graduate life.

Finally, I want to thank my whole family. Although I have been away from home for 5 years, I always feel the caring, understanding and love from my sweet family throughout my life. They give me all the courage, motivation, and confidence to keep going. None of this would have been possible without the supporting from my family. I deeply appreciate it.

Table of Contents

Chapter 1. Introduction of Dirhodium(II) Catalyzed Carbene Chemistry	1
1.1 Introduction	1
Chapter 2. In Situ Kinetic Studies of Dirhodium(II)-Catalyzed Asymmetric Cyclopropanation with Low Catalyst Loadings.	21
2.1 Introduction	21
2.2 Results and Discussions.....	22
2.3 Conclusions.....	45
Chapter 3. Copper(II)-catalyzed Aerobic Oxidation of Hydrazones to Diazo Compounds under Flow Conditions and Their Application in Carbene Reactions.	46
3.1 Introduction	46
3.2 Results and Discussions.....	49
3.3 Conclusions.....	61
Chapter 4. Pharmaceutically Relevant Asymmetric Cyclopropanation of Vinyl Heterocycles with Aryl- and Heteroaryldiazoacetates.	62
4.1 Introduction	62
4.2 Results and Discussions.....	65
4.3 Conclusions.....	75

Chapter 5. In Situ Kinetics Studies of Dirhodium (II)-Catalyzed C–H Functionalization to Achieve High Catalyst Turnover Numbers.....	77
5.1 Introduction	77
5.2 Results and Discussions.....	78
5.3 Conclusions.....	98
Experimental Part	99
6.1 General Considerations and Reagents.....	99
6.2 Experimental Part for Chapter 2	100
6.3 Experimental Part for Chapter 3	131
6.4 Experimental Part for Chapter 4	147
6.5 Experimental Part for Chapter 5.....	168
Reference	188

List of Schemes

Scheme 1.1 General mechanism of the dirhodium(II) complex catalyzed carbene reaction..	1
Scheme 1.2 Major classes of transient metal-carbene intermediates.....	2
Scheme 1.3 Vinyldiazoacetate underwent a thermal 6π electrocyclization to form pyrazole .	3
Scheme 1.4 Chiral auxiliary led to high level asymmetric induction in cyclopropanation	4
Scheme 1.5 Highly enantioselective cyclopropanation catalyzed by $\text{Rh}_2(\text{S-DOSP})_4$ (1.17)...	5
Scheme 1.6 $\text{Rh}_2(\text{S-PTAD})_4$ (1.25) was applied in asymmetric cyclopropanation with a range of donor/acceptor diazo compounds.....	5
Scheme 1.7 $\text{Rh}_2(\text{S-biTISP})_2$ (1.27) catalyzed cyclopropanation with high TONs.....	7
Scheme 1.8 $\text{Rh}_2(\text{S-DOSP})_4$ (1.17) and $\text{Rh}_2(\text{S-PTAD})_4$ (1.25) catalyzed solvent-free cyclopropanation with high TONs	8
Scheme 1.9 The steric and electronic influences on site selectivity of C–H functionalization	9
Scheme 1.10 Seminal examples of $\text{Rh}_2(\text{DOSP})_4$ (1.17) -catalyzed intermolecular reactions as classic disconnection equivalent	10
Scheme 1.11 High symmetry orientations of dirhodium(II) tetracarboxylate catalysts	11
Scheme 1.12 Second-generation C_4 Symmetric dirhodium(II) catalysts derived from N-phthalimido amino acids.....	12
Scheme 1.13 Third-generation C_2 , D_2 and C_4 Symmetric dirhodium(II) catalysts derived from TPCP ligands	13
Scheme 1.14 $\text{Rh}_2(\text{R-3,5-di}(p\text{-BuC}_6\text{H}_4)\text{TPCP})_4$ (1.50) catalyzed selective functionalization of unactivated secondary C–H bonds	14

Scheme 1.15 Rh ₂ (<i>S</i> -TCPTAD) ₄ (1.44) catalyzed selective functionalization of tertiary C–H bonds and the method application in late-stage functionalization of natural products	15
Scheme 1.16 Rh ₂ (<i>S</i> -2-Cl-5-BrTPCP) ₄ (1.49) catalyzed site selective functionalization of unactivated secondary C–H bonds	16
Scheme 1.17 Enantioselective synthesis of cylindrocyclophane core applying Rh ₂ (<i>S</i> -2-Cl-5-BrTPCP) ₄ (1.49) catalyzed C–H functionalization.....	17
Scheme 1.18 Rh ₂ [tris(<i>p</i> - ^t BuC ₆ H ₄)TPCP) ₄ (1.48) catalyzed site selective functionalization of unactivated primary C–H bonds	18
Scheme 1.19 Rh ₂ (<i>S</i> -TPPTTL) ₄ (1.45) catalyzed desymmetrization of cyclohexane derivatives.....	19
Scheme 1.20 Limitations of rhodium-carbene chemistry in practical applications	19
Scheme 2.1 Chiral dirhodium(II) catalysts capable of high TONs.....	22
Scheme 2.2 Influence of ester functionality on diazo compounds.....	23
Scheme 2.3 Proposed catalytic cycle for cyclopropanation of styrene	31
Scheme 2.4 Alternative dirhodium(II) catalysts applied to more sterically crowded substrates	43
Scheme 2.5 Asymmetric cyclopropanation in a key step in the synthesis of Beclabuvir 2.36	44
Scheme 3.1 Reaction conditions and representative scopes of the copper(II)-catalyzed oxidation of hydrazones to diazo compounds using oxygen as terminal oxidant	47
Scheme 3.2 Proposed mechanism of copper(II)-catalyzed oxidation of hydrazones to diazo compounds using oxygen as terminal oxidant.....	48

Scheme 3.3 Gram scale synthesis from the hydrazone 3.1 to the cyclopropane 3.4 with bench-top flow procedure.....	61
Scheme 4.1 Previous examples of Rh ₂ (<i>S</i> -DOSP) ₄ (4.1) catalyzed cyclopropanation reactions of styrene with heteroaryldiazoacetates	63
Scheme 4.2 Scopes of cyclopropanation of vinyl-heterocycle with diazo compounds containing chiral auxiliary (<i>R</i>)-pantolactone	64
Scheme 4.3 Scopes of cyclopropanation of vinyl-heterocycle with diazo compounds catalysed by Rh ₂ (<i>R-p</i> -Ph-TPCP) ₄ (4.17).....	66
Scheme 4.4 The additive effect of 2-chloropyridine on asymmetric cyclopropanation catalyzed by Rh ₂ (<i>S</i> -TPPTTL) ₄ (4.43).....	70
Scheme 4.5 Scopes of cyclopropanation of vinyl-heterocycle with various diazo compounds catalyzed by Rh ₂ (<i>S</i> -TPPTTL) ₄ (4.43).	73
Scheme 4.6 Scopes of cyclopropanation of various vinyl-heterocycle with diazo compounds catalyzed by Rh ₂ (<i>S</i> -TPPTTL) ₄ (4.43)	74
Scheme 4.7 Tandem copper-catalyzed diazo formation followed by a Rh ₂ (<i>S</i> -TPPTTL) ₄ (4.43)-catalyzed cyclopropanation.	75
Scheme 5.1 Dirhodium(II) catalysts with different steric structures tested in this study	79
Scheme 5.2 Proposed catalytical cycle of the dirhodium(II) catalyzed C–H insertion of cyclohexane.	85
Scheme 5.3 Scopes of asymmetric C–H functionalization with 0.001 mol% Rh ₂ (<i>R</i> -TPPTTL) ₄ (5.7) catalyst.....	96
Scheme 6.1 Elementary steps of the defined mechanism for the benchmark cyclopropanation reaction.....	108

List of Figures

Figure 2.1 Kinetic profiles of control experiment and the crude ¹ H-NMR.....	24
Figure 2.2 Kinetic profiles highlighting the importance of 4 Å molecular sieves	25
Figure 2.3 Reaction rates of various dirhodium(II) catalysts in the cyclopropanation reaction.	25
Figure 2.4 Variable time normalization analysis (VTNA) experiments for determining catalyst order.....	28
Figure 2.5 Kinetic profiles of cyclopropanation reaction with Rh ₂ (<i>S-p</i> -Br-TPCP) ₄ (2.6)....	30
Figure 2.6 High throughput cyclopropanation in a variety of solvents and chiral dirhodium(II) catalysts.	34
Figure 2.7 The decomposition curve of diazo compound 2.5a at 70 °C and 60 °C in (MeO) ₂ CO without catalyst.....	37
Figure 2.8 Kinetic profiles of the cyclopropanation reaction in (MeO) ₂ CO	38
Figure 2.9 Kinetic profiles of RPKA study for the cyclopropanation with Rh ₂ (<i>S-p</i> -Br- TPCP) ₄ (2.6) in (MeO) ₂ CO at 60 °C.....	39
Figure 2.10 Kinetic profiles of multiple addition experiment of the benchmark cyclopropanation.	40
Figure 2.11 Scopes of asymmetric cyclopropanation with 0.001 mol % Rh ₂ (<i>R-p</i> -Ph-TPCP) ₄ (2.8) at 60 °C in (MeO) ₂ CO	41
Figure 3.1 Kinetic investigation of the effect of DMAP and HFIP on Rh ₂ (<i>R-p</i> -Ph-TPCP) ₄ (3.3) catalyzed asymmetric cyclopropanation.....	52

Figure 3.2 HFIP and diazo compound 3.2 influenced each other's peak shifts on ¹ H-NMR	54
Figure 3.3 Tandem diazo compounds synthesis and the cyclopropanation scopes.....	57
Figure 3.4 Column robustness assessment experiments.....	59
Figure 3.5 Catalytic aerobic oxidation of hydrazone compounds in a three-phase packed bed reactor	60
Figure 4.1 Structural perturbations in Rh ₂ (<i>S</i> -TPPTTL) ₄ (4.43) enforced by the coordination of 2-chloropyridine based on X-ray analysis of a single crystal of Rh ₂ (<i>S</i> -TPPTTL) ₄ (4.43) coordinated to 2-chloropyridine	72
Figure 5.1 Reaction rates of various catalysts in C–H insertion of cyclohexane	80
Figure 5.2 Kinetic profiles of RPKA studies for Rh ₂ (<i>R</i> -TPPTTL) ₄ (5.7) catalyzed C–H insertion of cyclohexane.....	83
Figure 5.3 Kinetic profiles of condition optimization of C–H insertion of cyclohexane	87
Figure 5.4 Kinetic profiles of C–H insertion of cyclohexane catalyzed by various dirhodium(II) catalysts under neat condition.....	88
Figure 5.5 Rh ₂ (<i>S-p</i> -Br-TPPTTL) ₄ (5.11) catalyzed unreproducible C–H insertion reaction.	89
Figure 5.6 ¹ H-NMR spectrum revealed the reaction worked when the diazo compounds 5.8d contained DCC component.	90
Figure 5.7 Effect of different concentration of DCC additive on the reaction kinetic profiles at 60 °C with 0.0005 mol% Rh ₂ (<i>R</i> -TPPTTL) ₄ (5.7) catalyst loading	92
Figure 5.8 Kinetic profiles of control experiment with different additives.....	93

Figure 5.9 The reaction with 0.0005 mol% $\text{Rh}_2(\text{R-TPPTTL})_4$ (5.7) catalyst loading gives no progress until 1 mol% DCC and another 0.0005 mol% $\text{Rh}_2(\text{R-TPPTTL})_4$ (5.7) catalyst added.....	94
Figure 5.10 Computational study of the DCC additive effect.....	95
Figure 5.11 Kinetic profile of multiple-addition experiment of the C–H insertion reaction	97
Figure 6.1 <i>In situ</i> IR apparatus set-up.....	100
Figure 6.2 ReactIR run on software for a complete experiment.....	102
Figure 6.3 Initial 0.3 h kinetic profiles of the difference excess experiment to determine the order of the diazo compound in the benchmark cyclopropanation reaction.....	103
Figure 6.4 Initial 0.3 h kinetic profiles of the difference excess experiments to determine the order of styrene in the benchmark cyclopropanation reaction.....	104
Figure 6.5 The catalytic cycle for the benchmark cyclopropanation reaction according to the obtained rate law eq 6.13	107
Figure 6.6 The bench-top tandem Cu(II) catalyzed hydrazones oxidation in flow and sequential Rh(II) catalyzed asymmetric cyclopropanation reaction set-up.....	133

List of Tables

Table 1.1 Cyclopropanation with aryldiazoacetates conducted with low catalyst loadings...	6
Table 1.2 Catalyst-controlled benzylic C–H functionalization of ethyltoluene	14
Table 2.1 Lab scale cyclopropanation in a variety of solvents with Rh ₂ (<i>S-p</i> -Br-TPCP) ₄ (2.6)	35
Table 3.1 Optimization of aryldiazoacetate 3.2 synthesis in flow	49
Table 3.2 Batch-batch tandem reaction of copper(II) catalyzed hydrazone oxidation followed by dirhodium(II) catalyzed asymmetric cyclopropanation	51
Table 3.3 Optimization of flow-batch reaction conditions	55
Table 4.1 Optimization of the enantioselective cyclopropanation of a vinyl-heterocycle (4.37) with methyl 2-(2-methoxy-5-methylphenyl)-2-diazoacetate (4.38)	68
Table 4.2 Optimization of the enantioselective cyclopropanation of a vinyl-heterocycle (4.37) with methyl 2-(2-methoxy-5-methylphenyl)-2-diazoacetate (4.38) catalyzed by Rh ₂ (<i>R</i> -TPPTTL) ₄ (4.43)	69
Table 6.1 Initial conditions and the initial rate obtained from Figure 6.3 , the difference excess experiment, to determine the reaction order of the diazo compound in the benchmark cyclopropanation.	103
Table 6.2 Initial reagents' conditions and the initial rate obtained from Figure 6.4 , the difference excess experiment, to determine the reaction order of styrene in benchmark cyclopropanation.	105

List of Abbreviations

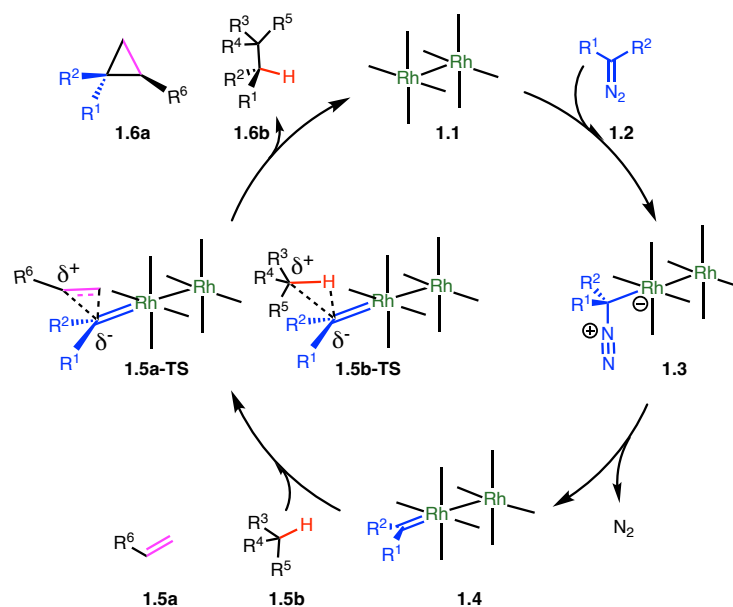
1,2-DCE	1,2-dichloroethane
Ac	acetyl
APCI	atmospheric pressure chemical ionization
Ar	aryl
Bn	benzyl
Boc	tert-butyloxycarbonyl
Bu	butyl
Cy	cyclohexyl
DBU	1,8-diazabicycloundec-7-ene
DCC	N,N'-dicyclohexylcarbodiimide
DCM	dichloromethane
DCU	N,N'-dicyclohexylurea
de	diastereomeric excess
DIC	N,N'-diisopropylcarbodiimide
DMAP	N,N'-4-(dimethylamino)pyridine
DMC	dimethyl carbonate
DMF	2,2-dimethylbutane
dr	diastereomeric ratio
EDG	electron-donating group
ee	enantiomeric excess
eq	equation
equiv	equivalents
ESI	electrospray ionization
Et	ethyl
EtOAc	ethyl acetate
EWG	electron-withdrawing group
g	gram
h	hour
HFIP	1,1,1,3,3,3-hexafluoro-2-propanol
HPLC	high performance liquid chromatography
HRMS	high-resolution mass spectrometry
<i>hν</i>	light
<i>i</i>-PrOAc	isopropyl acetate
IR	infrared spectroscopy
kcal	kilocalorie
L	ligand
LDA	lithium diisopropylamide
<i>m</i>	<i>meta</i>

M metal
m.p. melting point
Me methyl
min minute
mmol millimoles
mol mole
Ms mesyl
MS molecular sieves
NMR nuclear magnetic resonance
NSI nanospray ionization
o *ortho*
o-NBSA *ortho*-nitrobenzenesulfonyl azide
OMe methoxy
p *para*
p-ABSA *para*-acetamidobenzenesulfonyl azide
PG protecting group
Ph phenyl
Phth phthalimide
Piv pivaloyl
Pr propyl
r.t. room temperature
Rf retention factor
RPKA Reaction progress kinetic analysis
SiO₂ silica gel
TEA triethylamine
temp temperature
TFT trifluorotoluene
THF tetrahydrofuran
TLC thin layer chromatography
TMS trimethylsilyl
TMU tetramethylurea
TONs turnover numbers
tR retention time
Ts tosyl
TS transition state
VTNA Variable time normalization analysis

Chapter 1. Introduction of Dirhodium(II) Catalyzed Carbene Chemistry

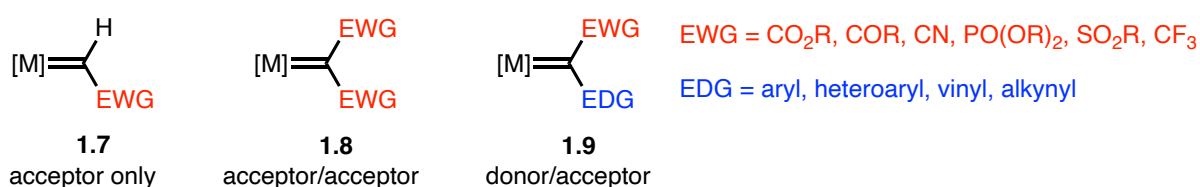
1.1 Introduction

Transition metal-catalyzed carbene chemistry has developed into a powerful methodology in organic synthesis.¹⁻¹⁴ Dirhodium(II) complexes have been found to be exceptional catalysts for a wide variety of highly regio-, diastereo-, and enantioselective carbene reactions.^{15, 16} The proposed mechanism of the dirhodium(II) catalyzed carbene reaction is shown in **Scheme 1.1**.¹⁷⁻²⁵ The catalytic cycle starts with the combination of dirhodium(II) complex **1.1** and diazo compound **1.2**, followed by nitrogen extrusion from the diazo compound **1.2** to form the rhodium carbene intermediate **1.4**. The highly electrophilic rhodium carbene **1.4** subsequently approaches the substrate (**1.5a** or **1.5b**) in the next step, and the positive charge builds up at the carbon of the intermediate. The process is concerted but asynchronous, forming a three-membered-ring transition state (**1.5a-TS** or **1.5b-TS**). Lastly, the carbene reaction product (**1.6a** or **1.6b**) is generated, and the dirhodium(II) complex **1.1** is released to initiate the next catalytic cycle.



Scheme 1.1 General mechanism of the dirhodium(II) complex catalyzed carbene reaction

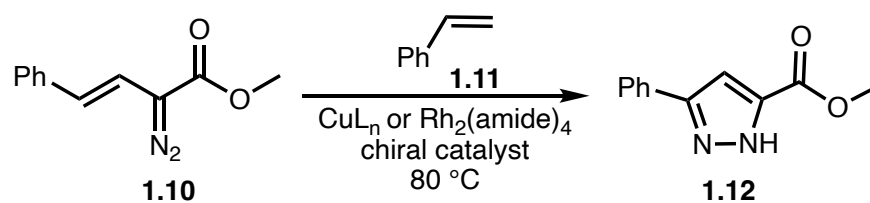
According to the mechanism described above, both electronic and steric effects of the substrate (**1.5a** or **1.5b**) and carbene intermediate **1.4** are crucial for the reaction outcome.²⁶⁻²⁸ The initial studies mainly applied acceptor only and acceptor/acceptor diazo compounds as carbene precursors. The “acceptor” was an electron withdrawing group that made the carbene intermediate highly electrophilic and extremely active. However, acceptor only **1.7** and acceptor/acceptor carbene **1.8** are often too reactive to achieve high selectivity in intermolecular reactions (**Scheme 1.2**). Carbene dimerization often occurs as an undesirable side-reaction, which leads to low yield of the desired products. A significant breakthrough to overcome the above limitations was the development of the donor/acceptor carbenes **1.9** pioneered by the Davies group (**Scheme 1.2**).²⁹ In contrast to the highly electrophilic acceptor-only carbene **1.7** and the acceptor/acceptor carbene **1.8**, the donor/acceptor carbene **1.9** has an electron-donating group to modulate its electrophilicity. The presence of the donor group enables the carbene to achieve excellent selectivity while the acceptor group still ensures high reactivity. Therefore, the donor/acceptor carbene **1.9** greatly expanded the scope of useful carbene reactions.



Scheme 1.2 Major classes of transient metal-carbene intermediates

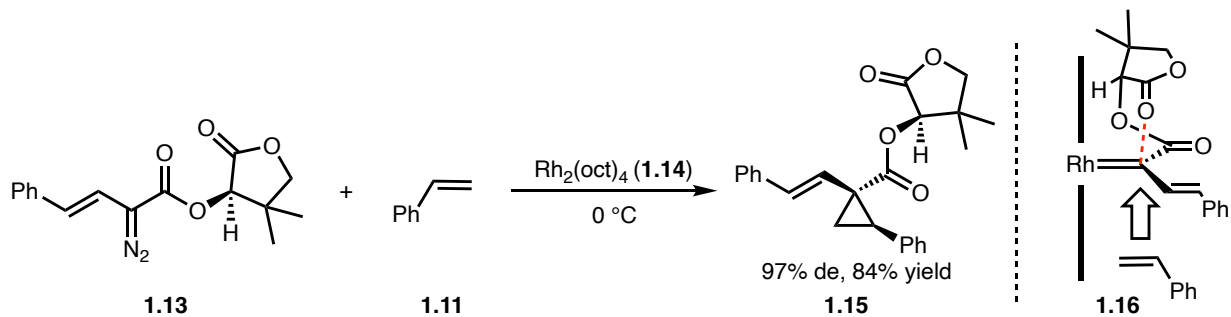
The high selectivity profile of donor/acceptor carbene **1.9** contributed to the development of asymmetric intermolecular carbene reactions catalyzed by chiral catalyst. However, the access to efficient chiral catalysts was limited at the early stage of donor/acceptor carbene chemistry studies. The traditional catalysts such as copper complexes and dirhodium(II) tetracarboxamidate catalysts

were not sufficiently active to generate carbene intermediate from donor/acceptor diazo compound **1.10**. More vigorous conditions with higher temperature were attempted to promote the reaction. However, the thermal cyclization of diazo compound **1.10** intervened to generate pyrazole **1.12** as product (**Scheme 1.3**).³⁰



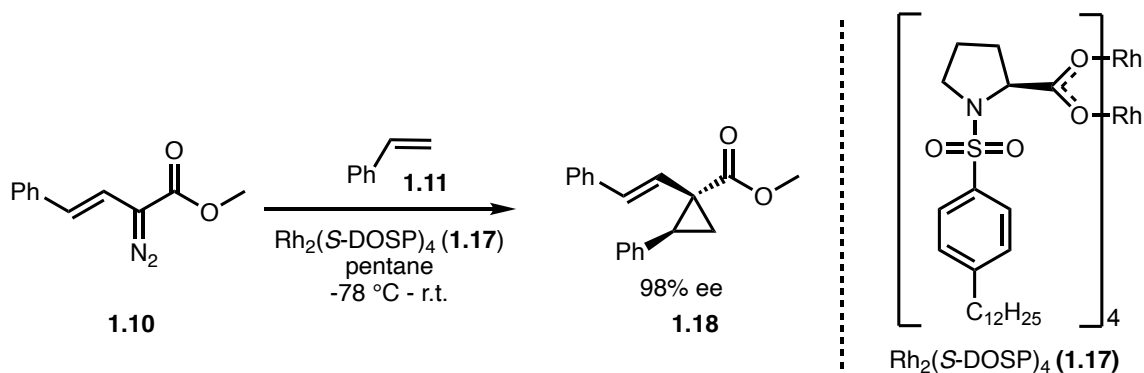
Scheme 1.3 Vinyl diazoacetate underwent a thermal 6π electrocyclicization to form pyrazole

To solve this problem, the Davies group explored an alternative approach to achieve asymmetric induction by using a chiral auxiliary. Specifically, donor/acceptor carbenes with (*R*)-pantolactone as the chiral auxiliary (**1.13**) were effective to achieve high levels of asymmetric induction in the cyclopropanation reaction. As illustrated in **Scheme 1.4**, cyclopropane **1.15** was generated with 97% de and 84% yield. It was proposed that the carbonyl group of the pantolactone interacted with the carbene center and generated a rigid intermediate **1.16** in the transition state. The rigid intermediate **1.16** blocked one face from attack and led to a high level of asymmetric induction.³⁰



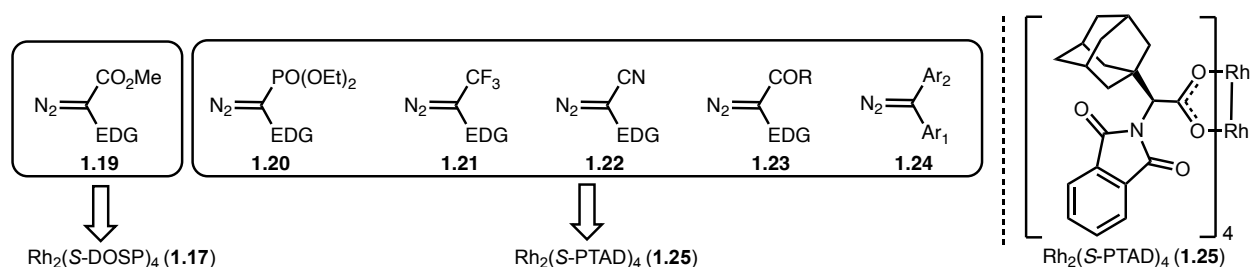
Scheme 1.4 Chiral auxiliary led to high level asymmetric induction in cyclopropanation reactions.

However, many chiral auxiliaries were expensive, and the stoichiometric amount of an auxiliary would be prohibitive in a large scale synthesis. Therefore, using a chiral catalyst in catalytic amounts to induce asymmetry in the reaction is desirable for practical application, and significant progress has been made. An early breakthrough was the development of the dirhodium(II) proline catalyst $\text{Rh}_2(\text{DOSP})_4$ (**1.17**) reported by the Davies group.³² As shown in **Scheme 1.5**, $\text{Rh}_2(S\text{-DOSP})_4$ (**1.17**) was disclosed as a superior catalyst to provide excellent levels of enantioselectivity in the carbene reaction. The optimization studies showed that nonpolar solvents such as pentane were beneficial for the catalyst performance. Applying lower temperature can further enhance the enantioselectivity and when the reaction was conducted at $-78\text{ }^\circ\text{C}$, cyclopropane **1.18** was obtained with 98% ee.³² Since then, the scope of $\text{Rh}_2(S\text{-DOSP})_4$ (**1.17**) catalyzed highly enantioselective cyclopropanation reactions have been expanded to a variety of alkenes with vinyl diazoacetates, aryldiazoacetates, heteroaryldiazoacetates, or alkynyl diazoacetates.¹⁴



Scheme 1.5 Highly enantioselective cyclopropanation catalyzed by $\text{Rh}_2(\text{S-DOSP})_4$ (**1.17**)

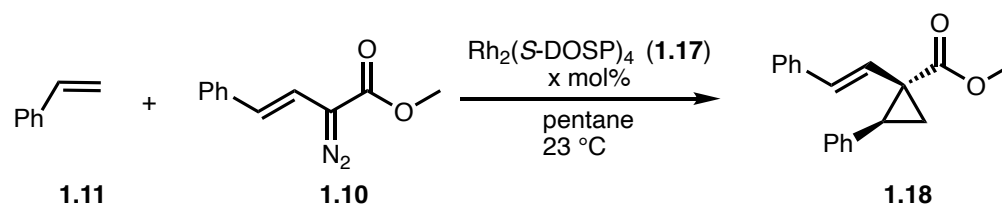
Methyl esters were originally used as the acceptor group for donor/acceptor carbenes, but since then, many other types of acceptor groups on the diazo compounds have been investigated. $\text{Rh}_2(\text{S-PTAD})_4$ (**1.25**) from the Davies group has been demonstrated as the optimal catalyst for those cases in cyclopropanation.³³ $\text{Rh}_2(\text{S-PTAD})_4$ (**1.25**) was derived from the N-phthalimido amino acids. The phthalimido catalysts were originally developed by Hashimoto³⁴ and further studied by Fox,^{35, 36} Charette³⁷ and Davies.^{33, 38, 39} By installing a bulky adamantyl group on the phthalimido ligand, $\text{Rh}_2(\text{S-PTAD})_4$ (**1.25**) was able to induce higher level of asymmetric induction in the carbene reactions. As listed in **Scheme 1.6**, $\text{Rh}_2(\text{S-PTAD})_4$ (**1.25**) was able to catalyze cyclopropanation reactions of aryldiazophosphonates **1.20**, trifluoromethylphenyldiazomethanes **1.21**, aryldiazoacetonitriles **1.22**, aryldiazoketones **1.23**, and diaryldiazomethanes **1.24**. These reactions consistently provided excellent results with high enantioselectivity and yield.⁴⁰



Scheme 1.6 $\text{Rh}_2(\text{S-PTAD})_4$ (**1.25**) was applied in asymmetric cyclopropanation with a range of donor/acceptor diazo compounds

Most of the reported carbene reactions normally used 1 mol % catalyst loading to guarantee consistent catalyst performance. To explore the potential of the dirhodium(II) catalyzed carbene reaction, low catalysts loading condition was also examined for achieving higher catalyst turnover numbers (TONs). In the initial study, the cyclopropanation reaction maintained good enantioselectivity (87% ee) with only 0.1 mol% $\text{Rh}_2(\text{S-DOSP})_4$ (**1.17**). However, further attempts to lower catalyst loadings showed the enantioselectivity dropped to 50% ee when 0.01 mol% catalyst loading was applied, and the reaction did not go to completion. (**Table 1.1**).

Table 1.1 Cyclopropanation with aryldiazoacetates conducted with low catalyst loadings

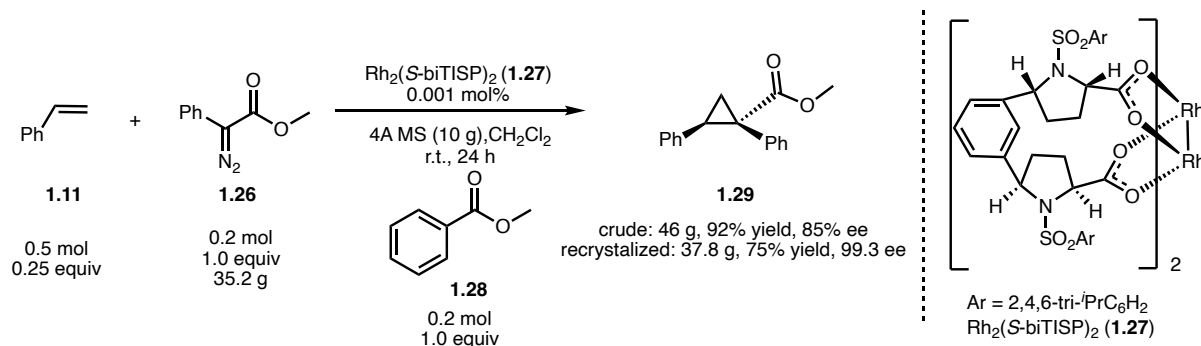


entry	x (mol%)	ee of 1.18 (%)
1	1	92
2	0.1	87
3	0.01	50*

*Reaction did not go to completion

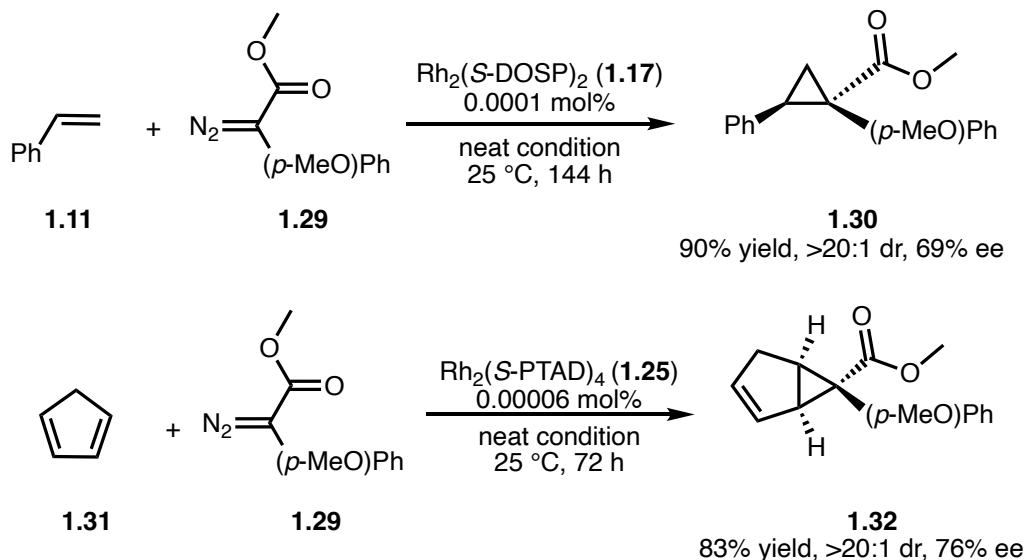
To further enhance the catalyst robustness, a new dirhodium(II) tetraproline complex $\text{Rh}_2(\text{S-biTISP})_2$ (**1.27**) was designed.^{41, 42} The proline ligands of $\text{Rh}_2(\text{S-biTISP})_2$ (**1.27**) were bridged to make the catalyst more durable under low loading conditions. With only 0.001 mol% $\text{Rh}_2(\text{S-biTISP})_2$ (**1.27**), the cyclopropanation between styrene **1.11** and methyl phenyldiazoacetate **1.26** achieved 92% yield and 85% ee at room temperature (**Scheme 1.7**). Notably, methyl benzoate **1.28** was an effective additive to promote the reaction to achieve higher TONs. The role of the methyl

benzoate **1.28** was possibly to stabilize the rhodium carbene complex either by coordination to the carbene or to the other rhodium center.



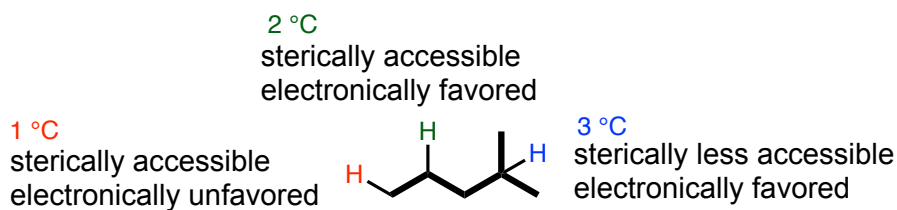
Scheme 1.7 $\text{Rh}_2(\text{S-biTISP})_2$ (**1.27**) catalyzed cyclopropanation with high TONs

Another method to achieve higher TONs was the use of a more stable carbene intermediate. $\text{Rh}_2(\text{S-DOSP})_4$ (**1.17**) had achieved 900,000 TONs in a cyclopropanation using *p*-methoxyphenyldiazoacetate **1.29** as the carbene precursor (**Scheme 1.8**).⁴³ The *p*-methoxyphenyl is a strong donor group that could stabilize the carbene intermediate. The more stable carbene intermediate was less likely to destroy the catalyst, leading to improved results. With *p*-methoxyphenyldiazoacetate **1.29** and the reactive trap reagent cyclopentadiene **1.31**, $\text{Rh}_2(\text{S-PTAD})_4$ (**1.25**) achieved 1,300,000 TONs in the cyclopropanation reaction (**Scheme 1.8**).⁴³ The reaction used 0.00006 mol% $\text{Rh}_2(\text{S-PTAD})_4$ (**1.25**) and generated product **1.32** in 83% yield and 76% ee. These results demonstrated that routinely applying extremely low catalyst loadings in the carbene reaction was promising. Inspired by these precedents, further high catalyst TONs investigation has been conducted to find a system that routinely achieves high levels of asymmetric induction. The extent of this work will be described in a subsequent Chapter.



Scheme 1.8 $\text{Rh}_2(\text{S-DOSP})_4$ and $\text{Rh}_2(\text{S-PTAD})_4$ catalyzed solvent-free cyclopropanation with high TONs

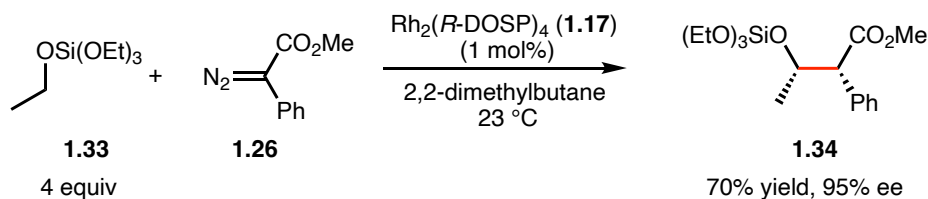
The donor/acceptor carbenes are effective in a range of other reactions beyond cyclopropanation. One reaction that has generated particular interest is C–H functionalization by means of inserting the metal carbene into a C–H bond. Earlier success of intermolecular C–H insertions largely relied on selecting substrates with an appropriate reactivity profile to give clean reactions. Substrates with the correct balance between electronic and steric influences enabled the C–H insertion reactions to occur in a selective manner. As illustrated in **Scheme 1.9**, while tertiary C–H bonds can lead to stabilized positive charge builds up during the transition state, their steric environment offers less opportunity for approach by the sterically encumbered carbene. Conversely, primary C–H bonds are the most sterically accessible sites but are not electronically preferred. Therefore, secondary C–H bonds were normally favored for the C–H insertion reaction, especially when the sites were electronically activated (allylic, benzylic, α to oxygen, α to nitrogen sites).



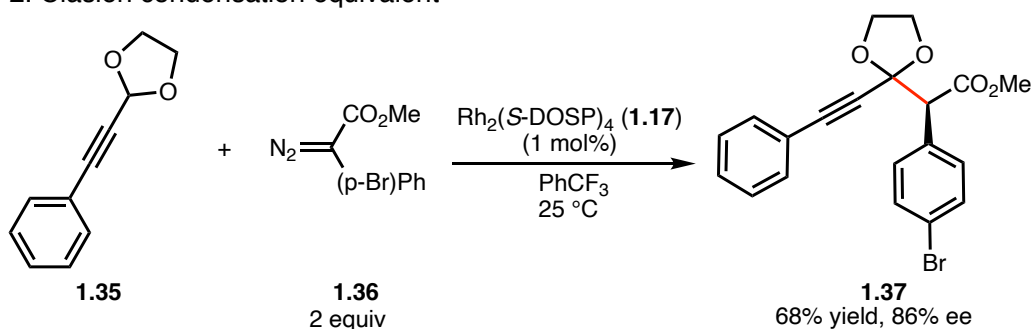
Scheme 1.9 The steric and electronic influences on site selectivity of C–H functionalization

Accordingly, a wide range of donor/acceptor carbene C–H insertions have been developed. Compared with the traditional methods, the C–H insertion methodology is significantly straightforward and effective. The C–H insertion reactions complement classic disconnection strategies and offer many alternative approaches in organic synthesis. For example, the C–H insertion of tetraethoxysilane **1.33** with phenyldiazoacetate **1.26** generated β -alkoxycarboxylate **1.34** with 95% ee and 70% yield (**Scheme 1.10.1**).⁴⁴ This particularly effective reaction catalyzed by $\text{Rh}_2(\text{S-DOSP})_4$ (**1.17**) can be considered as a surrogate of the aldol reaction to form β -hydroxyesters. Another representative example is the C–H insertion of allyl acetal **1.35** with the aryldiazoacetate **1.36** to deliver the ketal protected β -ketoester **1.37** with 86% ee in 68% yield (**Scheme 1.10.2**).⁴⁵ β -ketoesters are traditionally generated by a Claisen condensation. However, chiral β -ketoester products are likely to racemize under the Claisen condensation conditions. The C–H insertion method avoided the racemization because the ketal protection diminished the product CH acidity and ensured the product was readily isolated. A further example is the C–H insertion α to nitrogen to obtain β -amino acid derivatives, which is a Mannich reaction equivalent.⁴⁶ As shown in **Scheme 1.10.3**, C–H insertion of the phenyldiazoacetate **1.26** and N-Boc-pyrrolidine **1.38** generated β -amino acid derivative **1.39** in good yield with high levels of diastereo- and enantioselectivity.

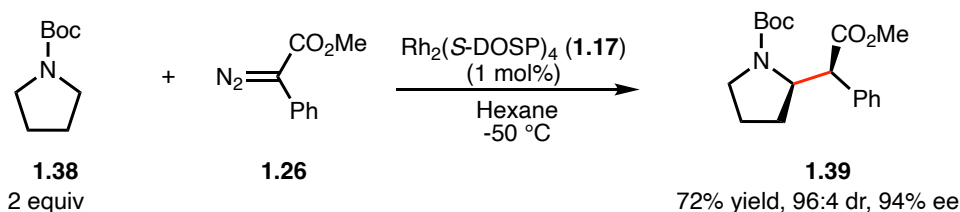
1. Aldol reaction equivalent



2. Claisen condensation equivalent



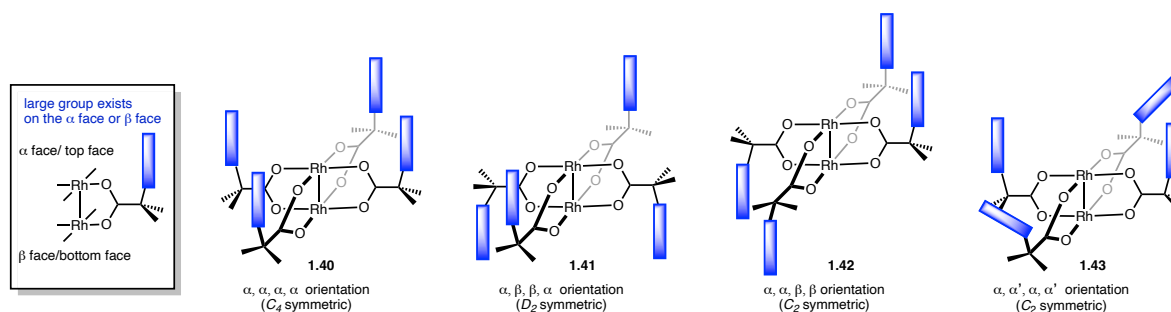
3. Mannich reaction equivalent



Scheme 1.10 Seminal examples of $\text{Rh}_2(\text{DOSP})_4$ -catalyzed intermolecular reactions as classic disconnection equivalent

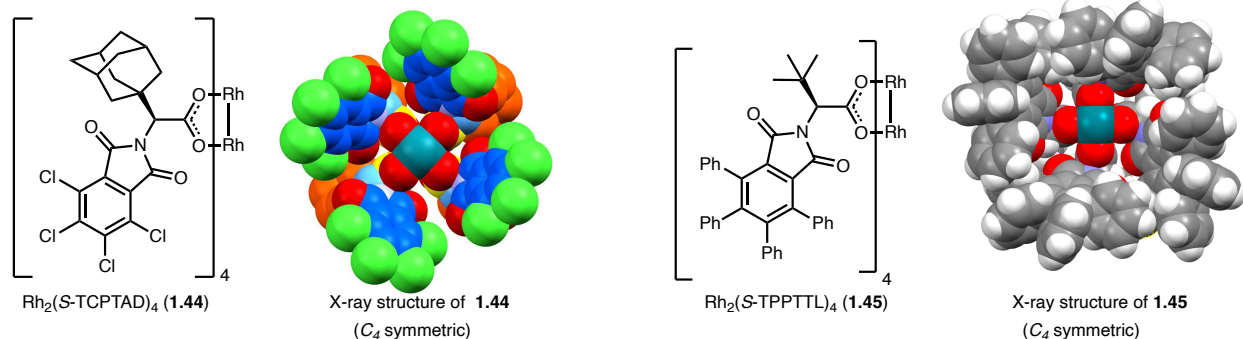
While various C–H insertion systems were explored, the early studies relied on selecting substrates with appropriate functionality for a clean reaction.^{47, 48} Therefore, alternative methods to control the reaction selectivity were required.^{5, 49–55} Remarkably, the Davies group has designed a series of chiral dirhodium(II) complexes that enable catalyst-controlled C–H functionalization.^{5, 49, 56–60} The principle was to utilize the steric environment around the catalysts to affect which C–H bonds could be accessed. The hypothesis was that less bulky catalysts would prefer to react at a tertiary C–H bond, while a sterically demanding catalysts would mitigate the reaction electronic preference and favor the sterically more accessible secondary or primary C–H bonds. Moreover, the high symmetry of the chiral dirhodium(II) complexes would further affect the reaction selectivity. The

achiral dirhodium(II) tetracarboxylate is D_{4h} symmetric with four identical ligands aligning in the periphery of the catalyst core. However, the chiral ligands with bulky substituent would exist on either the top (α) or bottom (β) face of the dirhodium(II) tetracarboxylate. The dirhodium(II) catalysts therefore could adopt higher symmetry than the ligands, depending on the specific orientations of the chiral ligands (**Scheme 1.11**).^{38, 55, 61} In recent years, a variety of chiral dirhodium(II) catalysts with high symmetry have been developed.



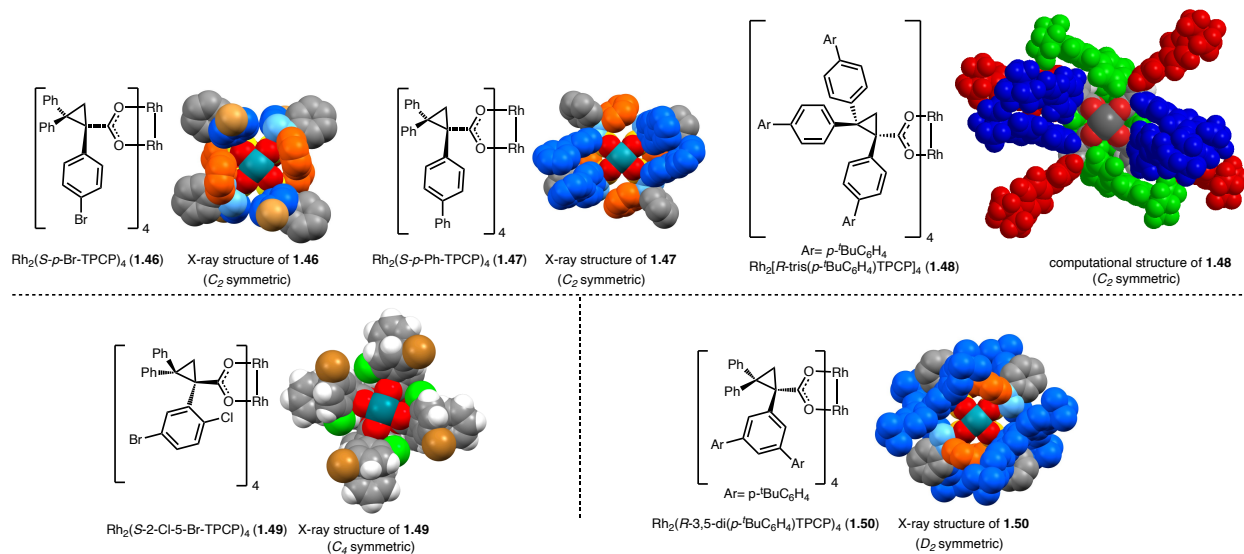
Scheme 1.11 High symmetry orientations of dirhodium(II) tetracarboxylate catalysts

$\text{Rh}_2(S\text{-TCPTAD})_4$ (**1.44**) and $\text{Rh}_2(S\text{-TPPTTL})_4$ (**1.45**), the second-generation catalysts developed in the Davies group, are derived from bulky N-phthalimido amino acids (**Scheme 1.12**).^{39, 59} Both $\text{Rh}_2(S\text{-TCPTAD})_4$ (**1.44**) and $\text{Rh}_2(S\text{-TPPTTL})_4$ (**1.45**) adopt the C_4 symmetric structure (**1.40**) and have some conformational flexibility to allow C–H functionalization at crowded sites. Intriguingly, the X-ray structure of $\text{Rh}_2(S\text{-TPPTTL})_4$ (**1.45**) showed that the 16 phenyl rings in the structure were tilted. While DFT calculations indicated that all 16 phenyl rings tilting one way is the lowest energy form, 12 phenyl rings are tilted one way and four are tilted in the opposite way.³⁹ This suggested the fixed stereogenic centers in the ligands led to a C_4 symmetric propeller-like structure, which could be a key feature for the high asymmetric induction exhibited by this catalyst.



Scheme 1.12 Second-generation C_4 Symmetric dirhodium(II) catalysts derived from N-phthalimido amino acids

The chiral dirhodium(II) complexes with triphenylcyclopropane (TPCP) carboxylate ligands are the third generation catalysts developed in the Davies group (**Scheme 1.13**).^{55, 61} They were designed to be more sterically demanding to overcome the electronic preference of the C–H insertion for tertiary sites. Depending on the functionality, TCPCP catalysts will adopt three possible high symmetry orientations. $\text{Rh}_2(p\text{-Br-TPCP})_4$ (**1.46**),⁵⁶ $\text{Rh}_2(p\text{-Ph-TPCP})_4$ (**1.47**)⁴⁹ and $\text{Rh}_2[R\text{-tris}(p\text{-}^t\text{BuC}_6\text{H}_4)\text{TPCP}]_4$ (**1.48**)⁶² are C_2 -symmetric (**1.42**). $\text{Rh}_2(S\text{-}2\text{-Cl-}5\text{-BrTPCP})_4$ (**1.49**) has an *o*-Cl substituent on the C-1 aryl ring, and the rotation between the cyclopropane and the *o*-Cl-aryl ring is hindered.⁶³⁻⁶⁵ $\text{Rh}_2(S\text{-}2\text{-Cl-}5\text{-BrTPCP})_4$ (**1.49**) preferentially adopts a C_4 -symmetric structure (**1.40**) with all four of the *o*-Cl phenyl rings on the same side. One extremely sterically demanding catalyst is $\text{Rh}_2(R\text{-}3,5\text{-di}(p\text{-}^t\text{BuC}_6\text{H}_4)\text{TPCP})_4$ (**1.50**), the aryl group of which is 3,5-disubstituted.⁵⁷ The four ligands of $\text{Rh}_2(R\text{-}3,5\text{-di}(p\text{-}^t\text{BuC}_6\text{H}_4)\text{TPCP})_4$ (**1.50**) adopt an up-down-up-down arrangement, which leads to a D_2 -symmetric structure (**1.41**).

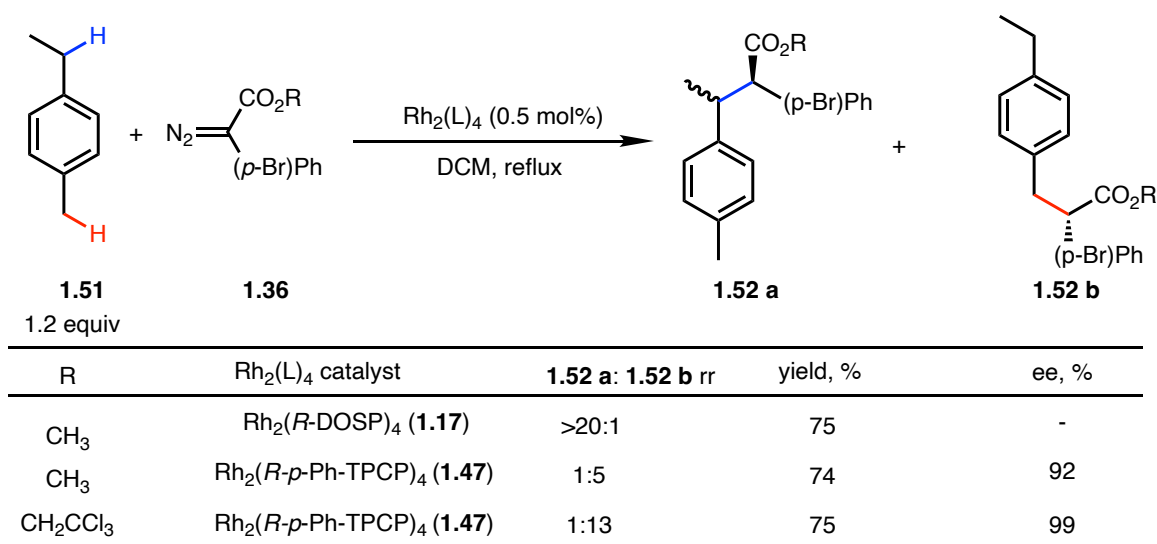


Scheme 1.13 Third-generation C_2 , D_2 and C_4 Symmetric dirhodium(II) catalysts derived from TPCP ligands

With all above novel dirhodium(II) catalysts in hand, relatively similar bonds can be differentiated in the C–H functionalization reaction. By applying appropriate dirhodium(II) catalysts to fit the steric environment, precisely controlled C–H functionalization reaction has been significantly developed. A significant example was the C–H functionalization of *p*-ethyl toluene **1.51** reported by the Davies group in 2014.⁴⁹ As demonstrated in **Table 1.2**, the reaction of methyl aryldiazoacetate **1.36** with *p*-ethyl toluene **1.51** was examined using two dirhodium(II) catalysts. The reaction catalyzed by $\text{Rh}_2(\text{R-DOSP})_4$ (**1.17**) generates cleanly the secondary benzylic C–H insertion product **1.52a** in 75% yield. With the more sterically bulky third generation catalyst, $\text{Rh}_2(\text{R-}p\text{-PhTPCP})_4$ (**1.47**), the reaction favors primary C–H bond and forms **1.52b** as product (1:5 rr and 92% ee). Furthermore, the selectivity can be further enhanced (1:13 rr and 99% ee) with the aryldiazoacetate **1.36**, in which the methyl ester has been replaced by a chloroethyl ester.

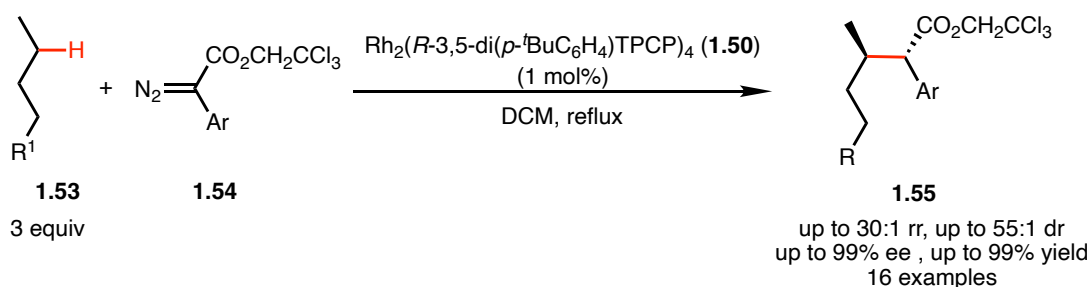
Table 1.2 Catalyst-controlled benzylic C–H functionalization of ethyltoluene

Davies (2014)



Compared with the active benzylic C–H insertion shown in **Table 1.2**, differentiation between unactivated secondary C–H bond needed a more sterically bulky catalyst to accurately control the selectivity. Rh₂(*R*-3,5-di(*p*-^tBuC₆H₄)TPCP)₄ (**1.50**) is the optimum catalyst in the C–H functionalization at the most accessible secondary site (**Scheme 1.14**).⁵⁷ This bulky *D*₂ symmetric catalyst is effective in the functionalization of pentane **1.53** at the most accessible C-2 position, with no competing reactions at the C-3 methylene site. The C–H products **1.55** are obtained with excellent site selectivity, diastereoselectivity, and enantioselectivity.

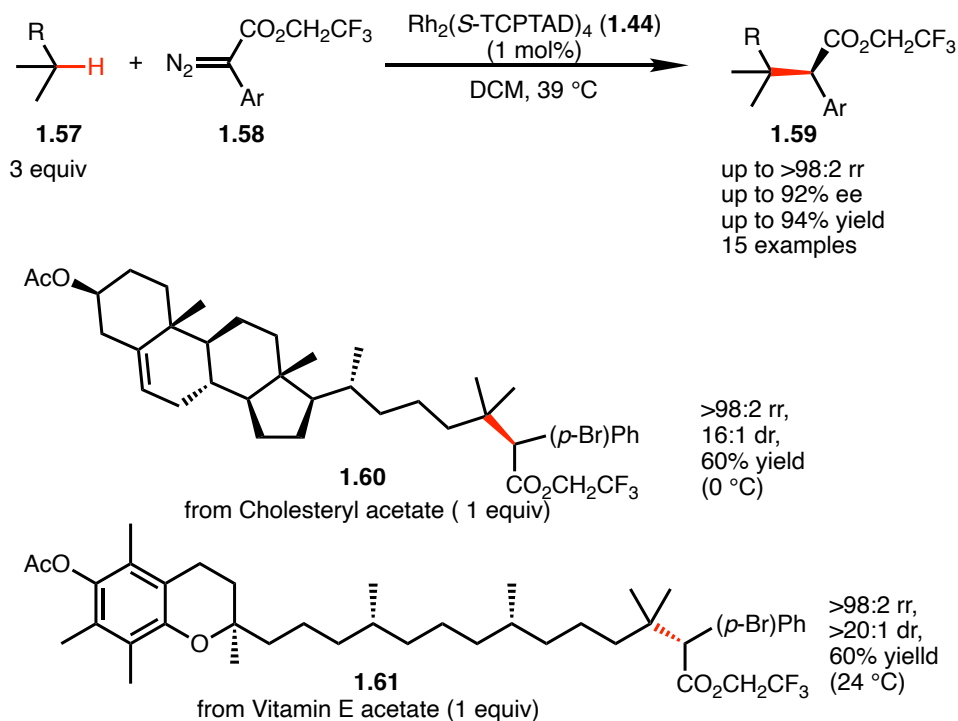
Davies (2016)



Scheme 1.14 Rh₂(*R*-3,5-di(*p*-^tBuC₆H₄)TPCP)₄ (**1.50**) catalyzed selective functionalization of unactivated secondary C–H bonds

Tertiary C–H bonds are electronically preferred in carbene-induced C–H functionalization reactions. However, the crowded environment of a tertiary C–H bond hinders approach to the rhodium-carbene center. Previous endeavors using $\text{Rh}_2(\text{DOSP})_4$ (**1.17**) in tertiary C–H insertion had limited scope and resulted in moderate levels of enantioselectivity. To further enhance the selectivity, the more rigid catalyst, $\text{Rh}_2(\text{S-TCPTAD})_4$ (**1.44**), was applied to the reaction.⁵⁹ As illustrated in **Scheme 1.15**, $\text{Rh}_2(\text{S-TCPTAD})_4$ (**1.44**) catalyzed tertiary bond C–H functionalization and generated products **1.59** with excellent site- and enantioselectivity. More remarkably, late-stage functionalization of natural products, including steroids (**1.60**) and a vitamin E derivative (**1.61**) has been carried out with satisfying results. While these elaborate substrates contained several tertiary C–H bonds, the C–H functionalization exclusively occurred at the most accessible one with high asymmetric induction.

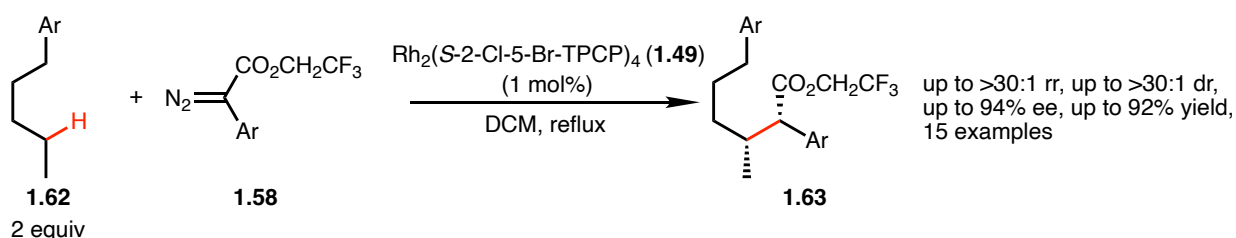
Davies (2017)



Scheme 1.15 $\text{Rh}_2(\text{S-TCPTAD})_4$ (**1.44**) catalyzed selective functionalization of tertiary C–H bonds and the method application in late-stage functionalization of natural products

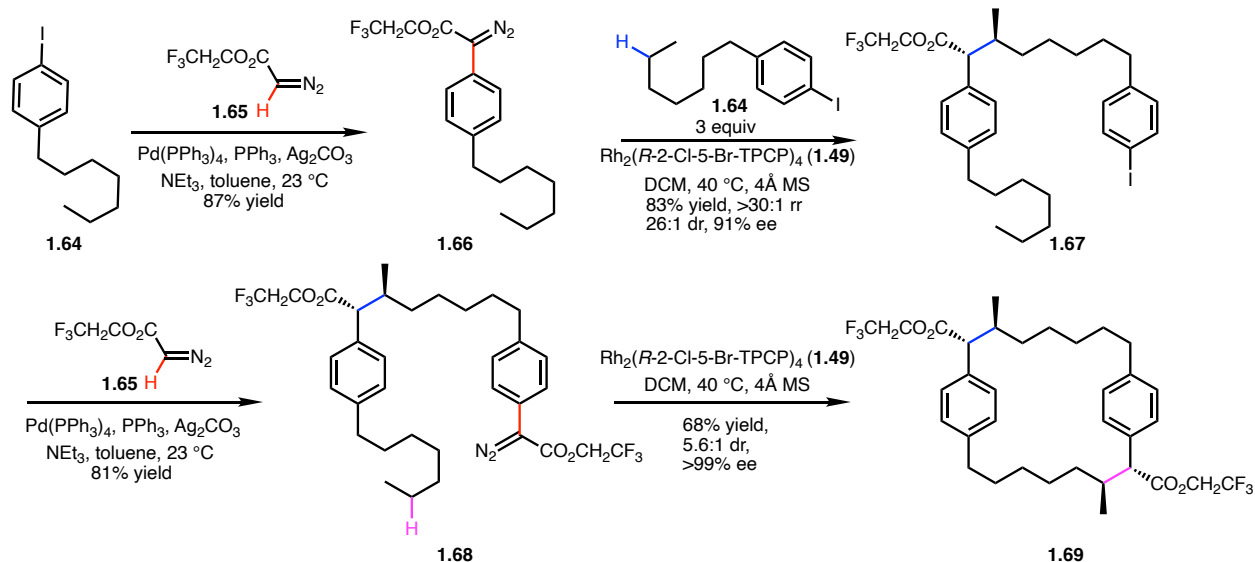
Recent research showed $\text{Rh}_2(\text{S-2-Cl-5-BrTPCP})_4$ (**1.49**) is capable of superior selectivity for reactions at the most accessible unactivated secondary C–H bond (**Scheme 1.16**).⁶³ Remarkably, C–H insertion happened at the most accessible methylene site of n-alkylbenzenes **1.62** in the presence of active benzylic C–H bond. The reaction has overcome the strong preference of electronically active site and displayed excellent steric control at the most accessible secondary C–H bond to obtain **1.63**.

Davies (2018)



Scheme 1.16 $\text{Rh}_2(\text{S-2-Cl-5-BrTPCP})_4$ (**1.49**) catalyzed site selective functionalization of unactivated secondary C–H bonds

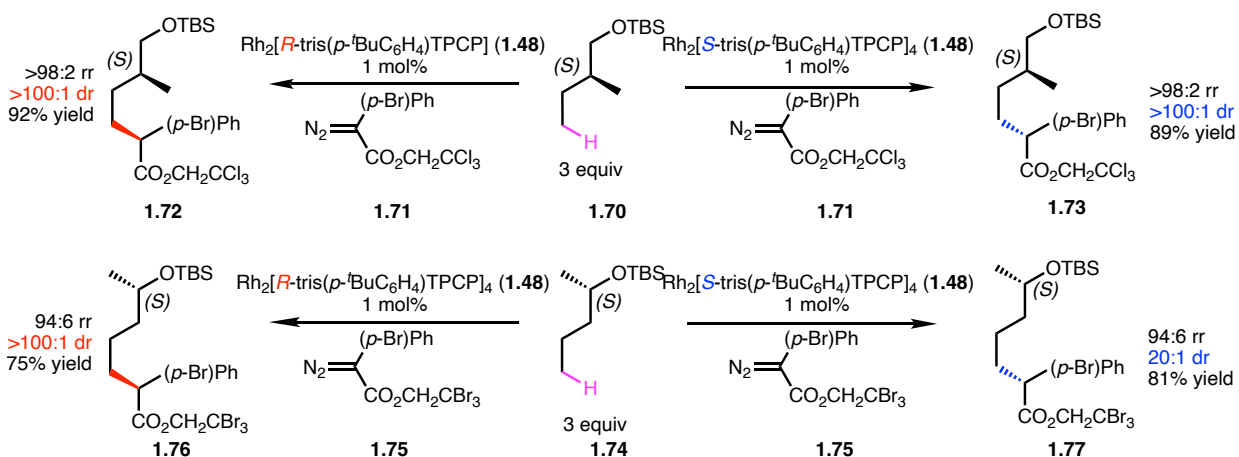
Notably, the method has been applied in synthesizing the macrocyclic core (**1.69**) of the cylindrocyclophane class of natural products (**Scheme 1.17**). $\text{Rh}_2(\text{S-2-Cl-5-BrTPCP})_4$ (**1.49**) catalyzed C–H functionalization was utilized in two key steps of the synthesis and controlled the stereochemistry precisely at four newly formed stereogenic centers. The example demonstrated the great efficiency of catalyst-controlled C–H functionalization to generate desired complex structures with accurate stereoselectivity.



Scheme 1.17 Enantioselective synthesis of cylindrocyclophane core applying $\text{Rh}_2(\text{S-2-Cl-5-BrTPCP})_4$ (**1.49**) catalyzed C–H functionalization

Functionalization of inert primary C–H bonds is more challenging, because they are electronically the least favored. Competition reactions from more active secondary or tertiary C–H bonds usually occur, leading to the formation of a mixture of products. Selective primary C–H insertion control needs very bulky dirhodium(II) catalysts. Accordingly, $\text{Rh}_2[\text{R-tris}(p\text{-}^t\text{BuC}_6\text{H}_4)\text{TPCP}]_4$ (**1.48**) was designed with fully *p*-phenyl substituted TPCP ligands.⁶² The catalyst (**1.48**) is sufficiently sterically demanding to overcome electronic preference for tertiary or secondary C–H insertion. As illustrated in **Scheme 1.18**, exceptionally high site selectivity and asymmetric induction has been achieved by $\text{Rh}_2[\text{R-tris}(p\text{-}^t\text{BuC}_6\text{H}_4)\text{TPCP}]_4$ (**1.48**). The C–H functionalization of the most sterically accessible primary C–H bonds was selectively targeted although the substrates (**1.70** and **1.74**) contain functional groups and electronically activated C–H bonds.

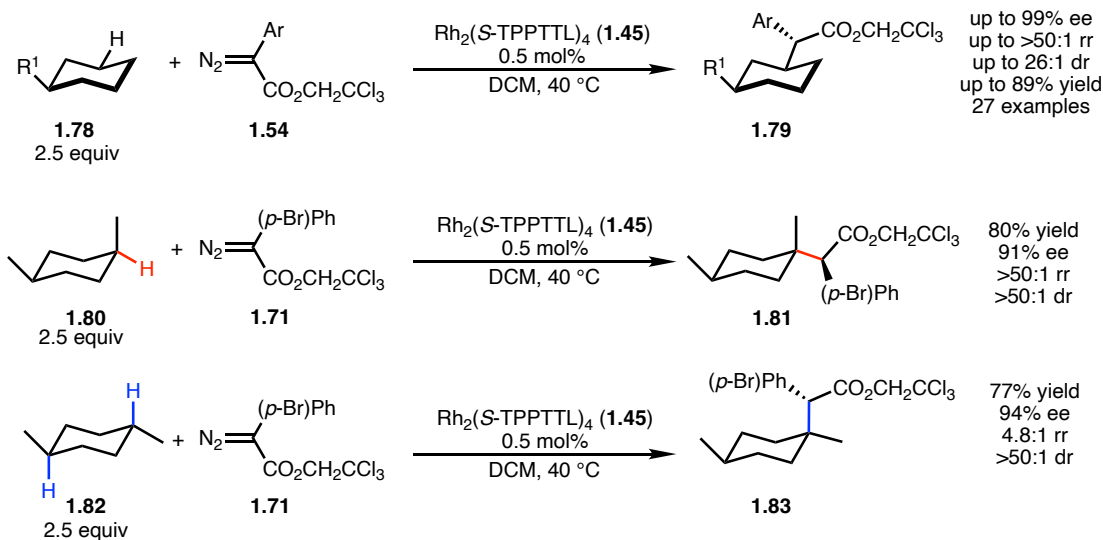
Davies (2018)



Scheme 1.18 $\text{Rh}_2[\text{tris}(p\text{-}^t\text{BuC}_6\text{H}_4)\text{TPCP}]_4$ (**1.48**) catalyzed site selective functionalization of unactivated primary C–H bonds

The C_4 symmetric catalyst $\text{Rh}_2(\text{S-TPPTTL})_4$ (**1.45**) achieved selectivity between similar unactivated secondary C–H bonds of cyclohexane derivatives.³⁹ As showed in **Scheme 1.19**, the substituted cyclohexane **1.78** has 11 different C–H bonds within the ring, 10 of which are secondary. While other tested dirhodium(II) catalysts generated mixture of products, $\text{Rh}_2(\text{S-TPPTTL})_4$ (**1.45**) catalyzed the reaction to generate cleanly the C-3 equatorial substituted product **1.79** with high regio-, diastereo- and enantioselectivity. According to the X-ray structure, the 16 phenyl groups on the ligands formed a well-defined wall at the periphery of $\text{Rh}_2(\text{S-TPPTTL})_4$ (**1.45**). Additionally, computational studies suggested this bowl-shape C_4 symmetric catalyst had some flexibility to adjust the pocket when the substrate approached the carbene center. This site selectivity was proposed to be controlled by how the substrate interacted with the wall of the catalyst rather than the influence of the steric environment at the carbene site itself.

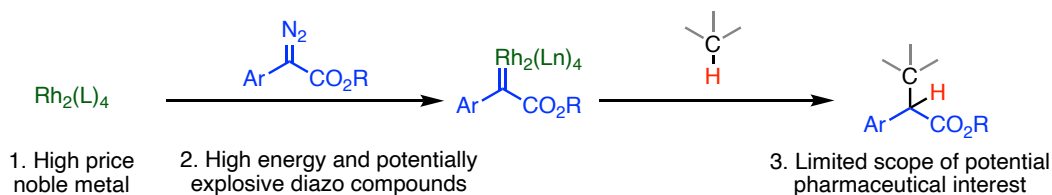
Davies (2018)



Scheme 1.19 $\text{Rh}_2(\text{S-TPPTTL})_4$ (**1.45**) catalyzed desymmetrization of cyclohexane derivatives

$\text{Rh}_2(\text{S-TPPTTL})_4$ (**1.45**) could catalyze C–H functionalization into a tertiary C–H site in both trans and cis 1,4-dimethylcyclohexane isomers (**1.80** and **1.82**), while the regioselectivity of trans-1,4-dimethylcyclohexane **1.83** was lower (4.8:1 r.r.). Competition experiments using mixtures of both isomers indicated that the equatorial C–H bond reacted approximately 140 times faster than an axial C–H bond. The results demonstrated the dramatic preference of equatorial position presented by $\text{Rh}_2(\text{S-TPPTTL})_4$ (**1.45**).

In summary, donor/acceptor carbenes and dirhodium(II) tetracarboxylates catalysts have been shown to be a privileged system, showing unique reactivity and selectivity in asymmetric reactions. However, challenges still exist for the broader application of carbene chemistry (**Scheme 1.20**).



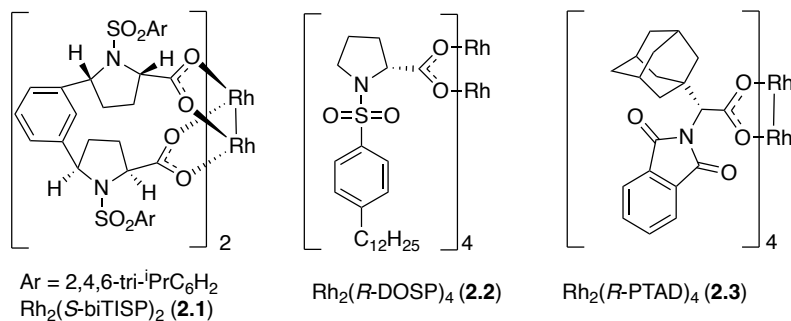
Scheme 1.20 Limitations of rhodium-carbene chemistry in practical applications

The work described in this thesis focused on studies aiming to overcome the practical limitations of the carbene chemistry. Each Chapter will discuss the efforts to enhance the practicality from different aspects. Firstly, considering the high price of precious rhodium metal, using less dirhodium(II) catalysts in the reaction is necessary to make the chemistry more economical.⁶⁶ Chapter 2 and Chapter 5 will introduce the work applying *in-situ* kinetic study to develop optimal low catalyst loadings conditions. The cyclopropanation (Chapter 2) and C–H insertion (Chapter 5) have achieved extremely high catalyst TONs while maintaining the excellent reactivity and selectivity. Secondly, diazo compounds are highly reactive and energetic.⁶⁷ The possibility of exothermic decomposition and explosion make diazo compounds undesirable for application in industrial-scale synthesis. Chapter 3 will describe a flow process using mild methods to synthesize and utilize diazo compounds *in-situ*. Moreover, the dirhodium(II) catalysts and electrophilic carbene intermediates are sensitive to the nucleophilic sites appearing in the substrates.⁶⁸⁻⁷⁰ Carbene reactions with nucleophilic heterocycles usually give lower yield or selectivity. As heterocyclic motifs are of pharmaceutical interest, Chapter 4 will introduce the efforts to develop asymmetric synthesis of pharmaceutically relevant cyclopropanes, which has accommodated a broad range of heterocycles.

Chapter 2. In Situ Kinetic Studies of Dirhodium(II)-Catalyzed Asymmetric Cyclopropanation with Low Catalyst Loadings.

2.1 Introduction

Dirhodium(II) tetracarboxylates have revolutionized the chemistry of transition-metal-catalyzed carbene reactions.^{38, 71} Under mild conditions, dirhodium(II) tetracarboxylates enable nitrogen extrusion from diazo compounds and generate carbene intermediates. The carbene intermediates, especially the donor/acceptor carbenes, can effectively undergo a wide range of synthetically useful reactions.⁵⁵ Considering the high cost of dirhodium(II) catalysts and the broad utility of carbene chemistry, we have a long-standing interest to conduct the reactions with extremely low catalyst loadings. A previous study established that the chiral bridged *N*-arylsulfonylprolinate catalyst, Rh₂(*S*-biTISP)₂ (**2.1**), enabled the cyclopropanation of styrene to be conducted with only 0.001 mol % catalyst loading and achieved 85% ee.⁷² However, Rh₂(*S*-biTISP)₂ (**2.1**) is difficult to synthesize on scale, which limits its general utility. In the absence of solvent, low catalyst loading conditions are also applicable for the carbene reactions catalyzed by Rh₂(*R*-DOSP)₄ (**2.2**) and Rh₂(*R*-PTAD)₄ (**2.3**).⁴³ For example, Rh₂(*R*-PTAD)₄ (**2.3**) achieved 1,300,000 TONs in cyclopropanation reaction under neat conditions. However, the enantioselectivity dropped dramatically comparing with normal catalyst loading conditions. Also, the neat reaction on large scale would have significant safety issues because of the high energy associated with the diazo compounds. The above high TONs studies mainly concentrated on Rh₂(*S*-biTISP)₂ (**2.1**), Rh₂(*R*-DOSP)₄ (**2.2**), and Rh₂(*R*-PTAD)₄ (**2.3**) because they were the only available chiral dirhodium(II) catalysts at that time (**Scheme 2.1**).^{42, 43} With various novel chiral dirhodium(II) catalysts developed recently, a systematic investigation is needed to examine the potential of these new catalysts to achieve extremely high TONs.

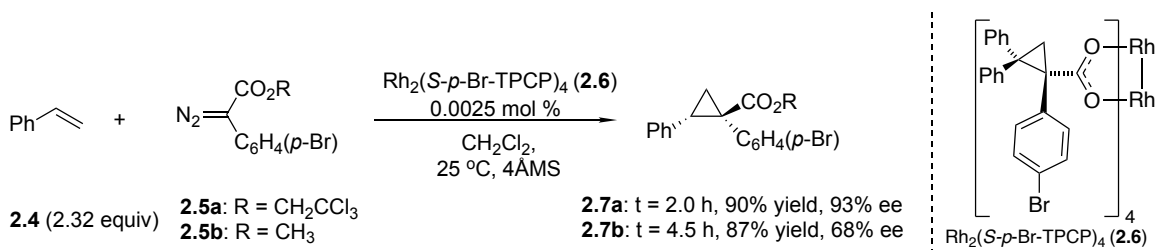


Scheme 2.1 Chiral dirhodium(II) catalysts capable of high TONs

In this study, detailed *in-situ* kinetic analysis was undertaken to reveal the relative reactivity of the catalysts and their performance as the reaction progresses. The kinetic information guided optimization of low catalyst loading conditions. Finally, a general process using 0.001 mol % catalyst loading was applied to cyclopropanation with a wide range of substrates, in which the level of enantioselectivity remained high (86-99% ee).

2.2 Results and Discussions

The first stage of the study was to determine the relative reactivity of the catalysts in a standard cyclopropanation of styrene (**2.4**) with *p*-bromophenyldiazoacetate (**2.5**) to form the cyclopropane (**2.7**). Previous research has shown that the trichloroethyl ester (**2.5a**) is superior compared with the traditional methyl ester (**2.5b**) in terms of site selectivity in C–H functionalization reactions, reaction efficiency, and faster reactions rate, at least under thermal conditions.^{73, 74} Therefore, we firstly compared the profiles of **2.5a** with **2.5b** in the cyclopropanation reaction catalyzed by Rh₂(*S*-*p*-Br-TPCP)₄ (**2.6**) with 0.0025 mol % loading (**Scheme 2.2**). The results showed diazo compound **2.5a** with trichloroethyl ester is more reactive and gives significantly higher enantioselectivity (93% ee versus 68% ee). Therefore, diazo compound **2.5a** was applied as the standard carbene precursor for exploring relative reactivity of the different dirhodium(II) catalysts.



Scheme 2.2 Influence of ester functionality on diazo compounds

Most reported studies on dirhodium(II)-catalyzed reactions of donor/acceptor carbenes rarely attempted to conduct the reactions at their lowest possible catalyst loadings.^{14, 75} The normal conditions usually used 0.5-1.0 mol % catalyst loading at rt, under which all the catalysts were very effective. Typically, the reactions are completed in a matter of minutes, although slow diazo compounds addition is commonly applied to prevent dimerization. The carbene reactions with reactive trapping substrates can even be conducted at -50 °C while maintaining good yield and selectivity. Prior to this study, information about the relative rates of the different dirhodium(II) catalysts was limited.⁷⁶⁻⁷⁸ Therefore, the reaction rates of the catalysts were firstly compared at relatively low loadings (0.0025 mol %), because under these conditions the kinetic difference between the catalysts should be perceptible. The reactions were conducted in dichloromethane (CH₂Cl₂) to avoid solubility issues. CH₂Cl₂ is also the established optimum solvent for most of the dirhodium(II) catalysts tested here. The two exceptions are the Rh₂(R-DOSP)₄ (**2.2**), and Rh₂(R-PTAD)₄ (**2.3**), which give higher levels of asymmetric induction when hydrocarbon solvents are used.⁷⁹ The reaction rates were determined by ReactIR, following the rate of disappearance of the distinctive signal for the diazo functionality [2103 cm⁻¹]. Control experiments were also conducted to show that the rate of disappearance of the diazo compound **2.5a** signal was directly proportional to the rate of appearance of the signals associated with the cyclopropane product **2.7a** (**Figure 2.1a-b**). The crude ¹H-NMR (**Figure 2.1c**) further showed the reaction is robust and clean with only 0.01 mol% catalyst loading, which is highly potential to achieve higher catalyst TONs.

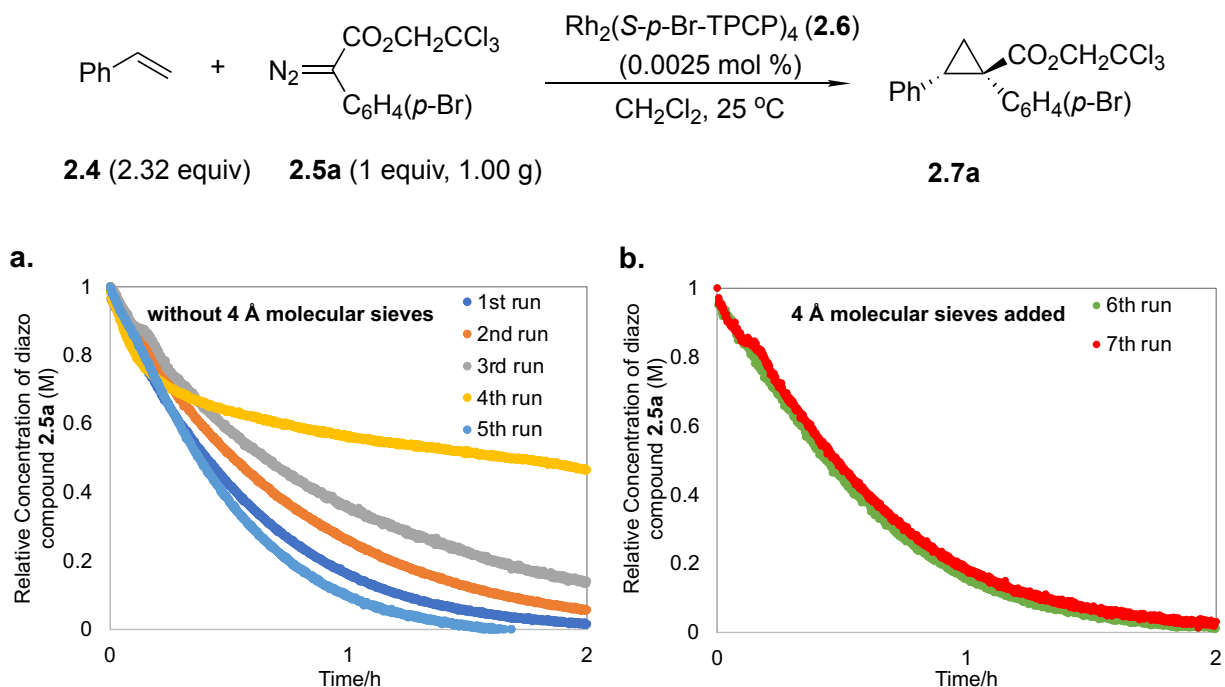


Figure 2.2 Kinetic profiles highlighting the importance of 4 Å molecular sieves **a.** Reaction kinetic profiles were inconsistent without 4 Å molecular sieves at 0.0025 mol % catalyst loading. **b.** Reaction kinetic profile became consistent upon inclusion of 4 Å molecular sieves in the reaction.

The influence of the catalysts on the rates of the reaction under the standard conditions is summarized in **Figure 2.3**. The tested dirhodium(II) catalysts displayed an unexpectedly wide range of reactivity with the most active catalyst being over 500 times faster than the slowest one. Even so, most catalysts finished the reaction in 30 min. The results implied that the catalytic cycle was robust and efficient, which was essential to achieve extremely high TONs. The most reactive catalyst is $\text{Rh}_2(\text{R-DOSP})_4$ (**2.2**), which had an initial TOF of 2,880,000/h and an overall TOF of 1,068,000/h. Among the second generation catalysts, $\text{Rh}_2(\text{R-PTAD})_4$ (**2.3**), and $\text{Rh}_2(\text{R-TCPTAD})_4$, are nearly as reactive as $\text{Rh}_2(\text{R-DOSP})_4$ (**2.2**), whereas $\text{Rh}_2(\text{R-TPPTTL})_4$ is about four times slower. The third generation catalysts, the TPCP series, tended to be the slowest catalysts. The trend is reasonable because the third generation catalysts were designed to be more sterically crowded than the first and second generation catalysts. The *ortho*-chloro-substituted catalysts, $\text{Rh}_2(\text{S-}o\text{-Cl-}$

TPCP)₄, and Rh₂(*S*-2-Cl-5-Br-TPCP)₄, are still relatively fast, with an initial TOF of >1,000,000/h but Rh₂(*S*-*p*-Br-TPCP)₄ (**2.6**), Rh₂(*R*-*p*-Ph-TPCP)₄ (**2.8**), and Rh₂[*R*-tris(*p*-^tBuC₆H₄)TPCP)₄ are about 20 times slower. The slowest catalyst of all is Rh₂(*R*-3,5-di(*p*-^tBuC₆H₄)TPCP)₄, which is a further order of magnitude slower and finished the reaction after 12 h.

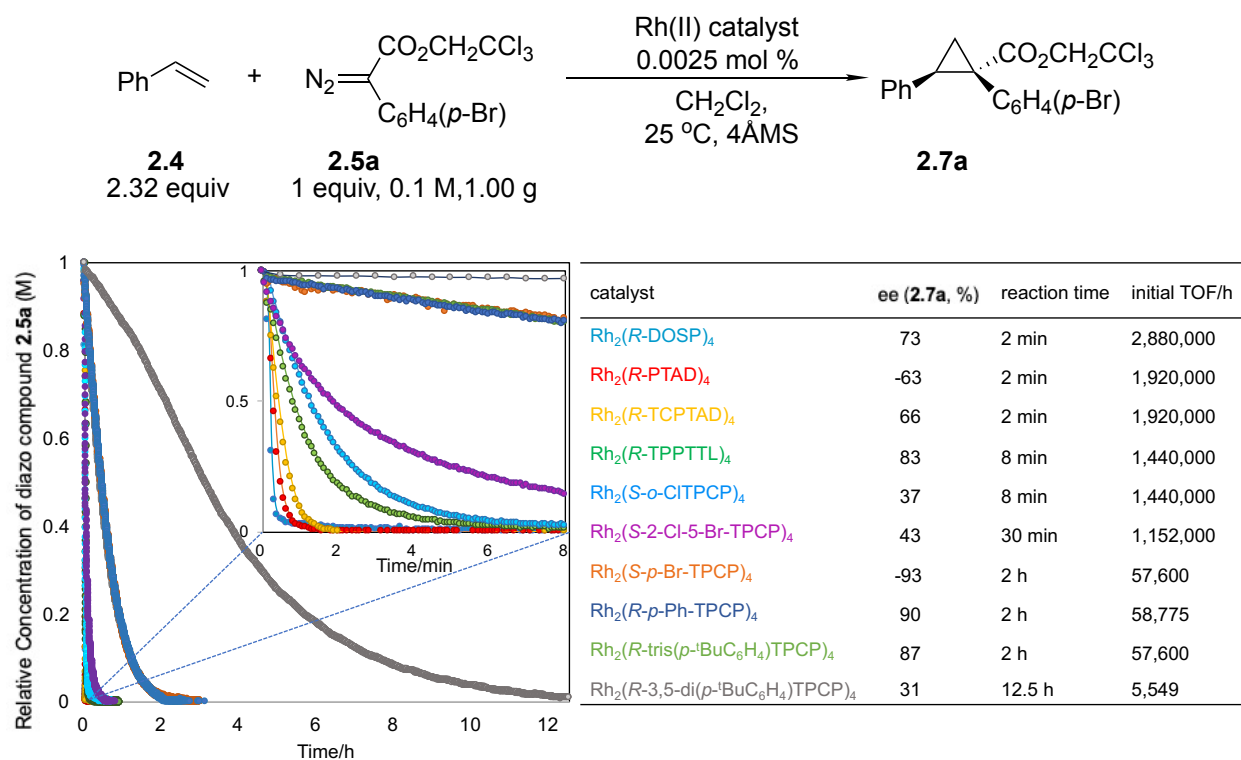


Figure 2.3 Reaction rates of various dirhodium(II) catalysts in the cyclopropanation reaction. (-) indicated that the opposite enantiomer was obtained. *The initial turnover frequency (TOF) was measured according to the initial rate of the reactions up to 20% conversion. All reactions gave the quantitative yield according to crude ¹H-NMR, and the overall TOFs were calculated by the isolated yields.

We have previously explored the high TONs catalysis of Rh₂(*R*-DOSP)₄ (**2.2**), and Rh₂(*R*-PTAD)₄ (**2.3**), two of the fastest catalysts.⁴³ Even though impressive overall TONs were obtained, the enantioselectivity of cyclopropanation dropped dramatically between 0.01-0.001 mol % catalyst loading. Therefore, we decided to explore whether some of the slower and more sterically constrained catalysts would be more robust to maintain the enantioselectivity under low catalyst

loading conditions. In this regard, further exploration focused on the $\text{Rh}_2(\text{S-}p\text{-Br-TPCP})_4$ (**2.6**)-catalyzed cyclopropanation because it gave the highest level of enantioselectivity (93% ee) in the standard reaction. Even though $\text{Rh}_2(\text{S-}p\text{-Br-TPCP})_4$ (**2.6**) is one of the slower catalysts, it still completed cyclopropanation at 0.0025 mol % catalyst loading in 2 h, and therefore still has the potential to achieve very high TONs, especially if the reaction is conducted under elevated temperatures.

To understand the behavior of $\text{Rh}_2(\text{S-}p\text{-Br-TPCP})_4$ (**2.6**) better, we conducted systematic kinetic studies on the $\text{Rh}_2(\text{S-}p\text{-Br-TPCP})_4$ (**2.6**) catalyzed cyclopropanation reaction. (**Figure 2.4** and **2.5**) Using the Variable Time Normalization Analysis (VTNA) methodology developed by Burés,⁸⁰ we determined the reaction order of the dirhodium(II) catalyst through a series of 1.0 g scale reactions with diazo-compound **2.5a** at a concentration of 0.1 M. The reactions were performed at various catalyst loadings: 0.02 mol %, 0.01 mol %, and 0.0025 mol % and the diazo compound concentration [**2.5a**] was plotted against a normalized time scale $t[\text{cat}]_T^n$ (t = time, T = total, n =catalyst order) (**Figure 2.4**), revealing that $\text{Rh}_2(\text{S-}p\text{-Br-TPCP})_4$ (**2.6**) was 1st order in the reaction.

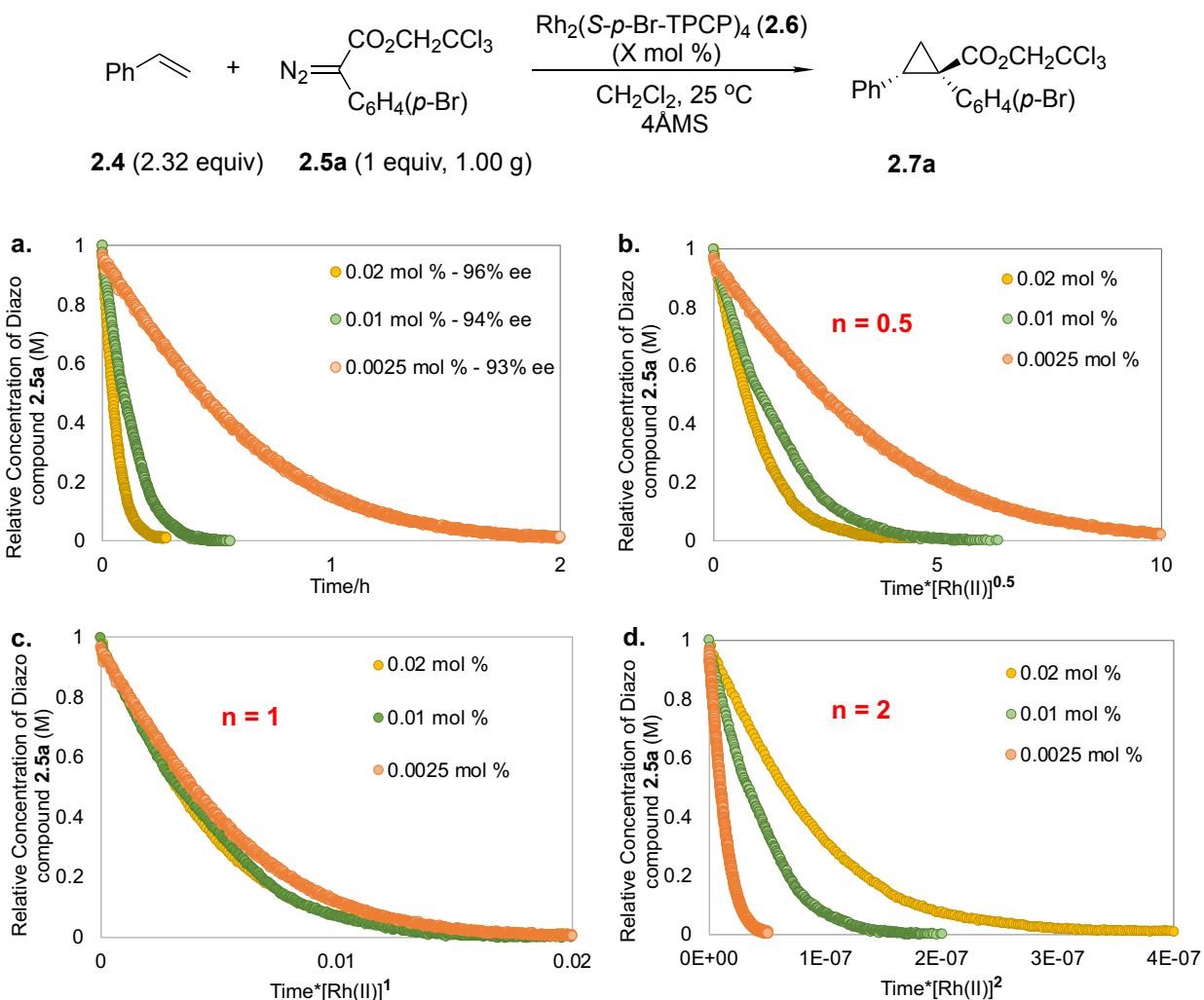


Figure 2.4 Variable Time Normalization Analysis (VTNA) experiments for determining catalyst order **a.** Primary kinetic curves of benchmark cyclopropanation reactions with different catalyst loadings. **b, c, d:** Three different normalized time scales showed that when $n = 1$, the curves overlap, meaning that the catalyst was 1st order in the benchmark cyclopropanation reaction.

After determining the reaction order of the catalyst, the robustness of the catalyst was evaluated using Reaction Progress Kinetic Analysis (RPKA) methodology by conducting “same excess” experiments.⁸¹ The [excess] was invariable over the course of the reaction and defined as shown in eq 1.

$$[\text{excess}] = [\mathbf{2.4}]_0 - [\mathbf{2.5a}]_0 = [\mathbf{2.4}] - [\mathbf{2.5a}] \quad (\text{eq 1})$$

The kinetic profiles of two reactions were investigated: one was the “standard condition” same as **Scheme 2.2** and the other was “same excess” with half the normal loading of the diazo compound **2.5a** (0.5 equiv) but the same [excess] of the styrene (**2.4**). When the “standard condition” reaction reached 50% conversion, if the catalyst is robust and does not show any deactivation or product inhibition, then the reaction rate should be equal to that of the “same excess” reaction. When tested, the kinetic curves of the “same excess” reaction and the “standard reaction” after 50% conversion showed good overlap between the data sets (**Figure 2.5b**). This result suggested that the catalytic performance of $\text{Rh}_2(\text{S-}p\text{-Br-TPCP})_4$ (**2.6**) was maintained after 20,000 TONs, and there was no product inhibition of the catalyst. After confirming the catalyst robustness, we moved forward to determine the concentration dependences of diazo compounds **2.5a** and styrene **2.4**. To achieve this goal, “different excess” experiments were performed. In these experiments, the amount of the diazo compound **2.5a** was decreased (0.5 equiv) while the concentration of styrene **2.4** (2.32 equiv) and the loading of the $\text{Rh}_2(\text{S-}p\text{-Br-TPCP})_4$ (**2.6**) (0.0025 mol %) were kept constant (**Figure 2.5c**). We found that the reaction rate (represented by change in the concentration of styrene **2.4**) became slower with decreased amount of diazo compound **2.5a**, but the high enantioselectivity was still maintained at 93% ee. This positive correlation demonstrates that the reaction order of diazo compound **2.5a** is positive. The data is also in agreement with earlier computational studies, which showed that the energy barrier for diazo decomposition to form the carbene intermediate is much higher than the cyclopropanation step in the reaction. Therefore, carbene formation is the rate determining step in the cyclopropanation reaction. Concentration dependence of styrene was also determined by the same method (**Figure 2.5d**). Interestingly, a higher concentration of styrene **2.4** (4.64 equiv) led to slower reaction rate, while lower concentration of styrene **2.4** (1.5 equiv) gave faster rate but diminished enantioselectivity (72% ee). The results suggested that although styrene

2.4 reduces the reaction TOF, possibly by competing coordination to the dirhodium(II) catalyst, this coordination effect may help to stabilize the catalyst or the carbene intermediate to maintain the high enantioselectivity.

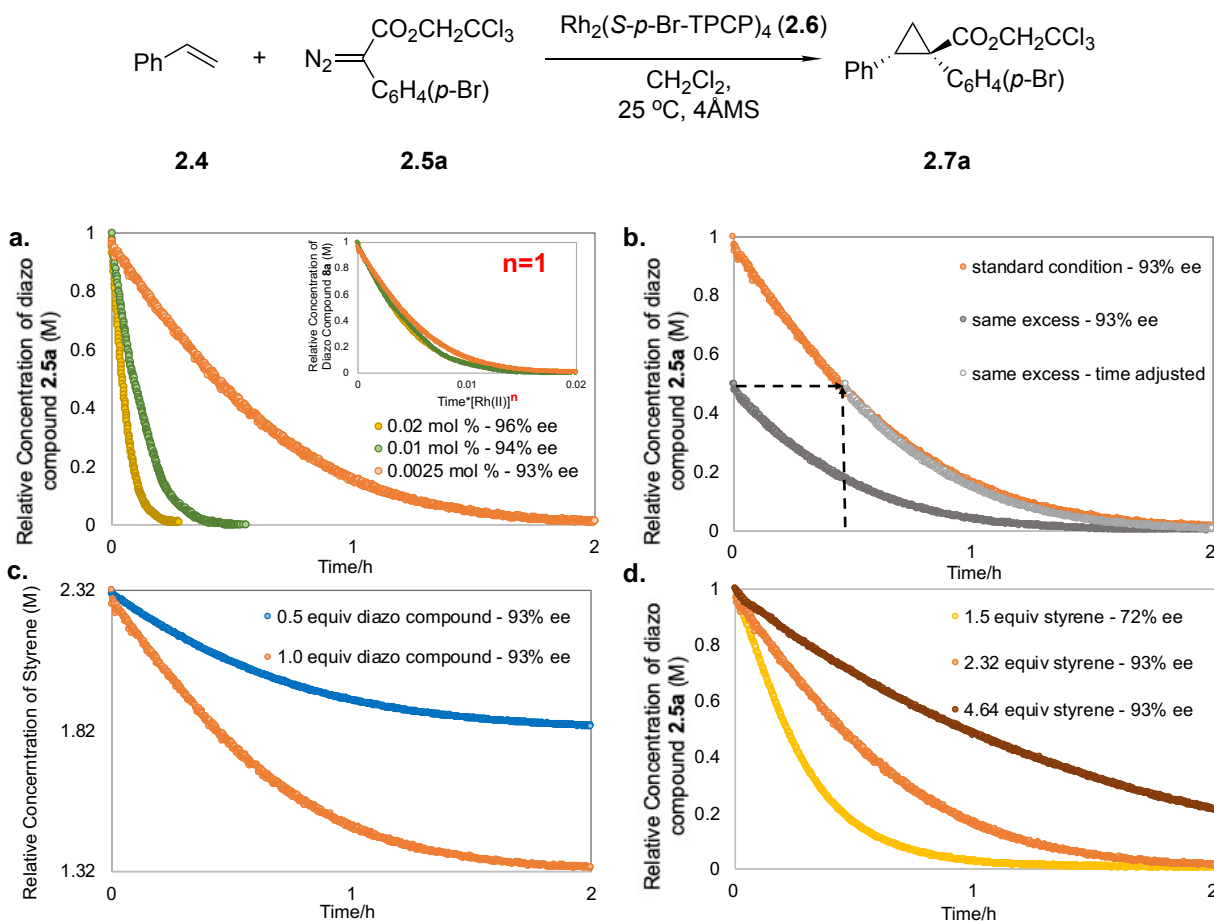
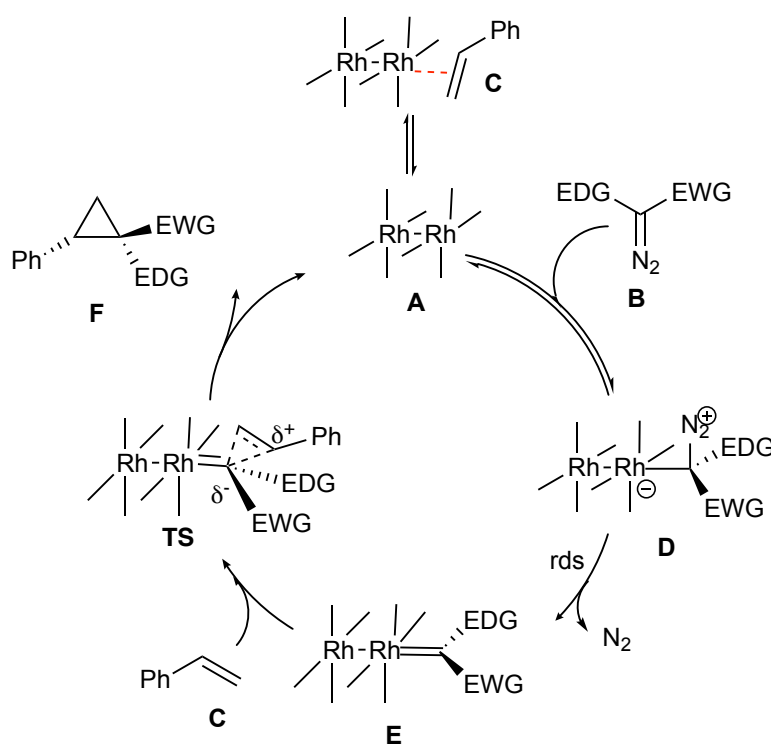


Figure 2.5 Kinetic profiles of cyclopropanation reaction with Rh₂(*S-p*-Br-TPCP)₄ (**2.6**) **a.** The Variable Time Normalization Analysis determined the catalyst was 1st order. **b.** Same excess reaction was carried out with [excess] = 0.132 M. “standard condition”: [2.4]₀ = 0.232 M, [2.5a]₀ = 0.1 M; “same excess”: [2.4]₀ = 0.182 M, [2.5a]₀ = 0.05 M. **c.** Different excess reaction determined positive reaction order of diazo compound **2.5a**. **d.** Different excess reaction determined negative reaction order of styrene **2.4**.

Based on above results and further derivation of the rate equation (See experimental part), a rate law for the cyclopropanation reaction is determined as shown in eq 2.

$$\text{rate} = k[\mathbf{2.5a}]^1 [\mathbf{2.4}]^{-1} [\text{Rh(II)}]^1 \quad (\text{eq 2})$$

A catalytic cycle based on the kinetic studies is described in **Scheme 2.3**. The dirhodium(II) carboxylate (**A**) coordinates to the aryldiazoacetate (**B**) in competition with styrene (**C**) coordination. This interaction would explain why the rate of the reaction had a reverse relationship to the concentration of styrene **C**. The rate determining step (rds) is the extrusion of nitrogen from the rhodium diazo complex (**D**) to form the rhodium carbene (**E**). Reaction of the rhodium carbene (**E**) with styrene (**C**) would then generate the final product (**F**) through a three-member transition state (**TS**) and recycle the catalyst (**A**).



Scheme 2.3 Proposed catalytic cycle for cyclopropanation of styrene

This mechanism is consistent with previous computational studies that have been carried out on the cyclopropanation reaction.²⁹ These studies showed that the carbene formation is the rate determining step and the barrier for the cyclopropanation step is very small. Dirhodium(II) tetracarboxylates are very stable complexes. They can be chromatographed and are stable in the

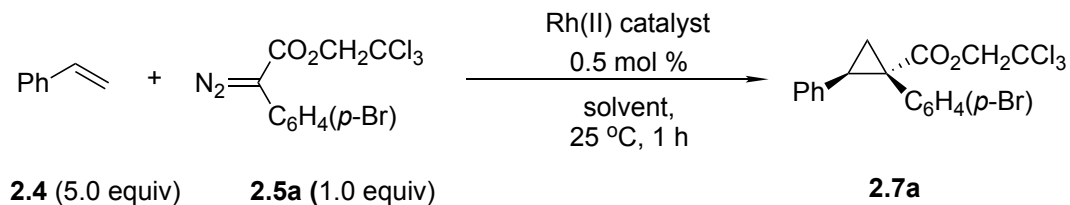
open-air for years. However, the rhodium carbene intermediate is likely to be unstable and needs to be trapped quickly to prevent its degradation. Consequently, an excess of styrene, despite its ability to decrease the overall reaction rate, is better for maintaining the high enantioselectivity under very low catalyst loadings. The X-ray structure of the catalyst always has molecules coordinating to the axial positions (water, ethyl acetate, etc). These axially coordinating ligands must be displaced for the catalytic reaction to proceed. However, our studies suggested that the kinetic barrier for the loss of the axial ligand must be insignificant since the reaction begins immediately after addition of the catalyst. However, dry conditions are required for reproducible reactions at extremely low catalyst loading, because excess water would likely interfere with the small amount of catalyst present.

Having established a deeper understanding of the catalytic system at 0.0025 mol % loading, we then explored how the catalyst can perform better at lower catalyst loadings. The reaction went to completion when it was conducted at 0.001 mol % catalyst loading, but the enantioselectivity decreased from 93% ee to 79% ee. The dropped enantioselectivity as one attempts to push the reaction to ultra-low catalyst loading is similar to the phenomenon observed in the earlier studies.⁴²

⁴³ Therefore, further studies were conducted to determine how to maintain the high level of enantioselectivity under low levels of catalyst loadings. The previous studies with $\text{Rh}_2(\text{S-biTISP})_2$ (**2.1**) reported that high enantioselectivity was maintained only when one equiv of methyl benzoate was added to the reaction mixture.⁴² It was reasoned that ester group of methyl benzoate weakly interacted with the carbene and increased the robustness and stability of the carbene. These results inspired us to explore whether the reaction would benefit from a solvent switch, with particular emphasis on solvents containing ester groups. Furthermore, higher boiling solvents were desired for further optimization, so that we would have the option to conduct the reactions with relatively

slow catalysts, such as $\text{Rh}_2(\text{S-}p\text{-Br-TPCP})_4$ (**2.6**), at higher temperatures to complete the reaction in a reasonable amount of time.

To quickly evaluate the effect of solvent on the enantioselectivity of the reaction, a series of reactions conditions were screened by Jack C. Sharland and Sam Mckinnon from our group using a robotic system. The small-scale reactions were conducted in the open-air without stirring. Control experiments showed that these reactions are effective to give reproducible diastereoselectivity and enantioselectivity. Each reaction was conducted for 1 h at rt with a catalyst loading of 0.5 mol %, which was sufficient for all of the catalysts to complete the cyclopropanation in CH_2Cl_2 . Despite the sensitivity of both the catalyst and the carbene to atmospheric water in C–H insertion reactions, the cyclopropanation was sufficiently favorable and robust that no diazo dimerization or O–H insertion byproducts were observed. The results of the high throughput screening were tabulated and transposed into a heat map to demonstrate the enantioselectivity of the reaction in each solvent for each of the catalyst tested (**Figure 2.6**).



Catalyst	EtOAc	CH ₂ Cl ₂	TFT	<i>i</i> -PrOAc	(MeO) ₂ CO	(EtO) ₂ CO	Pentane	 >99 % % ee 0 %
Rh ₂ (<i>R</i> -DOSP) ₄	78.1	63.1	77.9	83.9	67.1	66.7	77	
Rh ₂ (<i>R</i> -PTAD) ₄ *	90.9	56.6	56.9	53.5	40.5	47.1	58.9	
Rh ₂ (<i>R</i> -TCPTAD) ₄	90.7	71.5	72.9	66.7	68.1	90.7		
Rh ₂ (<i>R</i> -TPPTTL) ₄	95.6	88.5	90.5	91.3	91.9	87.9		
Rh ₂ (<i>S</i> - <i>o</i> -CITPCP) ₄	60.3	44.8	37.5	42.1	35.1	71.3		
Rh ₂ (<i>S</i> -2-Cl-5-Br-TPCP) ₄	39.7	72.2	70.9	77.9	63.5	70.2		
Rh ₂ (<i>S</i> - <i>p</i> -Br-TPCP) ₄ *	> 99	92	85.1	94.7	94.7	92.5	89.6	
Rh ₂ (<i>R</i> - <i>p</i> -Ph-TPCP) ₄	> 99	96.7	78.5	> 99	> 99	97.7		
Rh ₂ (<i>S</i> -tris(<i>p</i> - ^t BuC ₆ H ₄)TPCP) ₄ *	98.9	95.9	89.9	96.5	93.7	> 99		
Rh ₂ (<i>R</i> -3,5-di(<i>p</i> - ^t BuC ₆ H ₄)TPCP) ₄	87.1	73.3	91.3	82.7	61.8	89.5		

Figure 2.6 High throughput cyclopropanation in a variety of solvents and chiral dirhodium(II) catalysts. Color gradient proceeds from red to blue via white middle color which denotes middling % ee. The solvents tested were ethyl acetate (EtOAc), dichloromethane (CH₂Cl₂), trifluorotoluene (TFT), isopropyl acetate (*i*-PrOAc) dimethyl carbonate ((MeO)₂CO), and diethyl carbonate ((EtO)₂CO). Most of the tested catalysts were insoluble in pentane. *These catalysts provided the opposite enantiomer to the structure depicted in the representative reaction diagram above.

(Data from Jack C. Sharland and Sam Mckinnon)

According to **Figure 2.6**, several solvents emerged as promising candidates for further evaluation under high turnover conditions. Particularly interesting were ethyl acetate (EtOAc), isopropyl acetate (*i*-PrOAc), and dimethyl carbonate [(MeO)₂CO], which provided significant increases in enantioselectivity compared with dichloromethane (CH₂Cl₂). However, under these small-scale reaction conditions, the isolated yields were low and not truly representative. Before deciding which solvent would be best suited for low catalyst loading studies, larger laboratory-scale (100 mg) reactions using 0.5 mol % of catalyst were performed to both validate results obtained from the high throughput screen and determine the solvent impact on the yield (**Table 2.1**). Rh₂(*S*-*p*-Br-

enantioselectivity (94% ee) over CH₂Cl₂ (91% ee) (**Table 2.1, entry 1**). (MeO)₂CO is a high-boiling, environmentally benign solvent that has been widely used in organic synthesis as an alternative to potentially hazardous options like CH₂Cl₂ and diethyl ether (Et₂O).^{83, 84} Although previous studies reported that ester solvents like *i*-PrOAc can react with the rhodium carbene to form ylide,⁸⁵ we theorize that the solvent containing carbonates group like (MeO)₂CO would be more compatible due to the lack of labile α -hydrogens. Based on the above information, (MeO)₂CO was identified as the optimum solvent for lower catalyst loading exploration. Firstly, Rh₂(*S-p*-Br-TPCP)₄ (**2.6**)-catalyzed cyclopropanation of diazo compound **2.5a** with styrene **2.4** in (MeO)₂CO was examined at 0.0025 mol % catalyst loading (**Figure 2.8a**). The reaction rate at rt was much slower (incomplete conversion after 10 h) compared with the reaction in CH₂Cl₂ (2 h duration) (**Figure 2.3**). The slower reaction rate in (MeO)₂CO suggested an strong interaction between the solvent and the catalyst through coordination to either the carbene intermediate or the dirhodium(II) complex. We hypothesize that (MeO)₂CO may be weakly coordinating to the dirhodium(II) complex in a way similar to methyl benzoate as posited in our previous study on Rh₂(*S*-biTISP)₂ (**2.1**).⁴² Even so, the enantioselectivity of the reaction was greatly improved (97% ee in (MeO)₂CO compared with 93% ee in CH₂Cl₂). Control experiments revealed that at 60 °C, diazo compound **2.5a** underwent only about 3% decomposition over 10 h in (MeO)₂CO in the absence of the catalyst (**Figure 2.7**). Therefore, higher reaction temperature was applied to accelerate the reaction with lower catalyst loading.

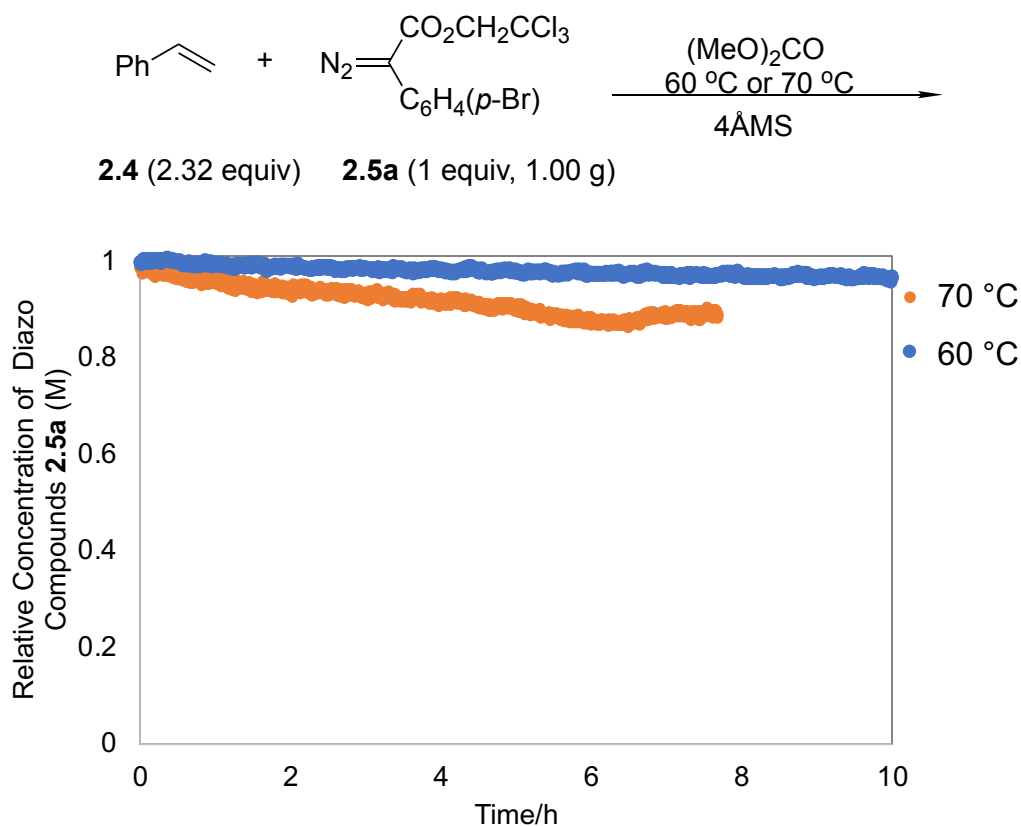


Figure 2.7 The decomposition curve of diazo compound **2.5a** at 70 °C and 60 °C in (MeO)₂CO without catalyst.

At 0.0025 mol % catalyst loading the cyclopropanation was finished within 6 h at 40 °C, and 2 h at 60 °C. More promisingly, the enantioselectivity of the reactions was successfully remained at 96% ee (**Figure 2.8a**). Therefore, exploration of lower catalyst loading was conducted as shown in **Figure 2.8b**. When the catalyst loading was decreased to 0.001 mol %, the enantioselectivity of the reaction maintained 94% ee. The reaction also went to completion with 0.00025 mol %, but the enantioselectivity dropped slightly to 90% ee. Furthermore, the reaction at 0.0001 mol % was incomplete even after 24 h and the enantioselectivity dropped further to 81% ee.

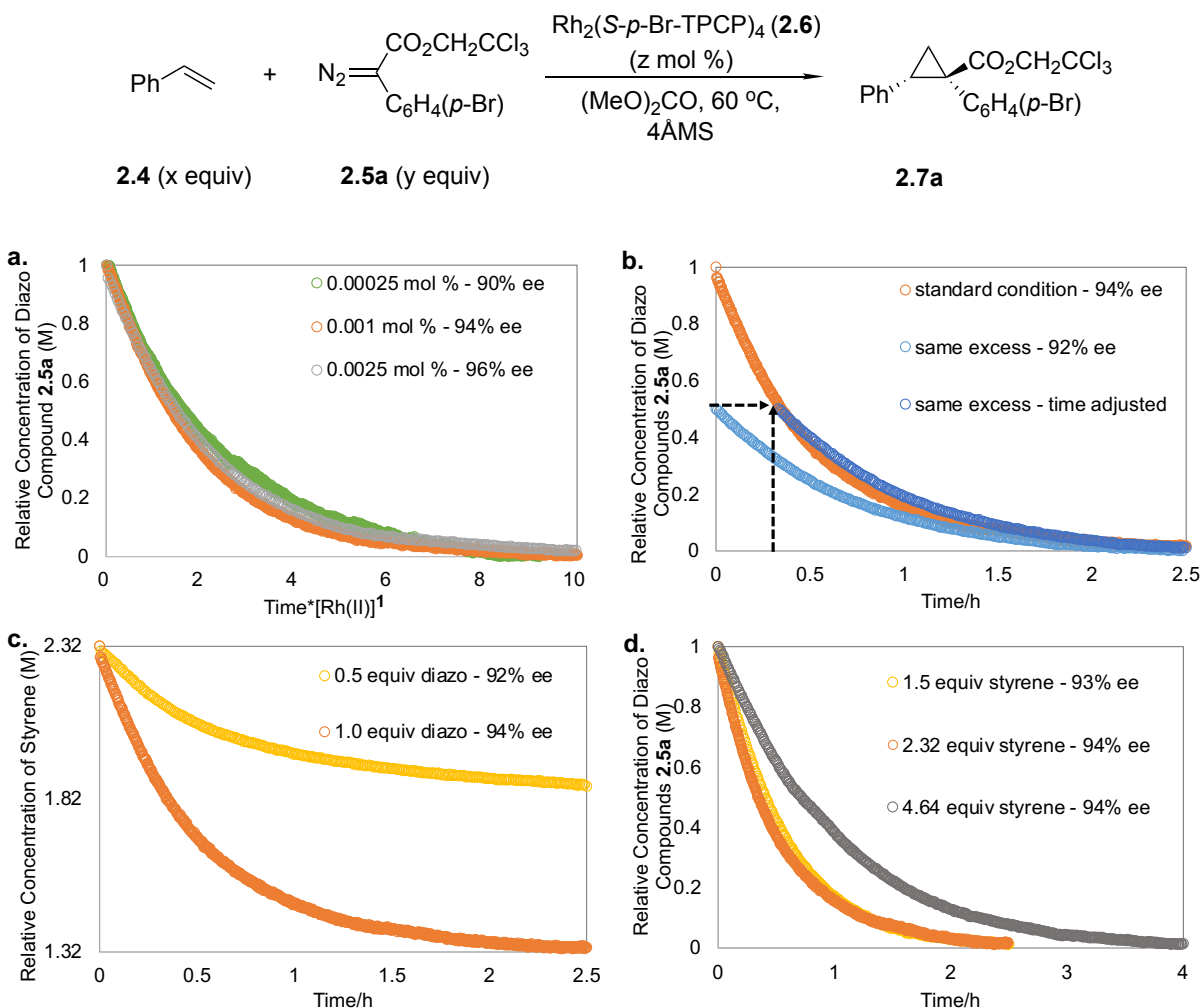


Figure 2.9 Kinetic profiles of RPKA study for the cyclopropanation with $\text{Rh}_2(\text{S-}i\text{p-Br-TPCP})_4$ (**2.6**) in $(\text{MeO})_2\text{CO}$ at 60°C **a.** The Variable Time Normalization Analysis determined the catalyst was 1st order in the reaction **b.** Time-adjusted kinetic profile of same excess reaction showed the catalyst was robust in the reaction **c.** Different excess reaction for diazo compound **2.5a** showed diazo compound was positive order in the reaction. **d.** Different excess reaction for styrene **2.4** showed styrene was negative order in the reaction.

To further investigate the robustness of the catalyst, we conducted a multiple addition experiment to practically demonstrate a higher turnover number (**Figure 2.10**). The new batches of diazo compound **2.5a** were recurrently added to the reaction solution upon the consumption of the prior batch diazo compound **2.5a**. In total, seven additions were completed in 20 h. Only a minor decrease of catalyst performance occurred, suggested by the observation of a slight increased

maximum diazo compound signal and a longer completion time of each batch. $\text{Rh}_2(\text{S-}p\text{-Br-TPCP})_4$ (**2.6**) remained robust to catalyze all seven additions and consistently generated cyclopropane **2.7a** with 90% ee.

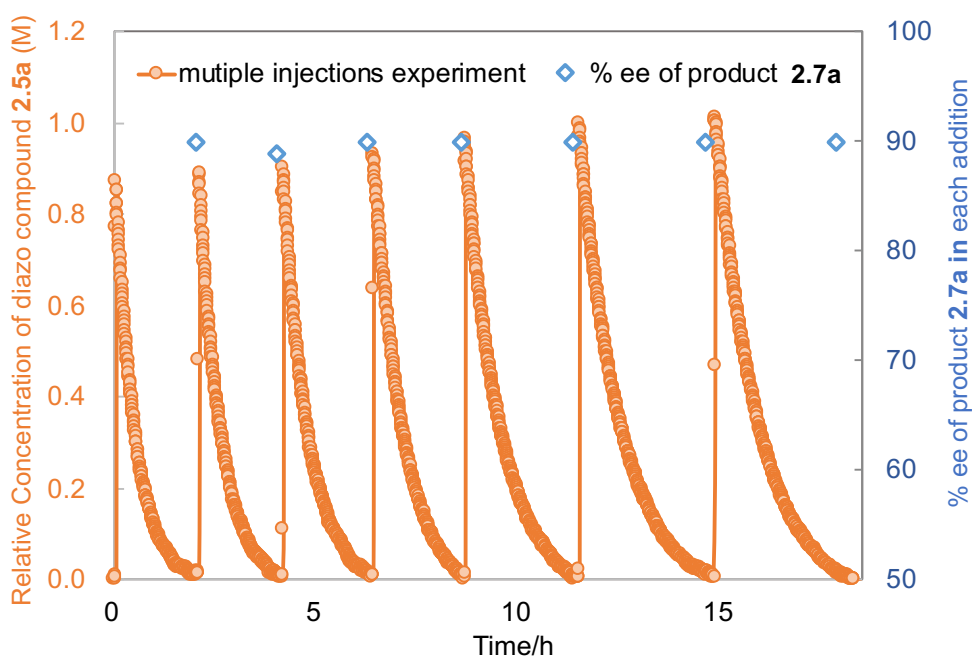
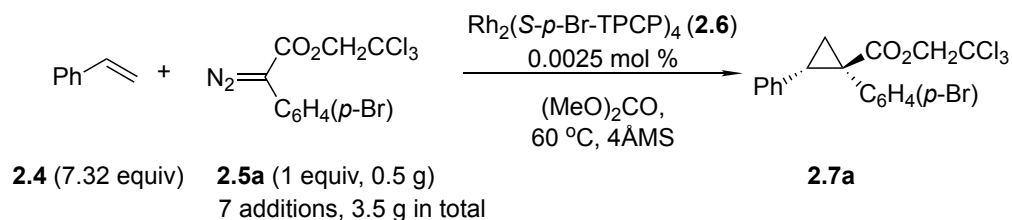


Figure 2.10 Kinetic profiles of multiple addition experiment of the benchmark cyclopropanation. Seven successive additions of diazo compound **2.5a** (1 equiv) were added into a solution of styrene **2.4** (7.32 equiv) and $\text{Rh}_2(\text{S-}p\text{-Br-TPCP})_4$ (**2.6**) (0.0025 mol %) in $(\text{MeO})_2\text{CO}$ at 60 °C.

The scope of the low catalyst loading cyclopropanation was then examined with a range of aryldiazoacetates. Unfortunately, while the $\text{Rh}_2(\text{S-}p\text{-Br-TPCP})_4$ (**2.6**)/ $(\text{MeO})_2\text{CO}$ system gave high enantioselectivity for some substrates, several substrates resulted in enantioselectivities well below 90% ee. According to the high throughput screen (**Figure 2.6**), $\text{Rh}_2(\text{R-}p\text{-Ph-TPCP})_4$ (**2.8**) was identified as another effective catalyst in $(\text{MeO})_2\text{CO}$ and gave very high asymmetric induction in

the cyclopropanation. The performance of $\text{Rh}_2(R\text{-}p\text{-Ph-TPCP})_4$ (**2.8**) was examined at low catalyst loading in $(\text{MeO})_2\text{CO}$. The kinetic profiles of $\text{Rh}_2(R\text{-}p\text{-Ph-TPCP})_4$ (**2.8**) were identical to $\text{Rh}_2(S\text{-}p\text{-Br-TPCP})_4$ (**2.6**), but $\text{Rh}_2(R\text{-}p\text{-Ph-TPCP})_4$ (**2.8**) routinely gave higher levels of enantioselectivity. Therefore, the full scope exploration of the asymmetric cyclopropanation at low catalyst loading applied $\text{Rh}_2(R\text{-}p\text{-Ph-TPCP})_4$ (**2.8**) as the optimum catalyst (**Figure 2.11**).

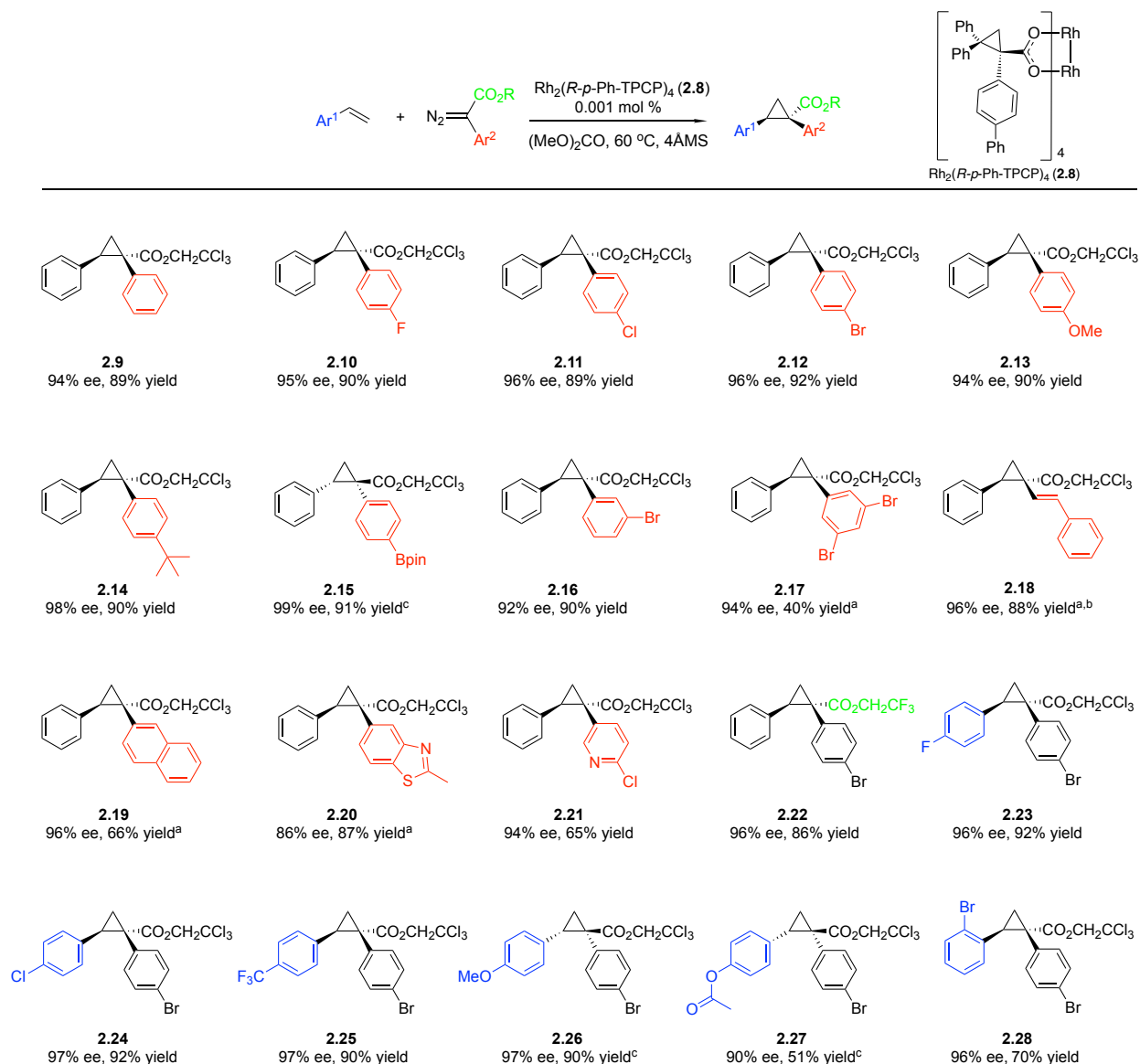
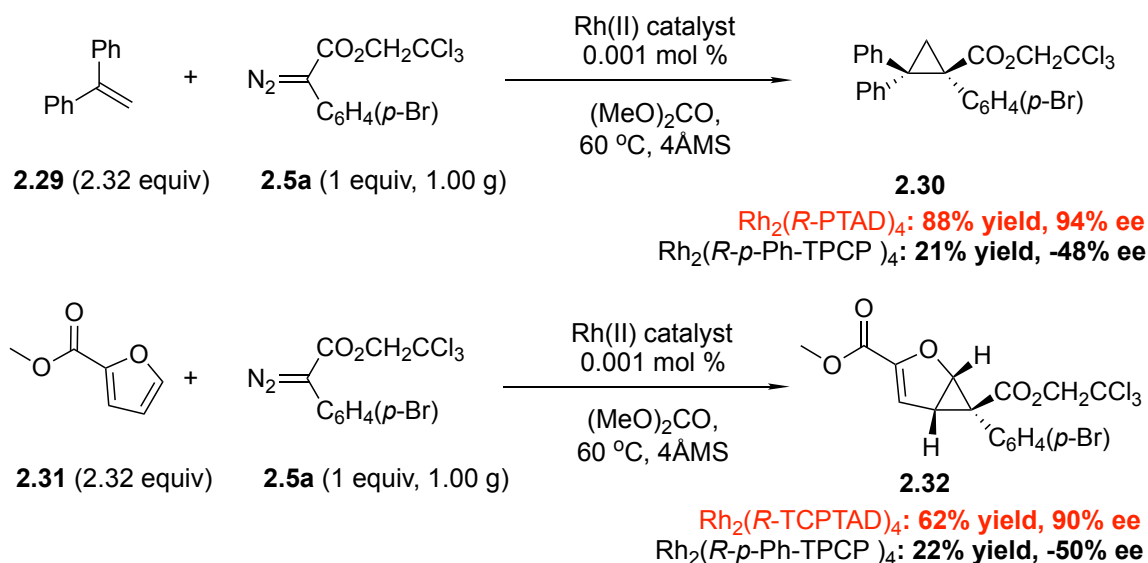


Figure 2.11 Scopes of asymmetric cyclopropanation with 0.001 mol % $\text{Rh}_2(R\text{-}p\text{-Ph-TPCP})_4$ (**2.8**) at 60 °C in $(\text{MeO})_2\text{CO}$. Compounds **2.9-2.22** illustrated the scopes of aryldiazoacetates. Compounds **2.23-2.28** illustrated the scopes of styrene derivatives. ^aReaction was conducted at

0.003 mol % catalyst loading to ensure reaction proceeds to completion. ^bReaction was conducted at 25 °C to avoid thermal rearrangement of the styryldiazoacetate to a pyrazole. ^cReaction was conducted with Rh₂(*S-p*-Ph-TPCP)₄.

The above results showed high enantioselectivity and yield were preserved across a broad scope of aryldiazoacetates and styrene derivatives. The method also successfully accommodated intriguing examples including boronate derivative **2.15**, the styryl derivative **2.18**, and the heterocycles (**2.20** and **2.21**). In the cases of **2.17**, **2.18**, **2.19**, and **2.20**, the reactions were incomplete in 12 h, and the conditions were revised using 0.003 mol % catalysts loading to increase the efficiency.

Extension of the Rh₂(*R-p*-Ph-TPCP)₄ (**2.8**)-catalyzed cyclopropanation to certain more rigid substrates was not as successful (**Scheme 2.4**). The cyclopropanation of 1,1-diphenylethylene (**2.29**), a key substrate for the enantioselective synthesis of the third generation (TPCP) catalyst ligands, did not perform very well and the cyclopropane **2.30** was obtained in only 21% yield and 48% ee. Diminished results with Rh₂(*R-p*-Ph-TPCP)₄ (**2.8**) also obtained in the cyclopropanation with methyl-2-furoate **2.31**, and compound **2.32** formed in 22% yield, 50% ee. To obtain better reactivity and selectivity for the above cases, other dirhodium(II) catalysts were tested to better match the substrates.⁸⁶ Rh₂(*R*-PTAD)₄ (**2.3**) was revealed as the optimum catalyst to furnish the cyclopropane **2.30** in 88% yield and 94% ee at 0.001 mol % catalyst loading. Also, Rh₂(*R*-TCPTAD)₄ enhanced the enantioselectivity of the cyclopropane **2.32** to 90% ee with 62% yield at 0.001 mol % catalyst loading.

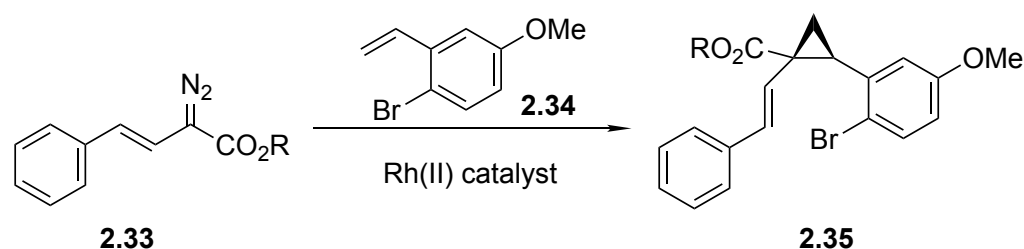


Scheme 2.4 Alternative dirhodium(II) catalysts applied to more sterically crowded substrates

The requirement for $\text{Rh}_2(\text{R-PTAD})_4$ (**2.3**) and $\text{Rh}_2(\text{R-TCPTAD})_4$ to achieve higher enantioselectivity of compound **2.30** and **2.32** is presumably because these catalysts are more sterically open and able to accommodate sterically crowded substrates like 1,1-diphenylethylene (**2.29**) and methyl-2-furoate (**2.31**). This trend is clearly visible in C–H insertion reactions as introduced in Chapter 1. The third generation catalysts like $\text{Rh}_2(\text{R-p-Ph-TPCP})_4$ (**2.8**) are highly selective for the most accessible C–H bonds due to their high steric demand. Complementarily, $\text{Rh}_2(\text{R-TCPTAD})_4$ enabled the more hindered C–H bonds insertion and was well established as a highly selective tertiary-C–H functionalization catalyst.

The cyclopropanation reaction is an important transformation and has been applied in drug discovery. The reaction is effective at constructing three membered ring motifs present in numerous drug molecules. Therefore, to demonstrate the utility of the new method in a practical application, we decided to optimize the previously reported synthesis of the cyclopropane **2.35** (**Scheme 2.5**). The compound **2.35a** was originally reported by BMS as a key intermediate in their

kilogram scale synthesis of the Hepatitis C drug, Beclabuvir (**2.36**).⁸⁷ Their synthesis was conducted via a $\text{Rh}_2(\text{R-DOSP})_4$ (**2.2**)-catalyzed cyclopropanation of methyl styryldiazoacetate **2.33a** with the styrene **2.34**. In the procedure, 0.2 mol % catalyst $\text{Rh}_2(\text{R-DOSP})_4$ (**2.2**) was used to afford cyclopropane **2.35a** in 94% yield and 83% ee. Compared with above industrial method, the reaction here used trichloroethyl styryldiazoacetate **2.33b** as carbene precursor and $(\text{MeO})_2\text{CO}$ as solvent in the presence of 0.001 mol % $\text{Rh}_2(\text{R-}p\text{-Ph-TPCP})_4$ (**2.8**) to generate the cyclopropane **2.35b** in 72% yield and 96% ee. The optimized reaction therefore enabled much higher asymmetric induction and was conducted using only 1/200th the amount of the dirhodium(II) catalyst as the industrial route.

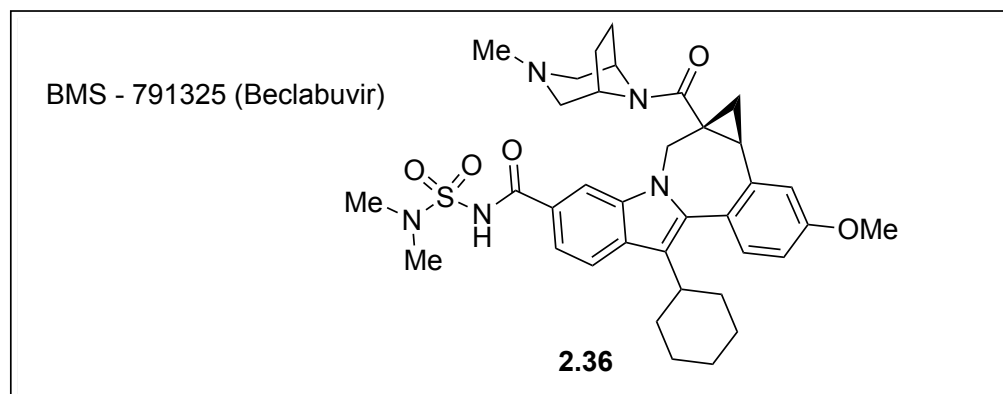


Industrial process:

a: R = CH₃
 $\text{Rh}_2(\text{S-DOSP})_4$: 0.2 mol %
 Heptane, 15~25 °C
 94% yield, 83% ee.

Optimized process:

b: R = CH₂CCl₃
 $\text{Rh}_2(\text{S-}p\text{-Ph-TPCP})_4$: 0.001 mol %
 $(\text{MeO})_2\text{CO}$, 25 °C, 4ÅMS
 72% yield, 96% ee



Scheme 2.5 Asymmetric cyclopropanation in a key step in the synthesis of Beclabuvir **2.36**

2.3 Conclusions

Over the course of this comprehensive study, the effect of the ligand on the performance of dirhodium(II) catalysts was investigated under *in-situ* monitoring by ReactIR. The kinetic profiles led us to choose $\text{Rh}_2(\text{S-}p\text{-Br-TPCP})_4$ (**2.6**), a highly enantioselective catalyst, for the optimization of reactions conducted at lower catalyst loading optimization. Detailed kinetic investigation using the RPKA method determined the rate law of the cyclopropanation reaction and revealed the catalyst is robust through at least the first 20,000 TONs. However, the catalyst failed to maintain high enantioselectivity in CH_2Cl_2 at over than 40,000 TONs. To achieve higher TONs, high throughput studies were performed and identified $(\text{MeO})_2\text{CO}$ as a superior solvent for achieving 100,000 catalyst TONs and conserving the high enantioselectivity. During these studies, the related catalyst $\text{Rh}_2(\text{R-}p\text{-Ph-TPCP})_4$ (**2.8**) was found to give reliably higher enantioselectivity than $\text{Rh}_2(\text{S-}p\text{-Br-TPCP})_4$ (**2.6**) across a broader range of cyclopropanation substrates. The study culminated in the optimization of a key step in the synthesis of the Hepatitis C drug Beclabuvir (**2.36**) at 200-fold lower catalyst loading with higher enantioselectivity compared with the published procedure. The kinetic analysis and condition optimization in this study resulted in a robust method to routinely apply 0.001 mol% catalyst loading in the cyclopropanation and maintain the high enantioselectivity. The results will inspire the high TONs method development for other donor/acceptor carbene reactions, such as C–H functionalization, tandem cyclopropanation/Cope rearrangement, and ylide-induced cascade reactions.

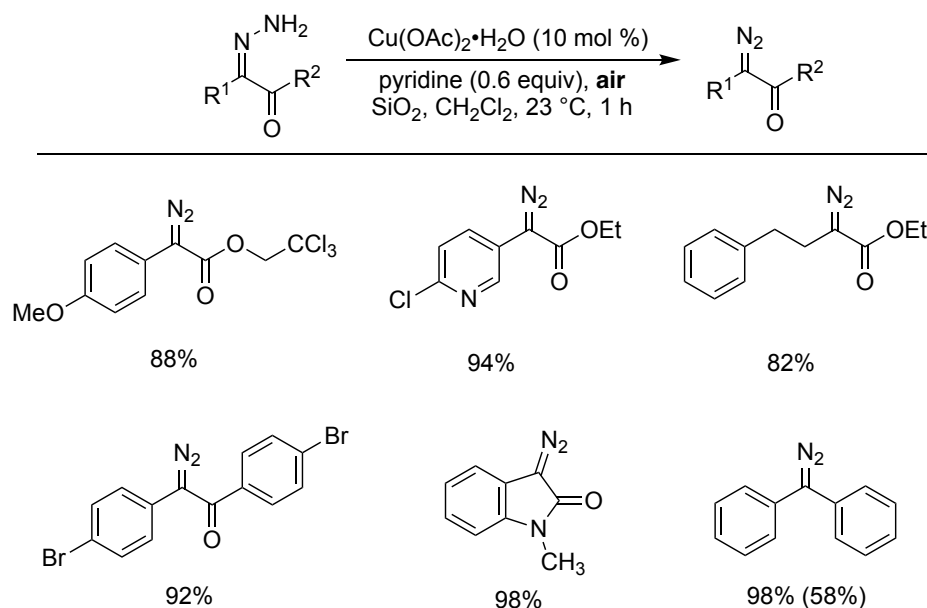
Chapter 3. Copper(II)-catalyzed Aerobic Oxidation of Hydrazones to Diazo Compounds under Flow Conditions and Their Application in Carbene Reactions.

3.1 Introduction

Diazo compounds are versatile reagents capable of initiating a wide variety of synthetically useful reactions.⁸⁸⁻⁹¹ Particularly important among these are metal-catalyzed carbene reactions. The diazo compound is used as the precursor to metal carbene intermediates in many enantioselective reactions such as cyclopropanation,^{66, 92, 93} cyclopropanation,^{90, 94, 95} C–H functionalization,^{55, 96-98} and ylide rearrangement.⁹⁹⁻¹⁰¹ However, diazo compounds are high energy compounds and potentially dangerous if the release of nitrogen from them is not controlled. The high reactivity feature of diazo compounds is advantageous because carbene generation can be achieved under mild conditions, but it also raises safety concerns.⁶⁷ The possibility of explosion and decomposition during the synthesis and storage of diazo compounds is a concern that needs to be addressed, especially if large scale reactions are contemplated. Most commonly, the reactions are conducted on relatively small scale in a research laboratory setting, although a few significant industrial scale processes involving diazo compound are known.^{87, 102-106}

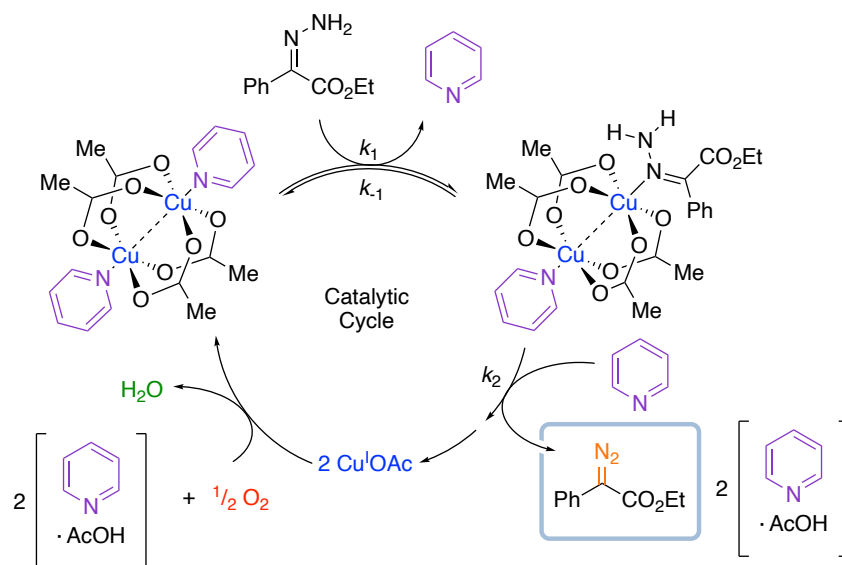
To overcome the above limitations, the examination of continuous-flow techniques for diazo synthesis has generated great interest.¹⁰⁷⁻¹¹⁹ Flow chemistry can enable the industrial scale synthesis and usage of diazo compounds without having large amounts of diazo compounds present at any one time. Traditional diazo synthesis methods applied in the flow process often require metal-based oxidants, which are toxic and/or expensive. Moreover, the established flow procedure routinely needed additional in-line purification processes to remove byproducts that may obstruct the downstream reaction.^{102, 105, 117, 120-128} Herein, a mild method to access diazo compound is desired for the further application in flow process. Through a collaboration with the

Stahl group, a new procedure to synthesize diazo compounds via hydrazone oxidation has been established.¹²⁹ The project was led by Dr. Wenbin Liu from the Davies group. $\text{Cu}(\text{OAc})_2\cdot\text{H}_2\text{O}$ and pyridine are revealed to be highly effective for the catalytic oxidation of hydrazones and generate the diazo compounds with high efficiency (**Scheme 3.1**).



Scheme 3.1 Reaction conditions and representative scope of the copper(II)-catalyzed oxidation of hydrazones to diazo compounds using oxygen as terminal oxidant (*Data collected with Dr. Wenbin Liu*)

The Stahl group conducted the kinetic investigation and proposed that an electron-rich pyridine is beneficial for the reaction by serving as the Brønsted base and helping to solubilize the $\text{Cu}(\text{OAc})_2\cdot\text{H}_2\text{O}$. 4-dimethylaminopyridine (DMAP) was determined to be the most practical additive.¹²⁹ The reactions happened under mild conditions using oxygen from air as the terminal oxidant. The catalyst $\text{Cu}(\text{OAc})_2\cdot\text{H}_2\text{O}$ is cheap and commercially available. Moreover, the reaction rate is fast with the pyridine additive, and the only byproduct is H_2O . Taking into consideration all the synthetic advantages described above, the system seemed promising to extend into an effective flow procedure for the safe synthesis of diazo compounds.



Scheme 3.2 Proposed mechanism of copper(II)-catalyzed oxidation of hydrazones to diazo compounds using oxygen as terminal oxidant¹²⁹

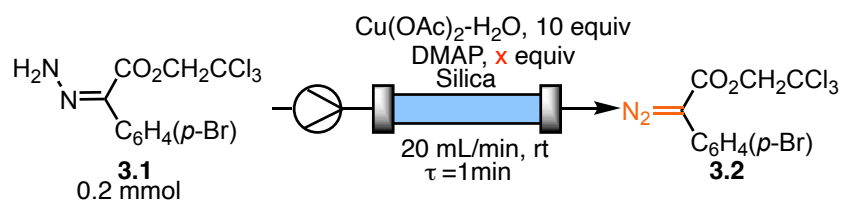
As introduced in Chapter 1, aryldiazoacetates are the most desired diazo compounds for many carbene reactions. When exposed to a dirhodium(II) catalyst, aryldiazoacetates can generate donor/acceptor carbenes, which have attenuated reactivity and better selectivity due to the presence of the aryl group acting as a donor group.^{55, 74} The study in this chapter concentrated on the aryldiazoacetate synthesis in a bench-top flow procedure. The starting hydrazone was first oxidized to the aryldiazoacetate using Cu(OAc)₂-H₂O/DMAP in a mixed silica column, and the diazo compound formed was dripped directly into the downstream flask for the dirhodium(II)-catalyzed cyclopropanation without any purification. Unlike the industrial-scale application, the cost of Cu(OAc)₂-H₂O was not a major concern for the lab scale procedure. Instead, it was more important to ensure the completion of the hydrazone conversion because any hydrazone residue eluted into the downstream dirhodium(II)-catalyzed carbene reaction would likely poison the reaction. Therefore, an excess of Cu(OAc)₂-H₂O was applied to guarantee the hydrazone conversion and eliminate the concern about catalyst regeneration. After optimizing upstream

column for the in-flow oxidation and the downstream cyclopropanation reaction conditions, we have developed a tandem procedure to convert hydrazones to cyclopropane derivatives with excellent overall yield and enantioselectivity.

3.2 Results and Discussions

The first stage of this study was to determine suitable flow conditions to guarantee full conversion of hydrazones **3.1** to diazo compounds **3.2** using a short residence time (τ). A stoichiometric amount of $\text{Cu}(\text{OAc})_2\text{-H}_2\text{O}$ catalyst and DMAP were mixed with silica to pack a column.⁴⁹ Hydrazone **3.1** was then added on the top of the packed column and eluted throughout to generate the corresponding diazo compound **3.2** in flow. As shown in **Table 3.1**, to minimize the eluted DMAP's hazardous effect to the downstream carbene reaction, 5 equiv of DMAP mixed with 10 equivalents of $\text{Cu}(\text{OAc})_2\text{-H}_2\text{O}$ were initially packed in the column (**Table 3.1**, **entries 1 and 2**).

Table 3.1 Optimization of aryldiazoacetate **3.2** synthesis in flow



entry	eluent	x	1st*	2nd*	3rd*
1	DCM	5	37%	33%	36% ^a
2	DMAP/DCM ^b	5	66%	47%	57% ^a
3	DMAP/DCM ^b	10	>99%	>99%	>99%

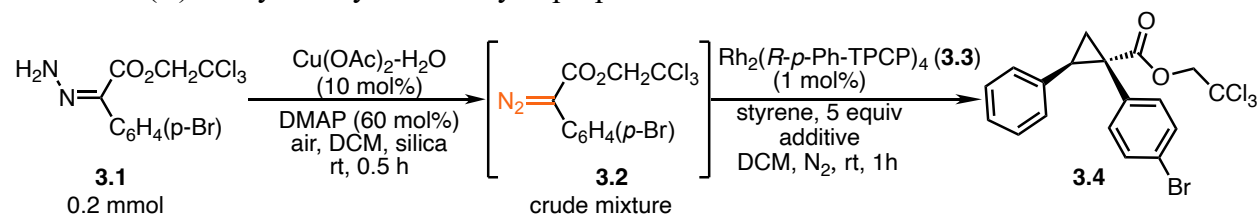
*Recycled the column for 3 times, conversion of hydrazone **3.1** calculated from crude ¹H-NMR.

^aflush the column with air before loading the 3rd batch hydrazone **3.1** to improve the column efficiency. ^beluent concentration is 0.06 mol/L DMAP in DCM.

However, the hydrazone **3.1** was not fully converted, although flushing the column with air after the second run and including DMAP in the eluent (0.06 M) increased the extent of conversion. According to the mechanism proposed in **Scheme 3.2**, we hypothesized that without enough base to entirely activate the copper(II) catalyst to accelerate the oxidation reaction, the column efficiency was insufficient with the limited residence time (1 min).¹²⁹ We therefore packed 10 equiv of DMAP with Cu(OAc)₂-H₂O in the column and used DMAP/DCM as the eluent to keep the Cu(OAc)₂-H₂O saturated with base coordination. The new conditions (**Table 3.1, entry 3**) gave full hydrazone **3.1** conversion in only 1 min and the efficiency was maintained for 3 batches without any further refreshment operation.

The next step was to combine the upstream hydrazone oxidation and downstream cyclopropanation reaction. In this stage, the compatibility issue was the major challenge to overcome. We first explored the batch-to-batch procedure to investigate the feasibility of the tandem process. The hydrazone **3.1** was converted to the diazo compound **3.2** with a catalytic amount of Cu(OAc)₂-H₂O (10 mol%) and DMAP (60 mol%) in a flask open to the air, and the resulting diazo compound **3.2** was directly injected into the other flask containing styrene, Rh₂(*R*-*p*-Ph-TPCP)₄ **3.3**, and 4Å MS in DCM in order to conduct the cyclopropanation reaction. However, as shown in **Table 3.2, entry 1**, the cyclopropanation product **3.4** was obtained in only 18% yield and 77% ee, while most of the diazo compound **3.2** remained unreacted.

Table 3.2 Batch-batch tandem reaction of copper(II) catalyzed hydrazone oxidation followed by dirhodium(II) catalyzed asymmetric cyclopropanation



entry	condition variation	additive	yield of 3.4 (%)	ee of 3.4 (%)
1	-	4Å MS	18	77
2	-	HFIP	67	98
3	No silica ^a	HFIP	64	97
4	Dropwise addition ^b	HFIP	72	97
5	Silica plug ^c	HFIP	57	97

^a Copper(II) catalyst and DMAP in the oxidation reaction vial without silica. ^b Crude diazo compound **3.2** mixture added to the cyclopropanation reactor, flow rate 0.05 mL/min. ^c The crude mixture was filter through a silica plug to get rid of most copper(II) catalyst and silica after oxidation step.

We anticipated that DMAP from the hydrazone oxidation step would suppressed the performance of the $\text{Rh}_2(\text{R-}p\text{-Ph-TPCP})_4$ **3.3** catalyst and the carbene intermediate in the cyclopropanation step, leading to the low reactivity and selectivity. HFIP has been recently revealed to be a useful additive for maintaining the performance of the cyclopropanation reactions in the presence of nucleophilic poisons.¹³⁰ The tandem procedure was then tested in the presence of HFIP as an additive. Significantly, the reaction yield of the product **3.4** increased to 67% and the enantioselectivity improved to 98% ee (**Table 3.2, entry 2**). Meanwhile, the control experiment with no silica in the oxidation step (**Table 3.2, entry 3**) led to an increased ratio of O–H insertion byproduct according to the crude ¹H-NMR. This result suggested that the silica likely benefited the downstream reaction by trapping the water byproduct produced from hydrazone oxidation. We further optimized the procedure by adding the diazo compound **3.2** dropwise and under these conditions the reaction yield increased to 72% (**Table 3.2, entry 4**).

According to the results shown in **Table 3.2**, HFIP is important for the success of the whole setup. To probe the role of HFIP in this tandem procedure, a kinetic investigation was performed. As shown in **Figure 3.1**, the concentration of the diazo compound **3.2** in the cyclopropanation reaction was *in-situ* monitored by ReactIR. First, the diazo compound **3.2**, styrene and DMAP were mixed in DCM. $\text{Rh}_2(\text{R-}p\text{-Ph-TPCP})_4$ **3.3** catalyst (1 mol %) was then injected in 0.1 mL DCM after 2 min. However, with DMAP in the system, the cyclopropanation reaction was inhibited with no further progress. HFIP (10 equiv) was subsequently injected, and the reaction was reinitiated to finally deliver cyclopropanation product **3.4** in 93% yield and 98% ee.

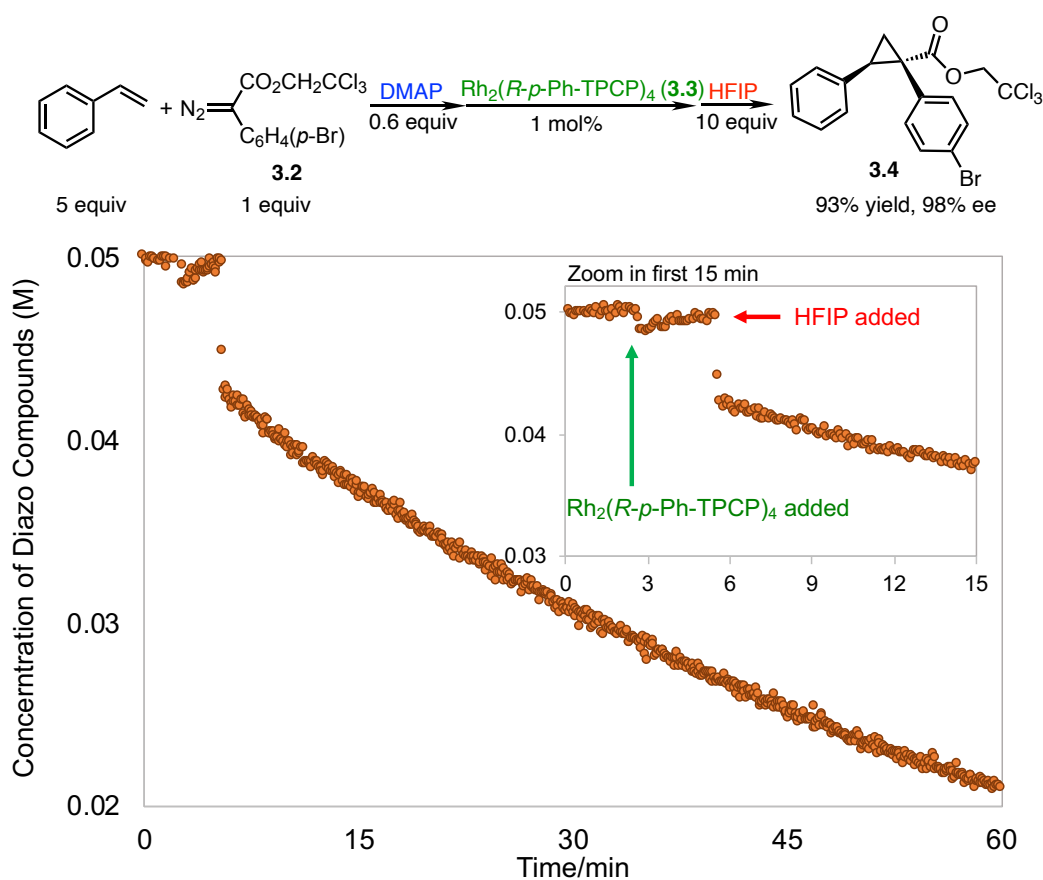


Figure 3.1 Kinetic investigation of the effect of DMAP and HFIP on $\text{Rh}_2(\text{R-}p\text{-Ph-TPCP})_4$ (**3.3**) catalyzed asymmetric cyclopropanation

We noted the diazo compound **3.2** concentration signal dropped in **Figure 3.1** as HFIP was injected, which was caused by dilution upon addition of HFIP (0.63 mL to the 12 mL reaction solution). The overall kinetic profile suggested that DMAP led to catalyst deactivation, likely by coordinating to the dirhodium(II) catalyst or the carbene intermediate.^{20, 131} HFIP was proposed to act as a hydrogen bond donor to interact with DMAP and suppress its deleterious coordination effect. The ¹H-NMR spectrum also showed that the HFIP and diazo compound **3.2** influenced each other's peak shifts (**Figure 3.2**) in CDCl₃ solution, which suggested that the reaction may also be affected by the hydrogen bonds between the diazo compound **3.2** and HFIP.^{132, 133}

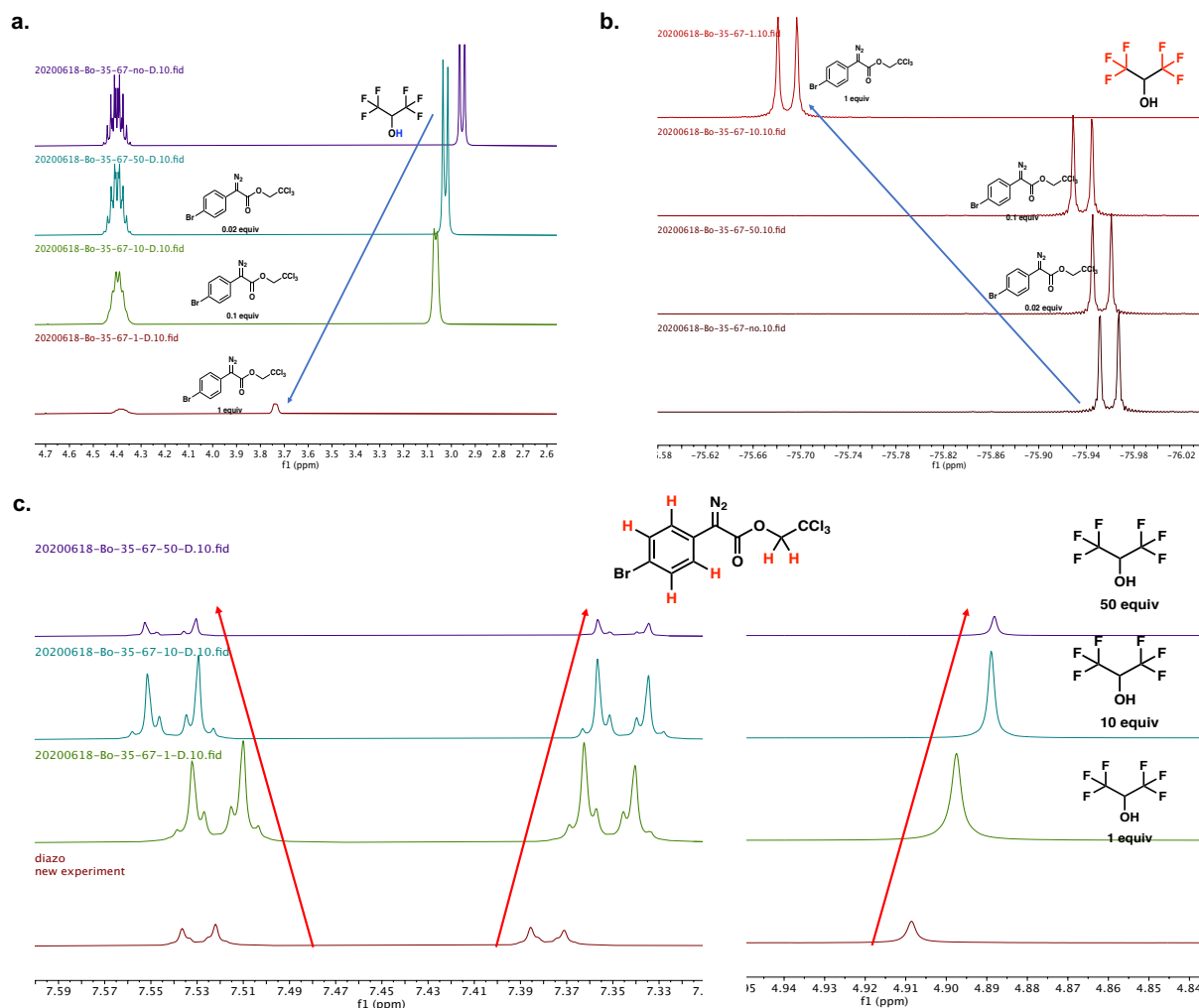
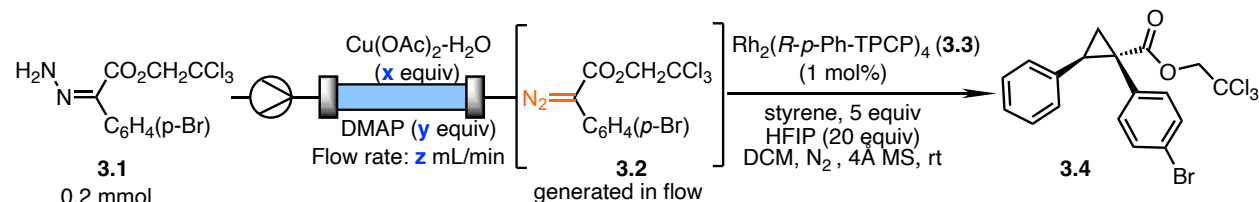


Figure 3.2 HFIP and diazo compound **3.2** influenced each other's peak shifts on ¹H-NMR **a**. The hydroxyl hydrogen peak of HFIP shifted on ¹H-NMR (400 HZ, CDCl₃ as solvent) from 2.97 ppm (no diazo compound **3.2** added) to 3.76 ppm (1 equiv diazo compound **3.2** added). **b**. The trifluoromethyl group peak of HFIP shifted on ¹⁹F-NMR (400 HZ, CDCl₃ as solvent) from -75.96 ppm (no diazo compound **3.2** added) to -75.68 ppm (1 equiv diazo compound **3.2** added). **c**. ¹H-NMR peak of diazo compound **3.2** shifted with HFIP added (400 HZ, CDCl₃ as solvent) .

After determining the key components needed in the tandem procedure, the benchtop flow system was set up to generate diazo compound **3.2** in the copper(II)-DMAP-silica mixed column, followed by its direct utilization in the downstream dirhodium(II)-catalyzed cyclopropanation reaction. To maximize the efficiency of the procedure, the column parameters were optimized as shown in **Table 3.3**.

Table 3.3 Optimization of flow-batch reaction conditions

entry	x	y	z	eluent	yield of 3.4 (%)	ee of 3.4 (%)
1	10	22	20	DCM	52	43
2	10	22	5	DCM	79	55
3	10	10	2	DCM	73	93
4	10	5	2	DCM	31	96
5	10	5	2	DMAP/DCM	43	90
6	10	10	2	DMAP/DCM	76	92
7	10	10	1	DMAP/DCM	75	97
8	10	5	0.5	DMAP/DCM	30	95
9	5	10	1	DMAP/DCM	73	97
10	2.5	10	1	DMAP/DCM	46	96
11 ^a	10	10	1	DMAP/DCM	21	90
12 ^b	10	10	1	DMAP/DCM	31	96

^aThe cyclopropanation reaction was performed with 0.1 mol% $\text{Rh}_2(R\text{-}p\text{-Ph-TPCP})_4$ (**3.3**) ^bThe cyclopropanation reaction was performed with 5 equiv HFIP.

We first applied excess copper(II)/DMAP (10 equiv of $\text{Cu}(\text{OAc})_2\cdot\text{H}_2\text{O}$, 22 equiv of DMAP), and 20 mL/min flow rate to ensure full hydrazone **3.1** conversion. The fast flow rate aimed to minimize the residence time and avoid excess eluent injection into the downstream reaction flask (**Table 3.3, entry 1**). Although the column fully converted the hydrazone **3.1** to diazo compound **3.2** according to $^1\text{H-NMR}$, the reactivity and selectivity in the cyclopropanation step were limited (52% yield, 43% ee). The disappointing results are likely caused by the overwhelming amount of DMAP eluted from the upstream column. Therefore, the flow rate, equivalents of DMAP, and the eluent were screened to obtain higher efficiency for both the upstream hydrazone oxidation and the downstream cyclopropanation. As showed in **Table 3.3, entry 7**, using 10 equiv of $\text{Cu}(\text{OAc})_2\cdot\text{H}_2\text{O}$

H₂O and DMAP, 1 mL/min flow rate, and DMAP/DCM as eluent generated the diazo compound **3.2** effectively and delivered the cyclopropanation product **3.4** in 75% yield and 97% ee. The promising result is an indication that DMAP and the byproduct, water, had been effectively trapped in the silica column. Additionally, HFIP as well as 4Å MS in the downstream flask helped to minimize the hazardous effects from the upstream reagents. The column system also enabled dropwise addition of the diazo compound **3.2** to decrease its possibility for dimerization in the downstream reaction. Subsequently, we investigated the reaction scope by applying this optimized benchtop flow-batch procedure to a range of substrates. To obtain more comprehensive evaluation, the tandem batch-batch catalytic condition was also tested on each example as shown in **Figure 3.3**.

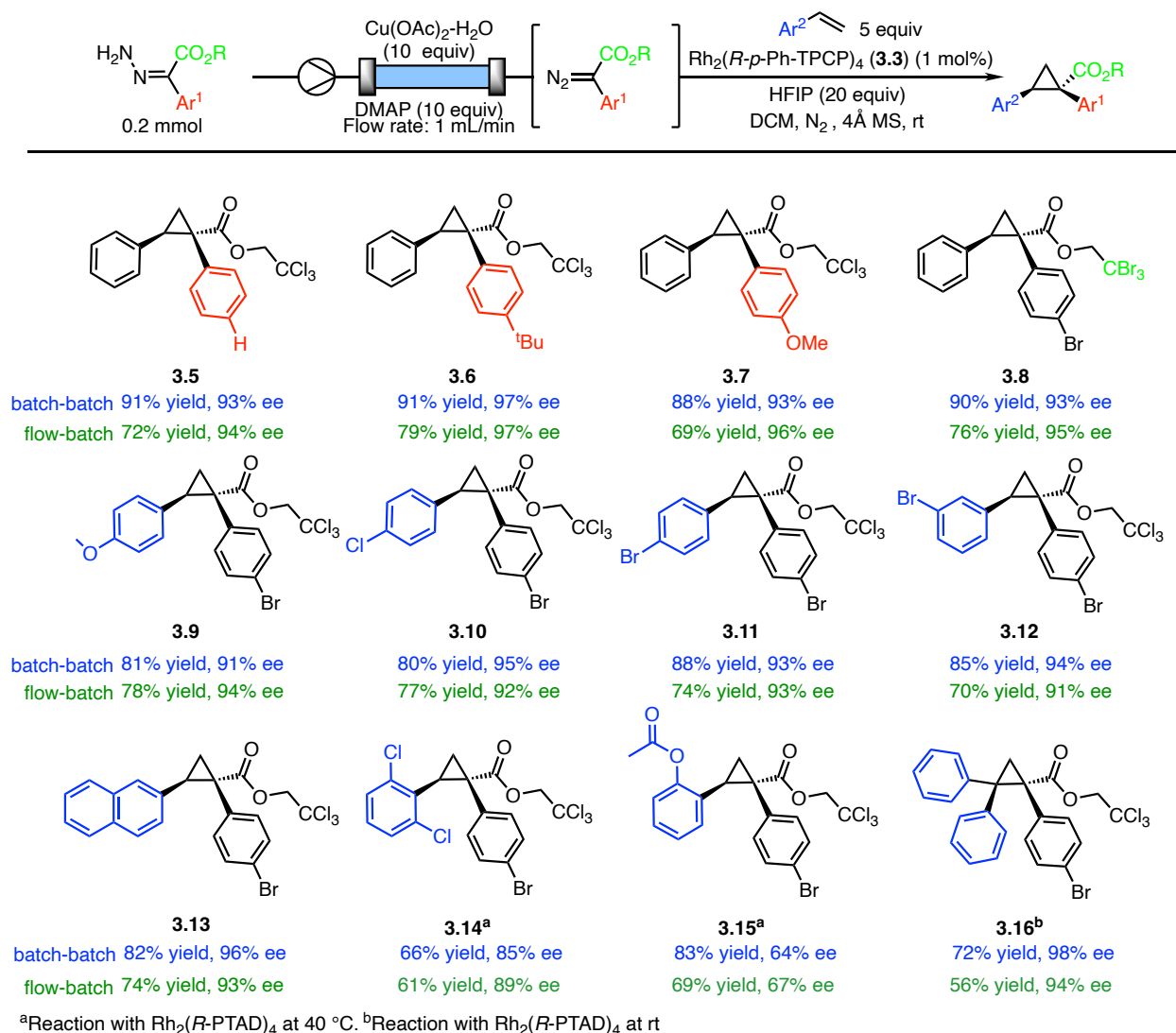


Figure 3.3 Tandem Diazo Compounds Synthesis and the Cyclopropanation Scopes

These studies revealed that both batch-batch and flow-batch procedures can accommodate a broad scope of substrates. $\text{Rh}_2(\text{R-}p\text{-Ph-TPCP})_4$ **3.3** is effective in catalyzing cyclopropanation reactions in the presence of the protective influence of HFIP. For the sterically hindered traps, $\text{Rh}_2(\text{R-PTAD})_4$ was applied to deliver the products (**3.14**, **3.15**, **3.16**) with good selectivity, which also demonstrates this tandem method is practical for various dirhodium(II) catalysts. Moreover, examples **3.5**, **3.7**, **3.8**, **3.9**, **3.14**, **3.15** showed the flow-batch procedure provided better

enantioselectivity compared with the batch-batch procedure. The outcome is likely caused by the beneficial effects of the dropwise addition procedure and less water content in the eluent.

The recyclability of the flow-batch setup was also assessed through reusing the silica column without any refreshment. The data in **Table 3.3, entry 9** showed that 5 equiv of $\text{Cu}(\text{OAc})_2\text{-H}_2\text{O}$ in the column delivered product **3.4** in 73% yield with 97% ee, which would suggest that 10 equiv of $\text{Cu}(\text{OAc})_2\text{-H}_2\text{O}$ catalyst packed in the column might catalyze more than a single batch of the reaction. Recycling experiments (**Figure 3.4a**) showed that the good enantioselectivity of the cyclopropanation product **3.4** is maintained over 5 cycles, but the overall yield decreased after each run. From the crude $^1\text{H-NMR}$ analysis, hydrazone **3.1** has been fully converted to product in the $\text{Cu}(\text{II})\text{-DMAP-silica}$ column. However, the relative quantity of OAc insertion, dimerization and O–H insertion byproducts when the column was recycled. Additionally, the control experiment showed that OAc insertion product was the major byproduct generated in the hydrazone oxidation step.

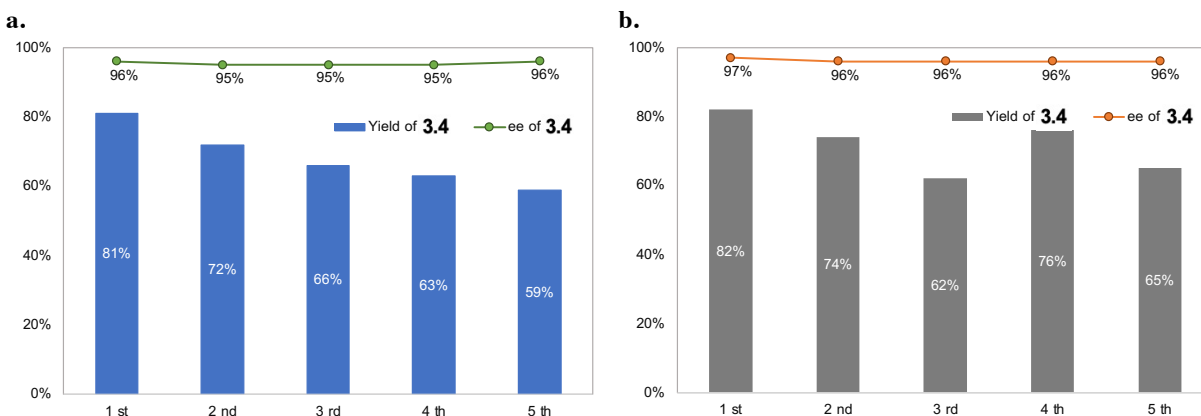
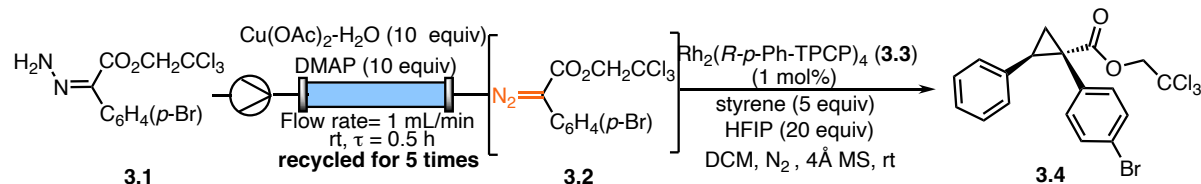


Figure 3.4 Column robustness assessment experiments. **a.** The column was recycled directly for all 5 tests without regeneration operation. **b.** The column was refreshed by flushing with air overnight after the 3rd test and reused in the 4th and 5th runs.

Based on the results in **Figure 3.4a**, the catalyst refreshing procedure was performed between the 3rd and the 4th run aiming to reactivate the copper(II) catalyst. The column was flushed with air overnight after the 3rd run and then reused in the 4th and the 5th runs. As the result showed in **Figure 3.4b**, the yield of the cyclopropanation product **3.4** was increased from 62% (the 3rd run) to 76% (the 4th run) and the high enantioselectivity was consistently maintained.

Compared with the recycling experiments without an air-flush regeneration procedure (**Figure 3.4a**), the result in **Figure 3.4b** suggests that the used copper(II) catalyst column can be reactivated by air to maintain the high efficiency. In collaboration with Taylor A. Hatridge from the Jones group, we have developed a three-phase packed bed reactor.¹³⁴ This setup continuously injected “ultra-zero” grade air to the silica column to keep the catalyst active. The system enabled catalytic aerobic oxidation to generate diazo compounds in flow and has achieved 74 TONs of

$\text{Cu}(\text{OAc})_2 \cdot \text{H}_2\text{O}$. The three-phase catalytic method herein would be most suited for an industrial-scale process, while the benchtop flow procedure is more practical for lab scientists wishing to access the diazo compound and carbene reaction in an effective and safe way.

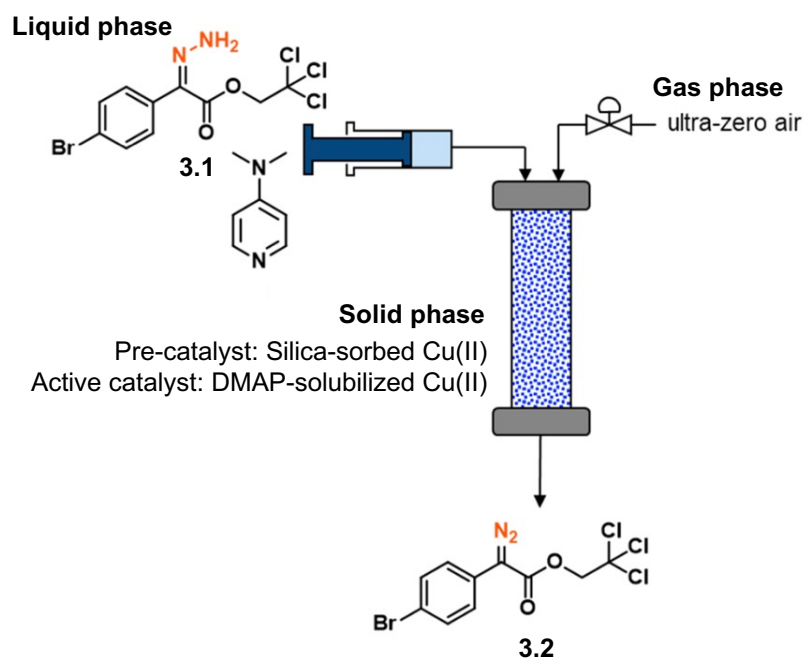
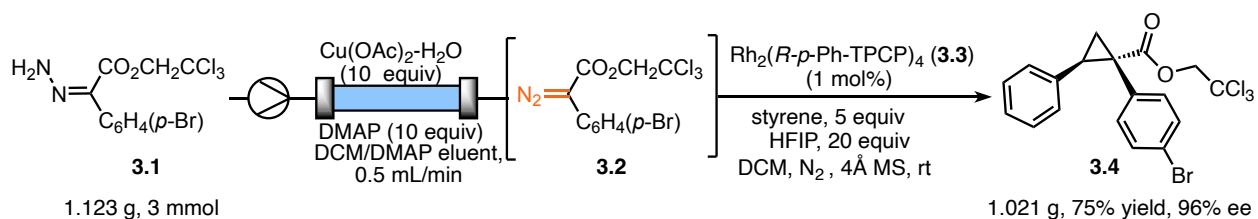


Figure 3.5 Catalytic aerobic oxidation of hydrazone compounds in a three-phase packed bed reactor

The bench-top flow procedure was further explored by conducting a gram-scale reaction with 5 equiv of $\text{Cu}(\text{OAc})_2 \cdot \text{H}_2\text{O}$ mixed with 10 equiv of DMAP in the column to convert 1.123 g, 3 mmol hydrazone **3.1** to diazo compound **3.2** and then the cyclopropane product **3.4**. As shown in **Scheme 3.3**, 1.021 g cyclopropane **3.4** was obtained in 75% yield with 96 ee%. The result demonstrated the efficiency of the procedure to access diazo compounds and the related cyclopropanation products in useful quantities.



Scheme 3.3 Gram scale synthesis from the hydrazone **3.1** to the cyclopropane **3.4** with bench-top flow procedure

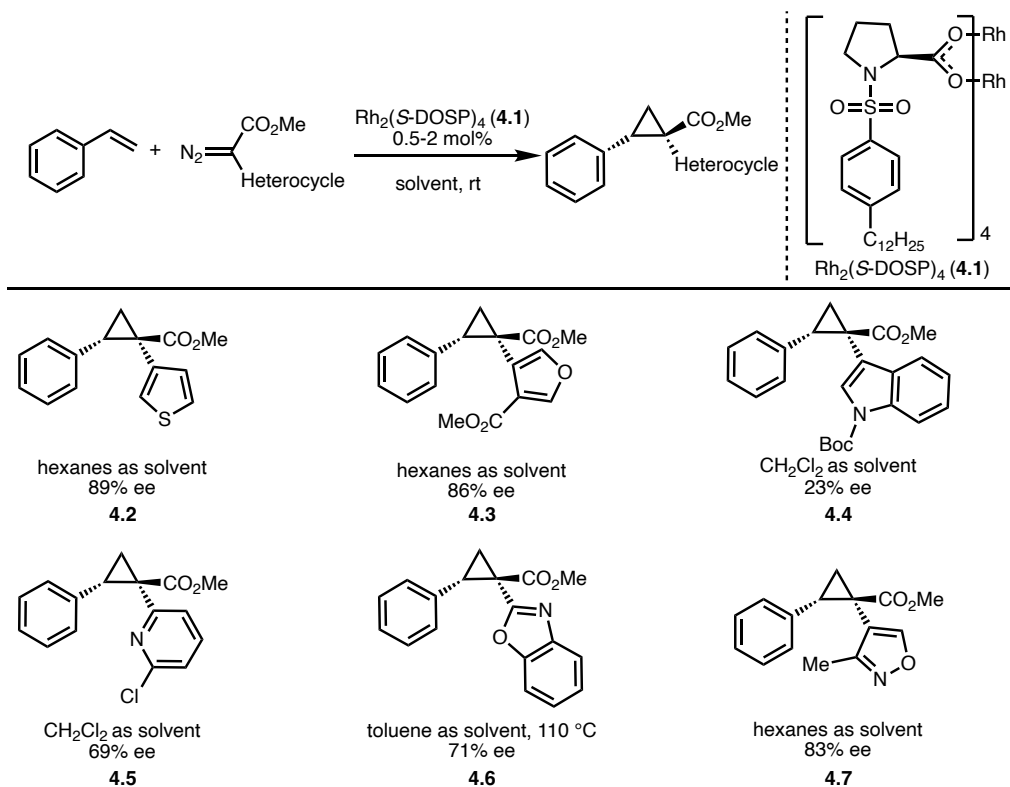
3.3 Conclusions

A bench-top flow procedure has been developed to generate diazo compounds by means of copper(II)-catalyzed hydrazone oxidation in a silica column. The diazo compound was formed *in situ* and directly used without any purification prior to the cyclopropanation reaction catalyzed by a dirhodium(II) catalyst. HFIP was revealed as the key component to solve the compatibility issue between the oxidation conditions and the carbene reaction. The process also avoided the engineering challenges of regenerating the reactive copper(II) catalyst. This method has been applied to a range of substrates to deliver various cyclopropanes with decent overall yield and high enantioselectivity. Recyclability assessment and large-scale experiments further demonstrated the practicality of this lab-based benchtop method. A process using catalytic amounts of copper(II) catalyst was also developed in the collaboration with the Jones group. This setup was more suitable for a sophisticated industrial-scale process.

Chapter 4. Pharmaceutically Relevant Asymmetric Cyclopropanation of Vinyl Heterocycles with Aryl- and Heteroaryldiazoacetates.

4.1 Introduction

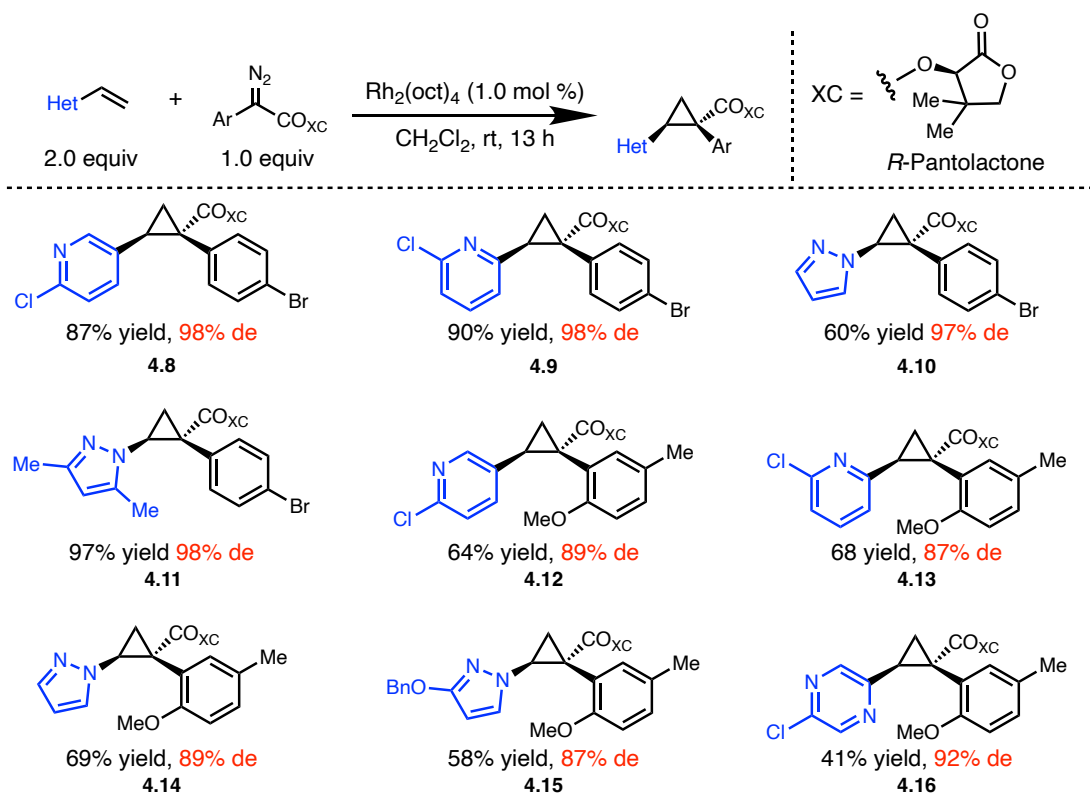
The cyclopropane is a common motif in natural products and pharmaceutical targets.¹³⁵⁻¹³⁸ Developing effective methods to construct chiral cyclopropanes has been of great industrial and academia interest.¹³⁹⁻¹⁴⁴ One of the most powerful methods is asymmetric cyclopropanation using chiral dirhodium(II) catalysts.¹⁴ Using donor/acceptor diazo compounds as carbene precursors and electron-rich alkenes as substrates, the cyclopropanation can be conducted with low catalyst loadings and high asymmetric induction.^{32, 66, 73, 145-147} However, once the substrates contain heterocyclic functionality, the efficiency of the reaction in terms of yield and stereoselectivity often drops because the dirhodium(II) complexes and the carbene intermediates are susceptible to undesirable interactions with nucleophilic sites within the heterocycles.^{14, 66, 68, 69, 148} Therefore, the synthesis of cyclopropanes containing heterocycles remains a challenge. Various methods have been developed intending to overcome this limitation. For example, the Davies group applied $\text{Rh}_2(\text{S-DOSP})_4$ (**4.1**)-catalyzed cyclopropanation of methyl heteroaryldiazoacetates with styrene (**Scheme 4.1**).³²



Scheme 4.1 Previous examples of $\text{Rh}_2(\text{S-DOSP})_4$ (**4.1**) catalyzed cyclopropanation reactions of styrene with heteroaryldiazoacetates

The reactions proceeded in high yield and diastereoselectivity while giving variable levels of enantioselectivity (23–89% ee). $\text{Rh}_2(\text{S-DOSP})_4$ (**4.1**) requires the use of nonpolar solvents to achieve high enantioselectivity, but such solvents cause solubility issues for many heterocyclic substrates, which limits the procedure's practicality. Another effective method developed by the Davies group uses chiral auxiliaries on the diazo compounds to induce high asymmetry. As introduced in Chapter 1, the optimum method used chiral pantolactone as auxiliaries and $\text{Rh}_2(\text{oct})_4$ as catalyst.³⁰ The procedure avoided the potential interference of heterocyclic substrates with chiral catalysts and was applied by AbbVie to access various heterocycle cyclopropanes. The reactions were conducted in CH_2Cl_2 at rt with 1 mol% $\text{Rh}_2(\text{oct})_4$. As shown in **Scheme 4.2**, excellent

enantioselectivity and good yield were consistently obtained, forming a variety of heterocyclic derivatives (**4.8-4.16**).



Scheme 4.2 Scopes of cyclopropanation of vinyl-heterocycle with diazo compounds containing chiral auxiliary (R)-pantolactone (*Data from AbbVie collaborators*)

Even though the AbbVie scientists had successfully developed a chiral auxiliary approach to the heterocyclic cyclopropanes, an asymmetric approach using chiral catalysts would be a more desirable solution. The use of a chiral auxiliary adds synthetic steps and is undesirable for a large-scale synthesis. Furthermore, only one enantiomer of the auxiliary, pantolactone, is relatively inexpensive.¹⁴⁹ Therefore, we were approached to determine if the chiral dirhodium(II) catalysts developed in the Davies lab would offer a practical enantioselective method to the desired cyclopropanes, which was substituted with heterocycles.

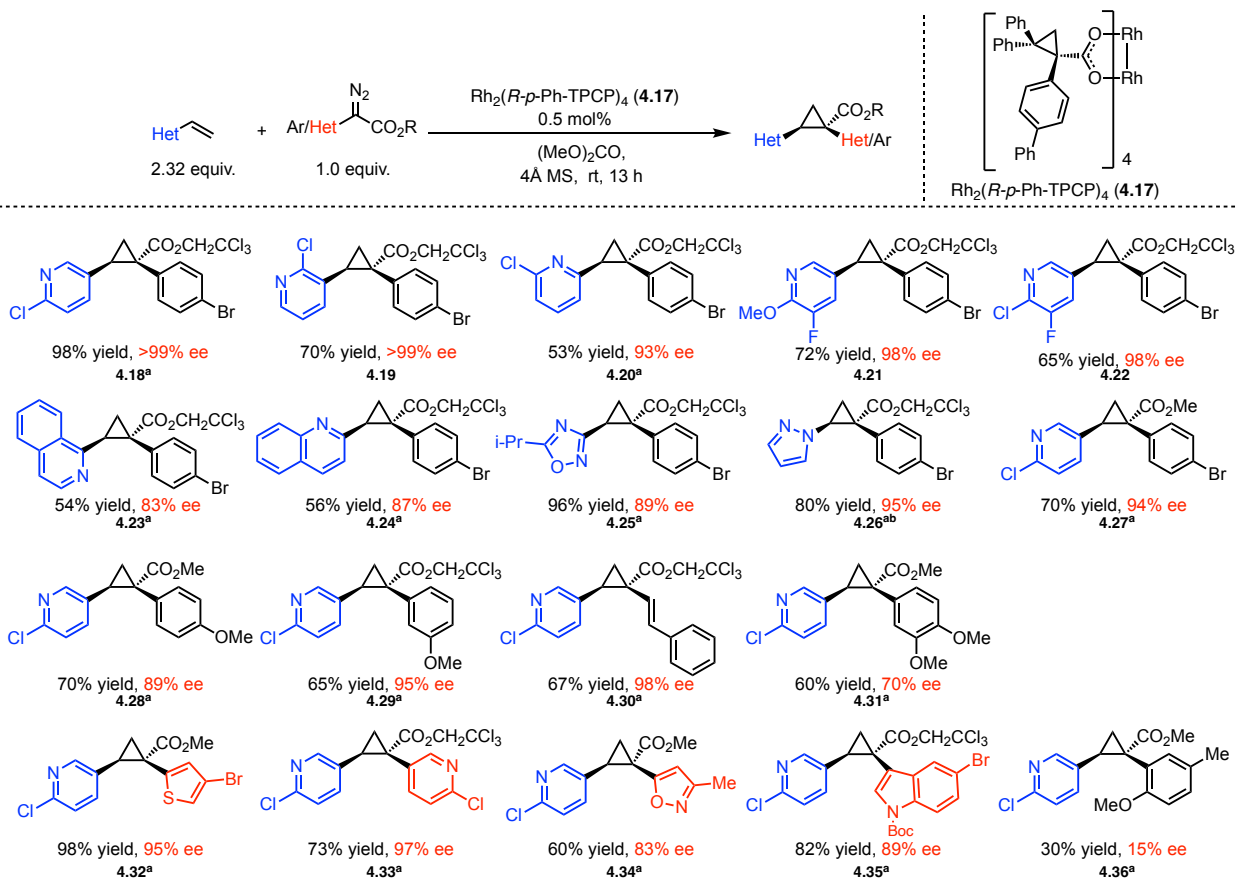
The study in this chapter identified two catalysts, $\text{Rh}_2(R\text{-p-Ph-TPCP})_4$ (**4.17**) and $\text{Rh}_2(S\text{-TPPTTL})_4$ (**4.43**) for the asymmetric synthesis of the heteroaryl cyclopropanes.^{39, 66} They are effective with a

variety of vinyl heterocycles and heteroaryldiazoacetates. The optimization process led to the discovery of 2-chloropyridine, which greatly enhances the enantioselectivity when *ortho*-substituted diazo compounds are used as substrates. Furthermore, the method has been adapted using the flow procedure described in Chapter 3 to generate and use the diazo compound *in situ*.

4.2 Results and Discussions

This study started by applying the procedure reported in Chapter 2 to a range of heterocyclic derivatives. $\text{Rh}_2(\text{R-}p\text{-Ph-TPCP})_4$ (**4.17**) has been demonstrated to be the most effective catalyst in the cyclopropanation of aryldiazoacetates with styrene derivatives.^{66, 148} Following the established procedure, reactions were conducted with 2.32 equiv of the vinyl heterocycles and 1.0 equiv of the diazo compounds with 0.5 mol % of catalyst loading.⁶⁶ The previous results showed that 4Å molecular sieves as additive and $(\text{MeO})_2\text{CO}$ as solvent were optimum conditions for catalyst high turnover numbers (TONs) while maintaining excellent selectivity.⁶⁶ Accordingly, 10 weight equiv of 4Å molecular sieves and $(\text{MeO})_2\text{CO}$ solvent were initially used in this study although CH_2Cl_2 was the solvent of choice in some cases. CH_2Cl_2 is the most widely-used solvent for donor/acceptor carbene transformations, and it can provide better solubility for some of the heterocyclic substrates. As shown in **Scheme 4.3**, my lab-collaborator, Jack C. Sharland, applied the established procedure and explored a wide range of substrates. The $\text{Rh}_2(\text{R-}p\text{-Ph-TPCP})_4$ (**4.17**)-catalyzed method was proved to be effective to construct various cyclopropanes accompanying with heterocycles as long as the aryl or heteroaryldiazoacetates did not contain an *ortho* substituent. Pyridine (**4.18-4.22**, **4.27-4.36**), quinoline (**4.23**, **4.24**) and various five-membered heterocycles (**4.25**, **4.26**) were all accommodated in the cyclopropanation with 2,2,2-trichloroethyl 2-(4-bromophenyl)-2-diazoacetate. A variety of *para*-, *meta*-substituted aryldiazoacetates and a styryldiazoacetate (**4.30**)

performed well in the cyclopropanation of 2-chloro-5-vinyl pyridine. High enantioselectivity (89-98% ee) was obtained except for the 3,4-dimethoxy derivative (**4.31**), which generated the cyclopropane in 70% ee. Furthermore, the cyclopropanes containing two heteroaryl rings (**4.32-4.35**) were obtained with high enantioselectivity (83-97% ee). One exception was the reaction with *ortho*-substituted aryldiazoacetate (**4.36**), which gave low yield (30%) and selectivity (15% ee).

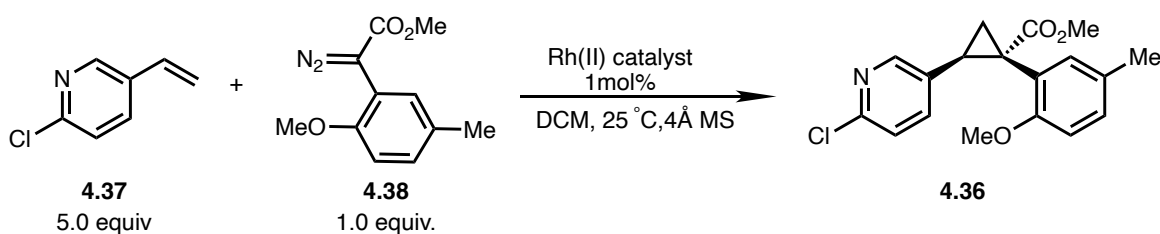


Scheme 4.3 Scopes of cyclopropanation of vinyl-heterocycle with diazo compounds catalysed by $\text{Rh}_2(R-p\text{-Ph-TPCP})_4$ (**4.17**). ^a CH_2Cl_2 was applied as solvent. ^b1 mol% $\text{Rh}_2(R-p\text{-Ph-TPCP})_4$ (**4.17**) was applied. (Data collected by Jack C. Sharland)

Some of the pharmaceutically most relevant derivatives in this AbbVie collaboration were *ortho*-substituted derivatives. Therefore, further studies were required to improve the reaction performance with *ortho*-substituted aryldiazoacetates. The standard reaction used in the optimization study was the cyclopropanation of 2-chloro-5-vinyl pyridine (**4.37**, 5.0 equiv), with

the *ortho*-substituted methyl 2-(2-methoxy-5-methylphenyl)-2-diazoacetate (**4.38**, 1.0 equiv) using 1 mol % of the dirhodium(II) catalyst. The results of the optimization study are summarized in **Table 4.1**. Rh₂(*S*-PTAD)₄ (**4.39**) and Rh₂(*R*-DOSP)₄ (**4.1**) had been previously reported to be effective catalysts in the stereoselective cyclopropanation of styrene with *ortho*-chlorophenyldiazoacetate.^{14, 145} These two established catalysts were therefore tested first, but both delivered the cyclopropane **4.36** with low enantioselectivity. Previous studies have demonstrated Rh₂(*R*-DOSP)₄ (**4.1**) and Rh₂(*S*-PTAD)₄ (**4.39**) worked better in nonpolar solvents like hexane and pentane. However, nonpolar solvents were not suitable here because of the solubility issues with the vinyl heterocycle (**4.37**).¹⁴ The disappointing results above showed that the most established dirhodium(II) catalysts did not offer a suitable solution in this case.. Hence, a series of the newly developed catalysts were screened. Among the tested catalysts, Rh₂(*R*-TPPTTL)₄ **4.43** showed promising results, forming the cyclopropane in 88% yield with 78% ee (**Table 4.1, entry 8**).^{39, 150}

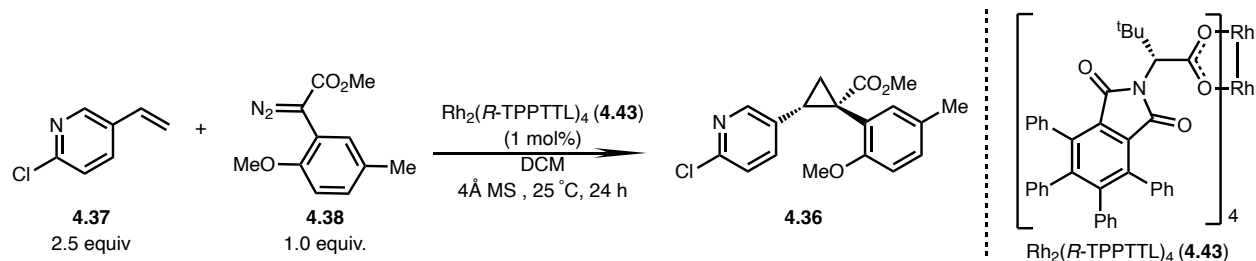
Table 4.1 Optimization of the enantioselective cyclopropanation of a vinyl-heterocycle (**4.37**) with methyl 2-(2-methoxy-5-methylphenyl)-2-diazoacetate (**4.38**)



Entry	Rh(II) Catalyst	condition variation	yield of 4.36 , %	ee of 4.36 , %
1	Rh ₂ (<i>R</i> -PTAD) ₄ (4.39)	-	79	9
2	Rh ₂ (<i>S</i> -NTTL) ₄ (4.40)	-	80	6
3	Rh ₂ (<i>R</i> -DOSP) ₄ (4.1)	Neat	70	4
4	Rh ₂ (<i>R</i> -DOSP) ₄ (4.1)	Pentane	66	27
5	Rh ₂ (<i>R</i> -DOSP) ₄ (4.1)	TFT	57	13
6	Rh ₂ (<i>R</i> -2-Cl-5-Br-TPCP) ₄ (4.41)	0 °C	46	35
7	Rh ₂ (<i>R</i> -TCPTAD) ₄ (4.42)	(MeO) ₂ CO	75	56
8	Rh₂(<i>R</i>-TPPTTL)₄ (4.43)	-	88	78

To achieve better enantioselectivity, further optimization of the Rh₂(*R*-TPPTTL)₄ (**4.43**)-catalyzed cyclopropanation were conducted by Jack C. Sharland. The results in **Table 4.2** showed lower temperature gave higher enantioselectivity (80% ee at 0 °C). Intriguingly, increasing the equivalent of trap reagent largely improved the reaction performance (**Table 4.2, entry 5**). Applying 5 equiv of 2-chloro-5-vinylpyridine in the reaction generated the cyclopropane **4.36** in 95% yield and with 98% ee.^{20, 44, 69, 151-153} To further enhance the practicality of the methodology, 4 Å molecular sieves were replaced by 10 equiv of hexafluoroisopropanol (HFIP) as drying reagent (**Table 4.2, entry 6**).¹⁵⁰ The procedure using HFIP generated a homogeneous reaction mixture, which would be more desired than the use of molecular sieves for a large scale industrial process.^{87, 104, 106, 154, 155}

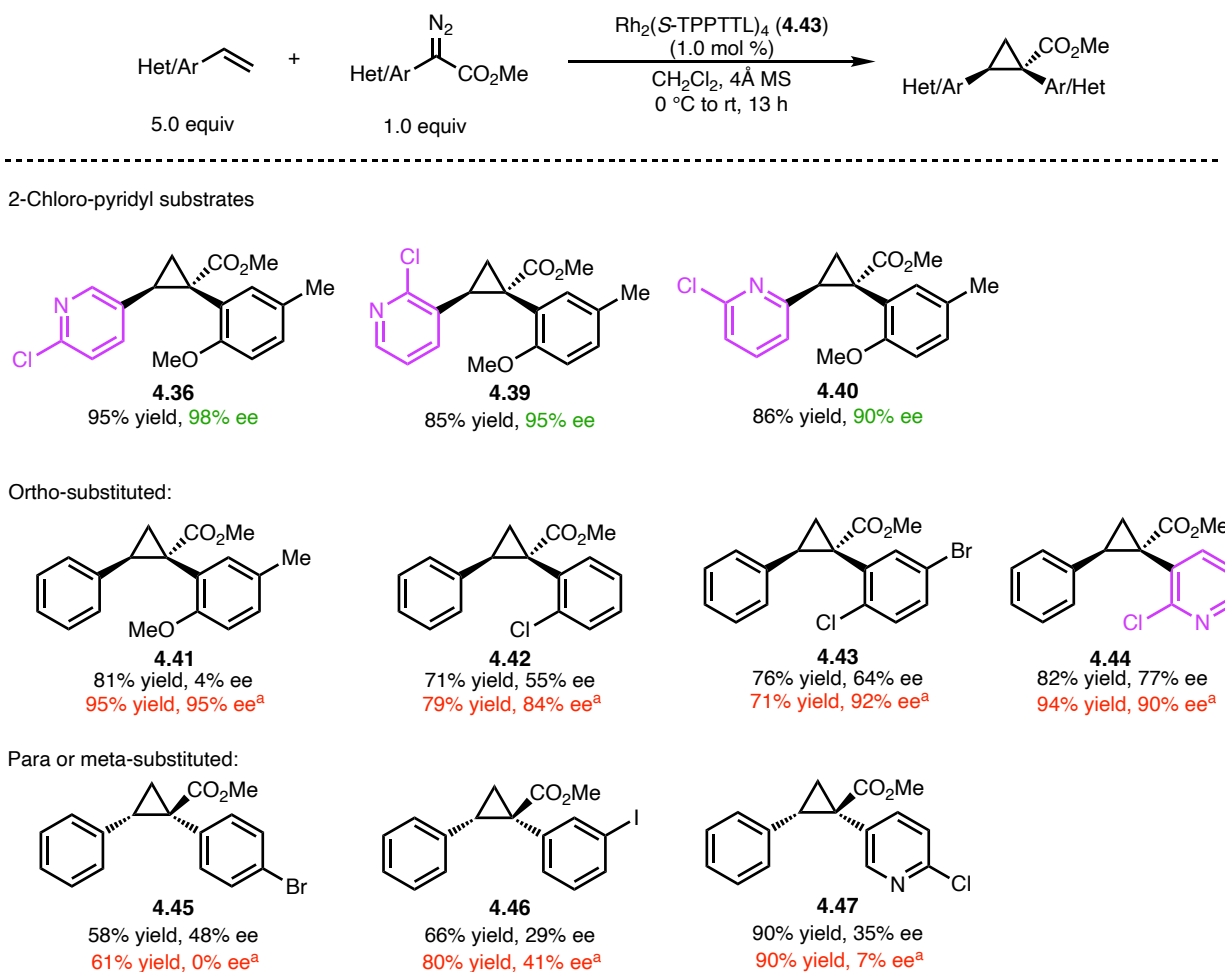
Table 4.2 Optimization of the enantioselective cyclopropanation of a vinyl-heterocycle (**4.37**) with methyl 2-(2-methoxy-5-methylphenyl)-2-diazoacetate (**4.38**) catalyzed by $\text{Rh}_2(\text{R-TPPTTL})_4$ (**4.43**)



Entry	condition variation	yield of 4.36 , %	ee of 4.36 , %
1	-	88	60
2	0 °C	85	80
3	(MeO) ₂ CO	74	35
4	TFT	58	58
5	0 °C, 5 equiv of 4.37	95	98
6	0 °C, 5 equiv of 4.37, 10 equiv HFIP	93	92

(Data collected by Jack C. Sharland)

Various *ortho*-substituted aryldiazoacetates were tested using the optimized conditions described above. As shown in **Scheme 4.4**, the reaction between aryldiazoacetate with vinyl 2-chloropyridines consistently gave high enantioselectivity (90-98% ee) (**4.36**, **4.39**, **4.40**). However, low selectivity still occurred when styrene was used in the cyclopropanation reaction with *ortho*-substituted aryldiazoacetates (4-64% ee) (**4.41-4.43**, **4.45-4.47**). The only exception was the cyclopropanation with 2-chloropyridyldiazoacetate, which achieved a moderate level of enantioselectivity (77% ee) (**4.44**).



Scheme 4.4 The additive effect of 2-chloropyridine on asymmetric cyclopropanation catalyzed by $\text{Rh}_2(\text{S-TPPTTL})_4$ (**4.43**). ^aThe reaction condition included 1.0 equiv of 2-chloropyridine as the additive. (*Data collected with Jack C. Sharland*)

The results in **Scheme 4.4** showed that a 2-chloropyridyl functionality had a positive influence on the enantioselectivity of the cyclopropanation. High enantioselectivity was observed with all the substrates containing a 2-chloropyridyl group. Furthermore, comparing **entry 5** with **entry 2** in **Table 4.2**, the results further suggested that more equivalents of the substrate with the 2-chloropyridyl group in the reaction led to higher levels of enantioselectivity. Based on the above observation, we proposed that 2-chloropyridyl functional group plays a critical role in influencing the enantioselectivity for $\text{Rh}_2(\text{S-TPPTTL})_4$ (**4.43**) catalyzed-cyclopropanation. To test this

hypothesis, control experiments were performed to confirm the positive effect of the pyridyl component on the reaction. In the control experiments, the reactions proceeding with low enantioselectivity in **Scheme 4.4** were rechecked under the same condition (**4.41-4.47**). The only difference was that 1 equivalent of 2-chloropyridine was included in the reaction as an additive. The new results are marked in red colour in **Scheme 4.4**. The inclusion of 2-chloropyridine caused a remarkable difference in the enantioselectivity compared with the previous no-additive condition. For example, the enantioselectivity of cyclopropane **4.41** increased from 4% ee to 95% ee in the presence of 2-chloropyridine additive. However, the positive effect caused by 2-chloropyridine is limited to *ortho*-substituted diazo compounds. For the diazo compounds lacking *ortho* substituents, the presence of 2-chloropyridine did not have a positive effect on the enantioselectivity in the cyclopropanation reaction. For compounds **4.45** and **4.47**, addition of 2-chloropyridine even lowered the enantioselectivity.

To obtain deeper understanding of the interaction between 2-chloropyridine additive with the dirhodium(II) catalyst, crystals suitable for X-ray crystallography were prepared by Jack C. Sharland (**Figure 4.1**). The additive-coordinated structures showed two 2-chloropyridine molecules bound to the two axial sites of $\text{Rh}_2(\text{S-TPPTTL})_4$ (**4.43**) complex, and a third 2-chloropyridine located in the bowl of the complex.

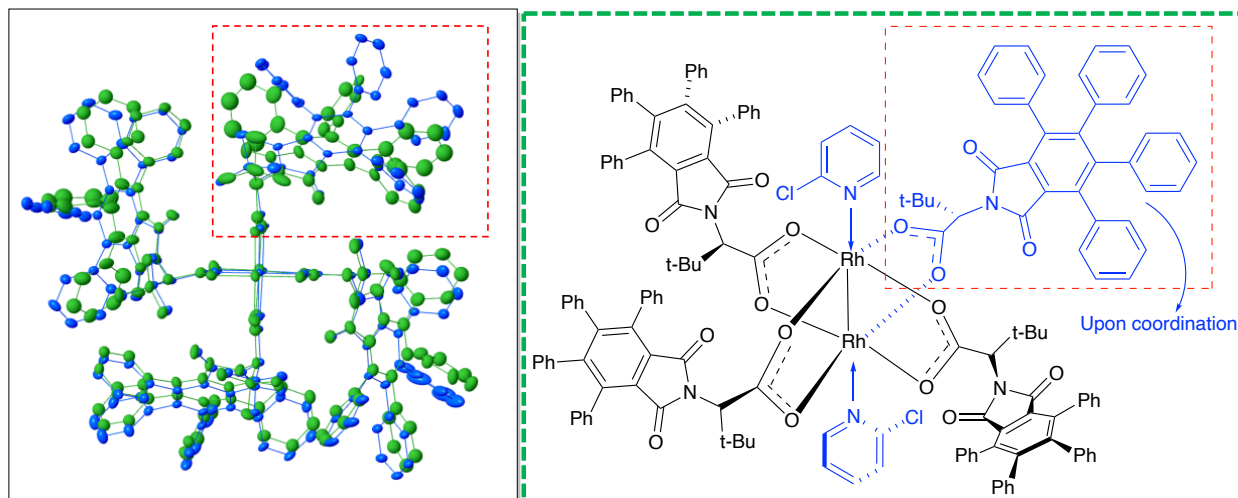
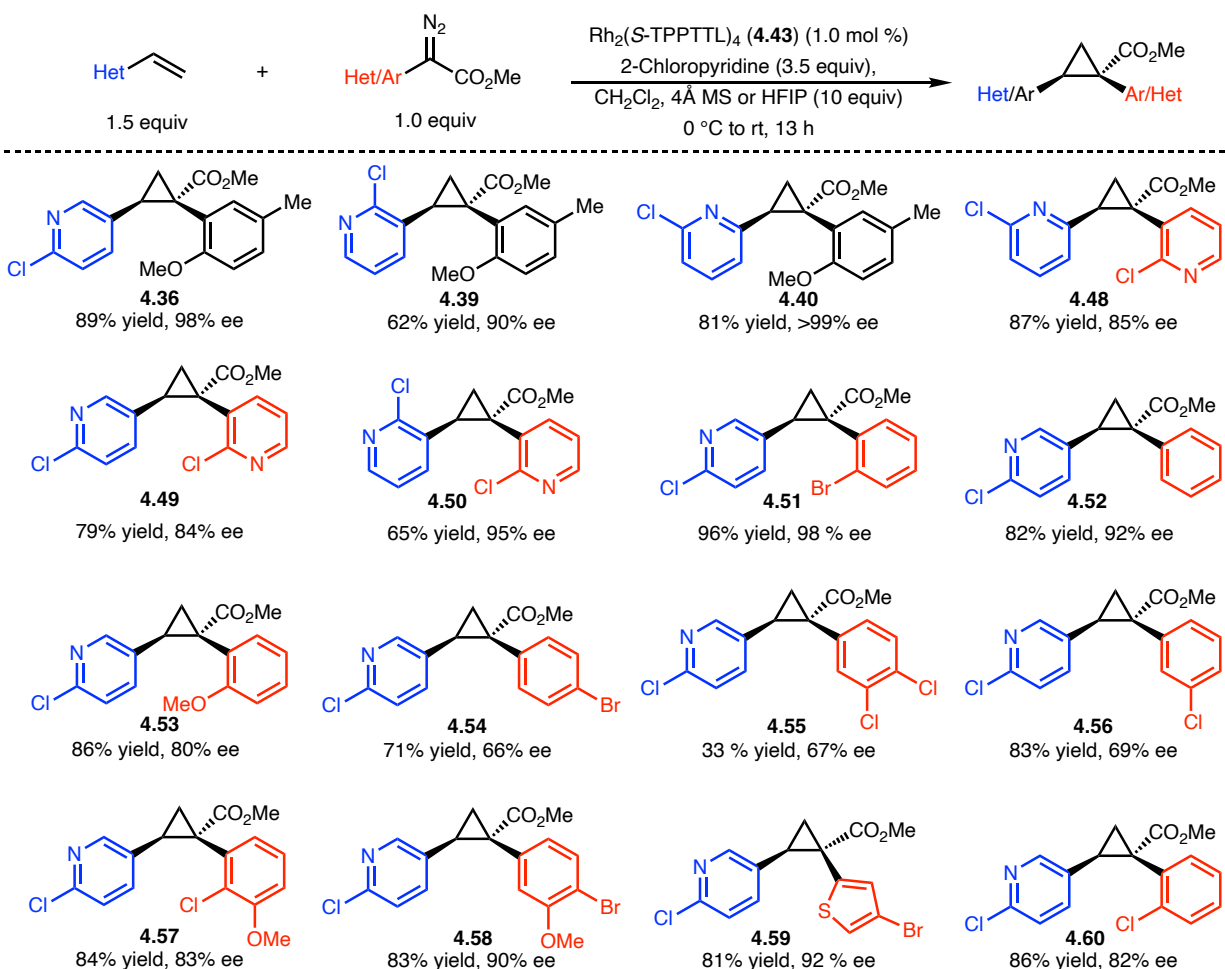


Figure 4.1 Structural perturbations in $\text{Rh}_2(\text{S-TPPTTL})_4$ (**4.43**) enforced by the coordination of 2-chloropyridine based on X-ray analysis of a single crystal of $\text{Rh}_2(\text{S-TPPTTL})_4$ (**4.43**) coordinated to 2-chloropyridine. (*Data collected by Jack C. Sharland*)

The additive-coordinated $\text{Rh}_2(\text{S-TPPTTL})_4$ (**4.43**) complex was compared with the original complex by overlapping the two crystal structures together.³⁹ We observed that one ligand of the $\text{Rh}_2(\text{S-TPPTTL})_4$ (**4.43**) catalyst was displaced upon 2-chloropyridine coordination. The observation here suggested the axial coordination effect from 2-chloropyridine changed the pocket conformation of the bowl shape catalyst $\text{Rh}_2(\text{S-TPPTTL})_4$ (**4.43**), and this effect may be the cause of the enantioselectivity variation in the cyclopropanation reaction.^{20, 66, 69, 131, 156-158}

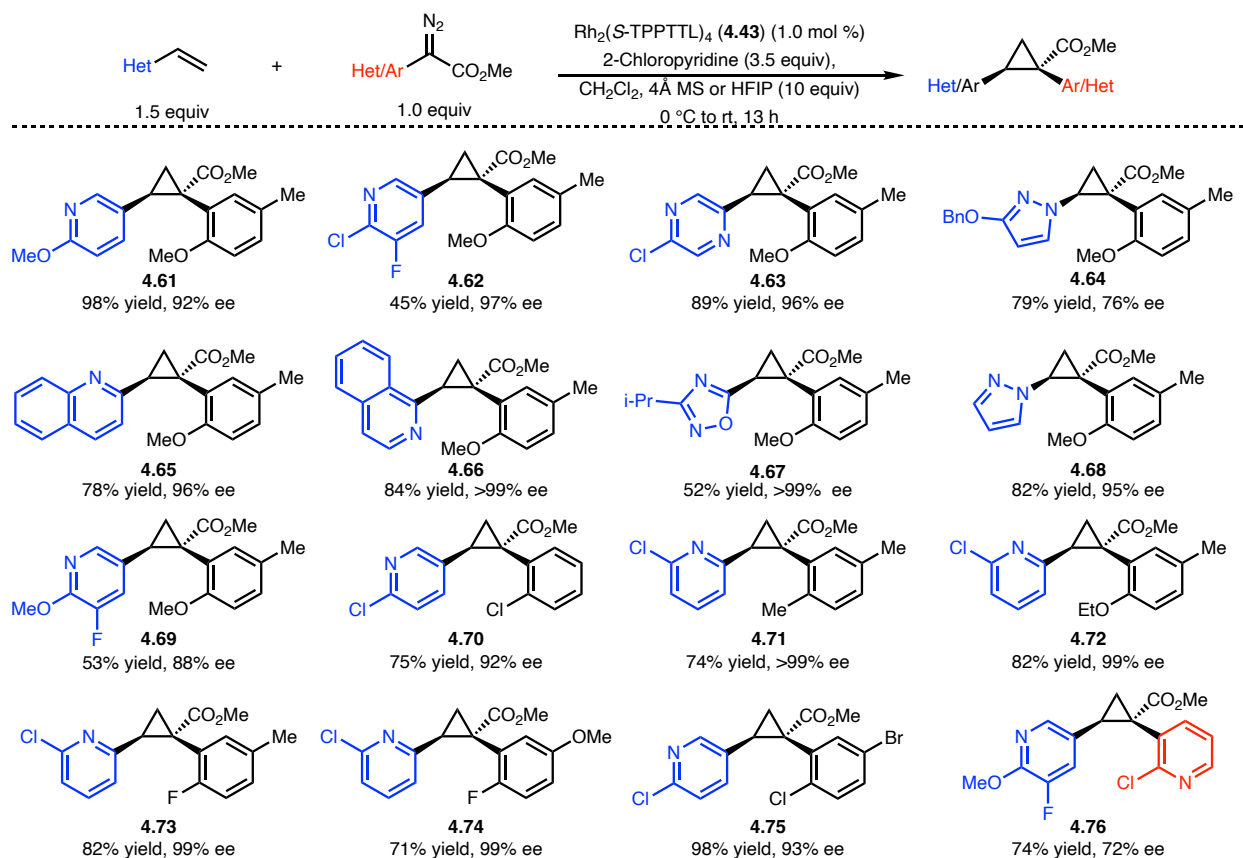
A range of substrates containing heterocycle motifs were explored in the presence of 2-chloropyridine (**Scheme 4.5**). The cyclopropanation of vinyl heterocycle with *ortho*- and *meta*-substituted aryldiazoacetates were completed in the presence of 2-chloropyridine. Since vinyl heterocycle substrates used in the reaction were usually expensive or not commercial-available, the reactions were conducted with only 1.5 equiv of the vinyl heterocycle substrates and 3.5 equiv of 2-chloropyridine additive. This combination of substrate and additive made the procedure more economical and practical while ensuring good enantioselectivity and yield. Several 1, 2-diheteroaryl cyclopropane carboxylates examples (**4.48-4.50**, **4.59**) were also generated with good

asymmetric induction (72% to 95% ee.) The reactions were carried out using either 4Å molecular sieves or HFIP as co-additive to avoid the interference from water in the reaction system.



Scheme 4.5 Scopes of cyclopropanation of vinyl-heterocycle with various diazo compounds catalyzed by $\text{Rh}_2(\text{S-TPPTTL})_4$ (**4.43**).

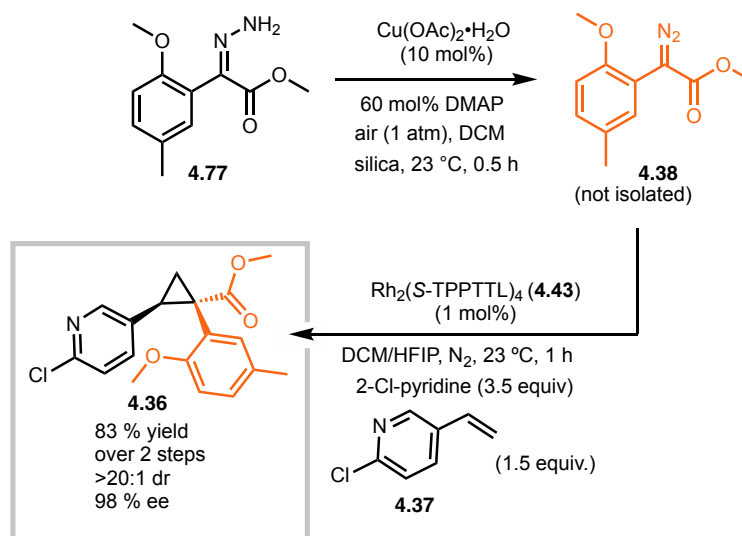
The exploration of vinyl-heteroaryls shown in **Scheme 4.6** was conducted by Jack C. Sharland. The study included various pyridines (**4.61-4.62**, **4.69-4.76**), pyrazines (**4.63**), pyrazoles (**4.64**, **4.68**), quinolines (**4.65**), isoquinolines (**4.66**) and oxadiazoles (**4.67**) structures. The yield of these reactions varies from 45% to 98% and the enantioselectivity range was 76% to >99% ee.



Scheme 4.6 Scopes of cyclopropanation of various vinyl-heterocycle with diazo compounds catalyzed by $\text{Rh}_2(\text{S-TPPTTL})_4$ (**4.43**). (Data collected by Jack C. Sharland and AbbVie collaborators)

To further illustrate the methodology's practicality in large scale synthesis, the procedure was incorporated into a tandem procedure to approach cyclopropane **4.36** starting from hydrazone **4.77** (Scheme 4.7).^{129, 159} In the procedure, the diazo compound **4.38** generated from the oxidation reaction was directly used in $\text{Rh}_2(\text{S-TPPTTL})_4$ (**4.43**) catalyzed cyclopropanation reaction without any purification. This tandem reaction procedure delivered the cyclopropane **4.36** in 83% overall yield and 98% ee. 20 equiv HFIP as additive in the cyclopropanation reaction flask was the crucial for the reaction success.¹⁵⁰ HFIP here not only desensitizes the reaction to H_2O , but also protects the dirhodium(II) catalyst and the carbene intermediate from the coordinating effect of DMAP,

which is used in the upstream oxidation.^{14, 20, 151} More detailed explanation about the role of HFIP is provided in Chapter 3.¹⁶⁰⁻¹⁶⁷



Scheme 4.7 Tandem copper-catalyzed diazo formation followed by a $\text{Rh}_2(\text{S-TPPTTL})_4$ (4.43)-catalyzed cyclopropanation.

4.3 Conclusions

This study developed effective methods to synthesize cyclopropane containing heterocycles of pharmaceutical interest. Two chiral dirhodium(II) catalysts were applied to deliver products with high yield and enantioselectivity. Firstly, $\text{Rh}_2(\text{R-}p\text{-Ph-TPCP})_4$ (4.17) was used to catalyze the cyclopropanation of vinyl heterocycles with a wide range of *para*, *meta*-substituted aryl and heteroaryldiazoacetates. This established method is robust and effective to deliver heteroarylcyclopropane carboxylates with high selectivity. However, the reaction accompanying *ortho*-substituted aryldiazoacetates delivered the modest result. $\text{Rh}_2(\text{S-TPPTTL})_4$ (4.43) is a superior catalyst to overcome the limitation involving *ortho*-substituted aryldiazoacetates. Furthermore, 2-chloropyridine was an effective additive to enhance the enantioselectivity. It was proposed that 2-chloropyridine coordination altered the $\text{Rh}_2(\text{S-TPPTTL})_4$ (4.43) catalyst pocket

conformation and subsequently effected the enantioselectivity of the reaction. The study herein established effective complementary methods for asymmetric cyclopropanation containing a wide range of heterocycle motifs. Moreover, the method was compatible with the tandem procedure to use aryldiazoacetate formed *in-situ* without purification. Above all, the optimization and the application in this study expanded the scope of the dirhodium(II) complexes catalyzed cyclopropanation reaction and enhanced its practical utility in a focused drug development program.

Chapter 5. In Situ Kinetics Studies of Dirhodium (II)-Catalyzed C–H Functionalization to Achieve High Catalyst Turnover Numbers.

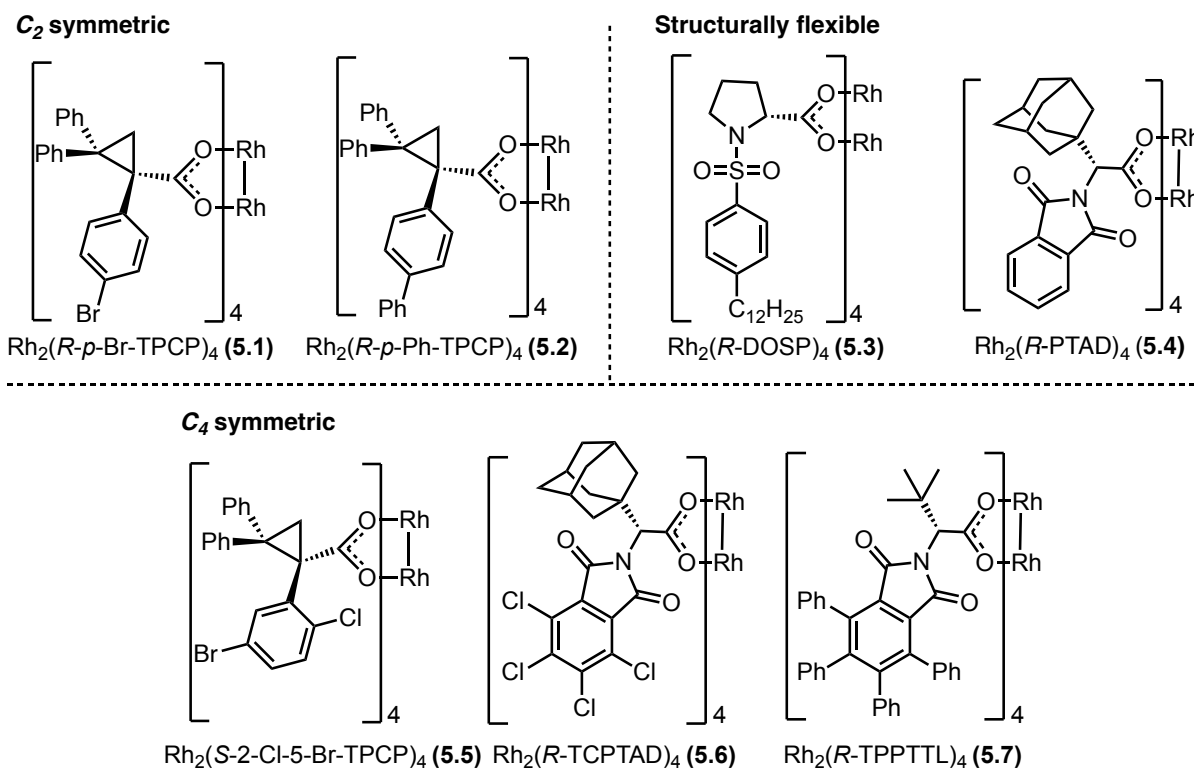
5.1 Introduction

Several chiral dirhodium(II) catalysts of high symmetry have been applied in C–H insertion functionalization reactions.⁴⁷ Depending on the steric environment, the dirhodium(II) catalysts can control precisely which C–H bond will be functionalized.⁵⁵ While significant advances have been made in dirhodium(II)-catalyzed C–H functionalization in recent years, only a few kinetic investigations have been conducted to analyze reactions progress, and most of the mechanistic interpretations are derived from computational studies.^{168, 29, 66, 97, 169-172} The experimental information about the kinetics of the C–H functionalization progress is underdeveloped. Furthermore, the high catalyst turnover numbers (TONs) achieved in dirhodium(II)-catalyzed carbene reactions are limited to reactions with very active substrates, such as the cyclopropanation of styrenes described in Chapter 2.⁶⁶ Using a low dirhodium(II) catalyst loading in C–H functionalization usually led to incomplete reactions and a considerable decrease in the overall asymmetric induction.^{43, 173} Therefore, it was necessary to determine what would be the factors limiting the turnover efficiency of the dirhodium(II) catalysts as the reaction progresses. The results from this study will guide rational reaction optimization as well as the design of better dirhodium(II)catalysts to achieve even higher TONs. Therefore, in this Chapter, using C–H insertion of cyclohexane as the model reaction, a comprehensive investigation of the reaction kinetics was undertaken. The results of this study demonstrated that the concentration of the substrate and the dirhodium(II) catalyst were the driving force in the C–H functionalization while the diazo compound showed zero order. Accordingly, the rate determining step was proposed to be carbene insertion rather than carbene formation. We also found 1 mol % of DCC as an additive

was crucial to help the reaction to achieve quantitative conversion with only 0.0005 mol% catalyst loading. Inspired by these results, further optimization was performed and more than 580,000 catalyst TONs were achieved in sequential diazo compound addition conditions. This low catalyst loading method was also applied to various substrates to demonstrate its versatility.

5.2 Results and Discussions

Dirhodium(II) catalyst-controlled intermolecular C–H functionalization was pioneered by the Davies in 1997 and studies in this area continue to the current times.^{47, 174, 175} Similar C–H bonds of a complex structure can be differentiated accurately by the dirhodium(II) complexes to achieve precise control of C–H functionalization. The superior selectivity achieved by the dirhodium(II) catalysts has led to many notable applications. To further optimize the chemistry, it is useful to seek deeper insights into how the catalyst behaves as the C–H reactions progresses. Firstly, in order to help further optimization of the C–H insertion reaction. Firstly, to understand the effect of the dirhodium(II) catalyst structure on the reaction rate, various dirhodium(II) complexes were tested in a standard C–H insertion reaction (**Scheme 5.1**).



Scheme 5.1 Dirhodium(II) catalyst with different steric structures tested in this study

In this reaction, 2,2,2-trichloroethyl aryldiazoacetate **5.8a** was selected as the precursor to the donor/acceptor carbene, because it is an established precursor for carbene reactions.⁷⁴ Cyclohexane **5.9** is an ideal substrate to begin the study because it is electronically neutral and had 12 identical unactivated methylene C–H bonds. A dirhodium(II) catalyst loading of 0.1 mol % in reactions conducted at 40 °C in CH_2Cl_2 were employed in the initial standard reactions.³⁹ The reaction kinetic profiles were *in-situ* monitored by ReactIR following the diazo compound **5.8a** concentration variation during the whole reaction progress (**Figure 5.1**).

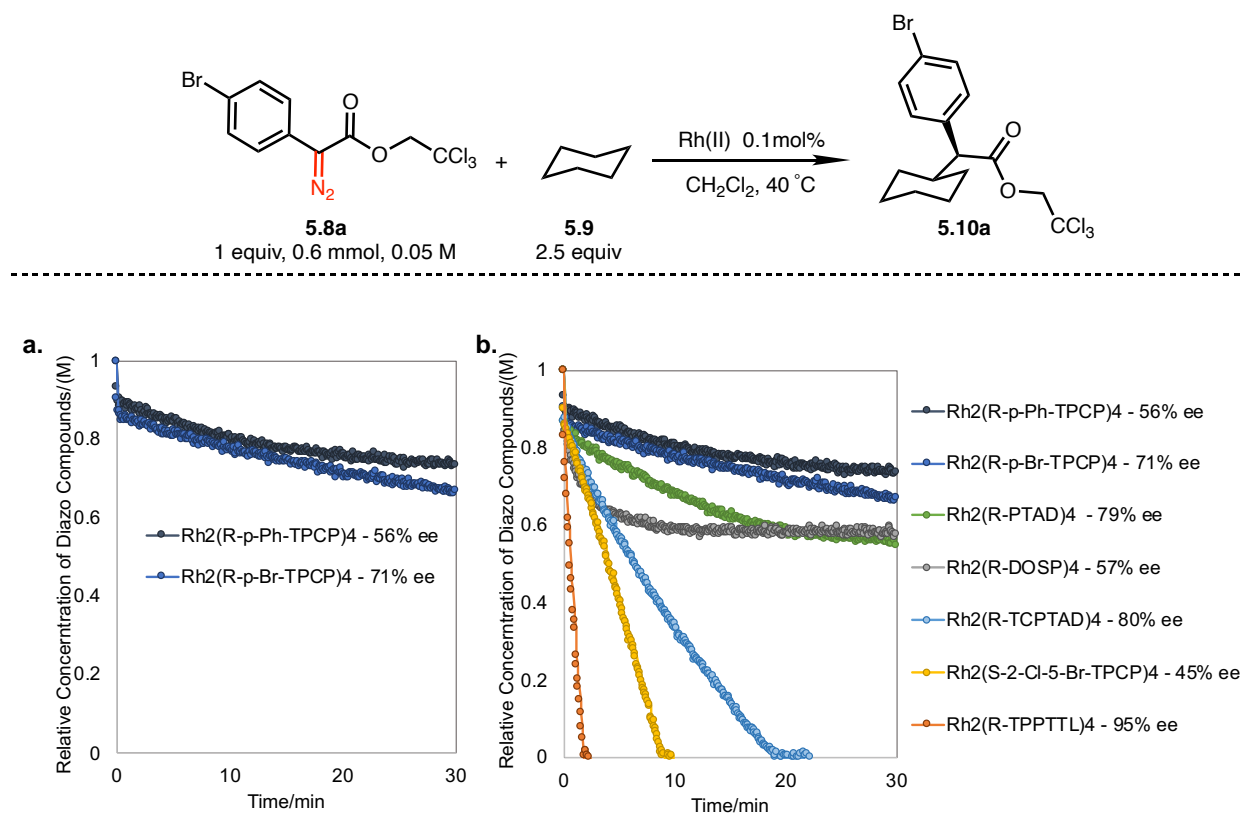


Figure 5.1 Reaction rates of various catalysts in C–H insertion of cyclohexane **a**. Kinetic profiles of C–H insertion of cyclohexane **5.9** catalyzed by previous reported high TONs dirhodium(II) catalysts in cyclopropanation reaction. **b**. Kinetic profiles of C–H insertion of cyclohexane **5.9** catalyzed by dirhodium(II) catalysts with various symmetric structures.

Rh₂(*R-p-Br*-TPCP)₄ (**5.1**) and Rh₂(*R-p-Ph*-TPCP)₄ (**5.2**) were tested under these standard conditions because they were the best catalysts for high TONs in the cyclopropanation reaction described in Chapter 2.⁶⁶ Accompanying with reactive trap reagent, styrene, both Rh₂(*R-p-Br*-TPCP)₄ (**5.1**) and Rh₂(*R-p-Ph*-TPCP)₄ (**5.2**) showed remarkable robustness and were able to deliver cyclopropanes with high yield and great enantioselectivity under 0.001 mol % catalyst loading. However, as shown in **Figure 5.1a**, 0.1 mol% Rh₂(*R-p-Br*-TPCP)₄ (**5.1**) and Rh₂(*R-p-Ph*-TPCP)₄ (**5.2**) both showed slow reaction rates and a limited level of enantioselectivity. Rh₂(*R-p-Br*-TPCP)₄ (**5.1**) and Rh₂(*R-p-Ph*-TPCP)₄ (**5.2**) are C₂ symmetric catalysts with bulky triarylcyclopropane

carboxylate ligands and can generate sterically crowded carbene intermediates.⁴⁷ We assumed it was difficult for the unreactive trap, cyclohexane **5.9**, to approach the carbene center when the carbene intermediate structures were rigid. In this situation, the interaction between the carbene intermediate and the trap reagent would be hindered and therefore retard the whole catalytic cycle. Compared with the cyclopropanation reaction accompanied with reactive trap reagent, the C–H insertion with unreactive trap reagent was more delicate in low catalyst loading condition and needed more effective catalysts to promote the reaction progress. Therefore, various high symmetry dirhodium(II) catalysts (**5.3-5.7**) were tested for their influence on the rate of the reaction.

To increase the reaction rate, the relatively uncrowded catalyst $\text{Rh}_2(R\text{-DOSP})_4$ (**5.3**) was firstly tested. 0.1 mol% $\text{Rh}_2(R\text{-DOSP})_4$ (**5.3**) catalyzed C–H insertion of cyclohexane **5.9** with methyl phenyldiazoacetate afforded 91% ee and 63% yield at 24 °C.⁹⁷ The reaction was conducted under neat conditions and a slow addition technique was used to avoid carbene or diazo compounds dimerization. In these experiments, $\text{Rh}_2(R\text{-DOSP})_4$ (**5.3**) showed a fast initial rate in the model reaction, but the rate slowed down quickly. Product **5.10a** was formed in 40% yield and 57% ee. It is known that $\text{Rh}_2(R\text{-DOSP})_4$ (**5.3**) is highly sensitive to solvent effect, and higher levels of enantioselectivity are favored in nonpolar solvents. Another sterically open catalyst, $\text{Rh}_2(R\text{-PTAD})_4$ (**5.4**),¹⁷⁶ was also tested, but the reaction was incomplete after 2 h while dimerization byproducts had formed. The above reactions with more sterically open dirhodium(II) catalysts enabled the unactive substrate cyclohexane **5.9** gave fast initial reaction rates but then the reactions stopped, presumably because the catalysts had decomposed or become deactivated. The carbene intermediates also tended to dimerize or react with the diazo compound to form azine dimer, which likely caused interference in the reactions.¹⁷⁷

The more promising results came from the C_4 symmetric dirhodium(II) catalysts, which displayed much faster reaction rates in the model C–H insertion reaction. $\text{Rh}_2(\text{S-2-Cl-5-Br-TPCP})_4$ (**5.5**)⁶³ and $\text{Rh}_2(\text{R-TCPATD})_4$ (**5.6**)⁶² accomplished the reaction rapidly with modest enantioselectivity and great yield. More remarkably, $\text{Rh}_2(\text{R-TPPTTL})_4$ (**5.7**)³⁹ completed the reaction in only 2 min in 94% yield with 95% ee, which demonstrate its superiority in this C–H insertion reaction. The C_4 symmetric dirhodium(II) catalysts showed high efficiency to catalyze the C–H insertion of cyclohexane **5.9**. We assume the great results come from the catalysts with matched steric conformation allowing cyclohexane **5.9** to involve a rapid C–H insertion process. The effective process possibly also prevented carbene intermediate from undesired decomposition or side reactions, which resulted in high reaction efficiency.

In the previous kinetic study of cyclopropanation catalyzed by various dirhodium(II) catalysts (**Chapter 2**),⁶⁶ the more sterically open dirhodium(II) catalysts gave the faster reaction rate. Since carbene formation was the rate-determining step in the cyclopropanation mode, more flexible dirhodium(II) catalysts tended to form carbene more effectively and resulted in faster reaction rate. However, with unactive substrates like cyclohexane **5.9**, the formation of the carbene may no longer be the rate determining step. To evaluate this possibility, more detailed kinetic experiment was needed. Moreover, the outstanding performance of the $\text{Rh}_2(\text{R-TPPTTL})_4$ (**5.7**) in C–H insertion of cyclohexane **5.9** also inspired us to conduct systematic kinetic studies for detailed reaction profiles. The kinetic insights could drive further optimization to achieve higher catalyst TONs. Therefore, we conducted a comprehensive kinetic study using $\text{Rh}_2(\text{R-TPPTTL})_4$ (**5.7**) as standard catalyst on the model C–H insertion of cyclohexane **5.9** (**Figure 5.2**).

Following the reaction progress kinetic analysis (RPKA) methods,⁸¹ the “same excess” experiments were conducted firstly to test the catalyst robustness (**Figure 5.2a**). The “excess” here

represented the concentration difference between cyclohexane **5.9** and diazo compound **5.8a**, which was supposed to be invariable during the catalytic reaction progress. Two reactions were performed correspondingly: one is the “standard condition”, and the other one is the “same excess”. Compared with the “standard condition” experiment, “same excess” experiment had 50% less amount of diazo compound **5.8a** and same excess of cyclohexane **5.9**. Two reaction progress kinetic profiles were compared with each other at same diazo compound **5.8a** concentration point.

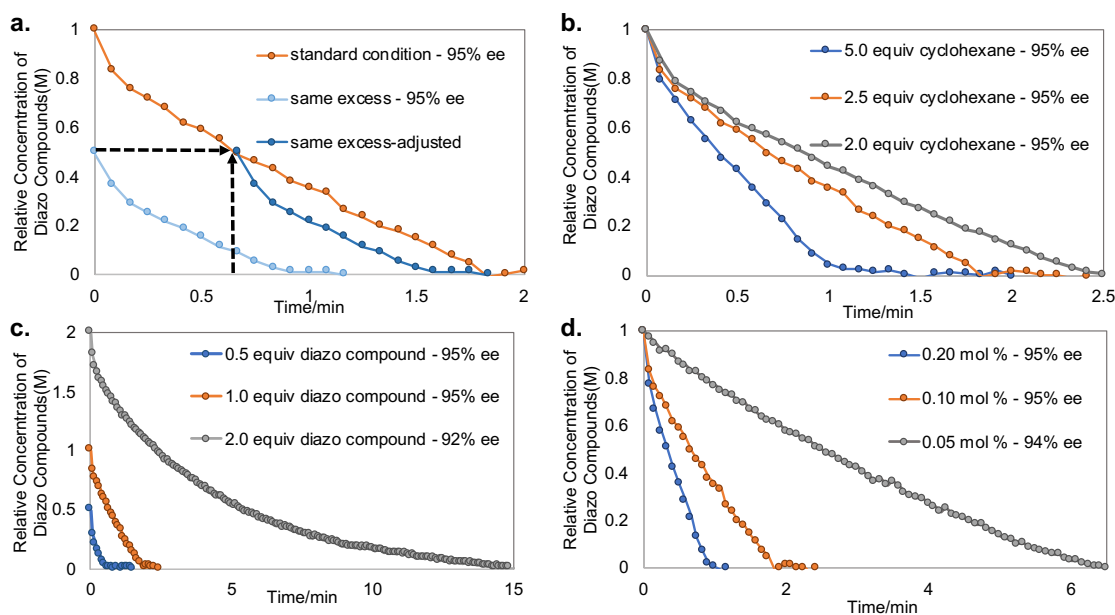
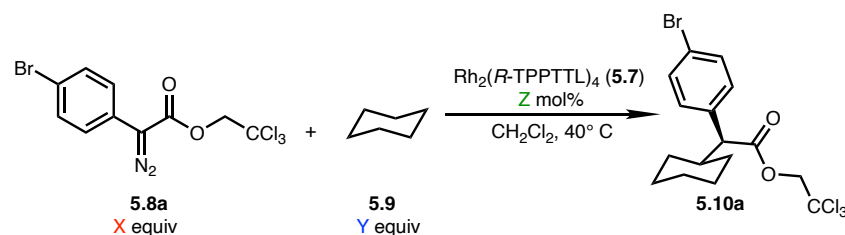
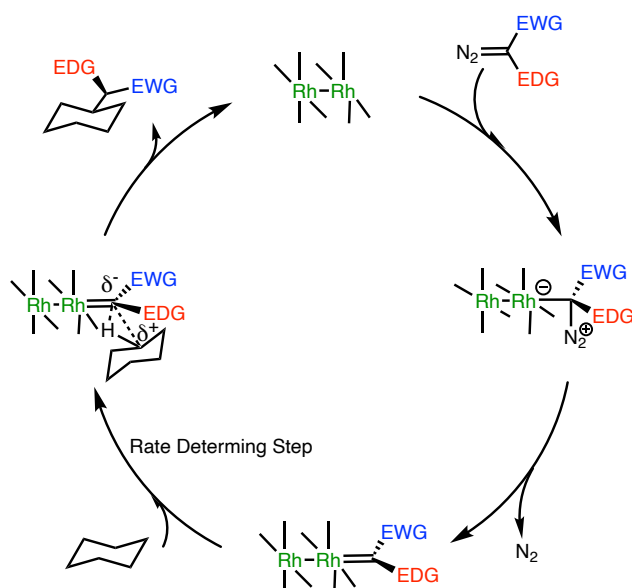


Figure 5.2 Kinetic profiles of RPKA studies for $\text{Rh}_2(\text{R-TPPTTL})_4$ (**5.7**) catalyzed C–H insertion of cyclohexane **5.9**. **a.** Same excess experiments were carried out with $[\text{excess}] = 0.075 \text{ M}$. Standard condition: $[\text{diazo}]_0 = 0.05 \text{ M}$, $[\text{cyclohexane}]_0 = 0.125 \text{ M}$; same excess: $[\text{diazo}]_0 = 0.025 \text{ M}$, $[\text{cyclohexane}]_0 = 0.1 \text{ M}$. **b.** Different excess experiments determined a positive reaction order of cyclohexane **5.9**. **c.** Different excess experiments determined a zero-order reaction of diazo compound **5.8a**. **d.** The variable time normalization analysis (VTNA) determined that the dirhodium(II) catalyst **5.7** was first order.

As showed in **Figure 5.2a**, the “standard condition” experiment exhibited a slower reaction rate at same reaction stage compared with the “same excess” one. The dirhodium(II) catalyst **5.7** in the “standard condition” had already finished 500 TONs and formed products **5.10a** while the “same excess” one has fresh catalyst without product **5.10a** present. The difference between the two kinetic profiles revealed that, at 0.1 mol% loading, some catalyst deactivation or product inhibition is occurring after 50% completion of the reaction. To further understand the driving force and encumbrance of the reaction, the “different excess” experiments were then conducted to determine the reagents’ roles in the reaction. The profiles in **Figure 5.2b** show 3 kinetic studies with varied equivalents of cyclohexane **5.9** while other factors are kept the same. The results showed more equivalents of cyclohexane **5.9** led to faster reaction rates, which indicates a positive order of cyclohexane **5.9** in the reaction. It is known that olefin moieties or Lewis basic sites in the reaction could coordinate with the dirhodium(II) catalyst and can possibly retard the reaction rate. The cyclohexane **5.9** had no functional sites to coordinate the catalysts, and might help with faster catalyst turnover frequency, which could benefit for achieving higher catalyst TON. The experiments with various equivalents of diazo compounds **5.8a**, keeping the other reaction conditions constant, were then performed (**Figure 5.2c**). The kinetic profiles showed the reactions with different diazo compound concentration gave the same initial reaction rates, which suggested zero order rate influence of the diazo compound **5.8a**. As only 0.1 mol% of the dirhodium(II) catalyst used in the reaction, higher concentration of the diazo compounds **5.8a** cannot increase the reaction rate, as the active catalyst sites were all saturated. The rate of the carbene formation step was therefore mainly controlled by the concentration of the catalyst. To further confirm the above hypothesis, the variable time normalization analysis (VTNA) method was applied to obtain the dirhodium(II) catalyst order (**Figure 5.2d**).⁸⁰ The reaction profiles at 0.2 mol%, 0.1 mol% and 0.05

mol% catalyst loading were placed in the same figure and the diazo compound **5.8a** concentration was plotted against a normalized timescale $t[\text{cat}]_T^n$ (t = time, $[\text{cat}]_T$ = total catalyst concentration, n = order of the catalyst to be determined). The “ n ” value was altered for overlapping the three curves to get the exact dirhodium(II) catalyst order. However, only when the “ n ” value equaled to 1, reaction curves of 0.2 mol% and 0.1 mol% catalyst loading overlapped, and no “ n ” value could drive 0.05 mol% catalyst loading curve to show identical trends with the other two. The result indicated that, the $\text{Rh}_2(R\text{-TPPTTL})_4$ (**5.7**) displayed the first order at normal catalyst loading. When the loading was as low as 0.05 mol%, the deactivated or decomposed dirhodium(II) catalyst ratio amplified and thus the turnover efficiency decreased. The results also suggested, with cyclohexane, the efficiency of the C–H insertion tended to significantly decrease in low catalyst loading condition. Based on above kinetic information, we proposed a catalytical cycle (**Scheme 5.2**), and accordingly a series of experiments were performed to optimize the reaction and overcome the dirhodium(II) catalysts TON limitation.



Scheme 5.2 Proposed catalytical cycle of the dirhodium(II) catalyzed C–H insertion of cyclohexane.

As cyclohexane **5.9** showed positive order in the reaction, neat conditions were applied to accelerate the reaction rate and potentially limit the chances for the rhodium carbene intermediate to destroy the catalyst.⁴³ Compared with the previous standard condition in **Figure 5.1**, the reaction using cyclohexane as solvent at 40 °C generated the products in quantitative yield and 98% ee with only 0.01 mol% catalyst loading (**Figure 5.3a**). Increasing the temperature to 60 °C further helped the reaction to finish in 20 seconds with only 0.005 mol% catalyst loading and gave 96% ee. However, the reaction with 0.0025 mol% catalyst loading did not go to completion even at higher temperature (80 °C). To further increase the catalyst TONs, adjustments were made to the carbene precursor, diazo compound **5.8** (**Figure 5.3b**). A more electron deficient diazo compound would generate a more electrophilic carbene intermediate, which would be more reactive in the rate determining step of C–H functionalization.²⁹ Therefore, a diazo compound with a strong electron withdrawing group on the aryl ring would be expected to be most effective. The result in **Figure 5.3b** showed the reaction with *p*-(trifluoromethyl)phenyldiazoacetate **5.8b** was more effective compared to the reaction with *p*-bromophenyldiazoacetate **5.8a**. The reaction completed in 1 min giving quantitative yield and 95% ee with only 0.0025 mol% catalyst loading. The electron-rich methoxy substitution **5.8c** was also tested to further clarify the carbene's electric effect on the reaction rate. With a stronger donor group, *p*-methoxy substituted diazo compound **5.8c** would form the carbene faster but the carbene would be more stable and less reactive. Virtually no reaction occurred with 0.0025 mol% catalyst loading, which is consistent with the observation that the C–H insertion is the rate determining step. A further improvement was obtained with the aryldiazoacetate **5.8d** with a trifluoroethyl ester. It gave even better enantioselectivity and results in a completed reaction in 1 min giving 96% ee and quantitative yield with 0.001 mol% catalyst

loading (**Figure 5.3c**). However, the reaction with even lower $\text{Rh}_2(R\text{-TPPTTL})_4$ (**5.7**) catalyst loading (0.0005 mol%) only proceeded to about 5% completion.

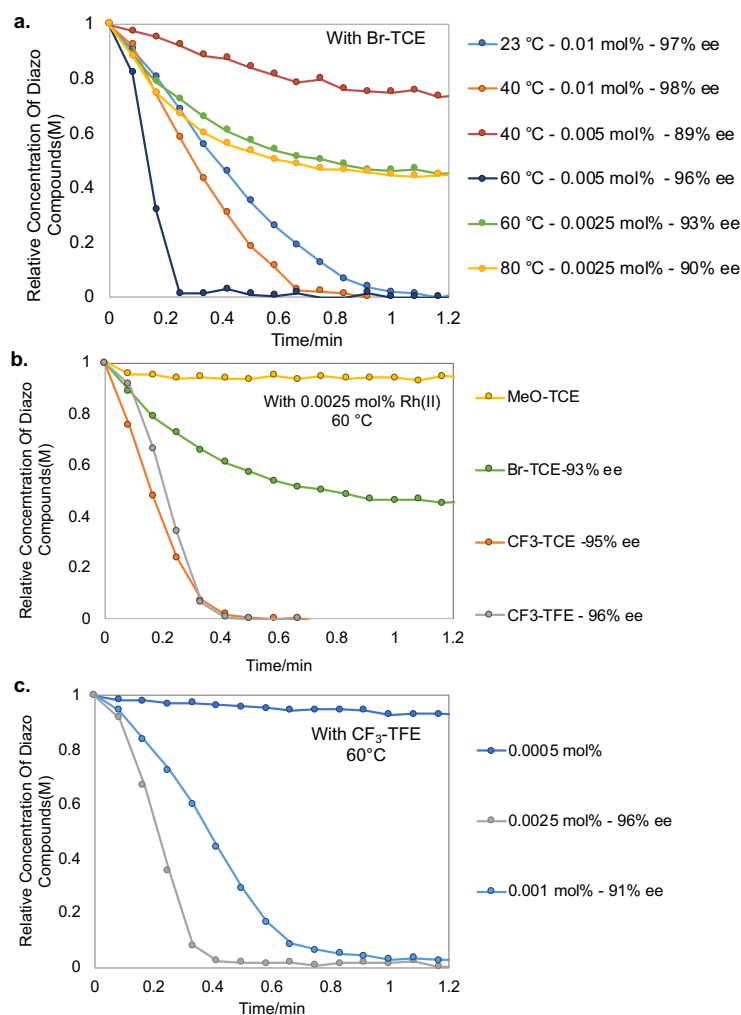
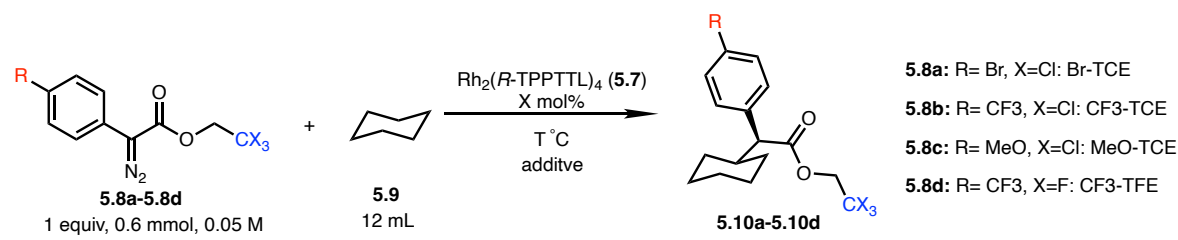


Figure 5.3 Kinetic Profiles of condition optimization of C–H insertion of cyclohexane **5.9**. **a.** Applying neat condition with various temperature and $\text{Rh}_2(R\text{-TPPTTL})_4$ (**5.7**) catalyst loading when R = Br, X = Cl. **b.** Effect of different aryldiazoacetates **5.8** structure on the reaction rate at 60 °C, 0.0025 mol% $\text{Rh}_2(R\text{-TPPTTL})_4$ (**5.7**) catalyst loading **c.** Effect of $\text{Rh}_2(R\text{-TPPTTL})_4$ (**5.7**) catalyst loading on the reaction rate when R = CF₃, X = F at 60 °C

To confirm the superior performance of the bowl-shape C_4 symmetrical catalyst $\text{Rh}_2(\text{R-TPPTTL})_4$ (**5.7**), we also compared it with the other catalysts under neat conditions with 0.005 mol% catalyst loading (**Figure 5.4**).

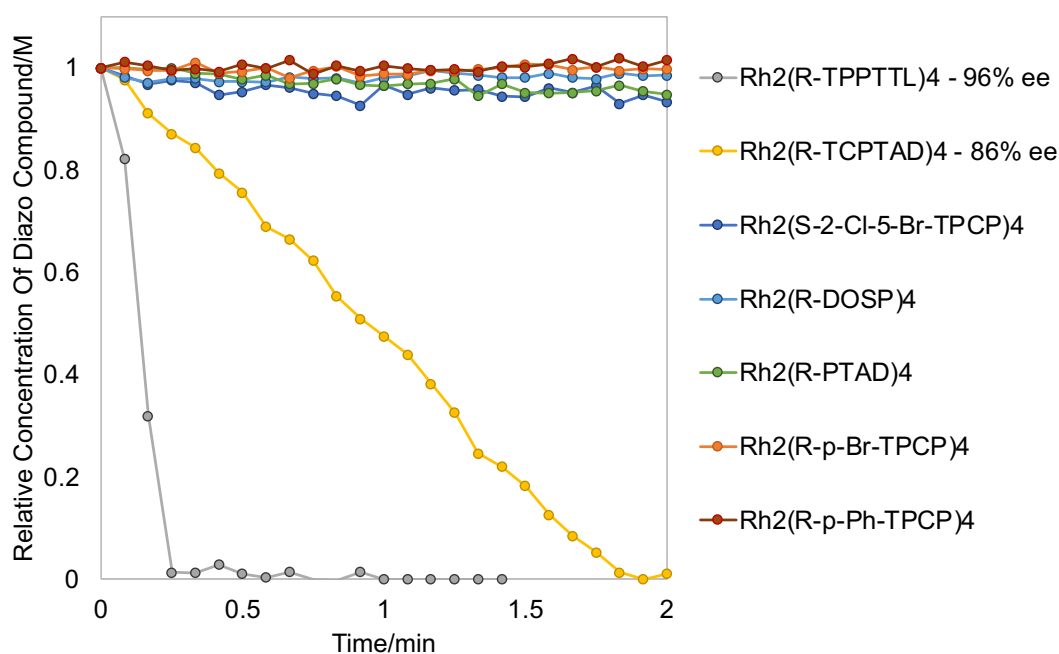
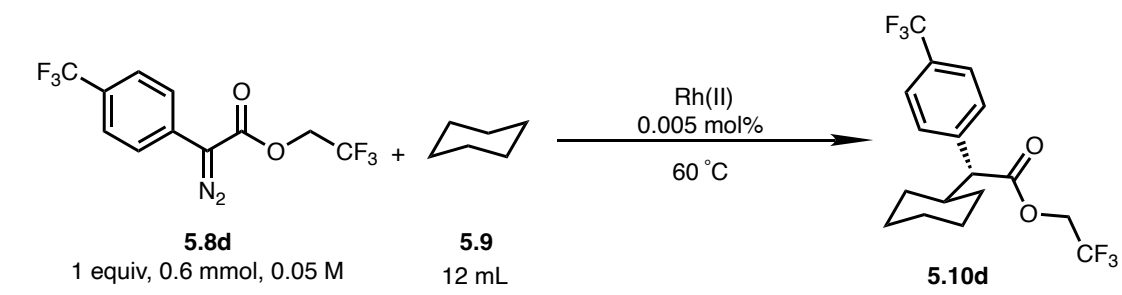


Figure 5.4 Kinetic profiles of C–H insertion of cyclohexane **5.9** catalyzed by various dirhodium(II) catalysts under neat condition.

The studies revealed that the C_4 symmetrical catalysts $\text{Rh}_2(\text{R-TPPTTL})_4$ (**5.7**), $\text{Rh}_2(\text{R-TCPTAD})_4$ (**5.6**) had high TONs and finished the reaction quickly. However, the other tested catalysts were ineffective at the low loading conditions. The results here further illustrate that the efficiency of C–H functionalization under high TON conditions was greatly influenced by the catalyst structure.

The Davies group had recently developed a series of more bulky C_4 symmetric catalysts derived from bulky N-phthalimido amino acids. As they are related to $\text{Rh}_2(R\text{-TPPTTL})_4$ (**5.7**), some were examined in this study. Among the tested catalysts, $\text{Rh}_2(S\text{-}p\text{-Br-TPPTTL})_4$ (**5.11**) showed superior performance. In the first attempted run, it completed the reaction in 3 min with only 0.0005 mol % catalyst loading and generated the product in quantitative yield and 95% ee (**Figure 5.5a**).

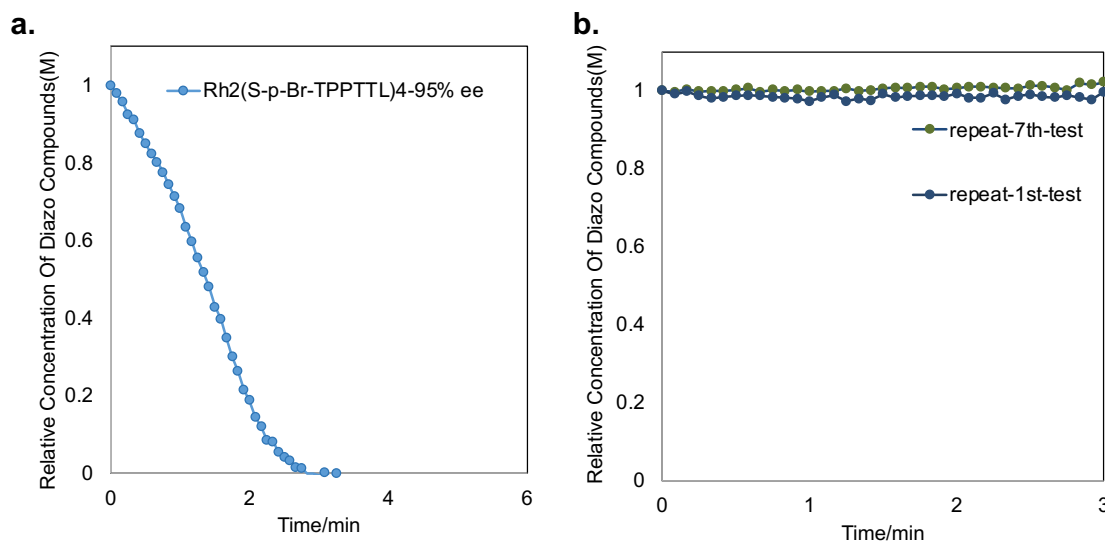
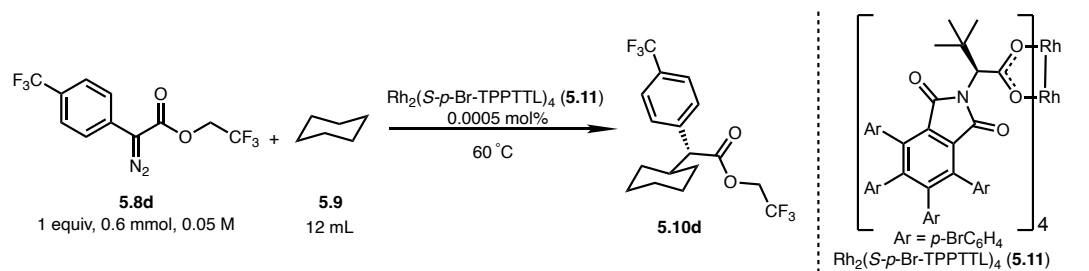


Figure 5.5 $\text{Rh}_2(S\text{-}p\text{-Br-TPPTTL})_4$ (**5.11**) catalyzed unreproducible C–H insertion reaction. **a.** $\text{Rh}_2(S\text{-}p\text{-Br-TPPTTL})_4$ (**5.11**) catalyzed C–H insertion reaction succeed at 0.0005 mol% loading. **b.** The repeated experiment showed the results were unreproducible.

However, the result could not be reproduced when a new batch of **5.8d** was used. As **Figure 5.5b** showed, the reaction failed 7 times with new batch of **5.8d** even though all the other aspects of the reaction conditions were identical to those used in **Figure 5.5a**. After checking the quality of the

starting material, the reactions worked only when the diazo compounds **5.8d** contained a small amount of N,N'-dicyclohexylcarbodiimide (**5.14**) (DCC) as an impurity. The DCC (**5.14**) was used during the esterification step to form **5.13** and in one batch of the diazo compound **5.8d** it remained as an impurity as can be seen from the $^1\text{H-NMR}$ spectrum (Figure 5.6).⁷⁴

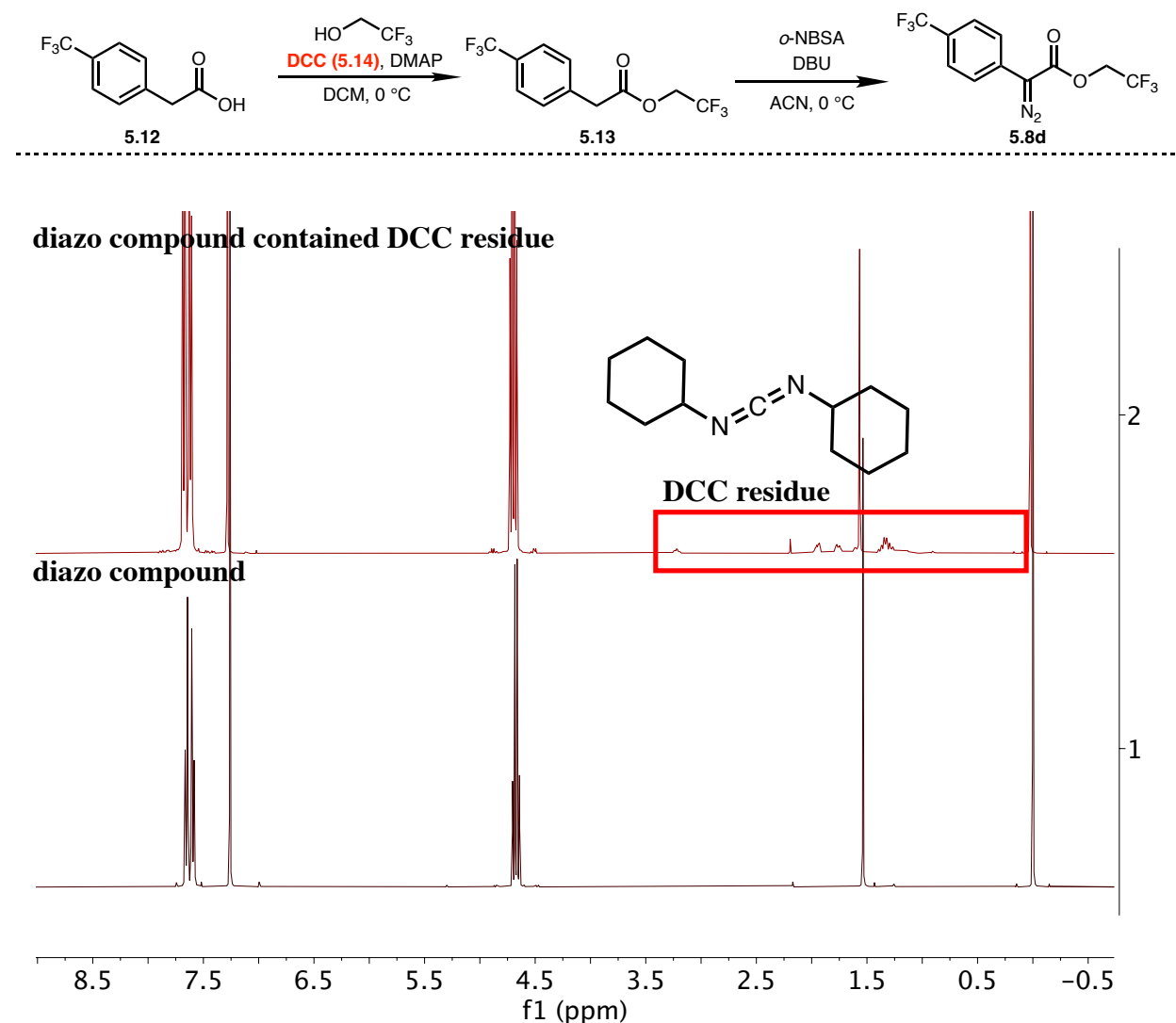


Figure 5.6 $^1\text{H-NMR}$ spectrum revealed the reaction worked when the diazo compounds **5.8d** contained DCC component: Top $^1\text{H-NMR}$: diazo compound **5.8d** contained DCC residue made the reaction worked. Bottom $^1\text{H-NMR}$: Diazo compound **5.8d** in the failed repeated reactions contained no DCC residue.

The unexpected discovery that DCC (**5.14**) had a major influence on maintaining the catalyst under high TONs conditions, motivated us to study in more detail the significance of this finding. We returned to the original high TON catalyst $\text{Rh}_2(R\text{-TPPTTL})_4$ (**5.7**) because it is easier to synthesize than the new catalysts $\text{Rh}_2(S\text{-}p\text{-Br-TPPTTL})_4$ (**5.11**) and its performance was already quite exceptional. As shown in **Figure 5.7**, the addition of 1 mol% DCC (**5.14**) dramatically helped the reaction at 0.0005 mol% $\text{Rh}_2(R\text{-TPPTTL})_4$ (**5.7**) loading to finish the reaction in 2.5 min and give the C–H functionalization product in essentially quantitative yield, 96% ee. When the reaction was conducted with 0.1 mol% DCC (**5.14**), the rate was faster but enantioselectivity was lower (91% ee). 2 mol% DCC (**5.14**) showed the slowest reaction rate, but still finished the reaction in 5 min and generated the product with 96% ee. In contrast, the C–H functionalization without DCC (**5.14**) additive showed very little reaction progress when 0.0005 mol% $\text{Rh}_2(R\text{-TPPTTL})_4$ (**5.7**) catalyst was applied.

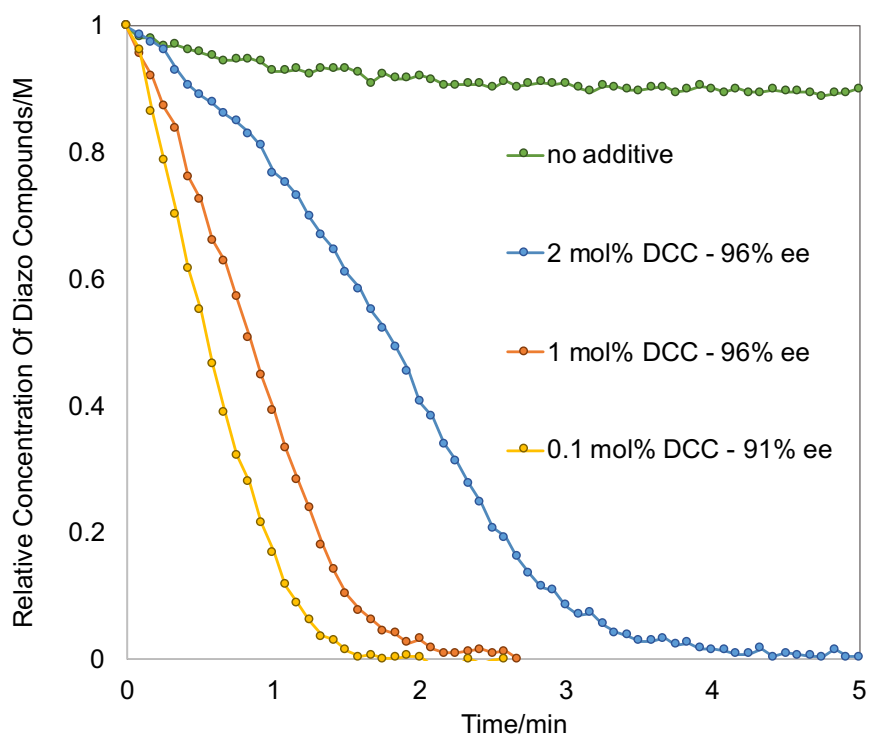
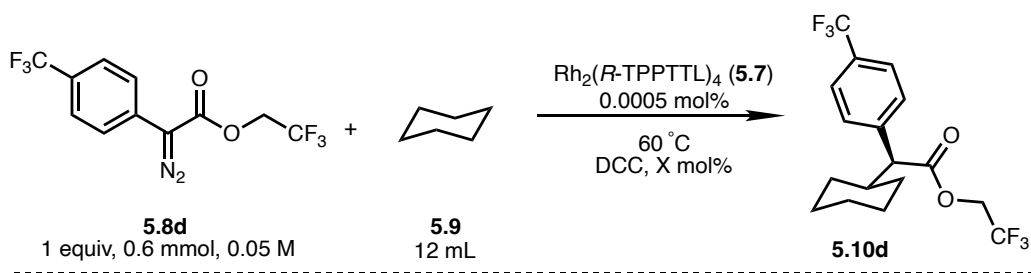


Figure 5.7 Effect of different concentration of DCC additive on the reaction kinetic profiles at 60 °C with 0.0005 mol% $\text{Rh}_2(\text{R-TPPTTL})_4$ (**5.7**) catalyst loading.

Previous studies have shown that tetramethylurea **5.15** (TMU) could modulate the reactivity and selectivity of the dirhodium(II) catalysts through the axial coordination.⁶⁹ Herein, we initially assumed DCC (**5.14**) possibly reacted with the trace water in the reaction solution and generated the urea derivatives dicyclohexylurea **5.16** (DCU) to help the reaction. To examine this assumption, both TMU (**5.15**) and DCU (**5.16**) were tested in the control experiments. As **Figure 5.8a** shown, the reaction in the presence of either urea derivatives **5.15** or **5.16** failed to proceed.

The results suggested urea derivative, which was the hydrolysis product of carbodiimide compound, had no beneficial effects on the reaction.

The other assumption was DCC (**5.14**) coordinated to the dirhodium (II) catalyst or the carbene intermediate and kept them from decomposing.^{20, 178} Therefore, a related carbodiimide compounds were screened as additives in the control experiments. Among them, N,N'-diisopropylcarbodiimide **5.17** (DIC) displayed an acceleration effect. 2 mol % DIC (**5.17**) enabled faster reaction rate, and more promisingly, 5 mol% DIC (**5.17**) further accelerated the reaction to finish in 5 min giving quantitative yield and 92% ee (**Figure 5.8b**). Therefore, carbodiimide derivatives were targeted as the useful additives to promote the reaction with extremely low catalyst loading, and DCC (**5.14**) was identified as a particularly effective one for further application.

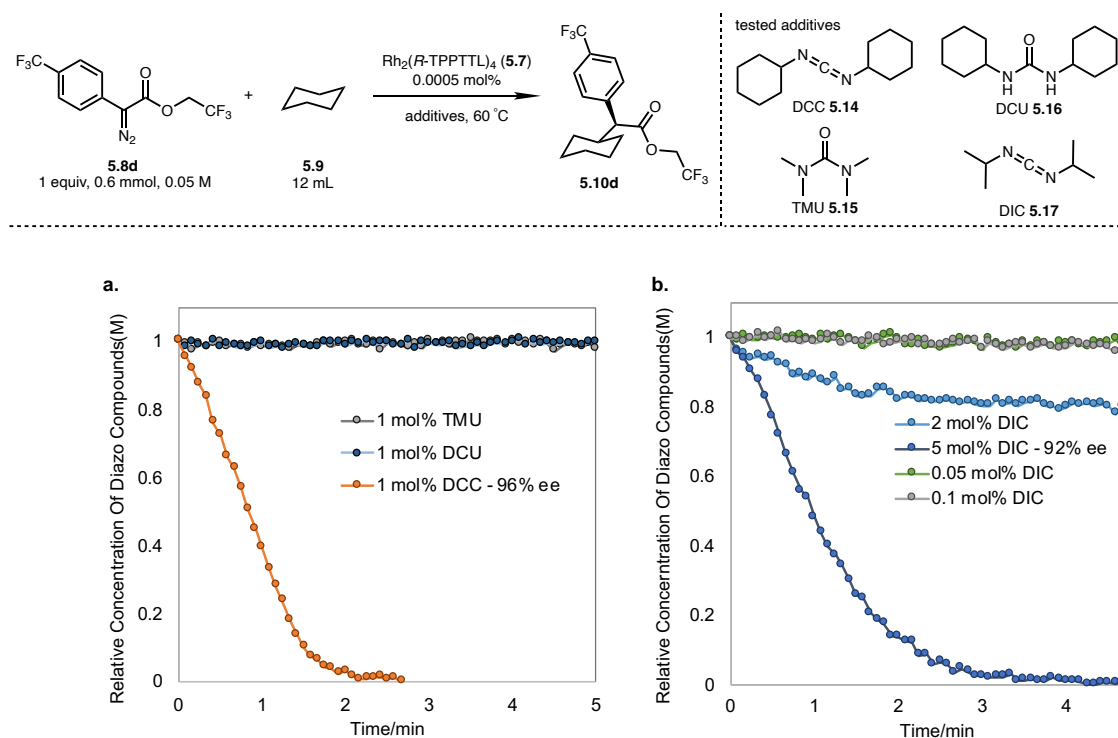


Figure 5.8 Kinetic profiles of control experiment with different additives. **a**. The reaction with 0.0005 mol% $\text{Rh}_2(\text{R-TPPTTL})_4$ (**5.7**) catalyst loading gave no progress with 1 mol% urea compounds (TMU and DCU). **b**. 5 mol% DIC showed acceleration effect on the reaction with 0.0005 mol% $\text{Rh}_2(\text{R-TPPTTL})_4$ (**5.7**) catalyst loading.

Control experiments were subsequently conducted to understand the role of DCC (**5.14**) in the reaction. As shown in **Figure 5.9**, the reaction with 0.0005 mol% $\text{Rh}_2(\text{R-TPPTTL})_4$ (**5.7**) catalyst showed little progress. When 1 mol % DCC (**5.14**) was added to the reaction, no further conversion was observed, which suggests that the original batch of catalyst has been destroyed. However, when a second batch of 0.0005 mol% $\text{Rh}_2(\text{R-TPPTTL})_4$ (**5.7**) was added, the reaction reinitiated and went to completion. The whole kinetic profile suggested the catalyst lost its reactivity without protection from DCC (**5.14**) and gave limited turnover numbers. At this stage it is considered that the presence of DCC (**5.14**) coordination prevents the rhodium-carbene intermediate from destroying the catalyst under high TON conditions.

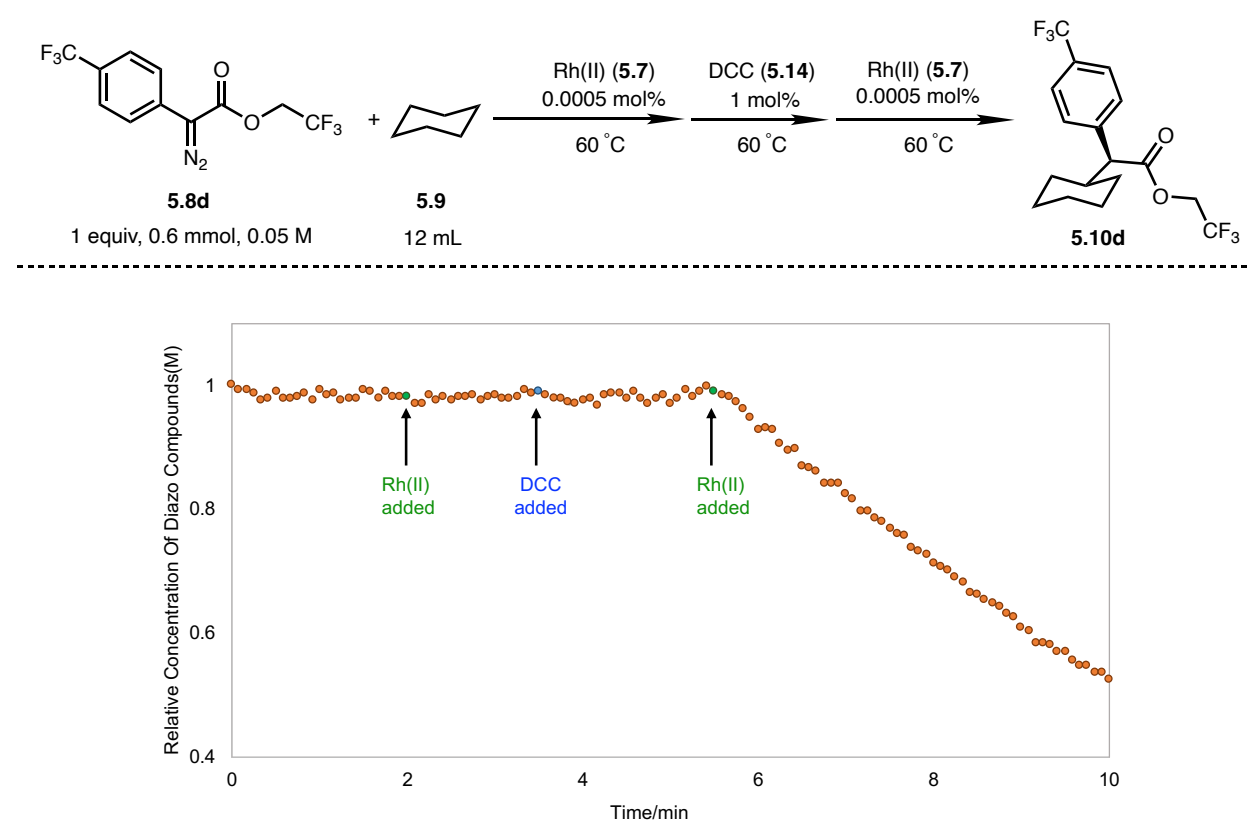


Figure 5.9 The reaction with 0.0005 mol% $\text{Rh}_2(\text{R-TPPTTL})_4$ (**5.7**) catalyst loading gives no progress until 1 mol% DCC and another 0.0005 mol% $\text{Rh}_2(\text{R-TPPTTL})_4$ (**5.7**) catalyst added.

To gain further understanding of the role of DCC (**5.14**), Jack C. Sharland conducted DFT calculations to rationalize the DCC (**5.14**) effect (**Figure 5.10**). The result showed that, compared with the normal carbene intermediate **5.18**, the carbene coordination with DCC (**5.14**) was thermodynamically favorable with -2.8 kcal/mol lower energy (**5.20**). The second DCC (**5.14**) molecule coordinated to the other rhodium atom via axial coordination further stabilized the carbene intermediate to form the lowest energy conformation (**5.21**). Based on all above information, we propose that DCC (**5.14**) coordinated to the carbene intermediate to form a low energy conformation. The coordination stabilized the carbene intermediate and protected it from decomposition. Additionally, higher concentration of DCC (**5.14**) in the reaction caused slower reaction rate because both metal centers of the dirhodium(II) catalysts were occupied by DCC (**5.14**) and cannot catalyze the reaction effectively.¹³¹

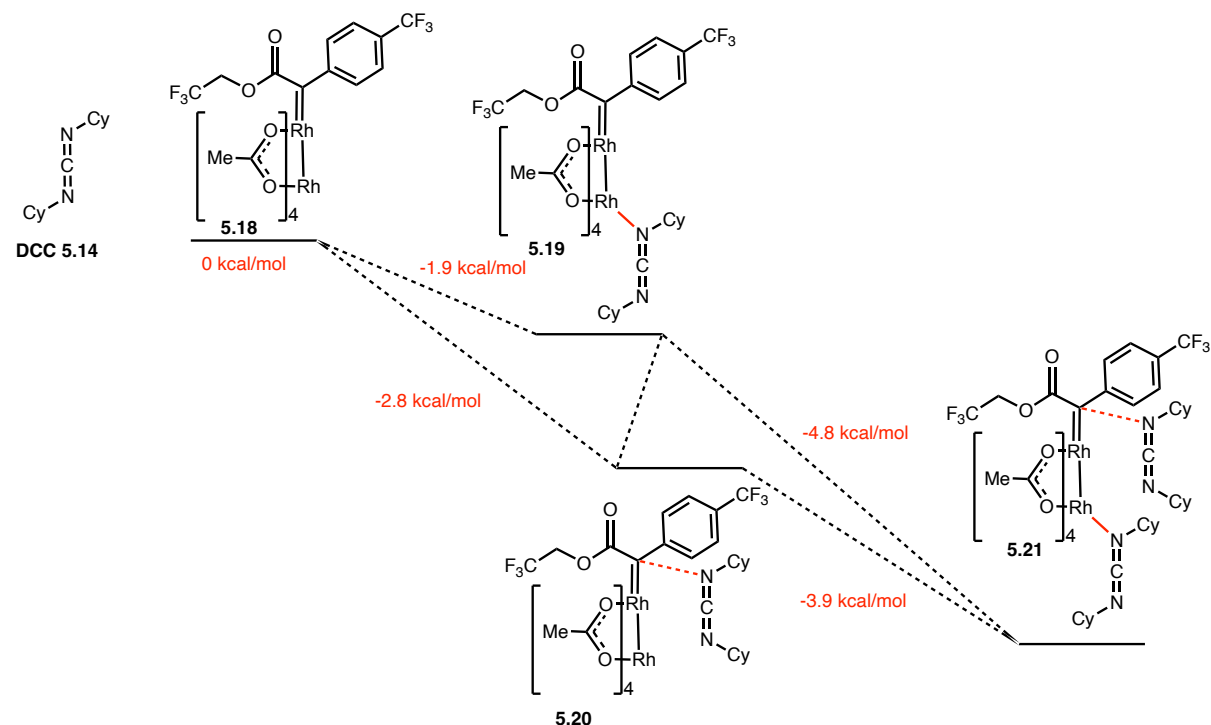
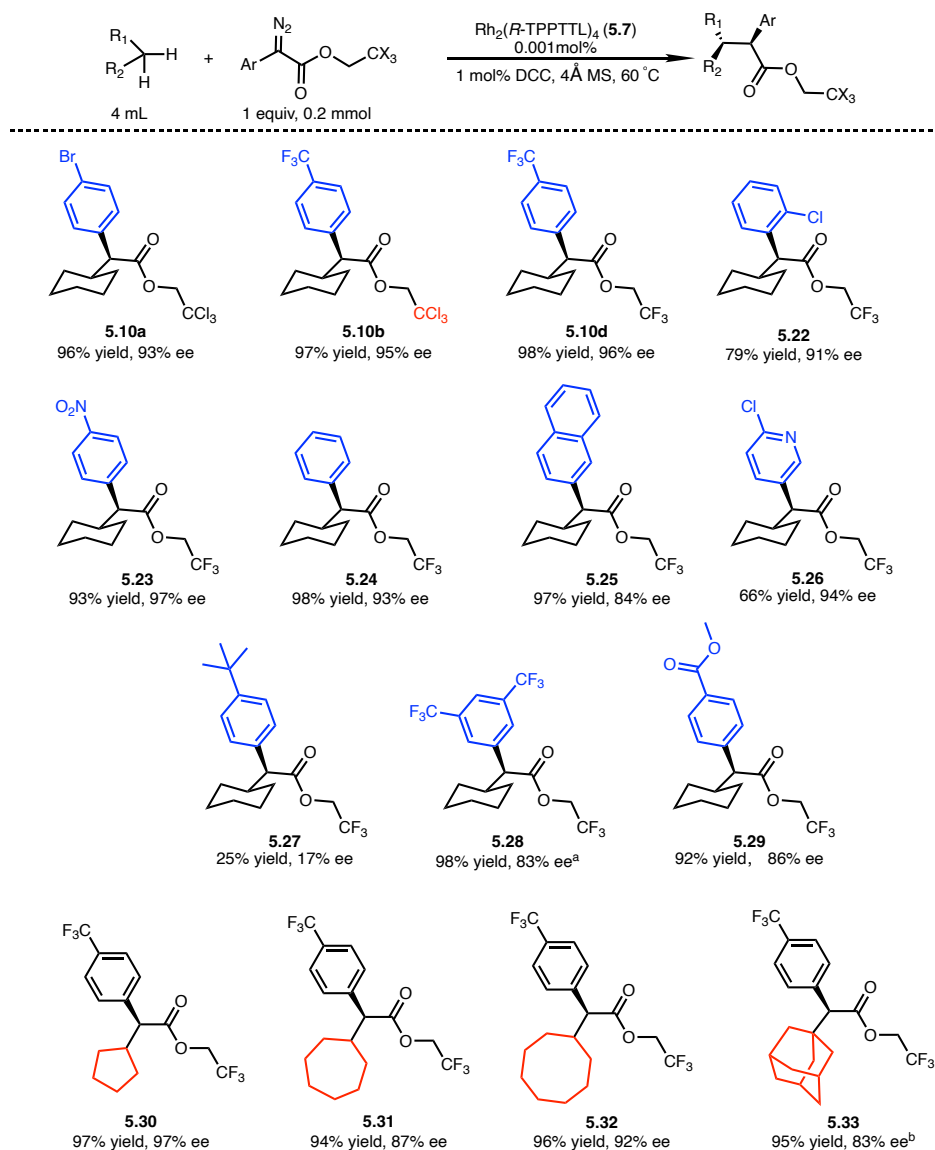


Figure 5.10 Computational study of the DCC additive effect.(DFT calculations performed at B3LYP-D3 level, 6-31G(d,p) basis set, LANL2DZ basis set used for Rh, DCM considered under PCM solvation model) (*Data from Jack C. Sharland*)

Based on the above information, 1 mol% DCC (**5.14**) as was set as optimum additive and the reaction scope was explored under these optimized conditions. As shown in **Scheme 5.3**, C–H functionalization reactions achieved high enantioselectivity and great yield consistently with various unactive substrates.



Scheme 5.3 Scopes of asymmetric C–H functionalization with 0.001 mol% $\text{Rh}_2(\text{R-TPPTTL})_4$ (**5.7**) catalyst. ^aThe reaction was conducted by $\text{Rh}_2(\text{S-2-Cl-5-Br-TPCP})_4$ (**5.5**) ^bThe reaction was conducted with 10 equiv of adamantane in 4 mL CHCl_3 .

The turnover potential of $\text{Rh}_2(\text{R-TPPTTL})_4$ (**5.7**) was further explored in a multiple additions experiment. As showed in **Figure 5.11**, cyclohexane **5.9**, 0.0005 mol% catalyst **5.7** and 1mol% DCC (**5.14**) were added first into the reaction flask. 1 equiv of diazo compound **5.8d** solid was directly added to the reaction in one portion and the reaction finished rapidly in 2.5 min. Consequently, two more batches of diazo compounds **5.8d** were added, and the catalyst finished the reaction in 96% yield and achieved about 580,000 TONs. After each addition finished, 0.2 mL mixture sample was taken to measure the enantioselectivity and the results showed that selectivity of the reaction was maintained at around 96% ee during the whole progress.

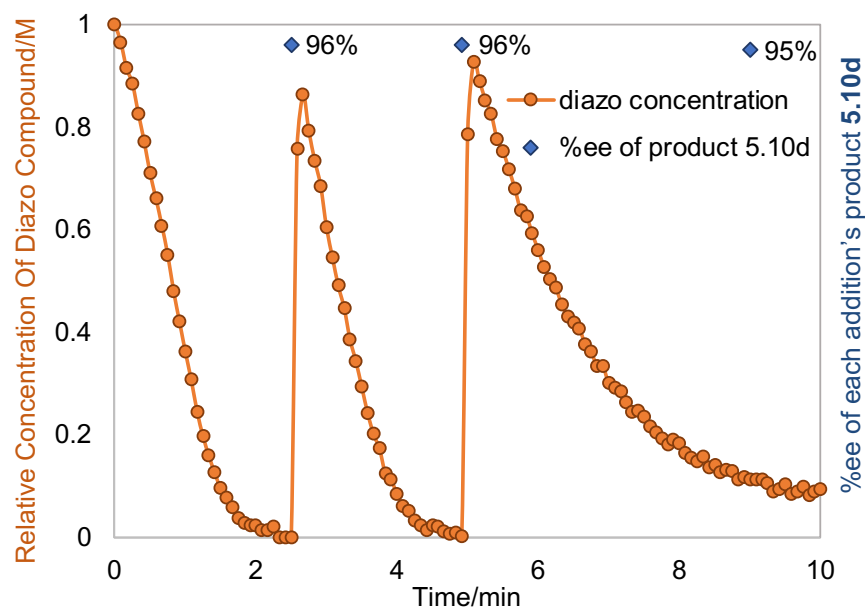
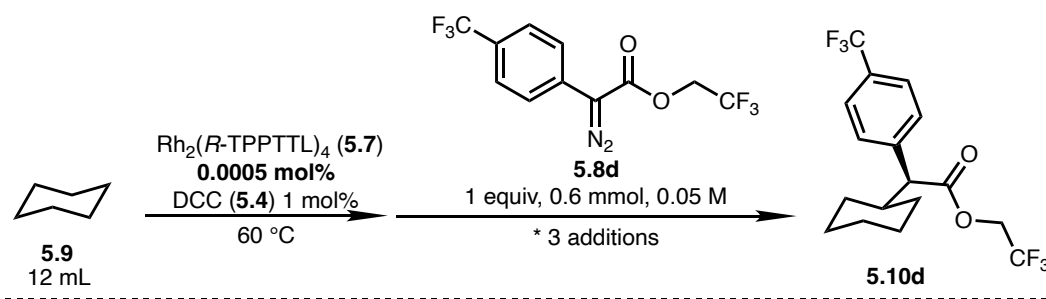


Figure 5.11 Kinetic profile of multiple-addition experiment of the C–H insertion reaction. Three successive additions of diazo compound **5.8d** (1 equiv.) were added into a solution of cyclohexane **5.9**, DCC **5.14** (1mol%) and $\text{Rh}_2(\text{R-TPPTTL})_4$ (**5.7**) (0.0005 mol %) at 60 °C.

5.3 Conclusions

In summary, a comprehensive kinetic investigation of dirhodium (II) catalyst catalyzed C–H insertion of cyclohexanes provided a deeper understanding of the reaction process. The rate law demonstrated carbene insertion was the rate determining step. Accordingly, rational optimization for higher catalyst TONs was conducted. Neat conditions, higher temperature, more electrophilic carbene intermediates were applied to help the dirhodium (II) catalysts effectively deliver the desired product under extremely low loading. Most surprisingly, 1 mol% DCC as additive was found to significantly promote the reaction. The coordination effect from DCC to the carbene intermediate was proposed to be the critical to lower the energy and prevent the carbene decomposition. Under the optimized condition, 0.001 mol% $\text{Rh}_2(\text{R-TPPTTL})_4$ (**5.7**) catalysts has been applied in a range of C–H functionalization reactions and showed great efficiency. Finally, multiple addition reaction further clarified the $\text{Rh}_2(\text{R-TPPTTL})_4$ (**5.7**) can achieve about 580,000 TONs with 96% ee. This study obtained detailed insights of the C–H functionalization progress. The kinetic profiles demonstrated the great reactivity and selectivity of the C_4 dirhodium(II) catalyzed C–H functionalization. The DCC coordination is revealed as a unique effect to enhance the catalyst robustness under extremely high TON condition. Above results will motivate more logical optimizations of C–H functionalization and inspire more rational dirhodium(II) catalysts design.

Experimental Part

6.1 General Considerations and Reagents

All reagents were obtained from commercial sources (Sigma Aldrich, Fisher, TCI Chemicals, Alfa-Aesar, Strem Chemicals, Oakwood Chemical and AK Scientific) and used as purchased or purified according to *Purification of Common Laboratory Chemicals* if necessary. Styrene was pre-purified by passing through a plug of silica gel. 4Å molecular sieves were activated under vacuum at 300 °C for 4 hours. After time elapsed, the flask was cooled to 60 °C under inert nitrogen atmosphere and stored in a 140 °C oven for future use. Dichloromethane (DCM) was purified and dried by a *Glass Contour Solvent System*, degassed by refluxing in the presence of activated 4Å molecular sieves and stored under nitrogen atmosphere. All flash column chromatography was performed on silica gel (SiliaFlash® P60, 40-63 µm). *In situ* IR reaction monitoring experiments were carried out with a Mettler Toledo ReactIR 45m instrument equipped with a 9.5 mm x 12'' AgX 1.5 m SiComp probe. ¹H, ¹³C, and ¹⁹F NMR spectra were recorded at either 400 MHz (¹³C at 101 MHz) on VNMR 400 spectrometer or 600 MHz (¹³C at 151 MHz) on INOVA 600 or Bruker 600 spectrometer. NMR spectra were run in solutions of deuterated chloroform (CDCl₃) with residual chloroform taken as an internal standard (7.26 ppm for ¹H, and 77.26 ppm for ¹³C), and were reported in parts per million (ppm). The abbreviations for multiplicity are as follows: s = singlet, d = doublet, t = triplet, q = quartet, p = pentet, m = multiplet, dd = doublet of doublet, etc. Coupling constants (J values) are obtained from the spectra. Mass spectra were taken on a Thermo Finnigan LTQ-FTMS spectrometer with APCI, ESI or NSI. Melting points (mp) were measured in open capillary tubes with a Mel-Temp Electrothermal melting points apparatus and are uncorrected. FTIR spectra were collected on a Nicolet iS10 FT-IR spectrometer from Thermo

Scientific and reported in unit of cm^{-1} . Thin layer chromatography was performed on aluminum-back silica gel plates with UV light to visualize. Optical rotations were measured on Jasco P-2000 polarimeters. Enantiomeric excess (ee) data were obtained on Chiral HPLC Varian Prostar 210, Agilent 1100, or Agilent 1290 Infinity II instruments, eluting the purified products using a mixed solution of HPLC-grade 2-propanol (iPrOH) and *n*-hexane.

6.2 Experimental Part for Chapter 2

6.2.1 General procedure for ReactIR set-up and the cyclopropanation reactions

The ReactIR instrument was filled with liquid nitrogen and allowed to equilibrate while the reaction flask was being set-up. An oven-dried 100 mL 3-neck round-bottom flask with 1.5 g 4 Å molecular sieves was fitted with a rubber septum (left neck, 14/20), ReactIR probe (center neck, 24/40 to 19/25 adapter, 19/25 neck), and argon inlet (right neck, 14/20)(**Figure 6.1**).

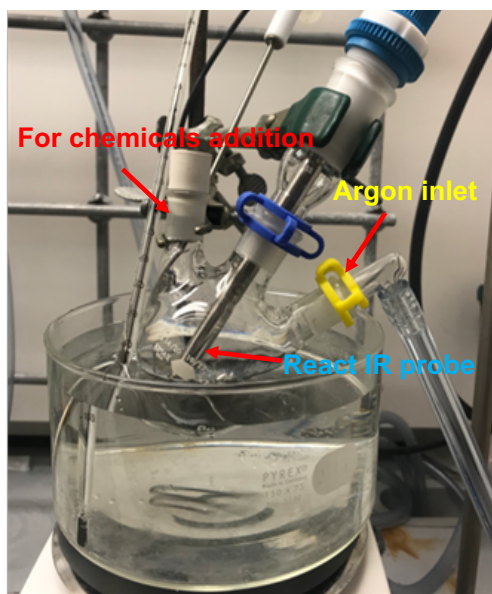


Figure 6.1 *In situ* IR apparatus set-up

The flask was cooled to room temperature under vacuum, then backfilled with argon and placed in a water or oil bath, with the temperature of the stir plate set to the desired temperature and stir

rate on 700 rpm. Once the reaction flask was at the desired temperature, the background and water vapor spectrum were taken via the ReactIR instrument. The syringe and needle used for the solvent was primed with argon before adding 27 ml solvent through the rubber septum. The data collection was started on the ReactIR™ software, and the solvent was allowed to stir for 15 min. After a reference spectrum of the solvent was taken, styrene (pre-purified by passing through a pipette column) was added using a plastic syringe. The reaction mixture was allowed to stir while the diazo compound was weighed out. A reference spectrum of styrene was taken after subtracting out the solvent spectrum, and then the diazo compound (solid) was added by removing and quickly replacing the rubber septum. A reference spectrum of the diazo compound was taken after subtracting out the reference spectrum of styrene, and the reaction mixture was allowed to stir for 15 min. 1 mL of the catalyst stock solution was added to the reaction mixture and allowed to stir until the complete consumption of the diazo compound by tracking the disappearance of the C=N₂ stretch frequencies (around 2103 cm⁻¹). Upon reaction completion, the solution was passed through a celite filter to remove molecular sieves and the solvent was removed in vacuo. The crude residue was purified based on R_f by flash column chromatography. Pure product fractions were combined, and solvent was evaporated to calculate yield. Product was characterized by chiral-HPLC. Varian Prostar to analyze enantioselectivity.

6.2.2 General Procedure for ReactIR Data Analysis

The completed diazo decomposition graph on the ReactIR™ software is shown below (**Figure 6.2**).

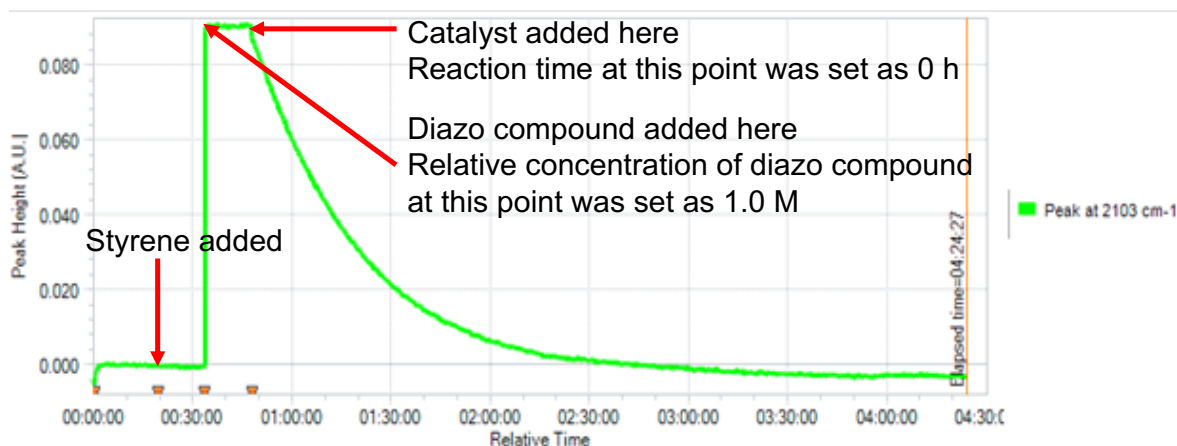


Figure 6.2 ReactIR run on software for a complete experiment

The data was extracted directly from the software as a text-file and copied into Microsoft Excel[®]. The point at which the curve rises sharply at a right angle, around the 30-min mark, was where the diazo compound was added to the reaction mixture. The catalyst solution was injected where the curve starts to decrease, around the 45-min mark. The absorbance point and relative time at which the catalyst was added, all the way until the end of the data collection period, was set as the diazo decomposition curve. The first time point in the diazo decomposition curve was set as “00:00:00” (HH:MM:SS) by subtracting the relative time at that point from itself, and all subsequent time points were set by subtracting the relative time of the beginning of the data set from the relative time extracted from **Figure 6.2**. To normalize the absorbance, the absorbance of the first point in the data set was set as “1.0 M” (actual concentration of diazo compound is 0.10 M), which was obtained from dividing the absorbance of the first point by itself, and all subsequent absorbances were divided by the absorbance of the first point. In doing so, it is possible to get the relative concentration of diazo compound over the course of the reaction and monitor the time of its decomposition.

6.2.3 Derivation of the Rate Equation

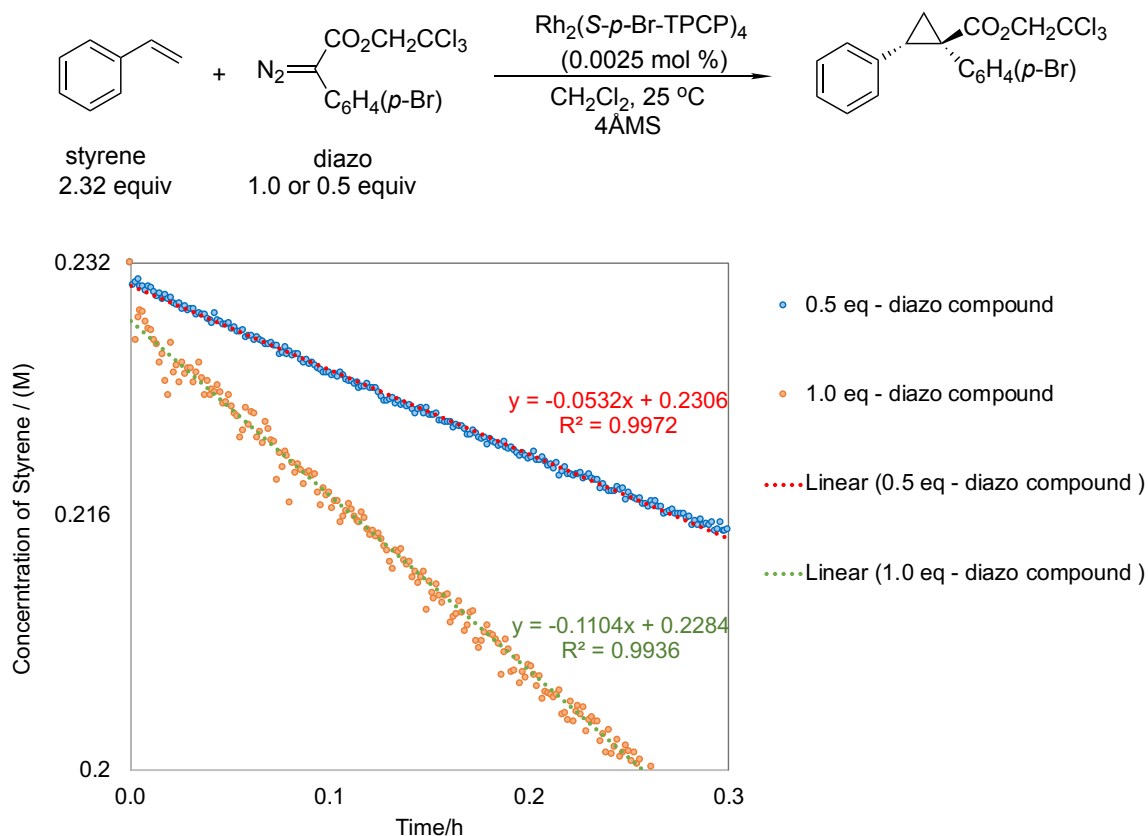


Figure 6.3 Initial 0.3 h kinetic profiles of the difference excess experiment to determine the order of the diazo compound in the benchmark cyclopropanation reaction

Table 6.1 Initial conditions and the initial rate obtained from **Figure 6.3**, the difference excess experiment, to determine the reaction order of the diazo compound in the benchmark cyclopropanation.

Entry	diazo	styrene	[excess]	ee (%)	yield (%)	initial rate (M/h)
a	0.1M	0.232M	0.132M	93	90	0.110
b	0.05M	0.232M	0.182M	93	93	0.0532

An empirical reaction rate law may be described by the power-law expression (eq 6.1):

$$\text{rate} = k_{obs} [\text{diazo}]^x [\text{styrene}]^y [\text{Rh(II)}]^z \quad \text{eq 6.1}$$

Taking the log of the rate expression gives:

$$\log[\text{rate}] = \log(k_{obs}) + x\log([\text{diazo}]) + y\log([\text{styrene}]) + z\log([\text{Rh(II)}])$$

For two sets of experiments, **a** and **b**, given in **Table 6.1**, the initial concentrations $[\text{styrene}]_0$ and $[\text{Rh(II)}]$ are identical:

$$[\text{styrene}]_{0, a} = [\text{styrene}]_{0, b}$$

$$[\text{Rh(II)}]_a = [\text{Rh(II)}]_b$$

Dividing the rates for the two conditions leaves only $[\text{diazo}]$ as a variable:

$$\frac{(\text{rate})_a = k_{obs} [\text{diazo}]_a^x [\text{styrene}]_a^y [\text{Rh(II)}]_a^z}{(\text{rate})_b = k_{obs} [\text{diazo}]_b^x [\text{styrene}]_b^y [\text{Rh(II)}]_b^z} = \frac{[\text{diazo}]_a^x}{[\text{diazo}]_b^x}$$

$$\log \left[\frac{(\text{rate})_a}{(\text{rate})_b} \right] = \log \left[\frac{[\text{diazo}]_a^x}{[\text{diazo}]_b^x} \right] = x \log \left[\frac{[\text{diazo}]_a}{[\text{diazo}]_b} \right]$$

According to the initial rate obtained in **Figure 6.3**, the reaction order of diazo compound can be determined as $x = 1$ by the following equations:

$$\log \left[\frac{(\text{rate})_a}{(\text{rate})_b} \right] = \log \left[\frac{k_{obs} [\text{diazo}]_a^x [\text{styrene}]_a^y [\text{Rh(II)}]_a^z}{k_{obs} [\text{diazo}]_b^x [\text{styrene}]_b^y [\text{Rh(II)}]_b^z} \right] = \log \left[\frac{[\text{diazo}]_a^x}{[\text{diazo}]_b^x} \right] = x \log \left[\frac{[\text{diazo}]_a}{[\text{diazo}]_b} \right] \quad \text{eq 6.2}$$

$$\log \left[\frac{(\text{rate})_a}{(\text{rate})_b} \right] = \log \left[\frac{0.110}{0.0532} \right] = x \log \left[\frac{[\text{diazo}]_a}{[\text{diazo}]_b} \right] = x \log \left[\frac{0.100}{0.0500} \right] \quad \text{eq 6.3}$$

$$x = 1.05 \approx 1 \quad \text{eq 6.4}$$

Similar treatment for the three experiments in **Figure 6.4** and **Table 6.3**, where $[\text{diazo}]_0$ and $[\text{Rh(II)}]$ are held constants, yields the order in $[\text{styrene}]$ by following steps:

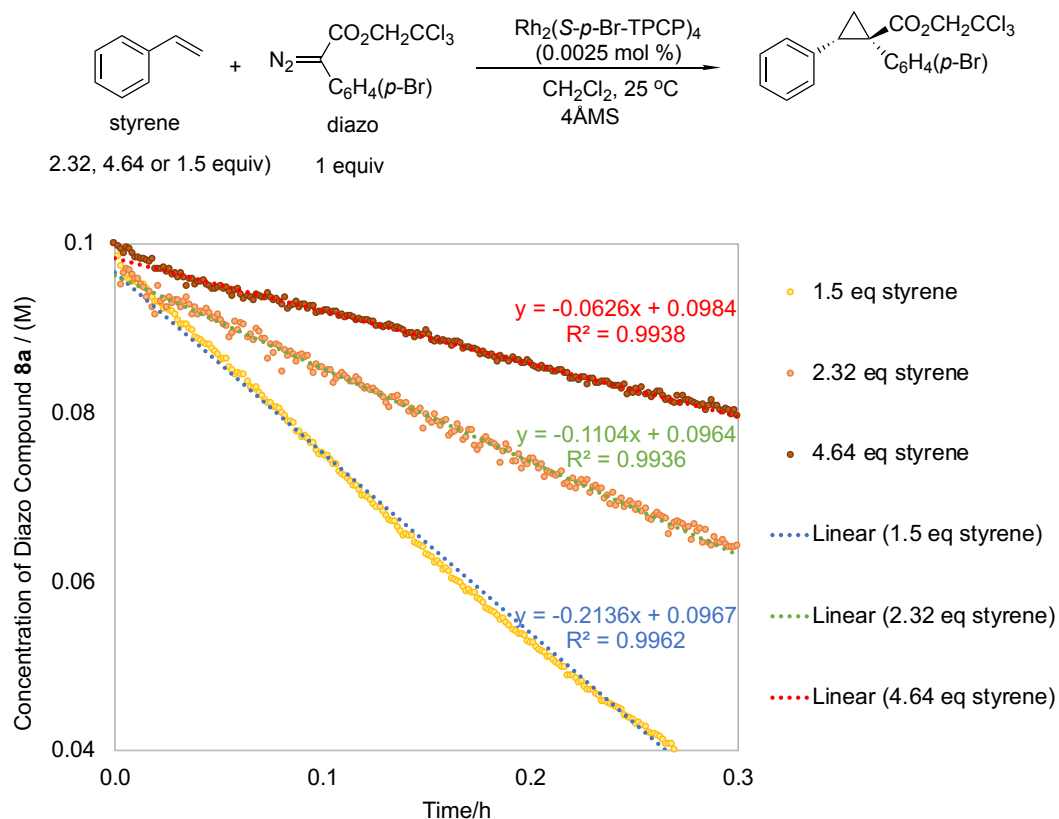


Figure 6.4 Initial 0.3 h kinetic profiles of the difference excess experiments to determine the order of styrene in the benchmark cyclopropanation reaction.

Table 6.2 Initial reagents' conditions and the initial rate obtained from **Figure 6.4**, the difference excess experiment, to determine the reaction order of styrene in benchmark cyclopropanation.

Entry	[diazo]	[styrene]	[excess]	ee (%)	yield (%)	Initial rate (M/h)
a	0.100M	0.232M	0.132M	93	90	0.110
c	0.100M	0.150M	0.05M	67	91	0.214
d	0.100M	0.464M	0.364M	93	90	0.0626

$$\begin{aligned} \log \left[\frac{(rate)_a}{(rate)_c} \right] &= \log \left[\frac{k_{obs} [diazo]_a^x [styrene]_a^y [Rh(II)]_a^z}{k_{obs} [diazo]_c^x [styrene]_c^y [Rh(II)]_c^z} \right] \\ &= \log \left[\frac{[styrene]_a^y}{[styrene]_c^y} \right] = y \log \left[\frac{[styrene]_a}{[styrene]_c} \right] \end{aligned} \quad \text{eq 6.5}$$

$$\log \left[\frac{(rate)_a}{(rate)_d} \right] = \log \left[\frac{0.110}{0.0626} \right] = y_{ad} \log \left[\frac{[styrene]_a}{[styrene]_d} \right] = y_{ad} \log \left[\frac{0.232}{0.464} \right] \quad \text{eq 6.6}$$

$$\log \left[\frac{(rate)_a}{(rate)_c} \right] = \log \left[\frac{0.110}{0.214} \right] = y_{ac} \log \left[\frac{[styrene]_a}{[styrene]_c} \right] = y_{ac} \log \left[\frac{0.232}{0.150} \right] \quad \text{eq 6.7}$$

$$\log \left[\frac{(rate)_d}{(rate)_c} \right] = \log \left[\frac{0.0626}{0.214} \right] = y_{dc} \log \left[\frac{[styrene]_d}{[styrene]_c} \right] = y_{dc} \log \left[\frac{0.464}{0.150} \right] \quad \text{eq 6.8}$$

$$y_{ad} = -0.813 \quad \text{eq 6.9}$$

$$y_{ac} = -1.53 \quad \text{eq 6.10}$$

$$y_{dc} = -1.09 \quad \text{eq 6.11}$$

$$\text{Take the average, } y = -1.14 \approx -1 \quad \text{eq 6.12}$$

Above all the rate expression is obtained in **eq 6.13**:

$$\text{rate} = k_{obs} [diazo]^1 [styrene]^{-1} [Rh(II)]^1 \quad \text{eq 6.13}$$

The catalytic cycle exhibits first order kinetics both in diazo compound [*diazo*] and [*Rh(II)*], which act as driving forces for the cyclopropanation reaction. And *styrene* has a reaction order of -1, which means it must become dissociated with the transition state complex in order to generate a carbene. Therefore, the mechanism can be stated explicitly (**Figure 6.5**).

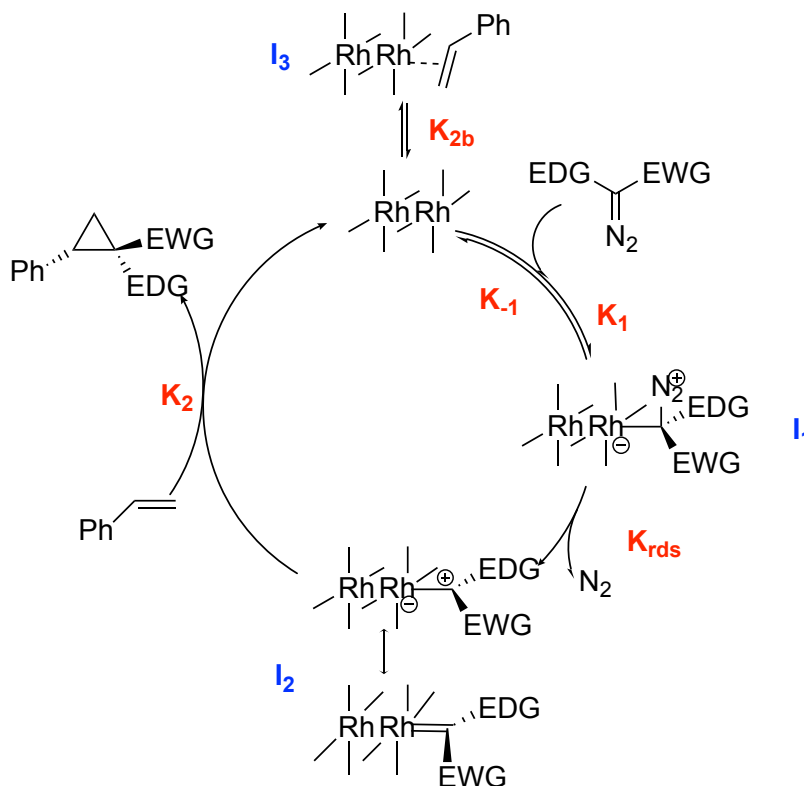


Figure 6.5 The catalytic cycle for the benchmark cyclopropanation reaction according to the obtained rate law eq 6.13.

The reaction cycle above is consistent with the kinetic data obtained from this work. The elementary steps of the reaction, as well as the mathematical descriptions of the intermediate species' concentration, are shown in **Scheme 6.1**. On-cycle steps can help reaction progression while off-cycle steps may contribute to deactivation/activation of the catalyst or slowing of the reaction rate.

On-cycle Steps	
Rh(II) + diazo I ₁	(S1-1)
I ₁ I ₂ + N ₂	(S1-2)
I ₂ + styrene product+ Rh(II)	(S1-3)
Off-cycle Step	
Rh(II)+ styrene I ₃	(S1-4)

Scheme 6.1 Elementary steps of the defined mechanism for the benchmark cyclopropanation reaction.

As shown in **Scheme 6.1** and **Figure 6.5**, on cycle step include: reversible dirhodium (II) catalyst (Rh(II)) complexation with diazo compound to generate intermediate **I**₁ (S1-1), extrusion of nitrogen to give the dirhodium (II) carbene **I**₂ (S1-2), **I**₂ combines with styrene to form the product and regeneration of the free dirhodium (II) catalyst (S1-3). The dirhodium (II) catalyst reversibly coordinates to styrene to form off-cycle reservoirs **I**₃ (S1-4). The rate-determining step is S1-2 and the elementary steps prior to S1-2 step are also important to the overall reaction. As shown in **eq 6.14**, the contributions of steps after the rate determining step S1-2 are negligible.

$$rate = K_{rds}[I_1] \quad \text{eq 6.14}$$

Here we use a steady-state approximation to get **eq 6.15**:

$$\begin{aligned}\frac{d[I_1]}{dt} &= K_1[\text{Rh(II)}][\mathbf{diazo}] - K_{-1}[I_1] - K_{rds}[I_1] \\ &= K_1[\text{Rh(II)}][\mathbf{diazo}] - (K_{-1} + K_{rds})[I_1] = 0 \quad \mathbf{eq\ 6.15}\end{aligned}$$

The **eq 6.15** is then rearranged to give the concentration of I_1 in **eq 6.16**

$$[I_1] = \frac{K_1[\text{Rh(II)}][\mathbf{diazo}]}{K_{-1} + K_{rds}} \quad \mathbf{eq\ 6.16}$$

Because K_1 , K_{-1} , K_{rds} are all constants, α is used to represent $\frac{K_1}{K_{-1} + K_{rds}}$ To get **eq 6.17**:

$$[I_1] = \alpha[\text{Rh(II)}][\mathbf{diazo}] \quad \mathbf{eq\ 6.17}$$

Then we move to determine the catalyst mass balance as **eq 6.18**

$$\begin{aligned}[\text{Rh(II)}]_{total} &= [\text{Rh(II)}] + [I_1] + [I_3] = [\text{Rh(II)}] + \alpha[\text{Rh(II)}][\mathbf{diazo}] + K_{2b}[\text{Rh(II)}][\mathbf{styrene}] \\ &= [\text{Rh(II)}](1 + \alpha[\mathbf{diazo}] + K_{2b}[\mathbf{styrene}]) \quad \mathbf{eq\ 6.18}\end{aligned}$$

eq 6.18 then is rearranged to give the $[\text{Rh(II)}]$ in **eq 6.19**:

$$[\text{Rh(II)}] = \frac{[\text{Rh(II)}]_{total}}{(1 + \alpha[\mathbf{diazo}] + K_{2b}[\mathbf{styrene}])} \quad \mathbf{eq\ 6.19}$$

According to **eq 6.17** and **eq 6.19**, the concentration of I_1 is defined by **eq 6.20**

$$[I_1] = \alpha \frac{[\text{Rh(II)}]_{\text{total}}}{(1 + \alpha[\text{diazo}] + K_{2b}[\text{styrene}])} [\text{diazo}] \quad \text{eq 6.20}$$

Once $[I_1]$ is fully defined, it is substituted into the generic rate **eq 6.14** to get **eq 6.21**, which is a mathematical description of the reaction.

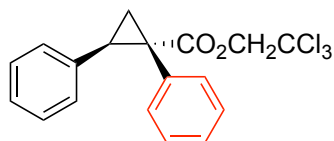
$$\text{rate} = \frac{K_{rds}\alpha[\text{Rh(II)}]_{\text{total}}[\text{diazo}]}{(1 + \alpha[\text{diazo}] + K_{2b}[\text{styrene}])} \quad \text{eq 6.21}$$

Here we can compare the steady-state catalytic form of the reaction law **eq 6.21** and the empirical description **eq 6.13**

$$\text{rate} = \frac{K_{rds}\alpha[\text{Rh(II)}]_{\text{total}}[\text{diazo}]}{(1 + \alpha[\text{diazo}] + K_{2b}[\text{styrene}])} = k_{\text{obs}} [\text{diazo}]^1 [\text{styrene}]^{-1} [\text{Rh(II)}]^1$$

Both forms demonstrate that the dirhodium (II) catalyst is first order with respect to benchmark cyclopropanation, which also confirms the dirhodium (II) complex is an active catalyst. The off-cycle reservoir, I_3 , decreased the active steady-state concentration of the dirhodium (II) catalyst within the catalytic cycle throughout the reaction. However, the enantioselectivity results in **Table 6.2** suggests that off-cycle reservoirs formed through styrene coordination may also prevent the dirhodium (II) catalyst catalysts from deactivation helping to maintain effectiveness and mitigate decomposition.

6.2.4 Characterization of the cyclopropanation products



2.9

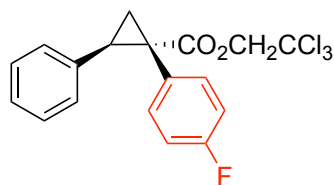
2,2-trichloroethyl (1*S*,2*R*)-1,2-diphenylcyclopropane-1-carboxylate

This compound was prepared according to the general procedure 3.1 for cyclopropanation reactions, using styrene (6.24 mmol, 650.0 mg, 2.32 equiv.) as the substrate, 2,2,2-trichloroethyl 2-diazo-2-phenylacetate (2.69 mmol, 789.6 mg, 1.0 equiv.) and $\text{Rh}_2(\text{R-}p\text{-Ph-TPCP})_4$ catalyst (0.0000269 mmol, 0.0474 mg, 0.001 mol %). After flash chromatography (0%, then 5% - 15% Et_2O in hexanes) the product was obtained as a white solid (885.2 mg, 89% yield).

$^1\text{H NMR}$ (400 MHz, Chloroform-*d*) δ 7.17 – 7.10 (m, 3H), 7.07 (hept, $J = 3.1$ Hz, 5H), 6.80 (dd, $J = 6.7, 3.0$ Hz, 2H), 4.84 (d, $J = 11.9$ Hz, 1H), 4.64 (d, $J = 11.9$ Hz, 1H), 3.22 (dd, $J = 9.4, 7.4$ Hz, 1H), 2.28 (dd, $J = 9.4, 5.1$ Hz, 1H), 2.01 (dd, $J = 7.4, 5.1$ Hz, 1H).

$^{13}\text{C NMR}$ (151 MHz, Chloroform-*d*) δ 172.26, 135.88, 133.81, 132.16, 128.26, 127.94, 127.83, 127.43, 126.73, 95.21, 74.51, 37.37, 33.99, 20.43.

Chiral HPLC: (OJ-H, 30 min, 1 mL/min, 1 % iPrOH in hexanes, UV 230 nm) tR: Major: 15.3 min, Minor: 9.0 min, 94% ee.



2.10

2,2,2-trichloroethyl (1*S*,2*R*)-1-(4-fluorophenyl)-2-phenylcyclopropane-1-carboxylate

This compound was prepared according to the general procedure 3.1 for cyclopropanation reactions, using styrene (6.24 mmol, 650.0 mg, 2.32 equiv.) as the substrate, 2,2,2-trichloroethyl

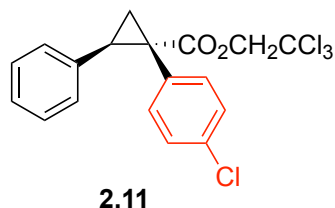
2-diazo-2-(4-fluorophenyl)acetate (2.69 mmol, 838.0 mg, 1.0 equiv.), and $\text{Rh}_2(\text{R-}p\text{-Ph-TPCP})_4$ catalyst (0.0000269 mmol, 0.0474 mg, 0.001 mol %). After flash chromatography (0 %, then 5 % - 15 % Et_2O in hexanes) the product was obtained as a white solid (938.5 mg, 90 % yield).

$^1\text{H NMR}$ (400 MHz, Chloroform-*d*) δ 7.16 – 7.08 (m, 3H), 7.07 – 6.98 (m, 2H), 6.87 – 6.74 (m, 4H), 4.82 (d, $J = 11.9$ Hz, 1H), 4.65 (d, $J = 11.9$ Hz, 1H), 3.21 (dd, $J = 9.4, 7.4$ Hz, 1H), 2.29 (dd, $J = 9.4, 5.2$ Hz, 1H), 1.98 (dd, $J = 7.4, 5.2$ Hz, 1H).

$^{13}\text{C NMR}$ (151 MHz, Chloroform-*d*) δ 172.08, 135.56, 133.77, 133.71, 129.78, 128.24, 128.08, 126.91, 114.91, 114.76, 95.13, 74.56, 36.57, 34.07, 20.55.

$^{19}\text{F NMR}$ (376 MHz, Chloroform-*d*) δ -114.59.

Chiral HPLC: (OJ-H, 30 min, 1 mL/min, 1 % *i*PrOH in hexanes, UV 230 nm) tR: Major: 14.4 min, Minor: 8.8 min, 95% ee.



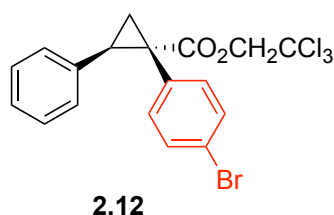
2,2,2-trichloroethyl (1*S*,2*R*)-1-(4-chlorophenyl)-2-phenylcyclopropane-1-carboxylate

This compound was prepared according to the general procedure 3.1 for cyclopropanation reactions, using styrene (6.24 mmol, 650.0 mg, 2.32 equiv.) as the substrate, 2,2,2-trichloroethyl 2-(4-chlorophenyl)-2-diazoacetate (2.69 mmol, 882.2 mg, 1.0 equiv.), and $\text{Rh}_2(\text{R-}p\text{-Ph-TPCP})_4$ catalyst (0.0000269 mmol, 0.0474 mg, 0.001 mol %). After flash chromatography (0%, then 5% - 15% Et_2O in hexanes) the product was obtained as a white solid (967.5 mg, 89% yield).

$^1\text{H NMR}$ (400 MHz, Chloroform-*d*) δ 7.17 – 7.06 (m, 5H), 7.04 – 6.95 (m, 2H), 6.80 (dd, $J = 6.6, 3.0$ Hz, 2H), 4.83 (d, $J = 11.9$ Hz, 1H), 4.64 (d, $J = 11.9$ Hz, 1H), 3.22 (dd, $J = 9.4, 7.5$ Hz, 1H), 2.29 (dd, $J = 9.4, 5.2$ Hz, 1H), 1.98 (dd, $J = 7.5, 5.2$ Hz, 1H).

^{13}C NMR (151 MHz, Chloroform-*d*) δ 171.83, 135.39, 133.44, 133.39, 132.55, 128.23, 128.16, 128.11, 127.00, 95.11, 74.55, 36.66, 34.12, 20.37.

Chiral HPLC: (OJ-H, 30 min, 1 mL/min, 1 % iPrOH in hexanes, UV 230 nm) tR: Major: 13.2 min, Minor: 8.3 min, 96% ee.



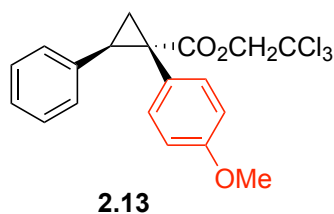
2,2,2-trichloroethyl (1*S*,2*R*)-1-(4-bromophenyl)-2-phenylcyclopropane-1-carboxylate

This compound was prepared according to the general procedure 3.1 for cyclopropanation reactions, using styrene (6.24 mmol, 650.0 mg, 2.32 equiv.) as the substrate, 2,2,2-trichloroethyl 2-(4-bromophenyl)-2-diazoacetate (2.69 mmol, 1000.0 mg, 1.0 equiv.) and $\text{Rh}_2(\text{R-}p\text{-Ph-TPCP})_4$ catalyst (0.0000269 mmol, 0.0474 mg, 0.001 mol %). After flash chromatography (0%, then 5% - 15% Et₂O in hexanes) the product was obtained as a white solid (1110.0 mg, 90% yield).

^1H NMR (400 MHz, Chloroform-*d*) δ 7.28 – 7.24 (m, 3H), 7.16 – 7.05 (m, 2H), 6.98 – 6.86 (m, 2H), 6.86 – 6.75 (m, 2H), 4.83 (d, $J = 11.9$ Hz, 1H), 4.64 (d, $J = 11.9$ Hz, 1H), 3.22 (dd, $J = 9.4$, 7.5 Hz, 1H), 2.28 (dd, $J = 9.4$, 5.2 Hz, 1H), 1.97 (dd, $J = 7.5$, 5.2 Hz, 1H).

^{13}C NMR (151 MHz, Chloroform-*d*) δ 171.74, 135.35, 133.79, 133.07, 131.06, 128.23, 128.18, 127.02, 121.67, 95.10, 74.54, 36.74, 34.09, 20.32.

Chiral HPLC: (OJ-H, 30 min, 1 mL/min, 1 % iPrOH in hexanes, UV 230 nm) tR: Major: 13.4 min, Minor: 8.8 min, 96% ee.



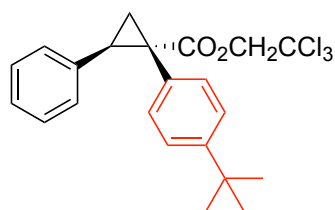
2,2,2-trichloroethyl (1*S*,2*R*)-1-(4-methoxyphenyl)-2-phenylcyclopropane-1-carboxylate

This compound was prepared according to the general procedure 3.1 for cyclopropanation reactions, using styrene (6.24 mmol, 650.0 mg, 2.32 equiv.) as the substrate, 2,2,2-trichloroethyl 2-diazo-2-(4-methoxyphenyl)acetate (2.69 mmol, 870.3 mg, 1.0 equiv), and Rh₂(*R-p*-Ph-TPCP)₄ catalyst (0.0000269 mmol, 0.0474 mg, 0.001 mol %). After flash chromatography (0%, then 5% - 15% Et₂O in hexanes) the product was obtained as a clear oil (967.6 mg, 90% yield).

¹H NMR (400 MHz, Chloroform-*d*) δ 7.15 – 7.05 (m, 3H), 7.05 – 6.95 (m, 2H), 6.88 – 6.78 (m, 2H), 6.73 – 6.63 (m, 2H), 4.86 (d, *J* = 11.9 Hz, 1H), 4.66 (d, *J* = 11.9 Hz, 1H), 3.72 (s, 3H), 3.20 (dd, *J* = 9.4, 7.4 Hz, 1H), 2.29 (dd, *J* = 9.4, 5.0 Hz, 1H), 1.97 (dd, *J* = 7.4, 5.0 Hz, 1H).

¹³C NMR (151 MHz, Chloroform-*d*) δ 172.52, 158.82, 136.03, 133.21, 128.33, 127.99, 126.71, 125.94, 113.33, 95.33, 74.49, 55.25, 36.71, 34.07, 20.66.

Chiral HPLC: (*R,R*-Whelk , 45 min, 1 mL/min, 1 % iPrOH in hexanes, UV 230 nm) tR: Major: 30.3 min, Minor: 19.7 min, 94% ee.



2.14

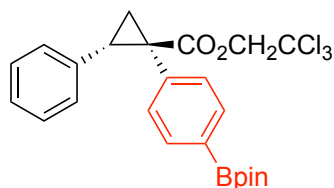
2,2,2-trichloroethyl (1*S*,2*R*)-1-(4-*tert*-butylphenyl)-2-phenylcyclopropane-1-carboxylate

This compound was prepared according to the general procedure 3.1 for cyclopropanation reactions, using styrene (6.24 mmol, 650.0 mg, 2.32 equiv.) as the substrate, 2,2,2-trichloroethyl 2-(4-(*tert*-butyl)phenyl)-2-diazoacetate (2.69 mmol, 940.5 mg, 1.0 equiv.), and Rh₂(*R-p*-Ph-TPCP)₄ catalyst (0.0000269 mmol, 0.0474 mg, 0.001 mol %). After flash chromatography (0%, then 5% - 15% Et₂O in hexanes) the product was obtained as a white solid (1030.8 mg, 90 % yield).

¹H NMR (400 MHz, Chloroform-*d*) δ 7.18 – 7.10 (m, 2H), 7.07(dd, $J=4.9, 1.8$ Hz, 3H), 7.01 – 6.95 (m, 2H), 6.79(dtd, $J=4.9, 3.2, 2.7, 1.4$ Hz, 2H), 4.84 (d, $J=11.9$ Hz, 1H), 4.66 (d, $J=11.9$ Hz, 1H), 3.20 (dd, $J=9.4, 7.4$ Hz, 1H), 2.29 (dd, $J=9.4, 5.0$ Hz, 1H), 1.98 (dd, $J=7.4, 5.1$ Hz, 1H), 1.23 (s, 9H).

¹³C NMR (151 MHz, Chloroform-*d*) δ 172.35, 150.27, 136.06, 131.70, 130.62, 128.25, 127.80, 126.59, 124.70, 95.29, 74.40, 37.01, 34.52, 33.87, 31.39, 20.49.

Chiral HPLC: (*R,R*-Whelk, 30 min, 1 mL/min, 1 % iPrOH in hexanes, UV 230 nm) tR: Major: 11.2min, Minor: 8.4 min, 98% ee.



2.15

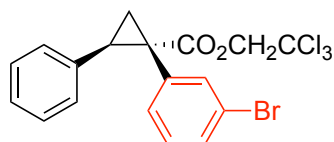
2,2,2-trichloroethyl(1*S*,2*R*)-2-phenyl-1-(4-(4,4,5,5-tetramethyl-1,3,2-dioxaborolan-2-yl)phenyl)cyclopropane-1-carboxylate

This compound was prepared according to the general procedure 3.1 for cyclopropanation reactions, using styrene (6.24 mmol, 650.0 mg, 2.32 equiv.) as the substrate, 2,2,2-trichloroethyl 2-diazo-2-(4-(4,4,5,5-tetramethyl-1,3,2-dioxaborolan-2-yl)phenyl)acetate (2.69 mmol, 1128.4 mg, 1.0 equiv), and Rh₂(*S*-p-Ph-TPCP)₄ catalyst (0.0000269 mmol, 0.0474 mg, 0.001 mol %). After flash chromatography (0%, then 5% - 15% Et₂O in hexanes) the product was obtained as a clear oil (1213.3 mg, 91 % yield).

¹H NMR (400 MHz, Chloroform-*d*) δ 7.64 – 7.52 (m, 2H), 7.14 – 7.03 (m, 5H), 6.88 – 6.74 (m, 2H), 4.86 (d, $J=11.9$ Hz, 1H), 4.63 (d, $J=11.9$ Hz, 1H), 3.23 (dd, $J=9.4, 7.5$ Hz, 1H), 2.28 (dd, $J=9.4, 5.1$ Hz, 1H), 2.02 (dd, $J=7.5, 5.1$ Hz, 1H), 1.32 (s, 12H).

^{13}C NMR (151 MHz, Chloroform-*d*) δ 172.02, 136.90, 135.68, 134.29, 131.48, 128.24, 128.04, 126.78, 95.18, 83.85, 74.44, 37.43, 34.12, 25.04, 24.99, 20.32.

Chiral HPLC: (*S,S*-Whelk, 30 min, 1 mL/min, 1 % iPrOH in hexanes, UV 230 nm) tR: Major: 10.5 min, Minor: 12.8 min, 99% ee.



2.16

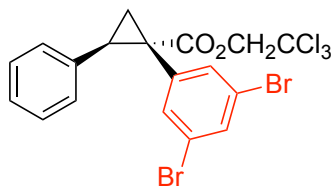
2,2,2-trichloroethyl (1*S*,2*R*)-1-(3-bromophenyl)-2-phenylcyclopropane-1-carboxylate

This compound was prepared according to the general procedure 3.1 for cyclopropanation reactions, using styrene (6.24 mmol, 650.0 mg, 2.32 equiv.) as the substrate, 2,2,2-trichloroethyl 2-(3-bromophenyl)-2-diazoacetate (2.69 mmol, 1000.0 mg, 1.0 equiv.) and $\text{Rh}_2(\text{R-}p\text{-Ph-TPCP})_4$ catalyst (0.0000269 mmol, 0.0474 mg, 0.001 mol %). After flash chromatography (0%, then 5% - 15% Et₂O in hexanes) the product was obtained as a clear oil (1086.0 mg, 90% yield).

^1H NMR (400 MHz, Chloroform-*d*) δ 7.26(dt, $J = 7.0, 1.7$ Hz, 2H), 7.17-7.05 (m, 3H), 7.02 – 6.90 (m, 2H), 6.87– 6.78 (m, 2H), 4.84 (d, $J = 11.9$ Hz, 1H), 4.62 (d, $J = 11.9$ Hz, 1H), 3.22 (dd, $J = 9.4, 7.5$ Hz, 1H), 2.27 (dd, $J = 9.4, 5.2$ Hz, 1H), 2.00 (dd, $J = 7.5, 5.3$ Hz, 1H).

^{13}C NMR (151 MHz, Chloroform-*d*) δ 171.64, 136.25, 135.21, 135.09, 130.92, 130.59, 129.26, 128.23, 128.14, 127.06, 121.69, 95.07, 74.57, 36.83, 34.18, 20.21.

Chiral HPLC: (OJ-H, 30 min, 1 mL/min, 1 % iPrOH in hexanes, UV 230 nm) tR: Major: 14.4 min, Minor: 10.2 min, 92% ee.



2.17

2,2,2-trichloroethyl (1*S*,2*R*)-1-(3,5-dibromophenyl)-2-phenylcyclopropane-1-carboxylate

This compound was prepared according to the general procedure 3.1 for cyclopropanation reactions, using styrene (6.24 mmol, 650.0 mg, 2.32 equiv.) as the substrate, 2,2,2-trichloroethyl 2-diazo-2-(3,5-dibromophenyl)acetate (2.69 mmol, 1214.1 mg, 1.0 equiv.), and Rh₂(*R-p*-Ph-TPCP)₄ catalyst (0.0000807 mmol, 0.1422 mg, 0.003 mol %). After flash chromatography (0%, then 5% - 15% Et₂O in hexanes) the product was obtained as a clear oil (567.5 mg, 40 % yield).

[α]²⁰_D = -5° (c = 0.20, CHCl₃)

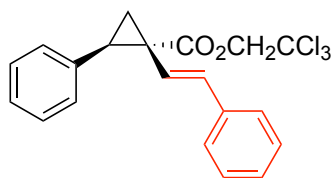
¹H NMR (400 MHz, Chloroform-*d*) δ 7.43 (t, *J* = 1.8 Hz, 1H), 7.21 – 7.05 (m, 5H), 6.85 (dd, *J* = 7.5, 2.1 Hz, 2H), 4.86 (d, *J* = 11.9 Hz, 1H), 4.62 (d, *J* = 11.9 Hz, 1H), 3.23 (dd, *J* = 9.5, 7.6 Hz, 1H), 2.27 (dd, *J* = 9.4, 5.4 Hz, 1H), 2.00 (dd, *J* = 7.5, 5.4 Hz, 1H).

¹³C NMR (151 MHz, Chloroform-*d*) δ 171.10, 137.96, 134.63, 134.02, 133.20, 128.36, 128.21, 127.43, 122.04, 94.97, 74.66, 36.40, 34.41, 20.00.

IR(neat): 3029, 2970, 1736, 1585, 1552, 1498, 1365, 1235, 1156, 1113, 860, 814, 698 cm⁻¹

HR-MS : (+p APCI) calcd for [C₁₈H₁₃Br₂Cl₃O₂+]⁺ 523.8348 found 523.83376

Chiral HPLC: (OD-H, 30 min, 1 mL/min, 1 % iPrOH in hexanes, UV 230 nm) tR: Major: 9.7 min, Minor: 9.0 min, 94% ee.



2.18

2,2,2-trichloroethyl (1*R*,2*R*)-2-phenyl-1-((*E*)-styryl)cyclopropane-1-carboxylate

This compound was prepared according to the general procedure 3.1 for cyclopropanation reactions, using styrene (6.24 mmol, 650.0 mg, 2.32 equiv.) as the substrate, 2,2,2-trichloroethyl (*E*)-2-diazo-4-phenylbut-3-enoate (2.69mmol, 859.6 mg, 1.0 equiv.), and Rh₂(*R*-*p*-Ph-TPCP)₄ catalyst (0.0000807 mmol, 0.1422 mg, 0.003 mol %) at 25°C. After flash chromatography (0 %, then 5 % - 15 % Et₂O in hexanes) the product was obtained as a white solid (936.7 mg, 88 % yield).

MP: 71 – 72 °C

[α]²⁰_D = +73° (c = 0.10, CHCl₃)

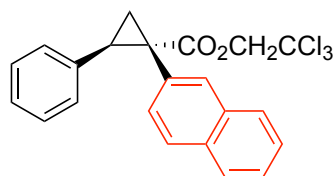
¹H NMR (400 MHz, Chloroform-*d*) δ 7.36 – 7.05 (m, 10H), 6.45 (d, *J* = 16.1 Hz, 1H), 6.19 (d, *J* = 16.2 Hz, 1H), 4.87 (qd, *J* = 12.2, 2.2 Hz, 2H), 3.20 (dd, *J* = 9.2, 7.4 Hz, 1H), 2.22 (dd, *J* = 9.3, 5.2 Hz, 1H), 1.97 (dd, *J* = 7.5, 5.2 Hz, 1H).

¹³C NMR (151 MHz, Chloroform-*d*) δ 172.03, 137.08, 135.10, 133.73, 129.34, 128.53, 128.26, 127.56, 127.20, 126.39, 123.17, 95.26, 74.47, 35.94, 33.04, 19.19.

IR(neat):3027, 2924, 1732, 1602, 1500, 1455, 1377, 1312, 1243, 1208, 1149, 1128, 1109, 1092, 1053, 975, 953, 897, 857, 813, 773, 747, 710, 694, 576, 477 cm⁻¹

HR-MS : (+p APCI) calcd for [C₂₀H₁₇Cl₃O₂+H] 395.0367 found 395.03652

Chiral HPLC: (ADH, 30 min, 1 mL/min, 1 % iPrOH in hexanes, UV 230 nm) tR: Major: 10.3 min, Minor: 8.8min, 96% ee.



2.19

2,2,2-trichloroethyl (1*S*,2*R*)-1-(naphthalen-2-yl)-2-phenylcyclopropane-1-carboxylate

This compound was prepared according to the general procedure 3.1 for cyclopropanation reactions, using styrene (6.24 mmol, 650.0 mg, 2.32 equiv.) as the substrate, 2,2,2-trichloroethyl 2-diazo-2-(naphthalen-2-yl)acetate (2.69 mmol, 924.2 mg, 1.0 equiv.), and $\text{Rh}_2(\text{R-}p\text{-Ph-TPCP})_4$ catalyst (0.0000807 mmol, 0.1422 mg, 0.003 mol %). After flash chromatography (0 %, then 5 % - 15 % Et_2O in hexanes) the product was obtained as a white solid (745.2 mg, 66 % yield).

MP: 127 – 128 °C

$[\alpha]^{20}_{\text{D}} = -81.3^\circ$ ($c = 0.10$, CHCl_3)

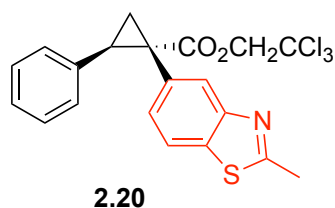
$^1\text{H NMR}$ (400 MHz, Chloroform- d) δ 7.77 – 7.68 (m, 2H), 7.66 (d, $J = 1.7$ Hz, 1H), 7.55 (d, $J = 8.5$ Hz, 1H), 7.45 – 7.37 (m, 2H), 7.11 (dd, $J = 8.5, 1.8$ Hz, 1H), 7.06 – 6.96 (m, 3H), 6.88 – 6.80 (m, 2H), 4.89 (d, $J = 11.9$ Hz, 1H), 4.63 (d, $J = 11.9$ Hz, 1H), 3.30 (dd, $J = 9.4, 7.4$ Hz, 1H), 2.38 (dd, $J = 9.4, 5.1$ Hz, 1H), 2.16 (dd, $J = 7.4, 5.1$ Hz, 1H).

$^{13}\text{C NMR}$ (151 MHz, Chloroform- d) δ 172.26, 135.66, 133.11, 132.72, 131.69, 130.87, 130.21, 128.26, 128.01, 127.91, 127.71, 127.25, 126.78, 126.04, 125.84, 95.20, 74.48, 37.49, 34.19, 20.52.

IR(neat): 3057, 2924, 1732, 1602, 1500, 1455, 1377, 1312, 1243, 1208, 1149, 1128, 1109, 1092, 1053, 975, 953, 897, 857, 813, 773, 747, 710, 694, 576, 477 cm^{-1}

HR-MS : (+p APCI) calcd for $[\text{C}_{22}\text{H}_{17}\text{Cl}_3\text{O}_2+\text{H}]$ 419.0367 found 419.03622

Chiral HPLC: (ADH, 30min, 1 mL/min, 1 % iPrOH in hexanes, UV 230 nm) tR: Major: 11.6 min, Minor: 10.1 min, 96% ee.



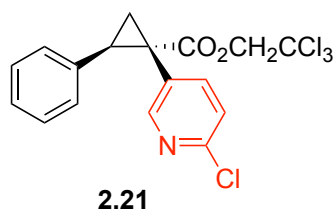
2,2,2-trichloroethyl(1S,2R)-1-(2-methylbenzo[d]thiazol-5-yl)-2-phenylcyclopropane-1-carboxylate

This compound was prepared according to the general 3.1 procedure for cyclopropanation reactions, using styrene (6.24 mmol, 650.0 mg, 2.32 equiv.) as the substrate, 2,2,2-trichloroethyl 2-diazo-2-(naphthalen-2-yl)acetate (2.69 mmol, 980.8 mg, 1.0 equiv.), and $\text{Rh}_2(\text{R-}p\text{-Ph-TPCP})_4$ catalyst (0.0000807 mmol, 0.1422 mg, 0.003 mol %). After flash chromatography (0%, then 5% - 15% Et_2O in hexanes) the product was obtained as a clear oil (1031.5 mg, 87 % yield).

$^1\text{H NMR}$ (400 MHz, Chloroform-*d*) δ 7.77 (d, $J = 1.7$ Hz, 1H), 7.51 (d, $J = 8.3$ Hz, 1H), 7.09 – 6.99 (m, 3H), 6.98 (dd, $J = 8.3, 1.7$ Hz, 1H), 6.86 – 6.77 (m, 2H), 4.85 (d, $J = 11.9$ Hz, 1H), 4.65 (d, $J = 11.9$ Hz, 1H), 3.29 (dd, $J = 9.4, 7.4$ Hz, 1H), 2.78 (s, 3H), 2.35 (dd, $J = 9.4, 5.2$ Hz, 1H), 2.11 (dd, $J = 7.5, 5.2$ Hz, 1H).

$^{13}\text{C NMR}$ (151 MHz, Chloroform-*d*) δ 172.04, 167.22, 153.26, 135.48, 134.77, 132.16, 129.23, 128.22, 128.03, 126.80, 125.49, 120.54, 95.12, 74.47, 37.27, 34.19, 20.50, 20.21.

Chiral HPLC: (OJ-H, 30 min, 1 mL/min, 1 % *i*PrOH in hexanes, UV 230 nm) tR: Major: 21.8min, Minor: 15.8 min, 86% ee.



2,2,2-trichloroethyl (1*S*,2*R*)-1-(6-chloropyridin-3-yl)-2-phenylcyclopropane-1-carboxylate

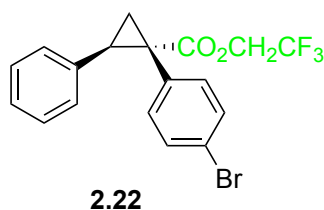
This compound was prepared according to the general procedure 3.1 for cyclopropanation reactions, using styrene (6.24 mmol, 650.0 mg, 2.32 equiv.) as the substrate, 2,2,2-trichloroethyl 2-(6-chloropyridin-3-yl)-2-diazoacetate (2.69 mmol, 884.9 mg, 1.0 equiv.), and $\text{Rh}_2(\text{R-}p\text{-Ph-TPCP})_4$ catalyst (0.0000269 mmol, 0.0474 mg, 0.001 mol %). After flash chromatography (0%,

then 5% - 10% EtOAc in hexanes) the product was obtained as a slight yellow oil (708.3 mg, 65 % yield).

$^1\text{H NMR}$ (400 MHz, Chloroform-*d*) δ 8.17-8.11 (m, 1H), 7.30-7.23 ppm (m, 1H), 7.14 (dd, J = 4.9, 1.9 Hz, 3H), 7.06 (d, J = 8.3 Hz, 1H), 6.83 (dd, J = 6.7, 2.9 Hz, 2H), 4.84 (d, J = 11.9 Hz, 1H), 4.65 (d, J = 11.9 Hz, 1H), 3.27 (dd, J = 9.5, 7.5 Hz, 1H), 2.35 (dd, J = 9.4, 5.4 Hz, 1H), 2.05 (dd, J = 7.5, 5.4 Hz, 1H).

$^{13}\text{C NMR}$ (151 MHz, Chloroform-*d*) δ 171.03, 152.54, 150.53, 142.52, 134.40, 129.25, 128.54, 128.25, 127.53, 123.40, 94.90, 74.68, 34.06, 34.00, 19.65.

Chiral HPLC: (OJ-H, 30 min, 1 mL/min, 1 % iPrOH in hexanes, UV 230 nm) tR: Major: 25.2 min, Minor: 21.9 min, 94% ee.



2,2,2-trifluoroethyl (1*S*,2*R*)-1-(4-bromophenyl)-2-phenylcyclopropane-1-carboxylate

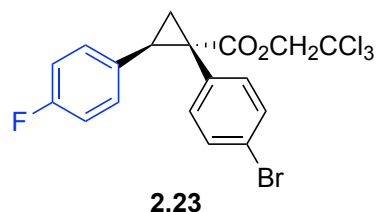
This compound was prepared according to the general procedure 3.1 for cyclopropanation reactions, using styrene (6.24 mmol, 650.0 mg, 2.32 equiv.) as the substrate and 2,2,2-trifluoroethyl 2-(4-bromophenyl)-2-diazoacetate (2.69 mmol, 869.1 mg, 1.0 equiv.) under the catalysis of $\text{Rh}_2(\text{R-}p\text{-Ph-TPCP})_4$ (0.0000269 mmol, 0.0474 mg, 0.001 mol%). After flash chromatography (0%, then 5% - 15% Et₂O in hexanes) the product was obtained as a clear oil (923.5 mg, 86 % yield).

$^1\text{H NMR}$ (400 MHz, Chloroform-*d*) δ 7.31 – 7.22 (m, 3H), 7.20 – 7.03 (m, 3H), 6.93 – 6.85 (m, 2H), 6.79 (dd, J = 6.7, 3.0 Hz, 2H), 4.54 (dq, J = 12.7, 8.4 Hz, 1H), 4.40 (dq, J = 12.6, 8.3 Hz, 1H), 3.17 (dd, J = 9.4, 7.5 Hz, 1H), 2.22 (dd, J = 9.4, 5.2 Hz, 1H), 1.96 (dd, J = 7.5, 5.2 Hz, 1H).

^{13}C NMR (151 MHz, Chloroform-*d*) δ 171.87, 135.21, 133.61, 132.98, 131.17, 128.22, 128.18, 127.06, 121.75, 61.20, 60.96, 36.52, 34.06, 20.56.

^{19}F NMR (376 MHz, Chloroform-*d*) δ -73.92, -73.94, -73.96.

Chiral HPLC: (OJ-H, 30 min, 1 mL/min, 1 % iPrOH in hexanes, UV 230 nm) tR: Major: 16.7 min, Minor: 9.6 min, 96% ee.



2,2,2-trichloroethyl (1*S*,2*R*)-1-(4-bromophenyl)-2-(4-fluorophenyl)cyclopropane-1-carboxylate

This compound was prepared according to the general procedure 3.1 for cyclopropanation reactions, using 1-fluoro-4-vinylbenzene (6.24 mmol, 762.3 mg, 2.32 equiv.) as the substrate, 2,2,2-trichloroethyl 2-(4-bromophenyl)-2-diazoacetate (2.69 mmol, 1000.0 mg, 1.0 equiv.), and $\text{Rh}_2(\text{R-}p\text{-Ph-TPCP})_4$ catalyst (0.0000269 mmol, 0.0474 mg, 0.001 mol %). After flash chromatography (0%, then 5% - 15% Et_2O in hexanes) the product was obtained as a white solid (1154.6 mg, 92 % yield).

$[\alpha]_D^{20}$: -10° ($c=0.10$, CHCl_3).

MP: 106 – 108 $^\circ\text{C}$

^1H NMR (400 MHz, Chloroform-*d*) δ 7.33 – 7.22 (m, 3H), 6.98 – 6.89 (m, 2H), 6.85 – 6.72 (m, 4H), 4.83 (d, $J = 11.9$ Hz, 1H), 4.64 (d, $J = 11.9$ Hz, 1H), 3.20 (dd, $J = 9.4, 7.4$ Hz, 1H), 2.28 (dd, $J = 9.5, 5.3$ Hz, 1H), 1.92 (dd, $J = 7.4, 5.3$ Hz, 1H).

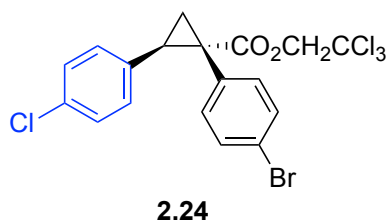
^{13}C NMR (151 MHz, Chloroform-*d*) δ 171.59, 133.74, 132.85, 131.18, 131.10, 129.69, 129.63, 121.80, 115.24, 115.09, 95.06, 74.56, 36.60, 33.29, 20.44.

^{19}F NMR (376 MHz, Chloroform-*d*) δ -115.40.

IR(neat): 2954, 1733, 1607, 1513, 1490, 1395, 1375, 1239, 1152, 1011, 838, 716, 575 cm^{-1}

HR-MS : (+p APCI) calcd for $[\text{C}_{18}\text{H}_{13}\text{BrCl}_3\text{FO}_2+\text{H}]$ 464.9221 found 464.92158

Chiral HPLC: (OJ-H, 30 min, 1 mL/min, 1 % iPrOH in hexanes, UV 230 nm) tR: Major: 17.8 min, Minor: 10.6 min, 96% ee.



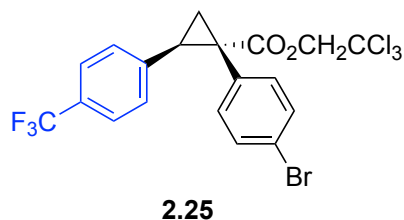
2,2,2-trichloroethyl (1*S*,2*R*)-1-(4-bromophenyl)-2-(4-chlorophenyl)cyclopropane-1-carboxylate

This compound was prepared according to the general procedure 3.1 for cyclopropanation reactions, using 1-chloro-4-vinylbenzene (6.24 mmol, 864.9 mg, 2.32 equiv.) as the substrate, 2,2,2-trichloroethyl 2-(4-bromophenyl)-2-diazoacetate (2.69 mmol, 1000 mg, 1.0 equiv.), and $\text{Rh}_2(\text{R-}p\text{-Ph-TPCP})_4$ catalyst (0.0000269 mmol, 0.0474 mg, 0.001 mol %). After flash chromatography (0%, then 5% - 15% Et_2O in hexanes) the product was obtained as a white solid. (1195.3 mg, 92 % yield).

^1H NMR (400 MHz, Chloroform-*d*) δ 7.31 – 7.26 (m, 2H), 6.96 – 6.90 (m, 2H), 6.85 – 6.77 (m, 2H), 6.77 (dd, $J = 8.5, 5.6$ Hz, 2H), 4.83 (d, $J = 11.9$ Hz, 1H), 4.64 (dd, $J = 11.9, 0.6$ Hz, 1H), 3.20 (dd, $J = 9.4, 7.4$ Hz, 1H), 2.28 (dd, $J = 9.4, 5.3$ Hz, 1H), 1.92 (dd, $J = 7.4, 5.3$ Hz, 1H).

^{13}C NMR (151 MHz, Chloroform-*d*) δ 171.59, 133.73, 132.85, 131.18, 131.10, 129.68, 129.63, 121.80, 115.23, 115.09, 95.06, 74.54, 36.59, 33.28, 20.42.

Chiral HPLC: (OJ-H, 30 min, 1 mL/min, 1 % iPrOH in hexanes, UV 230 nm) tR: Major: 25.1 min, Minor: 14.1 min, 96% ee.



2,2,2-trichloroethyl(1*S*,2*R*)-1-(4-bromophenyl)-2-(4-(trifluoromethyl)phenyl)cyclopropane-1-carboxylate

This compound was prepared according to the general procedure 3.1 for cyclopropanation reactions, using 1-(trifluoromethyl)-4-vinylbenzene (6.24 mmol, 1074.4 mg, 2.32 equiv.) as the substrate, 2,2,2-trichloroethyl 2-(4-bromophenyl)-2-diazoacetate (2.69 mmol, 1000 mg, 1.0 equiv.), and Rh₂(*R-p*-Ph-TPCP)₄ catalyst (0.0000269 mmol, 0.0474 mg, 0.001 mol %). After flash chromatography (0 %, then 5 % - 15 % Et₂O in hexanes) the product was obtained as a white solid (1250.6 mg, 90% yield).

MP: 98 - 100 °C

[α]²⁰_D = -13° (c = 0.10, CHCl₃)

¹H NMR (400 MHz, Chloroform-*d*) δ 7.37 (d, *J* = 8.1 Hz, 2H), 7.33 – 7.28 (m, 2H), 6.98 – 6.84 (m, 4H), 4.83 (d, *J* = 11.9 Hz, 1H), 4.64 (d, *J* = 11.9 Hz, 1H), 3.24 (dd, *J* = 9.4, 7.4 Hz, 1H), 2.33 (dd, *J* = 9.4, 5.3 Hz, 1H), 1.99 (dd, *J* = 7.4, 5.3 Hz, 1H).

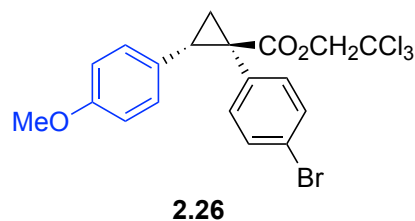
¹³C NMR (151 MHz, Chloroform-*d*) δ 171.36, 139.81, 133.64, 132.40, 131.36, 128.46, 125.14, 125.11, 125.09, 122.09, 94.97, 74.64, 37.23, 33.31, 20.75.

¹⁹F NMR (376 MHz, cdcl₃) δ -62.51.

IR(neat): 2955, 1735, 1620, 1489, 1323, 1239, 1154, 1115, 1067, 1011, 927, 842, 764, 715, 573, 509 cm⁻¹

HR-MS : (+p APCI) calcd for [C₁₉H₁₃BrCl₃F₃O₂+]⁺ 513.9111 found 513.91045

Chiral HPLC: (OJ-H, 30 min, 1 mL/min, 1 % iPrOH in hexanes, UV 230 nm) tR: Major:21.7 min, Minor: 12.0 min, 97% ee.



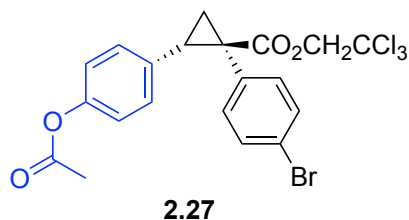
2,2,2-trichloroethyl(1*S*,2*R*)-1-(4-bromophenyl)-2-(4-methoxyphenyl)cyclopropane-1-carboxylate

This compound was prepared according to the general procedure for cyclopropanation reactions, using 1-methoxy-4-vinylbenzene (6.24 mmol, 837.4 mg, 2.32 equiv.) as the substrate, 2,2,2-trichloroethyl 2-(4-bromophenyl)-2-diazoacetate (2.69 mmol, 1000 mg, 1.0 equiv), and Rh₂(*S*-p-Ph-TPCP)₄ catalyst (0.0000269 mmol, 0.0474 mg, 0.001 mol %). After flash chromatography (0 %, then 5 % - 15 % Et₂O in hexanes) the product was obtained as a clear oil (1158.7 mg, 90 % yield).

¹H NMR (400 MHz, Chloroform-*d*) δ 7.29 – 7.22 (m, 2H), 6.97 – 6.87 (m, 2H), 6.70 (d, *J* = 8.7 Hz, 2H) 6.71-6.59 (m, 2H), 4.81 (dd, *J* = 11.9, 0.8 Hz, 1H), 4.61 (dd, *J* = 12.0, 0.8 Hz, 1H), 3.71 (s, 3H), 3.15 (dd, *J* = 9.5, 7.5 Hz, 1H), 2.25 (ddd, *J* = 9.4, 5.2, 0.8 Hz, 1H), 1.88 (dd, *J* = 7.5, 5.2 Hz, 1H).

¹³C NMR (151 MHz, Chloroform-*d*) δ 171.79, 158.62, 133.84, 133.25, 131.05, 129.24, 127.27, 121.59, 113.64, 95.14, 74.49, 55.29, 36.45, 33.74, 20.40.

Chiral HPLC: (*S,S*-Whelk, 30 min, 1 mL/min, 1 % iPrOH in hexanes, UV 230 nm) tR: Major: 15.0min, Minor: 18.4 min, 97% ee.



2,2,2-trichloroethyl (1*S*,2*R*)-2-(4-acetoxyphenyl)-1-(4-bromophenyl)cyclopropane-1-carboxylate

This compound was prepared according to the general procedure for cyclopropanation reactions, using 4-vinylphenyl acetate (6.24 mmol, 1012.2 mg, 2.32 equiv.) as the substrate, 2,2,2-trichloroethyl 2-(4-bromophenyl)-2-diazoacetate (2.69 mmol, 1000 mg, 1.0 equiv.), and Rh₂(*S*-*p*-Ph-TPCP)₄ catalyst (0.0000269 mmol, 0.0474 mg, 0.001 mol %). After flash chromatography (0 %, then 5 % - 15 % Et₂O in hexanes) the product was obtained as a white solid (695.0 mg, 51 % yield).

MP: 95 - 98 °C

[α]²⁰_D = -9.2° (c = 1.00, CHCl₃)

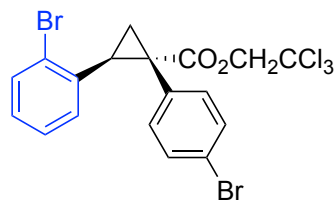
¹H NMR (400 MHz, Chloroform-*d*) δ 7.32 – 7.23 (m, 2H), 6.98 – 6.90 (m, 2H), 6.89 – 6.82 (m, 2H), 6.82 – 6.76 (m, 2H), 4.83 (d, *J* = 11.9 Hz, 1H), 4.63 (d, *J* = 12.0 Hz, 1H), 3.20 (dd, *J* = 9.5, 7.4 Hz, 1H), 2.29 (dd, *J* = 9.5, 5.2 Hz, 1H), 2.24 (s, 3H), 1.92 (dd, *J* = 7.4, 5.3 Hz, 1H).

¹³C NMR (151 MHz, Chloroform-*d*) δ 171.60, 169.35, 149.63, 133.77, 133.00, 132.84, 131.17, 129.10, 121.81, 121.27, 95.05, 74.54, 36.71, 33.43, 21.24, 20.64.

IR(neat): 3041, 1757, 1630, 1505, 1367, 1186, 1163, 1108, 1012, 907, 850, 626, 490 cm⁻¹

HR-MS : (+*p* APCI) calcd for [C₂₀H₁₆BrCl₃O₄+]⁺503.9298 found 503.92901

Chiral HPLC: (ADH, 40 min, 1 mL/min, 1 % *i*PrOH in hexanes, UV 230 nm) t_R: Major: 24.0 min, Minor: 30.0 min, 90% ee.



2.28

2,2,2-trichloroethyl (1*S*,2*S*)-2-(2-bromophenyl)-1-(4-bromophenyl)cyclopropane-1-carboxylate

This compound was prepared according to the general procedure for cyclopropanation reactions, using 1-bromo-2-vinylbenzene (6.24 mmol, 1142.4 mg, 2.32 equiv.) as the substrate, 2,2,2-trichloroethyl 2-(4-bromophenyl)-2-diazoacetate (2.69 mmol, 1000 mg, 1.0 equiv.), and Rh₂(*R*-*p*-Ph-TPCP)₄ catalyst (0.0000269 mmol, 0.0474 mg, 0.001 mol %). After flash chromatography (0%, then 5% - 15% Et₂O in hexanes) the product was obtained as a clear oil (993.2 mg, 70 % yield).

[α]²⁰_D = +4.0° (c = 0.03, CHCl₃)

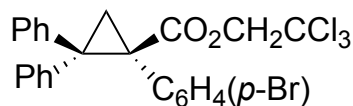
¹H NMR (400 MHz, Chloroform-*d*) δ 7.57 – 7.43 (m, 1H), 7.25 – 7.18 (m, 2H), 7.10 – 7.02 (m, 2H), 7.02 – 6.90 (m, 2H), 6.65 – 6.48 (m, 1H), 4.90 (d, *J* = 11.9 Hz, 1H), 4.65 (d, *J* = 11.9 Hz, 1H), 3.47 (dd, *J* = 9.2, 7.7 Hz, 1H), 2.26 (dd, *J* = 9.2, 5.3 Hz, 1H), 2.12 (dd, *J* = 7.7, 5.3 Hz, 1H).

¹³C NMR (151 MHz, Chloroform-*d*) δ 171.42, 135.01, 133.16, 133.01, 132.72, 131.03, 128.73, 127.85, 127.22, 127.20, 121.69, 95.01, 74.61, 35.90, 35.00, 18.98.

IR(neat): 2952, 1735, 1592, 1469, 1439, 1376, 1242, 1206, 1156, 1125, 1090, 1073, 1059, 1045, 1011, 969, 827, 768, 718, 575, 515 cm⁻¹

HR-MS : (+p APCI) calcd for [C₁₈H₁₃Br₂Cl₃O₂+H] 524.8421 found 524.84200

Chiral HPLC: (OD-H, 30 min, 1 mL/min, 1 % iPrOH in hexanes, UV 230 nm) tR: Major: 17.3 min, Minor: 11.9 min, 96% ee.

**2.30**

2,2,2-trichloroethyl (*R*)-1-(4-bromophenyl)-2,2-diphenylcyclopropane-1-carboxylate

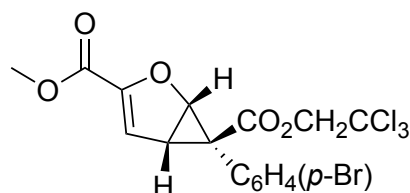
This compound was prepared according to the general procedure for cyclopropanation reactions, using 1,1-diphenylethylene (6.24 mmol, 1124.9 mg, 2.32 equiv.) as the substrate, 2,2,2-trichloroethyl 2-(4-bromophenyl)-2-diazoacetate (2.69 mmol, 1000 mg, 1.0 equiv.), and Rh₂(*R*-PTAD)₄ catalyst (0.0000269 mmol, 0.0419 mg, 0.001 mol %). After flash chromatography (0 %, then 5 % - 15 % Et₂O in hexanes) the product was obtained as a clear oil (1242.0 mg, 88 % yield).

¹H NMR (400 MHz, Chloroform-*d*) δ 7.58 – 7.52 (m, 2H), 7.37 – 7.23 (m, 7H), 7.11 – 6.95 (m, 5H), 4.54 (d, *J* = 11.8 Hz, 1H), 4.15 (d, *J* = 11.9 Hz, 1H), 2.78 (d, *J* = 5.7 Hz, 1H), 2.52 (d, *J* = 5.7 Hz, 1H).

¹³C NMR (151 MHz, Chloroform-*d*) δ 169.19, 134.05, 133.70, 130.86, 130.10, 128.80, 128.74, 128.04, 127.49, 126.77, 121.59, 94.42, 75.37, 45.77, 42.28, 23.10.

Chiral UHPLC: (IAU, 6 min, 0.500 mL/min, 1.0 % iPrOH in hexanes, UV 230 nm) tR: Major: 5.1 min, Minor: 3.3 min, 94% ee.

(Rh₂(*R*-*p*-Ph-TPCP)₄ as catalyst: AD-H, 30 min, 1 mL/min, 1 % iPrOH in hexanes, UV 230 nm) tR: Major: 10.5 min, Minor: 18.8 min, -48% ee)

**2.32**

3-methyl 6-(2,2,2-trichloroethyl) (1*S*,5*S*,6*R*)-6-(4-bromophenyl)-2-oxabicyclo[3.1.0]hex-3-ene-3,6-dicarboxylate

This compound was prepared according to the general procedure 3.1 for cyclopropanation reactions, using methyl furan-2-carboxylate (6.24 mmol, 787.0 mg, 2.32 equiv.) as the substrate, 2,2,2-trichloroethyl 2-(4-bromophenyl)-2-diazoacetate (2.69 mmol, 1000 mg, 1.0 equiv.), and $\text{Rh}_2(\text{R-TCPTAD})_4$ catalyst (0.0000269 mmol, 0.0568 mg, 0.001 mol %). After flash chromatography ((silica gel, hexanes/EtOAc = 50:1, 25:1, 15:1, 3:1) the product was obtained as a yellow oil (784.7 mg, 62 % yield).

$[\alpha]^{20}_{\text{D}} = -39.8^\circ$ ($c = 1.5$, CHCl_3)

$^1\text{H NMR}$ (600 MHz, Chloroform- d) δ 7.39 (d, $J = 8.0$ Hz, 1H), 7.11 (d, $J = 8.0$ Hz, 1H), 6.13 (d, $J = 3.0$ Hz, 1H), 5.33 (d, $J = 5.2$ Hz, 1H), 4.75 – 4.70 (m, 1H), 4.66 – 4.61 (m, 1H), 3.64 (d, $J = 2.3$ Hz, 3H), 3.50 (dd, $J = 5.4, 2.9$ Hz, 1H).

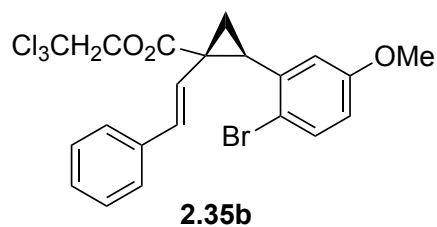
$^{13}\text{C NMR}$ (151 MHz, Chloroform- d) δ 170.49, 158.61, 149.58, 134.02, 131.49, 127.87, 122.32, 113.45, 94.71, 74.40, 71.22, 52.35, 40.22, 28.08.

IR (neat): 2954, 2257, 1727, 1611, 1490, 1438, 1396, 1338, 1264, 1226, 1208, 1115, 1040, 1012, 952, 906, 793, 725, 576, 524 cm^{-1}

HR-MS: (NSI) m/z : calculated for $\text{C}_{16}\text{H}_{13}\text{BrCl}_3\text{O}_5\text{H}^+$ 468.9012, observed 468.9015.

Chiral UHPLC: (IAU, 15 min, 0.500 mL/min, 5.0 % iPrOH in hexanes, UV 230 nm) tR: Major: 4.8 min, Minor: 9.1 min, 90% ee.

($\text{Rh}_2(\text{R-}p\text{-Ph-TPCP})_4$ as catalyst: OD-H, 40 min, 1 mL/min, 3 % iPrOH in hexanes, UV 230 nm) tR: Major: 25.7 min, Minor: 14.2 min, -50% ee)



2,2,2-trichloroethyl (1*S*,2*R*)-2-(2-bromo-5-methoxyphenyl)-1-styrylcyclopropane-1-carboxylate

This compound was prepared according to the general procedure 3.1 for cyclopropanation reactions, using 1-bromo-4-methoxy-2-vinylbenzene (6.24 mmol, 1329.7 mg, 2.32 equiv.) as the substrate, 2,2,2-trichloroethyl (1*S*, 2*R*)-2-diazo-4-phenylbut-3-enoate (2.69 mmol, 859.6 mg, 1.0 equiv.), and Rh₂(*R-p*-Ph-TPCP)₄ catalyst (0.0000269 mmol, 0.0474 mg, 0.001 mol%) at 25 °C. After flash chromatography (0%, then 5% - 15% Et₂O in hexanes) the product was obtained as a white solid (977.4 mg, 72% yield).

MP: 98 - 99 °C

[α]²⁰_D = -52.4° (c = 0.10, CHCl₃)

¹H NMR (400 MHz, Chloroform-*d*) δ 7.40 (d, *J* = 8.7 Hz, 1H), 7.24 – 7.09 (m, 5H), 6.72 – 6.59 (m, 2H), 6.34 (d, *J* = 16.1Hz, 1H), 6.24 (d, *J* = 16.1Hz, 1H), 4.91 (d, *J* = 11.9 Hz, 1H), 4.81 (d, *J* = 11.9 Hz, 1H), 3.72 (s, 3H), 3.22 – 3.08 (m, 1H), 2.28 – 2.11 (m, 1H), 1.94 (dd, *J* = 7.6, 5.3 Hz, 1H).

¹³C NMR (151 MHz, Chloroform-*d*) δ 171.84, 158.80, 137.05, 136.45, 132.99, 132.43, 128.50, 127.51, 126.42, 122.50, 117.81, 116.91, 113.95, 95.13, 74.60, 55.59, 37.58, 32.42, 19.06.

IR(neat):3024, 2954, 2836, 1734, 1596, 1571, 1472, 1449, 1419, 1375, 1294, 1274, 1228, 1195, 1169, 1137,1097, 1064, 1016, 961, 804, 787, 751, 730, 716, 693, 604, 576 cm⁻¹

HR-MS : (+p APCI) calcd for [C₂₁H₁₈BrCl₃O₃+H] 502.9578 found 502.95765

Chiral HPLC: (*R,R*-Whelk, 35 min, 1mL/min, 1 % iPrOH in hexanes, UV 230 nm) tR: Major: 24.8 min, Minor: 23.0 min.

6.3 Experimental Part for Chapter 3

6.3.1 General procedure for Cu(II) catalyzed hydrazone oxidation in flow

A 50 mL beaker was charged with $\text{Cu}(\text{OAc})_2 \cdot \text{H}_2\text{O}$ (0.40 g, 2.0 mmol, 10 equiv), DMAP (0.24 g, 2.0 mmol, 10 equiv), silica powder (4.0 g, SiliaFlash® P60, 40-63 μm), an egg-shape stir bar and 20 mL DCM. The mixture was stirred vigorously (700 rpm) under air for 10 min to be air saturated. In a column (Biotage® SNAP Cartridge, KP-Sil, 10 g) 6.0 g silica powder was firstly packed at the bottom layer. The air saturated $\text{Cu}(\text{OAc})_2 \cdot \text{H}_2\text{O}$ /DMAP/silica/DCM mixture was then packed on the top layer. After the column being rinsed with 0.06 mol/L DMAP in DCM eluent, 2,2,2-trichloroethyl (*Z*)-2-(4-bromophenyl)-2-hydrazineylideneacetate (74.9 mg, 0.2 mmol, 1.0 equiv) was added on the top of the column and flashed with eluent (20 mL/min flow rate). The fractions were collected and get the crude ^1H NMR to determine the yield.

6.3.2 General procedure for tandem reactions of Cu(II) catalyzed hydrazones oxidation and Rh(II) catalyzed asymmetric cyclopropanation under batch conditions.

A 20 mL scintillation vial was charged with $\text{Cu}(\text{OAc})_2 \cdot \text{H}_2\text{O}$ (4.0 mg, 0.020 mmol, 10 mol%), silica powder (40.0 mg, SiliaFlash® P60, 40-63 μm), and 1.0 mL solution of 0.06 mol/L DMAP in DCM. The initial mixture was stirred vigorously with a stir bar (600 rpm) under air for 5 min before hydrazone was added. The hydrazone (0.2 mmol, 1 equiv) was dissolved in 1.0 mL of the 0.06 mol/L DMAP in DCM solution and transferred by syringe in one portion to the $\text{Cu}(\text{OAc})_2 \cdot \text{H}_2\text{O}$ /DMAP/silica DCM solution. The reaction was stirred for 30 minutes before next step. Another 20 mL scintillation vial equipped with a stir bar was flame dried under vacuum. After cooling down, the vial was charged with $\text{Rh}_2(\text{R-}p\text{-Ph-TPCP})_4$ (3.5 mg, 0.002 mmol, 1.0 mol%) and 4Å MS (1000% wt). The vial was then flushed with nitrogen for 3 times and the nitrogen balloon was left on the septum. HFIP (672.2 mg, 0.42 mL, 4.0 mmol, 20 equiv), styrene (104.2

mg, 115 μ L, 1.0 mmol, 5.0 equiv) and 2.0 mL distilled DCM were injected sequentially to the vial, this mixture was stirred at 600 rpm for 10 min before diazo compounds injection. The crude diazo compound from copper-catalyzed oxidation step (in \sim 1.5 mL DCM solution) was injected to the styrene/ $\text{Rh}_2(\text{R-}p\text{-Ph-TPCP})_4$ DCM solution by syringe with 0.05 mL/min flow rate. After addition, the reaction was stirred for another 1 h under nitrogen at room temperature. After completion, the solution was concentrated under rotovap and purified by flash column chromatography (0%, then 5%-15% Et₂O in Hexanes) to get the cyclopropanation products.

6.3.3 General procedure for tandem reactions of Cu(II) catalyzed hydrazones oxidation and Rh(II) catalyzed asymmetric cyclopropanation under flow-Batch Conditions

A 50 mL beaker was charged with $\text{Cu}(\text{OAc})_2\cdot\text{H}_2\text{O}$ (0.40 g, 2.0 mmol, 10 equiv), DMAP (0.24 g, 2.0 mmol, 10 equiv), silica powder (4.0 g, SiliaFlash® P60, 40-63 μ m), and 20 mL DCM. The mixture was stirred vigorously with a stir bar (700 rpm) under air for 10 min. In a column (Biotage® SNAP Cartridge, KP-Sil, 10 g) 6.0 g silica powder was firstly packed and the air saturated $\text{Cu}(\text{OAc})_2\cdot\text{H}_2\text{O}$ /DMAP/silica/DCM mixture was packed on the top layer. After the column being rinsed with 0.06 mol/L DMAP in DCM eluent, hydrazone was added on the top of the column and flashed with eluent injected by syringe pump. A 50 mL flask equipped with a stir bar was flame dried under vacuum. After cooling down, the flask was charged with $\text{Rh}_2(\text{R-}p\text{-Ph-TPCP})_4$ and 4Å MS, flushed with nitrogen for 3 times and the nitrogen balloon was left on the septum. Then HFIP, styrene derivatives and 2.0 mL distilled DCM were injected sequentially. The mixture was then stirred at 600 rpm for 10 min before upstream crude diazo compound injection. The crude diazo compound solution from the $\text{Cu}(\text{OAc})_2\cdot\text{H}_2\text{O}$ /DMAP/silica column was eluted drop-wisely to the styrene/ $\text{Rh}_2(\text{R-}p\text{-Ph-TPCP})_4$ flask for cyclopropanation reaction. **(Figure 6.6)** After diazo compound addition, the reaction was stirred for another 1 h under nitrogen at

room temperature. After reaction completion the solution was concentrated under rotovap and purified by flash column chromatography (0%, then 5% - 15% Et₂O in Hexanes) to obtain the cyclopropanation products.

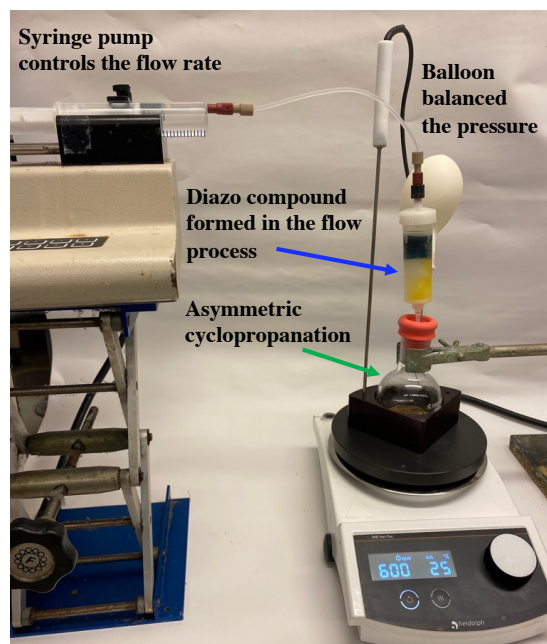


Figure 6.6 The bench-top tandem Cu(II) catalyzed hydrazones oxidation in flow and sequential Rh(II) catalyzed asymmetric cyclopropanation reaction set-up

6.3.4 Procedure for Column Robustness Assessment Experiment

A 50 mL beaker was charged with Cu(OAc)₂·H₂O (0.40 g, 2.0 mmol, 10 equivalents), DMAP (0.2443 g, 2.0 mmol, 10.0 equiv), silica powder (4.0 g, SiliaFlash® P60, 40-63 μm), and 20 mL DCM. The mixture was stirred vigorously with a stir bar (700 rpm) under air for 10 min before packed to the column. In a column (Biotage® SNAP Cartridge, KP-Sil, 10 g) 6.0 g silica powder was firstly packed. The air saturated Cu(OAc)₂·H₂O/DMAP/silica/DCM mixture was then packed on the top layer. After the column being rinsed with 0.06 mol/L DMAP in DCM eluent. The 2,2,2-trichloroethyl (Z)-2-(4-bromophenyl)-2-hydrazineylideneacetate (74.9 mg, 0.2 mmol, 1.0 equiv) in 1 mL DCM was added on the top of the column and flashed with eluent injected by syringe

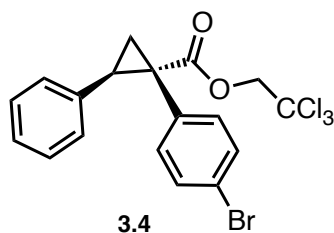
pump. A 50 mL flask equipped with a stir bar was flame dried under vacuum. After cooling down, the flask was charged with $\text{Rh}_2(\text{R-}p\text{-Ph-TPCP})_4$ (3.5 mg, 1.0 mol%, 0.002 mmol) and 4 Å MS (1000% wt), flushed with nitrogen for 3 times and the nitrogen balloon was left on the septum. Then HFIP (672.2 mg, 0.42 mL, 20 equiv, 4.0 mmol), styrene (104.2 mg, 0.115 mL, 5.0 equiv, 1.0 mmol) and 2.0 mL distilled DCM were injected to the flask sequentially. The mixture was then stirred at 600 rpm for 10 min before upstream crude diazo compound injection. The crude diazo compound solution from the $\text{Cu}(\text{OAc})_2\text{-H}_2\text{O}/\text{DMAP}/\text{silica}$ column was eluted drop-wisely to the styrene/ $\text{Rh}_2(\text{R-}p\text{-Ph-TPCP})_4$ flask for cyclopropanation reaction. After each batch of hydrazone conversion, the subsequent batch of the hydrazone was added on the top of the column again. After each addition of diazo compound to the cyclopropanation flask, the cyclopropanation reaction flask was replaced and the reaction was stirred for another 1 h. After reaction completion the solution was concentrated under rotovap and purified by flash column chromatography (0%, then 5%-15% Et_2O in Hexanes) to obtain the cyclopropanation product.

6.3.5 Procedure for Gram Scale Synthesis with Bench-top Flow procedure

A 50 mL beaker was charged with $\text{Cu}(\text{OAc})_2\text{-H}_2\text{O}$ (2.995 g, 15.0 mmol, 5 equiv), DMAP (3.665 g, 30 mmol, 10 equiv), silica powder (10.0 g, SiliaFlash® P60, 40-63 μm), and 40 mL DCM. The mixture was stirred vigorously with a stir bar (700 rpm) under air for 10 min. In a column (Biotage® SNAP Cartridge, KP-Sil, 50 g) 40 g silica powder was firstly packed and the air saturated $\text{Cu}(\text{OAc})_2\text{-H}_2\text{O}/\text{DMAP}/\text{silica}/\text{DCM}$ mixture was packed on the top layer. After the column being rinsed with 0.06 mol/L DMAP in DCM eluent, 2,2,2-trichloroethyl (Z)-2-(4-bromophenyl)-2-hydrazineylideneacetate (1.123 g, 3.0 mmol, 1.0 equiv) in 3 mL DMAP/DCM solution was added on the top of the column and flashed through the column with 0.5 mL/min flow rate controlled by syringe pump. A 100 mL flask equipped with a stir bar was flame dried under

vacuum. After cooling down, the flask was charged with $\text{Rh}_2(\text{R-}p\text{-Ph-TPCP})_4$ (52.91 mg, 0.030 mmol, 1 mol%), and 4Å MS (11.23 g, 1000% wt), flushed with nitrogen for 3 times and the nitrogen balloon was left on the septum. Then HFIP (10.08 g, 6.3 mL, 60 mmol, 20 equiv), styrene (1.56 mg, 1.72 mL, 5.0 equiv, 15 mmol) and 20 mL distilled DCM were injected sequentially. The mixture was then stirred at 600 rpm for 10 min before upstream crude diazo compound injection. The crude diazo compound solution from the $\text{Cu}(\text{OAc})_2\text{-H}_2\text{O}/\text{DMAP}/\text{silica}$ column was eluted drop-wisely to the styrene/ $\text{Rh}_2(\text{R-}p\text{-Ph-TPCP})_4$ flask for cyclopropanation reaction. After diazo compound addition, the reaction was stirred for another 1 h under nitrogen at room temperature. After reaction completion the solution was concentrated under rotovap and purified by flash column chromatography (0%, then 5% - 15% Et_2O in Hexanes) to obtain the cyclopropanation product (1.021g, 75% yield, 96% ee).

6.3.6 Characterization of the Cyclopropanation Products



2,2,2-trichloroethyl (1*S*,2*R*)-1-(4-bromophenyl)-2-phenylcyclopropane-1-carboxylate

This compound was prepared following both methods of General procedure 6.3.2 (batch-batch) and General procedure 6.3.3 (flow-batch). Starting material is 2,2,2-trichloroethyl (*Z*)-2-(4-bromophenyl)-2-hydrazineylideneacetate (74.9 mg, 0.2 mmol, 1.0 equiv). Cyclopropanation step condition applied styrene (104.2 mg, 1.0 mmol, 0.115 mL, 5.0 equiv.) as substrate, $\text{Rh}_2(\text{R-}p\text{-Ph-TPCP})_4$ (3.5 mg, 0.002 mmol, 1.0 mol%) as catalyst. After flash chromatography (0%, then 5% - 15% Et_2O in hexanes) the product was obtained as a white solid (64.6 mg, 72% yield with batch-

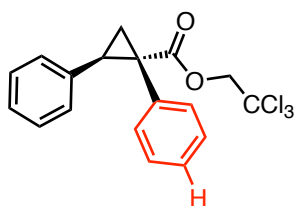
batch procedure, 67.3 mg, 75% yield with flow-batch procedure). The ^1H NMR data are consistent with literature values.⁵

^1H NMR (400 MHz, Chloroform- d) δ 7.27 – 7.25 (m, 2H), 7.20 – 7.06 (m, 3H), 6.99 – 6.89 (m, 2H), 6.80 (dd, J = 6.7, 2.9 Hz, 2H), 4.83 (d, J = 11.9 Hz, 1H), 4.64 (d, J = 11.9 Hz, 1H), 3.22 (dd, J = 9.4, 7.5 Hz, 1H), 2.28 (dd, J = 9.4, 5.2 Hz, 1H), 1.97 (dd, J = 7.5, 5.2 Hz, 1H).

Chiral HPLC:

Batch-batch: (OJ-H, 30 min, 1 mL/min, 1 % iPrOH in hexanes, UV 230 nm.) t_{R} : Major: 13.2 min, Minor: 8.5 min, 97% ee.

Flow-batch: (AD-H, 30 min, 1 mL/min, 1 % iPrOH in hexanes, UV 230 nm.) t_{R} : Major: 8.3 min, Minor: 6.6 min, 97% ee.



3.5

2,2-trichloroethyl (1*S*,2*R*)-1,2-diphenylcyclopropane-1-carboxylate

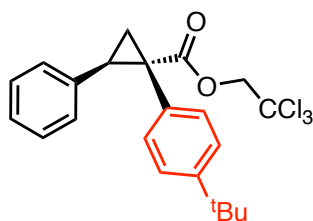
This compound was prepared following both methods of General procedure 6.3.2 (batch-batch) and General procedure 6.3.3 (flow-batch). Starting material is 2,2,2-trichloroethyl (*Z*)-2-hydrazineylidene-2-phenylacetate (59.1 mg, 0.2 mmol, 1.0 equiv). Cyclopropanation step condition applied styrene (104.2 mg, 1.0 mmol, 0.115 mL, 5.0 equiv.) as substrate, $\text{Rh}_2(\text{R-}p\text{-Ph-TPCP})_4$ (3.5 mg, 0.002 mmol, 1.0 mol%) as catalyst. After flash chromatography (0%, then 5% - 15% Et_2O in hexanes) the product was obtained as a white solid (67.3mg, 91% yield with batch-batch procedure, 53.2 mg, 72% yield with flow-batch procedure). The ^1H NMR data are consistent with literature values.⁵

$^1\text{H NMR}$ (400 MHz, Chloroform- d) δ 7.15 – 7.11 (m, 3H), 7.10 – 7.04 (m, 5H), 6.79 (dd, J = 6.7, 3.0 Hz, 2H), 4.84 (d, J = 11.9 Hz, 1H), 4.64 (d, J = 11.9 Hz, 1H), 3.22 (dd, J = 9.4, 7.4 Hz, 1H), 2.28 (dd, J = 9.4, 5.1 Hz, 1H), 2.01 (dd, J = 7.4, 5.1 Hz, 1H).

Chiral HPLC:

Batch-batch: (OJ-H, 60 min, 1 mL/min, 1 % iPrOH in hexanes, UV 230 nm) tR: Major: 29.2 min, Minor: 17.3 min, 93% ee.

Flow-batch: (OD-H, 30 min, 1 mL/min, 1 % iPrOH in hexanes, UV 230 nm) tR: Major: 7.5 min, Minor: 14.9 min, 94% ee.



3.6

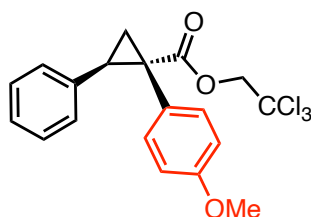
2,2,2-trichloroethyl (1*S*,2*R*)-1-(4-(tert-butyl)phenyl)-2-phenylcyclopropane-1-carboxylate

This compound was prepared following both methods of General procedure 6.3.2 (batch-batch) and General procedure 6.3.3 (flow-batch). Starting material is 2,2,2-trichloroethyl (*Z*)-2-(4-(tert-butyl)phenyl)-2-hydrazineylideneacetate (70.3 mg, 0.2 mmol, 1.0 equiv). Cyclopropanation step condition applied styrene (104.2 mg, 1.0 mmol, 0.115 mL, 5.0 equiv.) as substrate, $\text{Rh}_2(\text{R-}p\text{-Ph-TPCP})_4$ (3.5 mg, 0.002 mmol, 1.0 mol%) as catalyst. After flash chromatography (0%, then 5% - 15% Et_2O in hexanes) the product was obtained as a white solid (77.7 mg, 91% yield with batch-batch procedure, 67.5 mg, 79% yield with flow-batch procedure). The $^1\text{H NMR}$ data are consistent with literature values.⁵

$^1\text{H NMR}$ (400 MHz, Chloroform- d) δ 7.14 - 7.12 (m, 2H), 7.07 – 7.05 (m, 3H), 6.98 (d, J = 2.0 Hz, 1H), 6.96 (d, J = 1.9 Hz, 1H), 6.78 (dd, J = 6.7, 3.0 Hz, 2H), 4.83 (d, J = 11.9 Hz, 1H), 4.65

(d, $J = 11.9$ Hz, 1H), 3.18 (dd, $J = 9.4, 7.4$ Hz, 1H), 2.27 (dd, $J = 9.4, 5.1$ Hz, 1H), 1.97 (dd, $J = 7.4, 5.1$ Hz, 1H), 1.22 (s, 9H).

Chiral HPLC: (*R,R*-Whelk, 30 min, 1 mL/min, 1 % iPrOH in hexanes, UV 230 nm) tR: Major: 8.1 min, Minor: 6.0 min, Batch-batch: 97% ee, Flow-batch: 97% ee.



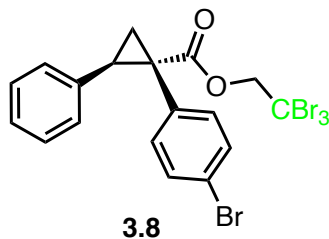
3.7

2,2,2-trichloroethyl (1*S*,2*R*)-1-(4-methoxyphenyl)-2-phenylcyclopropane-1-carboxylate

This compound was prepared following both methods of General procedure 6.3.2 (batch-batch) and General procedure 6.3.3 (flow-batch). Starting material is 2,2,2-trichloroethyl (*Z*)-2-hydrazineylidene-2-(4-methoxyphenyl)acetate (65.1 mg, 0.2 mmol, 1.0 equiv). Cyclopropanation step condition applied styrene (104.2 mg, 1.0 mmol, 0.115 mL, 5.0 equiv.) as substrate, Rh₂(*R-p*-Ph-TPCP)₄ (3.5 mg, 0.002 mmol, 1.0 mol%) as catalyst. After flash chromatography (0%, then 5% - 15% Et₂O in hexanes) the product was obtained as a white solid (70.7 mg, 88% yield with batch-batch procedure, 55.2 mg, 69% yield with flow-batch procedure). The ¹H NMR data are consistent with literature values.⁵

¹H NMR (400 MHz, Chloroform-*d*) δ 7.17 – 7.03 (m, 3H), 7.03 – 6.90 (m, 2H), 6.85 – 6.73 (m, 2H), 6.71 – 6.57 (m, 2H), 4.83 (d, $J = 11.9$ Hz, 1H), 4.65 (d, $J = 11.9$ Hz, 1H), 3.72 (s, 3H), 3.18 (dd, $J = 9.4, 7.4$ Hz, 1H), 2.27 (dd, $J = 9.4, 5.0$ Hz, 1H), 1.95 (dd, $J = 7.4, 5.0$ Hz, 1H).

Chiral HPLC: (AD-H, 30 min, 1 mL/min, 1 % iPrOH in hexanes, UV 230 nm) tR: Major: 10.4 min, Minor: 8.7 min, Batch-batch: 93% ee, Flow-batch: 96% ee.



2,2,2-tribromoethyl (1*S*,2*R*)-1-(4-bromophenyl)-2-phenylcyclopropane-1-carboxylate

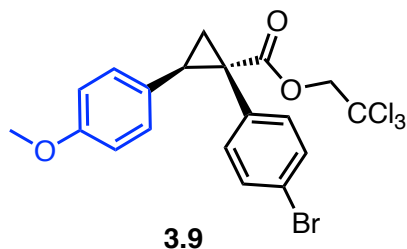
This compound was prepared following both methods of General procedure 6.3.2 (batch-batch) and General procedure 6.3.3 (flow-batch). Starting material is 2,2,2-tribromoethyl (*Z*)-2-(4-bromophenyl)-2-hydrazineylideneacetate (101.6 mg, 0.2 mmol, 1.0 equiv). Cyclopropanation step condition applied styrene (104.2 mg, 1.0 mmol, 0.115 mL, 5.0 equiv.) as substrate, Rh₂(*R-p*-Ph-TPCP)₄ (3.5 mg, 0.002 mmol, 1 mol%) as catalyst. After flash chromatography (0%, then 5% - 15% Et₂O in hexanes) the product was obtained as a white solid (105.1 mg, 90% yield with batch-batch procedure, 88.5 mg, 76% yield with flow-batch procedure). The ¹H NMR data are consistent with literature values.⁶

¹H NMR (400 MHz, Chloroform-*d*) δ 7.32 – 7.17 (m, 2H), 7.17 – 7.04 (m, 3H), 7.03 – 6.88 (m, 2H), 6.88 – 6.75 (m, 2H), 5.00 (d, *J* = 12.2 Hz, 1H), 4.83 (d, *J* = 12.2 Hz, 1H), 3.26 (dd, *J* = 9.4, 7.5 Hz, 1H), 2.32 (dd, *J* = 9.4, 5.2 Hz, 1H), 1.98 (dd, *J* = 7.5, 5.2 Hz, 1H).

Chiral HPLC:

Batch-batch: (*R,R*-Whelk, 60 min, 1 mL/min, 1 % *i*PrOH in hexanes, UV 230 nm) t_R: Major: 36.4 min, Minor: 27.6 min, 93% ee.

Flow-batch:(OD-H, 30 min, 1 mL/min, 1 % *i*PrOH in hexanes, UV 230 nm) t_R: Major: 10.2 min, Minor: 12.8 min, 95% ee.

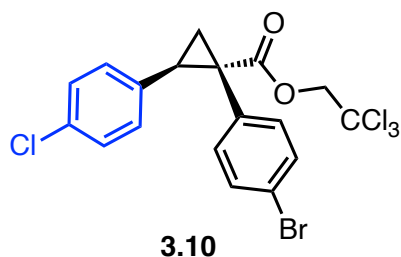


2,2,2-trichloroethyl(1*S*,2*R*)-1-(4-bromophenyl)-2-(4-methoxyphenyl)cyclopropane-1-carboxylate

This compound was prepared following both methods of General procedure 6.3.2 (batch-batch) and General procedure 6.3.3 (flow-batch). Starting material is 2,2,2-trichloroethyl (*Z*)-2-(4-bromophenyl)-2-hydrazineylideneacetate (74.9 mg, 0.2 mmol, 1.0 equiv). Cyclopropanation step applied 1-methoxy-4-vinylbenzene (134.2 mg, 1.0 mmol, 5.0 equiv.) as substrate, Rh₂(*R-p*-Ph-TPCP)₄ (3.5 mg, 0.002 mmol, 1 mol%) as catalyst. After flash chromatography (0%, then 5% - 15% Et₂O in hexanes) the product was obtained as a white solid (77.8 mg, 81% yield with batch-batch procedure, 75.1 mg, 78% yield with flow-batch procedure). The ¹H NMR data are consistent with literature values.⁵

¹H NMR (400 MHz, Chloroform-*d*) δ 7.28 (s, 2H), 7.01 – 6.87 (m, 2H), 6.76 – 6.69 (m, 2H), 6.69 – 6.61 (m, 2H), 4.82 (d, *J* = 11.9 Hz, 1H), 4.63 (d, *J* = 11.9 Hz, 1H), 3.72 (s, 3H), 3.17 (dd, *J* = 9.5, 7.5 Hz, 1H), 2.26 (dd, *J* = 9.5, 5.2 Hz, 1H), 1.90 (dd, *J* = 7.5, 5.2 Hz, 1H).

Chiral HPLC: (AD-H, 30 min, 1 mL/min, 1 % *i*PrOH in hexanes, UV 230 nm) tR: Major: 16.4 min, Minor: 12.0 min, Batch-batch: 91% ee, Flow-batch: 94% ee.

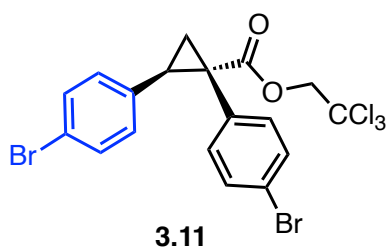


2,2,2-trichloroethyl (1*S*,2*R*)-1-(4-bromophenyl)-2-(4-chlorophenyl)cyclopropane-1-carboxylate

This compound was prepared following both methods of General procedure 6.3.2 (batch-batch) and General procedure 6.3.3 (flow-batch). Starting material is 2,2,2-trichloroethyl (Z)-2-(4-bromophenyl)-2-hydrazineylideneacetate (74.9 mg, 0.2 mmol, 1.0 equiv). Cyclopropanation step applied 1-chloro-4-vinylbenzene (138.6 mg, 1.0 mmol, 5.0 equiv.) as substrate, Rh₂(*R-p*-Ph-TPCP)₄ (3.5 mg, 0.002 mmol, 1 mol%) as catalyst. After flash chromatography (0%, then 5% - 15% Et₂O in hexanes) the product was obtained as a white solid (77.5 mg, 80% yield with batch-batch procedure, 74.6 mg, 77% yield with flow-batch procedure). The ¹H NMR data are consistent with literature values.⁵

¹H NMR (400 MHz, Chloroform-d) δ 7.33 – 7.22 (m, 2H), 7.10 – 7.01 (m, 2H), 6.99 – 6.83 (m, 2H), 6.82 – 6.62 (m, 2H), 4.82 (d, J = 11.9 Hz, 1H), 4.64 (d, J = 11.9 Hz, 1H), 3.18 (dd, J = 9.4, 7.4 Hz, 1H), 2.29 (dd, J = 9.4, 5.3 Hz, 1H), 1.92 (dd, J = 7.4, 5.3 Hz, 1H).

Chiral HPLC: (AD-H, 30 min, 1 mL/min, 1 % iPrOH in hexanes, UV 230 nm) tR: Major: 11.5 min, Minor: 8.8 min, Batch-batch: 95% ee, Flow-batch: 92% ee.



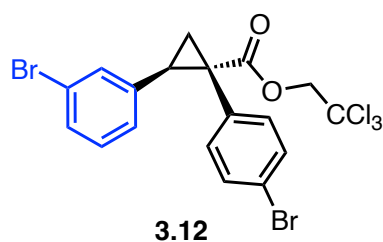
2,2,2-trichloroethyl (1*S*,2*R*)-1,2-bis(4-bromophenyl)cyclopropane-1-carboxylate

This compound was prepared following both methods of General procedure 6.3.2 (batch-batch) and General procedure 6.3.3 (flow-batch). Starting material is 2,2,2-trichloroethyl (Z)-2-(4-bromophenyl)-2-hydrazineylideneacetate (74.9 mg, 0.2 mmol, 1.0 equiv). Cyclopropanation step applied 1-bromo-4-vinylbenzene (183.1 mg, 1.0 mmol, 5.0 equiv.) as substrate, Rh₂(*R-p*-Ph-

TPCP)₄ (3.5 mg, 0.002 mmol, 1 mol%) as catalyst. After flash chromatography (0%, then 5% - 15% Et₂O in hexanes) the product was obtained as a white solid (93.1 mg, 88% yield with batch-batch procedure, 78.1 mg, 74% yield with flow-batch procedure). The ¹H NMR data are consistent with literature values.⁵

¹H NMR (400 MHz, Chloroform-d) δ 7.32 – 7.27 (m, 2H), 7.25 – 7.20 (m, 2H), 7.01 – 6.85 (m, 2H), 6.72 – 6.51 (m, 2H), 4.82 (d, J = 11.9 Hz, 1H), 4.63 (d, J = 11.9 Hz, 1H), 3.16 (dd, J = 9.4, 7.4 Hz, 1H), 2.28 (dd, J = 9.4, 5.3 Hz, 1H), 1.91 (dd, J = 7.4, 5.3 Hz, 1H).

Chiral HPLC: (AD-H, 30 min, 1 mL/min, 1 % iPrOH in hexanes, UV 230 nm) tR: Major: 12.1 min, Minor: 9.4 min, Batch-batch: 93% ee, Flow-batch: 93% ee.



2,2,2-trichloroethyl (1S,2R)-2-(3-bromophenyl)-1-(4-bromophenyl)cyclopropane-1-carboxylate

This compound was prepared following both methods of General procedure 6.3.2 (batch-batch) and General procedure 6.3.3 (flow-batch). Starting material is 2,2,2-trichloroethyl (Z)-2-(4-bromophenyl)-2-hydrazineylideneacetate (74.9 mg, 0.2 mmol, 1.0 equiv). Cyclopropanation step applied 1-bromo-3-vinylbenzene (183.1 mg, 1.0 mmol, 5.0 equiv.) as substrate, Rh₂(*R-p*-Ph-TPCP)₄ (3.5 mg, 0.002 mmol, 1 mol%) as catalyst. After flash chromatography (0%, then 5% - 15% Et₂O in hexanes) the product was obtained as a white solid (90.2 mg, 85% yield with batch-batch procedure, 74.3 mg, 70% yield with flow-batch procedure).

mp: 108-109°C

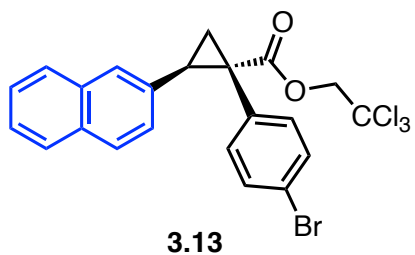
IR(neat) 2952, 1736, 1594, 1566, 1489, 1370, 1239, 1154, 1072, 1011, 828, 805, 764, 717, 697 cm^{-1}

^1H NMR (400 MHz, Chloroform- d) δ 7.34 – 7.27 (m, 2H), 7.23 (ddd, J = 8.0, 2.0, 1.0 Hz, 1H), 7.04 (t, J = 1.9 Hz, 1H), 6.95 (dd, J = 8.6, 7.1 Hz, 3H), 6.63 (dt, J = 8.0, 1.5 Hz, 1H), 4.82 (d, J = 11.9 Hz, 1H), 4.65 (d, J = 11.9 Hz, 1H), 3.17 (dd, J = 9.4, 7.4 Hz, 1H), 2.28 (dd, J = 9.4, 5.3 Hz, 1H), 1.94 (dd, J = 7.4, 5.3 Hz, 1H).

^{13}C NMR (101 MHz, CDCl_3) δ 171.5, 138.0, 133.8, 132.6, 131.7, 131.3, 130.2, 129.7, 126.6, 122.4, 122.0, 95.1, 74.7, 37.0, 33.4, 20.5.

HR-MS:(+p APCI) calcd for $[\text{C}_{18}\text{H}_{13}\text{O}_2\text{Br}_2\text{C}_3+\text{H}]$ 524.8421 found 524.8424

Chiral HPLC: (AD-H, 30 min, 1 mL/min, 1 % iPrOH in hexanes, UV 230 nm) tR: Major: 9.9 min, Minor: 7.5 min, Batch-batch: 94% ee, Flow-batch: 91% ee.



2,2,2-trichloroethyl (1*S*,2*R*)-1-(4-bromophenyl)-2-(naphthalen-2-yl)cyclopropane-1-carboxylate

This compound was prepared following both methods of General procedure 6.3.2 (batch-batch) and General procedure 6.3.3 (flow-batch). Starting material is 2,2,2-trichloroethyl (*Z*)-2-(4-bromophenyl)-2-hydrazineylideneacetate (74.9 mg, 0.2 mmol, 1.0 equiv). Cyclopropanation step applied 2-vinylnaphthalene (154.2 mg, 1.0 mmol, 5.0 equiv.) as substrate, $\text{Rh}_2(\textit{R-p-Ph-TPCP})_4$ (3.5 mg, 0.002 mmol, 1 mol%) as catalyst. After flash chromatography (0%, then 5% - 15% Et_2O in hexanes) the product was obtained as a white solid (82.1 mg, 82% yield with batch-batch procedure, 74.1 mg, 74% yield with flow-batch procedure).

mp: 95-98 °C

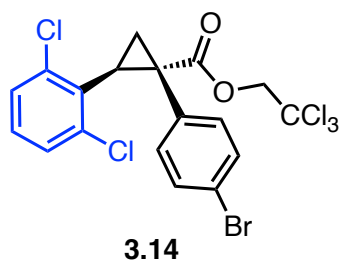
IR(neat) 2953, 1732, 1627, 1598, 1489, 1395, 1367, 1239, 1128, 1148, 1011, 858, 817, 766, 748, 715, 574 cm⁻¹

¹H NMR (400 MHz, Chloroform-d) δ 7.75 – 7.68 (m, 1H), 7.67 – 7.61 (m, 1H), 7.57 (d, J = 8.5 Hz, 1H), 7.44 – 7.38 (m, 2H), 7.38 – 7.35 (m, 1H), 7.23 – 7.20 (m, 2H), 7.01 – 6.93 (m, 2H), 6.84 (dd, J = 8.5, 1.9 Hz, 1H), 4.84 (d, J = 11.9 Hz, 1H), 4.67 (d, J = 11.9 Hz, 1H), 3.38 (dd, J = 9.4, 7.4 Hz, 1H), 2.36 (dd, J = 9.4, 5.2 Hz, 1H), 2.11 (dd, J = 7.5, 5.2 Hz, 1H).

¹³C NMR (101 MHz, Chloroform-d) δ 171.9, 133.8, 133.3, 133.2, 133.1, 132.6, 131.2, 127.8, 127.8, 127.5, 126.4, 126.1, 126.0, 121.8, 95.2, 74.7, 37.0, 34.4, 20.7.

HR-MS:(+p APCI) calcd for [C₂₂H₁₆BrC₁₃O₂+H] 496.9472 found 496.9473

Chiral HPLC: (AD-H, 30 min, 1 mL/min, 1 % iPrOH in hexanes, UV 230 nm) tR: Major: 12.4 min, Minor: 10.1 min, Batch-batch: 96% ee, Flow-batch: 93% ee.



2,2,2-trichloroethyl (1*S*,2*S*)-1-(4-bromophenyl)-2-(2,6-dichlorophenyl)cyclopropane-1-carboxylate

This compound was prepared following both methods of General procedure 6.3.2 (batch-batch) and General procedure 6.3.3 (flow-batch). Starting material is 2,2,2-trichloroethyl (Z)-2-(4-bromophenyl)-2-hydrazineylideneacetate (74.9 mg, 0.2 mmol, 1.0 equiv). Cyclopropanation step applied 1,3-dichloro-2-vinylbenzene (173.0 mg, 1.0 mmol, 5.0 equiv.) as substrate, Rh₂(R-PTAD)₄ (3.1 mg, 0.002 mmol, 1 mol%) as catalyst, 40 °C as reaction temperature. After flash

chromatography (0%, then 5% - 15% Et₂O in hexanes) the product was obtained as a clear oil (68.6 mg, 66% yield with batch-batch procedure, 63.4 mg, 61% yield with flow-batch procedure).

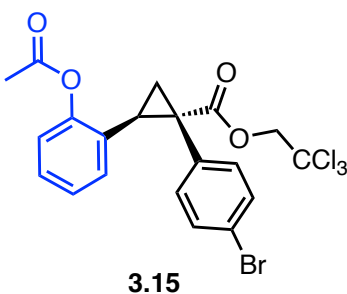
IR(neat) 2924, 1739, 1558, 1491, 1430, 1374, 1245, 1196, 1156, 1092, 1010, 769, 719, 575, 515 cm⁻¹

¹H NMR (400 MHz, Chloroform-d) δ 7.24 - 7.23 (m, 2H), 7.21 - 7.18 (m, 2H), 7.13 (s, 2H), 7.00 - 6.95 (m, 1H), 4.94 (d, J = 11.9 Hz, 1H), 4.66 (d, J = 11.9 Hz, 1H), 3.35 (dd, J = 9.8, 8.3 Hz, 1H), 3.10 (dd, J = 8.3, 6.0 Hz, 1H), 2.40 (dd, J = 9.9, 5.9 Hz, 1H).

¹³C NMR (151 MHz, Chloroform-d) δ 171.8, 132.8, 132.3, 132.2, 131.1, 130.9, 129.8, 128.9, 121.9, 95.1, 74.8, 34.9, 34.1, 23.1.

HR-MS:(+p APCI) calcd for [C₁₈H₁₂BrCl₃O₂+H] 514.8536 found 514.8537

Chiral HPLC: (AD-H, 30 min, 1 mL/min, 1 % iPrOH in hexanes, UV 230 nm) tR: Major: 7.1 min, Minor: 13.2 min, Batch-batch: 85% ee, Flow-batch: 89% ee.



2,2,2-trichloroethyl (1S,2R)-2-(2-acetoxyphenyl)-1-(4-bromophenyl)cyclopropane-1-carboxylate

This compound was prepared following both methods of General procedure 6.3.2 (batch-batch) and General procedure 6.3.3 (flow-batch). Starting material is 2,2,2-trichloroethyl (Z)-2-(4-bromophenyl)-2-hydrazineylideneacetate (74.9 mg, 0.2 mmol, 1.0 equiv). Cyclopropanation step applied 2-vinylphenyl acetate (162.2 mg, 1.0 mmol, 5.0 equiv.) as substrate, Rh₂(R-PTAD)₄ (3.1 mg, 0.002 mmol, 1 mol%) as catalyst, 40 °C as reaction temperature. After flash chromatography

(0%, then 5% - 15% Et₂O in hexanes) the product was obtained as a white solid (84.3 mg, 83% yield with batch-batch procedure, 70.1 mg, 69% yield with flow-batch procedure).

mp: 101-102 °C

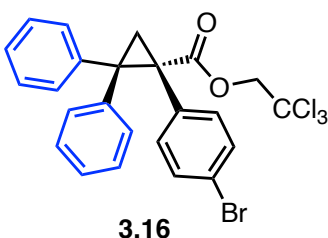
IR(neat) 2954, 1760, 1732, 1490, 1453, 1433, 1368, 1243, 1203, 1174, 1152, 1101, 1072, 1010, 971, 942, 911, 824, 768, 716, 682, 575, 530 cm⁻¹

¹H NMR (400 MHz, Chloroform-d) δ 7.27 (d, J = 1.9 Hz, 1H), 7.25 (d, J = 2.0 Hz, 1H), 7.14 (ddd, J = 8.1, 7.4, 1.6 Hz, 1H), 7.10 – 6.96 (m, 3H), 6.87 (td, J = 7.6, 1.3 Hz, 1H), 6.37 (dd, J = 7.8, 1.6 Hz, 1H), 4.84 (d, J = 11.9 Hz, 1H), 4.61 (d, J = 11.9 Hz, 1H), 3.22 (dd, J = 9.4, 7.6 Hz, 1H), 2.34 (s, 3H), 2.19 (dd, J = 9.4, 5.2 Hz, 1H), 2.01 (dd, J = 7.6, 5.2 Hz, 1H).

¹³C NMR (151 MHz, Chloroform-d) δ 171.9, 169.5, 150.8, 133.6, 133.0, 131.2, 128.2, 127.9, 127.3, 125.8, 122.4, 121.9, 95.1, 74.7, 36.3, 28.2, 21.2, 19.7.

HR-MS:(+p APCI) calcd for [C₂₀H₁₆BrCl₃O₄⁺] 503.9292 found 503.9289

Chiral HPLC: (AD-H, 30 min, 1 mL/min, 1 % iPrOH in hexanes, UV 230 nm) tR: Major: 14.6 min, Minor: 22.6 min, Batch-batch: 64% ee, Flow-batch: 67% ee.



2,2,2-trichloroethyl (R)-1-(4-bromophenyl)-2,2-diphenylcyclopropane-1-carboxylate

This compound was prepared following both methods of General procedure 6.3.2 (batch-batch) and General procedure 6.3.3 (flow-batch). Starting material is 2,2,2-trichloroethyl (Z)-2-(4-bromophenyl)-2-hydrazineylideneacetate (74.9 mg, 0.2 mmol, 1.0 equiv). Cyclopropanation step applied ethene-1,1-diyldibenzene (180.3 mg, 1.0 mmol, 5.0 equiv.) as substrate, Rh₂(R-PTAD)₄ (3.1 mg, 0.002 mmol, 1 mol%) as catalyst. After flash chromatography (0%, then 5% - 15% Et₂O

in hexanes) the product was obtained as a white solid (75.9 mg, 72% yield with batch-batch procedure, 59.1 mg, 56% yield with flow-batch procedure). The ^1H NMR data are consistent with literature values.⁵

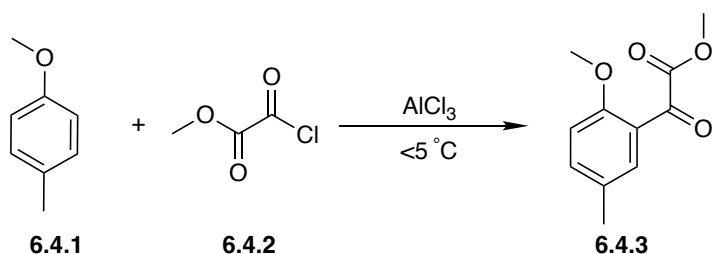
^1H NMR (400 MHz, Chloroform-d) δ 7.59 – 7.43 (m, 2H), 7.36 – 7.26 (m, 5H), 7.24 – 7.21 (m, 2H), 7.10 – 6.89 (m, 5H), 4.51 (d, J = 11.9 Hz, 1H), 4.12 (d, J = 11.9 Hz, 1H), 2.75 (d, J = 5.7 Hz, 1H), 2.48 (d, J = 5.8 Hz, 1H).

Chiral HPLC: (AD-H, 30 min, 1 mL/min, 1 % iPrOH in hexanes, UV 230 nm) tR: Major: 17.9 min, Minor: 10.0 min, Batch-batch: 98% ee, Flow-batch: 94% ee.

6.4 Experimental Part for Chapter 4

6.4.1 Procedure for starting material synthesis

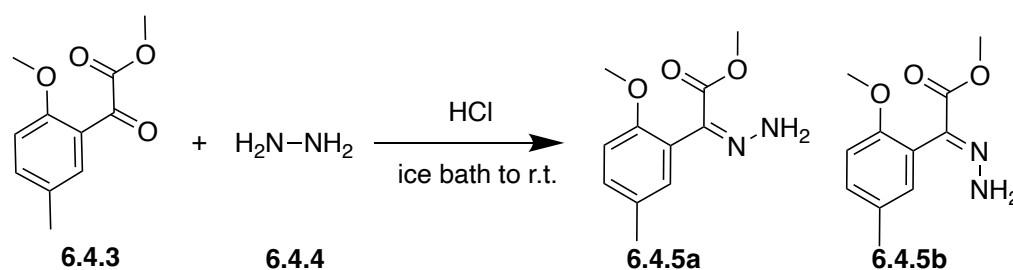
Methyl 2-(2-methoxy-5-methylphenyl)-2-oxoacetate(6.4.3)



A solution of 1-methoxy-4-methylbenzene (**6.4.1**) (2.443 g, 20 mmol) and methyl 2-chloro-2-oxoacetate (**6.4.2**) (2.756 g, 22.5 mol) in 20 ml CH_2Cl_2 was added dropwise to a stirred suspension of AlCl_3 (4.667 g, 35 mmol) in 13 ml of CH_2Cl_2 with the temperature maintained below 5°C throughout. When the addition was complete, the mixture was stirred at 25°C for 2.5 h and then poured onto 75 g of ice- H_2O . The aqueous layer was washed once with CH_2Cl_2 . The combined organic extracts were washed with 3 M HCl, 1 M HCl, H_2O , and saturated NaCl, and the organic

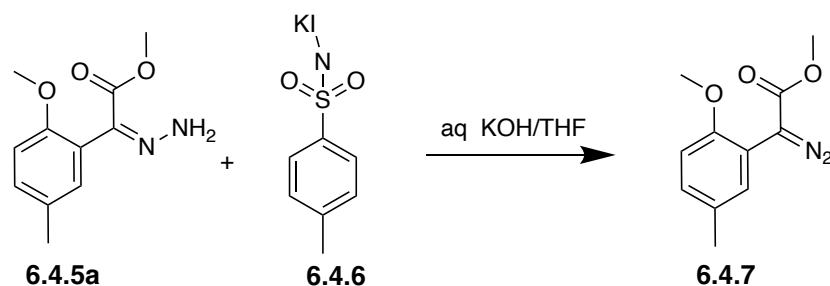
solvent was evaporated. The crude product **6.4.3** was then chromatographed (0-5% Diethyl Ether in Hexane) and get slight yellow liquid (77% yield)

Methyl (E or Z)-2-hydrazineylidene-2-(2-methoxy-5-methylphenyl)acetate (**6.4.5**)



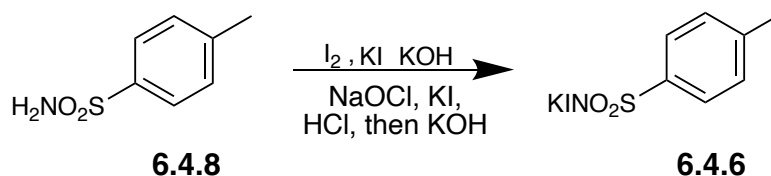
A 500 mL round-bottom flask was charged with hydrazine monohydrate (**6.4.4**) (12 mL, 6.5 g, 200 mmol, 10.0 equiv.) and MeOH (300 mL). The reaction mixture was cooled to 0 °C in an ice-H₂O bath. HCl (3.0 M, 60 mL, 180 mmol, 9 equiv.) was added slowly. To this solution methyl 2-(2-methoxy-5-methylphenyl)-2-oxoacetate (**6.4.3**) (4 g, 20 mmol, 1.0 equiv.) in 10 ml MeOH was added dropwise over about 5 min. The reaction mixture was stirred at 0 °C until full consumption of starting material was observed by TLC control (unnecessary longer reaction times lead to significantly lower yields). The reaction mixture was quenched by the addition of sat. NaHCO₃ (50 mL), MeOH was evaporated under reduced pressure, the residue was transferred into a separatory funnel and extracted with EtOAc (3*50 mL). The organic layers were washed with brine (50 mL), filtered, and evaporated under reduced pressure to give the crude products **6.4.5** as yellow liquid. The crude was purified by automatic flash silica gel chromatography. (0-6 % EtOAc in Hexane) (81% yield)

Methyl 2-diazo-2-(2-methoxy-5-methylphenyl)acetate (**6.4.7**)



A suspension of potassium N-iodo *p*-toluenesulfonamide (TsNIK) (**6.4.6**) (3.2 g, 9.4 mmol) in a solution of methyl (Z)-2-hydrazineylidene-2-(2-methoxy-5-methylphenyl)acetate (**6.4.5a**) in THF (8.5 mmol in 36 mL) was prepared. Aqueous potassium hydroxide (1 M, 9 mL) was slowly added to the THF suspension (the final volume ratio KOH (1 M) : THF was equal to 1:4). This caused dissolution of the potassium salt in the mixture and the appearance of a yellow to red coloration. The reaction was complete after stirring for 1 h at room temperature. The mixture was poured into aqueous potassium hydroxide (1 M, 20 mL) and extracted with ether (30 mL). The ethereal phase was washed with aqueous potassium hydroxide (1 M, 25 mL), saturated brine (5 mL) and dried over MgSO₄. Crude diazo compound **6.4.7** was purified by column (0-5% diethyl ether in hexane) and obtained with 70% yield.

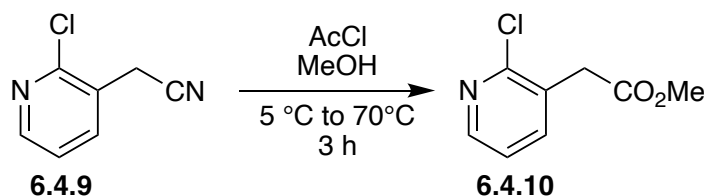
Potassium N-iodo *p*-toluenesulfonamide (TsNIK) (**6.4.6**)



A solution of *p*-Toluenesulfonamide **6.4.8** (4.55 g, 26.6 mmol) in aqueous potassium hydroxide (10%; 11.5 mL) was added to a solution of potassium iodide (17.6 g, 106 mmol) and iodine (9.00 g, 35.5 mmol) in water (20 mL). Aqueous potassium hydroxide (50%; 6 mL) was added, upon which loss of the colorations due to iodine occurred and a yellow precipitate appeared. The yellow solid was filtered, dried under suction, and washed with ether (20 mL) to give the title compound

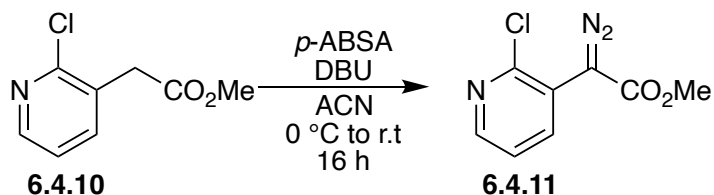
6.4.6 as a yellow solid The product showed no signs of decomposition when stored in the dark at room temperature over several weeks but decomposes with iodine release when heated above 220 °C.

Methyl 2-(2-chloropyridin-3-yl)acetate (**6.4.10**)



To a suspension of 2-(2-chloropyridin-3-yl)acetonitrile **6.4.9** (1.0 equiv, 8.31 g, 54.5 mmol) in methanol (50 ml) was added acetyl chloride (5.0 equiv, 19.36 mL, 272 mmol) dropwise. A reflux condenser was fitted, and the mixture was refluxed at 70°C for 16 h. The reaction mixture was concentrated via rotovap. DCM (20 mL) was added to the resulting light red oil was added along with a saturated NaHCO₃ solution (20 ml). The aqueous phase was extracted with DCM (2*10 mL). The organic phase was combined, dried over Na₂SO₄, and concentrated. The crude product was purified by flash column chromatography (0-30% Ethyl Acetate in hexanes over 24 CV) to give compound **6.4.10** as a yellow oil (87% yield, 9.9 g, 47.4 mmol).

Methyl 2-(2-chloropyridin-3-yl)-2-diazoacetate(**6.4.11**)



Methyl 2-(2-chloropyridin-3-yl)acetate (**6.4.10**) (1.0 equiv, 1.68 g, 9.05 mmol) and *p*-ABSA (1.2 equiv, 2.61 g, 10.9 mmol) were added to a flame-dried 250ml round bottom flask under an inert

nitrogen atmosphere. They were dissolved in dry acetonitrile (ACN, 50 mL) and cooled to 0 °C in an ice-bath. Then DBU (1.2 equiv, 1.65 g, 1.64 mL, 10.9 mmol) was added dropwise to the stirring solution which slowly became deep yellow. The reaction was allowed to warm to room temperature over 18 hours. Reaction was then quenched with saturated NH₄Cl (50 mL) and the organic layer was separated. The aqueous layer was extracted with DCM (2 x 20 mL) and organic extracts were combined, dried over Na₂SO₄, and dry-loaded onto silica (5 g). Diazo compound was then isolated by flash column chromatography (0-50% EtOAc/hexanes). Yellow fractions were combined and evaporated to yield methyl 2-(2-chloropyridin-3-yl)-2-diazoacetate **6.4.11** as a bright yellow solid.

6.4.2 General procedure for asymmetric cyclopropanation experiments

A 10 mL vial containing 4Å activated molecular sieves (0.5 g) and a stir bar was flame dried under vacuum along with a small round-bottom flask. Vessels were evacuated and purged with nitrogen 2 times to establish an inert atmosphere. Then catalyst Rh₂(S-TPPTTL)₄ (1.0 mol %, 4.9 mg, 0.002 mmol) was added to the vial. Solid diazo compound (1.0 equiv, 0.20 mmol) was added to the flame dried round bottom flask. Then vacuum was reestablished on both the vial and the flask to further remove air from the system. After 5 min, the system was flushed with nitrogen and vinyl pyridine (5.0 equiv, 1.0 mmol) was added to the vial via preweighed syringe and 2 mL distilled CH₂Cl₂ was added to the vial. The nitrogen line attached to the vial was then replaced by a balloon filled with argon and the vial was added to an ice bath to maintain the temperature at 0 °C and let stir. Temperature of the ice bath was monitored by thermocouple external to the reaction vessel. While the vial cooled for approximately 10 min, the diazo compound was dissolved in 3 mL distilled CH₂Cl₂ added via syringe. The round bottom flask was swirled to ensure all diazo had dissolved before the solution was loaded into the syringe. The syringe was then inserted through the vial

septum and the full contents were injected into the vial in one portion maintaining the bath at 0 °C throughout the addition. The reaction was stirred overnight under argon in the ice bath which slowly warmed to room temperature (at least 13 h). The reaction solution was subjected to TLC to determine reaction completion (20% EtOAc/hexanes). After completion the solution was filtered through celite to remove molecular sieves before concentrating via rotovap. The crude concentrate was then directly purified by flash column chromatography (5% EtOAc/hexanes 3 CV, 5% EtOAc/hexanes to 30% EtOAc/hexanes 15 CV, 30% EtOAc/hexanes for 3-10 CV). Fractions containing only product by TLC were aggregated and concentrated via rotovap. Enantioselectivity was determined by chiral HPLC.

6.4.3 General procedure for the 2-Chloropyridine promoted cyclopropanation involving ortho-substituted aryl/heteroaryl-diazoacetates.

A 10 mL vial containing 4Å activated molecular sieves (0.5 g) and a stir bar was flame dried under vacuum along with a small round-bottom flask. Vessels were evacuated and purged with nitrogen 2 times to establish an inert atmosphere. Then catalytic $\text{Rh}_2(\text{S-TPPTTL})_4$ (1.0 mol %, 4.9 mg, 0.002 mmol) was added to the vial. Solid diazo compound (1.0 equiv, 0.20 mmol) was added to the flame dried round bottom flask. Then vacuum was reestablished on both the vial and the flask to further remove air from the system. After 5 min, the system was flushed with nitrogen, vinyl-heterocycle (1.5 equiv, 0.30 mmol), and 2-Chloropyridine (3.5 equiv, 79 mg, 66 μl , 0.70 mmol) was added to the vial via syringe along with 2 mL dry CH_2Cl_2 . The nitrogen line attached to the vial was then replaced by a balloon filled with argon and the vial was added to an ice bath to maintain the temperature at 0 °C and let stir. Temperature of the ice bath was monitored by thermocouple external to the reaction vessel. While the vial cooled for approximately 10 min, the diazo compound was dissolved in 3 mL dry CH_2Cl_2 added via syringe. The round bottom flask

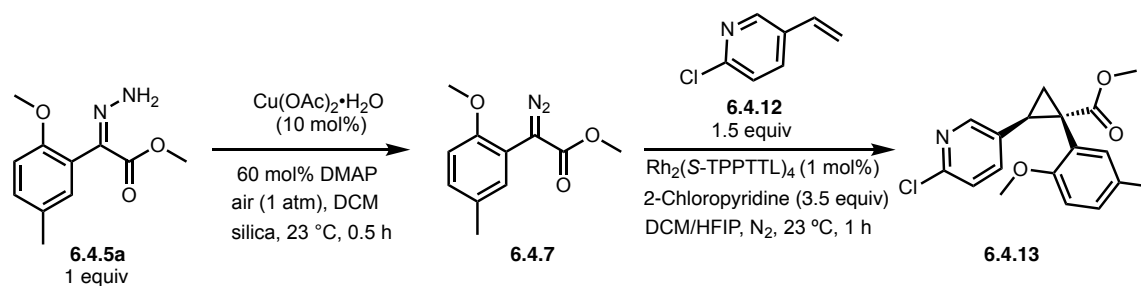
was swirled to ensure all diazo compound had dissolved before the solution was loaded into the syringe. The syringe was then inserted through the vial septum and the full contents were injected into the vial in one portion maintaining the bath at 0 °C throughout the addition. The reaction was stirred overnight under argon in the ice bath which slowly warmed to room temperature (at least 13 h). The reaction solution was subjected to TLC to determine reaction completion (20% EtOAc/hexanes). After completion the solution was filtered through celite to remove molecular sieves before concentrating via rotovap. The crude concentrate was then directly purified by flash column chromatography (5% EtOAc/hexanes 3 CV, 5% EtOAc/hexanes to 30% EtOAc/hexanes 15 CV, 30% EtOAc/hexanes for 3-10 CV). Fractions containing only product by TLC were aggregated and concentrated via rotovap. Enantioselectivity was determined by chiral HPLC.

6.4.4 General procedure for the 2-Chloropyridine promoted cyclopropanation involving ortho-substituted aryl/heteroaryl-diazoacetates and HFIP.

A 10 mL vial containing a stir bar was flame dried under vacuum along with a small round-bottom flask. Vessels were evacuated and purged with nitrogen 2 times to establish an inert atmosphere. Then catalytic $\text{Rh}_2(\text{S-TPPTTL})_4$ (1.0 mol %, 4.9 mg, 0.002 mmol) was added to the vial. Solid diazo compound (1.0 equiv, 0.20 mmol) was added to the flame dried round bottom flask. Then vacuum was reestablished on both the vial and the flask to further remove air from the system. After 5 min, the system was flushed with nitrogen, vinyl-heterocycle (1.5 equiv, 0.30 mmol), 2-Chloropyridine (3.5 equiv, 79 mg, 66 μl , 0.70 mmol), and 1,1,1-3,3,3-hexafluoroisopropanol (HFIP, 10 equiv, 340 mg, 0.21 mL, 2.0 mmol) was added to the vial via syringe along with 2 mL dry CH_2Cl_2 . The nitrogen line attached to the vial was then replaced by a balloon filled with argon and the vial was added to an ice bath to maintain the temperature at 0 °C and let stir. Temperature of the ice bath was monitored by thermocouple external to the reaction vessel. While the vial

cooled for approximately 10 min, the diazo compound was dissolved in 3 mL distilled CH_2Cl_2 added via syringe. The round bottom flask was swirled to ensure all diazo compound had dissolved before the solution was loaded into the syringe. The syringe was then inserted through the vial septum and the full contents were injected into the vial in one portion maintaining the bath at 0°C throughout the addition. The reaction was stirred overnight under argon and allowed to warm to room temperature (at least 13 h). The reaction solution was subjected to TLC to determine reaction completion (20% EtOAc/hexanes). After completion the solution was filtered through celite to remove molecular sieves before concentrating via rotovap. The crude concentrate was then directly purified by flash column chromatography (5% EtOAc/hexanes 3 CV, 5% EtOAc/hexanes to 30% EtOAc/hexanes 15CV, 30% EtOAc/hexanes for 3-10 CV). Fractions containing product by TLC were aggregated and concentrated via rotovap. Enantioselectivity was determined by chiral HPLC.

6.4.5 Procedure for tandem hydrazone oxidation/cyclopropanation reaction

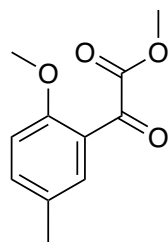


In the first step: A 20 mL scintillation vial was charged with $\text{Cu}(\text{OAc})_2 \cdot \text{H}_2\text{O}$ (3.9 mg, 0.020 mmol, 10 mol %), silica powder (44.4 mg, 100 wt%, SiliaFlash® P60, 40-63 μm), and 1.0 mL solution of 0.06 mol/L DMAP in CH_2Cl_2 . The initial mixture was stirred vigorously with a stir bar (600 rpm) under air for 5 min before hydrazone was added. In a 4 mL scintillation vial, methyl (Z)-2-hydrazineylidene-2-(2-methoxy-5-methylphenyl)acetate (**6.4.5a**) (44.4 mg, 0.20 mmol, 1.0 equiv) was dissolved in 1.0 mL of the 0.06 mol/L DMAP in CH_2Cl_2 solution. The hydrazone/DMAP

CH₂Cl₂ solution was then transferred by syringe in one portion to the initial mixture of Cu(OAc)₂-H₂O/silica/DMAP CH₂Cl₂ solution. The reaction was stirred for 0.5 h before next step to afford a crude solution of diazo compound **6.4.7**

In the second step: a 20 mL scintillation vial equipped with a stir bar was flame dried under vacuum. After cooling down, the vial was charged with Rh₂(*S*-TPPTTL)₄ (4.9 mg, 1.0 mol %, 0.0020 mmol), then flushed with nitrogen for 3 times and the nitrogen balloon was left on the septum. Then HFIP (672.2 mg, 0.42 mL, 20 equiv, 4.0 mmol), 2-Chloropyridine (79.5 mg, 66 μL, 3.5 equiv, 0.70 mmol), 2-Chloro-5-vinylpyridine (**6.4.12**), 41.9 mg, 1.5 equiv, 0.30 mmol) and 2.0 mL CH₂Cl₂ were added sequentially via syringe, the mixture was stirred at 600 rpm for 10 min before crude diazo compound **6.4.7** injection. The crude diazo compound mixture from step 1 (~1.5 mL) was added by syringe to the 2-Chloro-5-vinylpyridine/Rh₂(*S*-TPPTTL)₄/HFIP/2-Chloropyridine solution in one portion. The reaction was then stirred 1 h under nitrogen at r.t. After completion the solution was concentrated under rotovap and purified by flash column chromatography (5 % EtOAc/hexanes 3 CV, 5 % EtOAc/hexanes to 30 % EtOAc/hexanes 15 CV, 30 % EtOAc/hexanes 10 CV). Fractions containing cyclopropanation product **6.4.13** were aggregated and concentrated via rotovap to give a clear colorless oil in 83% yield (55.2 mg, 0.166 mmol) and 98% ee.

6.4.6 Characterization of the starting materials



6.4.3

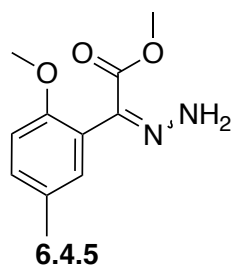
Methyl 2-(2-methoxy-5-methylphenyl)-2-oxoacetate

$^1\text{H NMR}$ (600 MHz, CDCl_3) δ 7.67 (d, $J = 2.5$ Hz, 1H), 7.39 (dd, $J = 8.5, 2.4$ Hz, 1H), 6.88 (d, $J = 8.5$ Hz, 1H), 3.91 (s, 3H), 3.84 (s, 3H).

$^{13}\text{C NMR}$ (151 MHz, CDCl_3) δ 186.4, 165.7, 158.5, 137.1, 130.9, 130.6, 122.4, 112.2, 56.3, 52.3, 20.2.

HRMS: (+p APCI) calculated for $[\text{C}_{11}\text{H}_{13}\text{O}_4]^+$ 209.0808, found 209.0806

IR(neat): 2951, 1739, 1667, 1608, 1581, 1497, 1412, 1272, 1245, 1224, 1179, 1155, 1133, 1019, 947, 901, 864, 813, 778, 712, 669, 588, 537, 489 cm^{-1}



Methyl (*E/Z*)-2-hydrazineylidene-2-(2-methoxy-5-methylphenyl)acetate.

MP: *Z*-isomer: 63-65 °C *E*-isomer: 72-75 °C

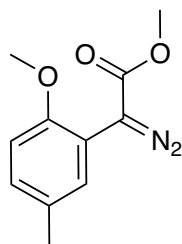
$^1\text{H NMR}$ (400 MHz, CDCl_3) *Z*-Isomer: δ 8.13 (s, 2H), 7.14 – 7.12 (m, 2H), 7.10 (dt, $J = 2.4, 0.8$ Hz, 1H), 6.79 (d, $J = 8.1$ Hz, 1H), 3.76 (s, 3H), 3.73 (s, 3H), 2.30 (d, $J = 0.8$ Hz, 3H). *E*-isomer: δ 7.21 (ddq, $J = 8.6, 2.3, 0.7$ Hz, 1H), 6.97 (dt, $J = 2.3, 0.6$ Hz, 1H), 6.90 (d, $J = 8.4$ Hz, 1H), 6.11 (s, 2H), 3.83 (s, 3H), 3.77 (s, 3H).

$^{13}\text{C NMR}$ (151 MHz, CDCl_3) *Z*-Isomer: δ 163.7, 155.9, 130.7, 130.3, 130.2, 126.3, 111.1, 56.0, 51.6, 20.6. *E*-isomer: δ 165.3, 155.1, 136.1, 131.9, 130.8, 130.7, 118.3, 111.9, 56.1, 52.6, 20.7.

HRMS: (+p APCI) calculated for $[\text{C}_{11}\text{H}_{15}\text{O}_3\text{N}_2]^+$ 223.1077, found 223.1077 for *Z* isomer, found 223.1079 for *E* isomer.

IR(neat): *Z*-Isomer: 3454, 3293, 2948, 2836, 1695, 1575, 1498, 1463, 1435, 1295, 1266, 1245, 1186, 1150, 1130, 1037, 1025, 993, 887, 808, 730, 670, 496. *E*-Isomer: 3407, 3294, 3210, 2948,

2838, 1708, 1608, 1557, 1496, 1435, 1316, 1238, 1185, 1119, 1046, 1025, 950, 872, 810, 781, 729, 468 cm^{-1}



6.4.7

Methyl 2-diazo-2-(2-methoxy-5-methylphenyl)acetate

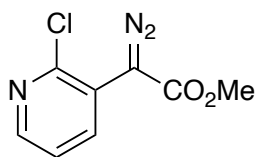
MP: 55-60 °C

$^1\text{H NMR}$ (600 MHz, CDCl_3) δ 7.36 (s, 1H), 7.06 (d, $J = 8.41$ Hz, 1H), 6.79 (d, $J = 8.42$ Hz, 1H), 3.83 (s, 3H), 3.82 (s, 3H), 2.31 (s, 3H).

$^{13}\text{C NMR}$ (151 MHz, CDCl_3) δ 166.8, 153.5, 130.7, 130.5, 129.2, 113.3, 110.9, 55.7, 51.9, 20.6.

HRMS: (+p APCI) calculated for $[\text{C}_{11}\text{H}_{13}\text{O}_3\text{N}_2]^+$ 221.0921, found 221.0922

IR(neat): 2090, 1693, 1503, 1434, 1339, 1291, 1248, 1186, 1138, 1048, 804, 743 cm^{-1}



6.4.11

Methyl 2-(2-chloropyridin-3-yl)-2-diazoacetate

MP: 71-73 °C

$^1\text{H NMR}$ (400 MHz, CDCl_3) δ 8.35 (dd, $J = 4.7, 1.9$ Hz, 1H), 7.95 (dd, $J = 7.8, 1.9$ Hz, 1H), 7.32 (dd, $J = 7.8, 4.7$ Hz, 1H), 3.86 (s, 3H).

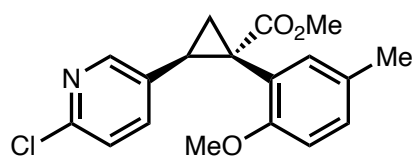
$^{13}\text{C NMR}$ (151 MHz, CDCl_3) δ 165.4, 149.2, 148.9, 140.5, 122.7, 121.6, 52.5. Please note that the diazo carbon was not visible by $^{13}\text{C NMR}$.

HRMS: (+p APCI) calculated for $[\text{C}_8\text{H}_7\text{O}_2\text{N}_3^{35}\text{Cl}]^+$ 212.0221, found 212.0222

IR(neat): 2097, 1694, 1555, 1455, 1435, 1402, 1344, 1272, 1211, 1193, 1162, 1128, 1099, 1060, 1023, 1006, 798, 737, 727 cm^{-1}

6.4.7 Characterization of the cyclopropanation products

**All products shown with absolute stereo-configuration generated with $\text{Rh}_2(\text{S-TPPTTL})_4$*



4.36

Methyl (1*S*,2*R*)-2-(6-chloropyridin-3-yl)-1-(2-methoxy-5-methylphenyl)cyclopropane-1-carboxylate

This compound was prepared according to General procedure 6.4.2, General procedure 6.4.3, and General procedure 6.4.4.

General procedure 6.4.2: 95% yield and 98% ee (0.19 mmol, 63 mg)

General procedure 6.4.3: 87% yield and 98% ee (0.17 mmol, 58 mg).

General procedure 6.4.4: 89% yield and 98% ee (0.18 mmol, 59 mg). After isolation, enantio-enriched product was obtained as a clear colorless oil, racemate is obtained as colorless orthorhombic crystals.

MP: 126-127 °C

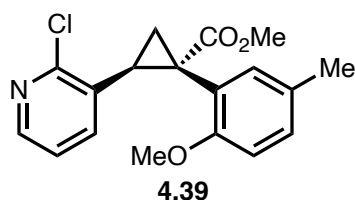
^1H NMR (600 MHz, CDCl_3) δ 8.00 (d, J = 2.53 Hz, 1H), 6.98 (s, 1H), 6.94 (d, J = 8.19 Hz, 1H), 6.89 (d, J = 8.23 Hz, 1H), 6.81 (dd, J = 2.51, 8.33 Hz, 1H), 6.44 (d, J = 8.24 Hz, 1H), 3.63 (s, 3H), 3.37 (s, 3H), 3.17 (m, 1H), 2.23 (s, 3H), 1.98 (m, 1H), 1.78 (m, 1H).

^{13}C NMR (151 MHz, CDCl_3) δ 173.8, 156.2, 149.6, 148.8, 136.6, 131.9, 129.7, 129.3, 122.3, 110.2, 55.0, 52.6, 34.1, 28.7, 25.3, 20.4, 20.0

HRMS: (+p APCI) calculated for $[\text{C}_{18}\text{H}_{19}\text{O}_3\text{N}^{35}\text{Cl} +]$ 332.1048, found 332.1046

IR(neat): 1716, 1562, 1501, 1461, 1434, 1348, 1262, 1241, 1158, 1140, 1107, 1029, 972, 905, 808, 732, 671, 548 cm^{-1}

Chiral HPLC: (OD-H, 30 min, 1 mL/min, 1% *i*-PrOH in *n*-hexane, UV 230 nm) RT: 19.46 min, 22.97 min.



Methyl (1*S*,2*S*)-2-(2-chloropyridin-3-yl)-1-(2-methoxy-5-methylphenyl)cyclopropane-1-carboxylate

This compound was prepared according to General procedure 6.4.2 and General procedure 6.4.3.

General procedure 6.4.2: 85% yield and 95% ee (0.17 mmol, 56 mg)

General procedure 6.4.3: 62% yield and 90% ee (0.12 mmol, 41 mg). After isolation, enantio-enriched product was obtained as a white solid.

MP: 143-152 °C

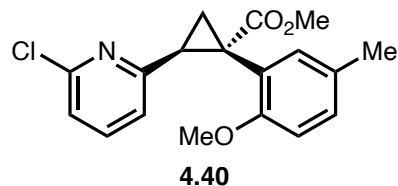
¹H NMR (600 MHz, CDCl₃) δ 8.03 (dd, *J*=1.94, 4.73, 1H), 7.01 (t, *J*=3.70, 1H), 6.93 (d, *J*=8.460, 1H), 6.72 (dd, *J*=4.67, 7.66), 6.47 (d, *J*=1.94, 1H), 6.40 (d, *J*=8.15, 1H), 3.67 (s, 3H), 3.63 (m, 1H), 3.38 (s, 3H), 2.25 (s, 3H), 2.05 (m, 1H), 1.84 (m, 1H)

¹³C NMR (151 MHz, CDCl₃) δ 173.5, 156.4, 153.2, 146.3, 133.8, 132.5, 131.7, 129.5, 128.9, 122.4, 120.8, 109.8, 54.8, 52.6, 34.4, 28.5, 20.4, 19.9.

HRMS: (+p APCI) calculated for [C₁₈H₁₉O₃N³⁵Cl +] 332.1048, found 332.1048

IR(neat): 2919, 1720, 1585, 1557, 1433, 1264, 1244, 1158, 1140, 1034, 910, 800, 733 cm^{-1}

Chiral HPLC: (OD-H, 30 min, 1 mL/min, 1% *i*-PrOH in *n*-hexane, UV 230 nm) RT: 12.44 min, 22.31 min.



Methyl (1*S*,2*S*)-2-(6-chloropyridin-2-yl)-1-(2-methoxy-5-methylphenyl)cyclopropane-1-carboxylate

This compound was prepared according to General procedure 6.4.2 and General procedure 6.4.3.

General procedure 6.4.2: 86% yield and 90% ee (0.17 mmol, 57 mg)

General procedure 6.4.3: 81% yield and >99% ee (0.16 mmol, 54 mg). After isolation, enantio-enriched product was obtained as a white solid.

MP: 114-116 °C

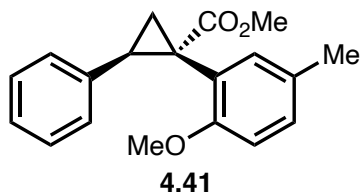
¹H NMR (400 MHz, CDCl₃) δ 7.31 – 7.16 (m, 2H), 7.02 (d, *J* = 2.3 Hz, 1H), 6.91 (ddd, *J* = 7.7, 5.6, 1.3 Hz, 2H), 6.74 (dd, *J* = 7.6, 0.8 Hz, 1H), 6.41 (d, *J* = 8.3 Hz, 1H), 3.64 (s, 3H), 3.44 – 3.31 (buried m under main s, 4H), 2.28 – 2.17 (buried m under main s, 4H), 1.96 (dd, *J* = 8.9, 4.7 Hz, 1H).

¹³C NMR (151 MHz, CDCl₃) δ 173.8, 157.9, 156.3, 149.5, 137.2, 132.6, 129.0, 128.9, 122.7, 121.0, 121.0, 109.6, 55.0, 52.5, 34.8, 32.9, 29.7, 20.4

HRMS: (+p APCI) calculated for [C₁₈H₁₉O₃N³⁵Cl +] 332.1048, found 332.1044

IR(neat): 2916, 2849, 1721, 1585, 1557, 1502, 1433, 1376, 1263, 1242, 1158, 1141, 1033, 910, 800, 720 cm⁻¹

Chiral HPLC: (OD-H, 60 min, 1 mL/min, 1% *i*-PrOH in *n*-hexane, UV 230 nm) RT: 22.93 min, 36.26 min.



Methyl (1*S*,2*R*)-1-(2-methoxy-5-methylphenyl)-2-phenylcyclopropane-1-carboxylate

This compound was prepared according to General procedure 6.4.2 and General procedure 6.4.3.

General procedure 6.4.2: 81% yield and 4% ee (0.16 mmol, 48 mg)

General procedure 6.4.3: 95% yield and 95% ee (0.19 mmol, 56 mg). After isolation, enantio-enriched product was obtained as a clear colorless oil.

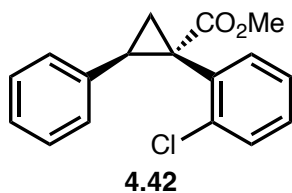
¹H NMR (400 MHz, CDCl₃) δ 7.02 (dd, *J* = 5.1, 1.9 Hz, 3H), 6.96 (d, *J* = 2.3 Hz, 1H), 6.94 – 6.86 (m, 1H), 6.83 – 6.71 (m, 2H), 6.43 (d, *J* = 8.2 Hz, 1H), 3.65 (s, 3H), 3.31 (s, 3H), 3.21 (dd, *J* = 9.3, 7.4 Hz, 1H), 2.23 (s, 3H), 1.97 (dd, *J* = 9.3, 4.9 Hz, 1H), 1.82 (dd, *J* = 7.3, 5.0 Hz, 1H).

¹³C NMR (151 MHz, CDCl₃) δ 174.5, 156.9, 136.9, 132.3, 129.0, 128.8, 127.7, 127.7, 127.0, 125.8, 123.5, 110.1, 55.0, 55.0, 52.4, 34.0, 32.4, 20.6, 20.5.

HRMS: (+p APCI) calculated for [C₁₉H₂₀O₃+]⁺ 296.1407, found 296.1409

IR(neat): 1716, 1502, 1460, 1436, 1410, 1354, 1263, 1244, 1186, 1159, 1144, 1067, 1031, 907, 806, 729, 683, 646, 503 cm⁻¹

Chiral HPLC: (OD-H, 30 min, 1 mL/min, 1% *i*-PrOH in *n*-hexane, UV 230 nm) RT: 10.89 min, 12.80 min. or (AD-H, 30 min, 1 mL/min, 1% *i*-PrOH in *n*-hexane, UV 230 nm) RT: 9.61 min, 11.17 min.



Methyl (1*S*,2*R*)-1-(2-chlorophenyl)-2-phenylcyclopropane-1-carboxylate

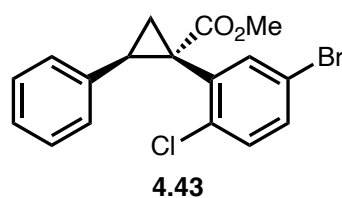
This compound was prepared according to General procedure 6.4.2 and General procedure 6.4.3.
General procedure 6.4.2: 71% yield and 55% ee (0.14 mmol, 40 mg).

General procedure 6.4.3: 79% yield and 84% ee (0.16 mmol, 45 mg). After isolation, enantio-enriched product was obtained as a clear colorless oil.

$^1\text{H NMR}$ (400 MHz, CDCl_3) δ 7.15 (broad m, 4H), 7.08 (m, 3H), 6.87 – 6.76 (dd, $J = 6.9, 2.0$ Hz 2H), 3.70 (s, 3H), 3.34 (t, $J = 8.4$ Hz, 1H), 2.13 (s, 1H), 1.94 (dd, $J = 7.5, 5.2$ Hz, 1H).

$^{13}\text{C NMR}$ (151 MHz, CDCl_3) δ 173.4, 137.3, 133.3, 129.3, 128.6, 127.9, 129.4, 126.4, 126.1, 64.4, 52.7, 33.3, 25.4, 21.5

Chiral HPLC: (OJ-H, 30 min, 1 mL/min, 1% *i*-PrOH in *n*-hexane, UV 230 nm) RT: 12.80 min, 20.73 min



Methyl (1*S*,2*R*)-1-(5-bromo-2-chlorophenyl)-2-phenylcyclopropane-1-carboxylate

This compound was prepared according to General procedure 6.4.2 and General procedure 6.4.3.
General procedure 6.4.2: 76% yield and 64% ee (0.15 mmol, 56 mg)

General procedure 6.4.3: 71% yield and 92% ee (0.14 mmol, 52 mg). After isolation, enantio-enriched product was obtained as a clear colorless oil.

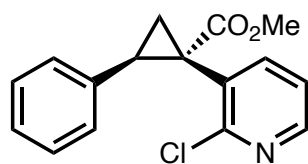
$^1\text{H NMR}$ (600 MHz, CDCl_3) δ 7.23 (dd, $J = 2.23, 8.46$ Hz, 1H), 7.10 (s, 4H), 7.02 (broad s, 1H), 6.86 (m, 2H), 3.68 (s, 3H) 3.32 (m, 1H), 2.10 (broad s, 1H), 1.90 (m, 1H)

$^{13}\text{C NMR}$ (151 MHz, CDCl_3) δ 172.6, 136.8, 135.5, 134.0, 131.5, 130.6, 127.9, 127.6, 127.6, 119.5, 52.7, 33.3, 33.3, 21.4

HRMS: (+p APCI) calculated for $[\text{C}_{17}\text{H}_{15}\text{O}_2^{79}\text{Br}^{35}\text{Cl}]^+$ 364.9938, found 364.9932

IR(neat): 3027, 2970, 2949, 1720, 1458, 1433, 1266, 1246, 1208, 1192, 116, 1115, 1085, 1045, 969, 814, 770, 731, 695, 526 cm^{-1}

Chiral HPLC: (OJ-H, 30 min, 1 mL/min, 1% *i*-PrOH in *n*-hexane, UV 230 nm) RT: 9.07 min, 11.82 min



4.44

Methyl (1*S*,2*R*)-1-(2-chloropyridin-3-yl)-2-phenylcyclopropane-1-carboxylate

This compound was prepared according to General procedure 6.4.2 and General procedure 6.4.3.

General procedure 6.4.2: 82% yield and 77% ee (0.16 mmol, 47 mg)

General procedure 6.4.3: 94% yield and 90% ee (0.19 mmol, 54 mg). After isolation, enantio-enriched product was obtained as a clear crystalline solid.

MP: 115-119 °C

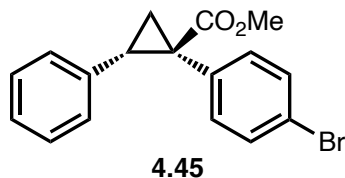
^1H NMR (600 MHz, CDCl_3) δ 8.19 (m, 1H), 7.09 (broad s, 5H), 6.85 (m, 2H), 3.68 (s, 3H), 3.34 (m, 1H), 2.18 (broad s, 1H), 1.92 (dd, J = 5.46, 7.59 Hz, 1H)

^{13}C NMR (151 MHz, CDCl_3) δ 172.5, 154.3, 148.1, 141.3, 134.9, 130.4, 129.3, 128.0, 127.8, 126.9, 121.6, 52.7, 34.1, 33.5, 25.3, 20.0

HRMS: (+p APCI) calculated for $[\text{C}_{16}\text{H}_{15}\text{O}_2\text{N}^{35}\text{Cl} +]$ 288.0785, found 288.0786

IR(neat): 1720, 1452, 1433, 1397, 1262, 1221, 1163, 1132, 1059, 966, 908, 776, 750, 728, 697, 646, 562 cm^{-1}

Chiral HPLC: (AD-H, 30 min, 1 mL/min, 1% *i*-PrOH in *n*-hexane, UV 230 nm) RT: 20.19 min, 23.41 min.



Methyl (1*R*,2*S*)-1-(4-bromophenyl)-2-phenylcyclopropane-1-carboxylate

This compound was prepared according to General procedure 6.4.2 and General procedure 6.4.3.

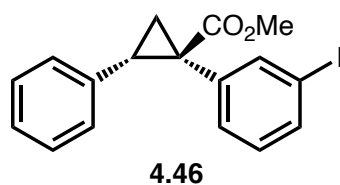
General procedure 6.4.2: 58% yield and 48% ee (0.11 mmol, 38 mg).

General procedure 6.4.3: 61% yield and 0% ee (0.12 mmol, 40 mg). After isolation, product was obtained as a white solid.

¹H NMR (400 MHz, CDCl₃) δ 7.28 – 7.24 (m, 3H), 7.16 – 7.05 (m, 2H), 6.98 – 6.86 (m, 2H), 6.86 – 6.75 (m, 2H), 4.83 (d, *J* = 11.9 Hz, 1H), 4.64 (d, *J* = 11.9 Hz, 1H), 3.22 (dd, *J* = 9.4, 7.5 Hz, 1H), 2.28 (dd, *J* = 9.4, 5.2 Hz, 1H), 1.97 (dd, *J* = 7.5, 5.2 Hz, 1H).

¹³C NMR (151 MHz, CDCl₃) δ 171.7, 135.4, 133.8, 133.1, 131.1, 128.2, 128.2, 127.0, 121.7, 95.1, 74.6, 36.7, 34.1, 20.3.

Chiral HPLC: (OJ-H, 30 min, 1 mL/min, 1% *i*-PrOH in *n*-hexane, UV 230 nm) RT: 10.03 min, 14.97 min.



Methyl (1*R*,2*S*)-1-(3-iodophenyl)-2-phenylcyclopropane-1-carboxylate

This compound was prepared according to General procedure 6.4.2 and General procedure 6.4.3.

General procedure 6.4.2: 66% yield and 29% ee (0.13 mmol, 50 mg)

General procedure 6.4.3: 80% yield and 41% ee (0.16 mmol, 61 mg). After isolation, product was obtained as a colorless oil.

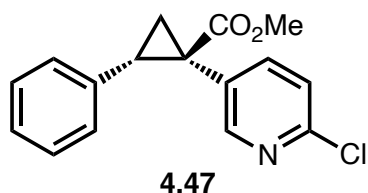
$^1\text{H NMR}$ (400 MHz, CDCl_3) δ 7.52 – 7.38 (m, 2H), 7.10 (dd, $J = 5.2, 2.0$ Hz, 3H), 6.98 – 6.85 (m, 1H), 6.84 (d, $J = 7.7$ Hz, 1H), 6.82 – 6.72 (m, 2H), 3.67 (s, 3H), 3.11 (dd, $J = 9.3, 7.3$ Hz, 1H), 2.13 (dd, $J = 9.3, 5.0$ Hz, 1H), 1.85 (dd, $J = 7.4, 5.0$ Hz, 1H).

$^{13}\text{C NMR}$ (151 MHz, CDCl_3) δ 173.6, 140.7, 137.2, 136.1, 135.7, 131.4, 129.2, 128.0, 127.8, 126.6, 93.3, 52.7, 36.7, 33.1, 20.2.

HRMS: (+p APCI) calculated for $[\text{C}_{17}\text{H}_{16}\text{O}_2^{127}\text{I} +]$ 379.0189, found 379.0184

IR(neat): 1713, 1590, 1559, 1474, 1455, 1431, 1250, 1209, 1190, 1095, 1054, 995, 965, 936, 908, 884, 789, 763, 729, 696, 678, 645, 592, 565 cm^{-1}

Chiral HPLC: (OD-H, 30 min, 1 mL/min, 1% *i*-PrOH in *n*-hexane, UV 230 nm) RT: 8.23 min, 9.27 min.



Methyl (1*R*,2*S*)-1-(6-chloropyridin-3-yl)-2-phenylcyclopropane-1-carboxylate

This compound was prepared according to General procedure 6.4.2 and General procedure 6.4.3.

General procedure 6.4.2: 90% yield and 35% ee (0.18 mmol, 52 mg)

General procedure 6.4.3: 90% yield and 7% ee (0.18 mmol, 52 mg). After isolation, enantio-enriched product was obtained as a clear colorless oil.

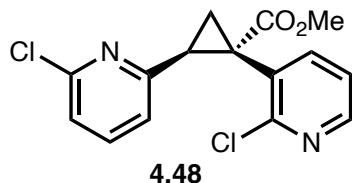
$^1\text{H NMR}$ (600 MHz, CDCl_3) δ 8.08 (dd, $J = 2.6, 0.8$ Hz, 1H), 7.21 (dd, $J = 8.2, 2.5$ Hz, 1H), 7.11 (dq, $J = 4.5, 2.3$ Hz, 3H), 7.05 (dd, $J = 8.2, 0.7$ Hz, 1H), 6.87 – 6.71 (m, 2H), 3.67 (d, $J = 3.5$ Hz, 3H), 3.16 (dd, $J = 9.3, 7.3$ Hz, 1H), 2.21 (dd, $J = 9.4, 5.2$ Hz, 1H), 1.96 – 1.86 (m, 1H).

$^{13}\text{C NMR}$ (151 MHz, CDCl_3) δ 173.2, 152.7, 150.2, 142.4, 135.1, 130.3, 128.5, 128.2, 127.3, 123.5, 53.0, 34.3, 33.1, 19.7.

HRMS: (+p APCI) calculated for [C₁₆H₁₅O₂N³⁵Cl⁺] 288.0785, found 288.0786

IR(neat): 2952, 1720, 1588, 1560, 1499, 1463, 1433, 1366, 1261, 1164, 1112, 1022, 965, 779, 742, 719, 696, 559, 485 cm⁻¹

Chiral HPLC: (OD-H, 30 min, 1 mL/min, 1% *i*-PrOH in *n*-hexane, UV 230 nm) RT: 22.14 min, 25.67 min.



Methyl (1*S*,2*S*)-2-(6-chloropyridin-2-yl)-1-(2-chloropyridin-3-yl)cyclopropane-1-carboxylate

This compound was prepared according to General procedure 6.4.3 and obtained 87% yield and 85% ee (0.17 mmol, 56 mg). After isolation, enantio-enriched product was obtained as a clear colorless oil.

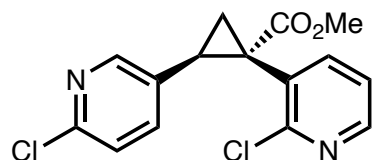
¹H NMR (400 MHz, CDCl₃) δ 8.21 (ddd, *J* = 10.3, 4.9, 1.9 Hz, 2H), 7.32 (broad s, 1H), 7.03 (broad s, 1H), 6.88 (broad s, 1H), 6.65 (broad s, 1H), 3.72 (s, 3H), 3.65 (broad s, 1H), 2.33 (broad s, 1H), 1.90 (dd, *J* = 7.8, 5.7 Hz, 1H).

¹³C NMR (151 MHz, CDCl₃) δ 171.7, 154.1, 153.4, 148.6 (2 C), 147.8, 141.6, 129.6, 121.9 (2 C), 121.7, 53.1, 29.6, 25.3, 20.9.

HRMS: (+p APCI) calculated for [C₁₅H₁₃O₂N₂³⁵Cl₂⁺] 323.0348, found 323.0340

IR(neat): 1724, 1563, 1436, 1411, 1398, 1357, 1268, 1220, 1196, 1166, 1132, 1063, 756, 732, 682cm⁻¹

Chiral HPLC: (AD-H, 30 min, 1 mL/min, 1% *i*-PrOH in *n*-hexane, UV 230 nm) RT: 10.65 min, 11.71 min.



4.49

Methyl (1*S*,2*R*)-1-(2-chloropyridin-3-yl)-2-(6-chloropyridin-3-yl)cyclopropane-1-carboxylate

This compound was prepared according to General procedure 6.4.3 and obtained 79% yield and 84% ee (0.16 mmol, 51 mg). After isolation, enantio-enriched product was obtained as a clear colorless oil.

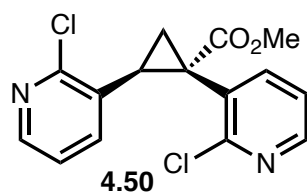
¹H NMR (600 MHz, CDCl₃) δ 8.27 (s, 1H), 7.98 (s, 1H), 7.19 (s, 1H), 7.03 (s, 3 H), 3.70 (s, 3H), 3.36 (m, 1 H), 2.18 (broad s, 1H), 1.69 (broad s, 1H)

¹³C NMR (151 MHz, CDCl₃) δ 171.7, 153.9, 149.9, 149.1, 148.8, 137.5, 129.4, 123.1, 122.1, 53.0, 36.0, 29.6, 29.6, 25.3

HRMS: (+p APCI) calculated for [C₁₅H₁₃O₂N₂³⁵Cl₂+]⁺ 323.0348, found 323.0349

IR(neat): 3016, 2970, 2950, 1721, 1562, 1464, 1434, 1397, 1348, 1265, 1221, 1165, 1132, 1108, 1058, 1023, 967, 911, 835, 801, 779, 754, 728, 659, 647, 633, 437 cm⁻¹

Chiral HPLC: (AD-H, 60 min, 1 mL/min, 1% *i*-PrOH in *n*-hexane, UV 230 nm) RT: 29.56 min, 34.74 min.



Methyl (1*S*,2*S*)-1,2-bis(2-chloropyridin-3-yl)cyclopropane-1-carboxylate

This compound was prepared according to General procedure 6.4.3 and obtained 65% yield and 95% ee (0.13 mmol, 42 mg). After isolation, enantio-enriched product was obtained as a clear colorless oil.

¹H NMR (400 MHz, CDCl₃) δ 8.20 (dd, *J* = 4.8, 1.9 Hz, 1H), 7.77 (s, 1H), 7.43 (t, *J* = 7.7 Hz, 1H), 7.20 (broad s, 1H), 6.94 (d, *J* = 7.9 Hz, 1H), 3.69 (s, 3H), 3.49 – 3.40 (m, 1H), 2.44 (broad s, 1H), 2.05 (broad s, 1H).

¹³C NMR (151 MHz, CDCl₃) δ 172.1, 155.7, 153.3, 149.9, 148.1, 141.8, 138.1, 130.1, 123.6, 121.8, 52.9, 37.0, 33.0, 29.7, 22.7, 20.9.

HRMS: (+p APCI) calculated for [C₁₅H₁₃O₂N₂³⁵Cl₂+]⁺ 323.0348, found 323.0346

IR(neat): 1722, 1583, 1558, 1434, 1398, 1377, 1265, 1220, 1162, 1132, 1096, 1058, 991, 941, 910, 810, 796, 770, 752, 730, 714, 654 cm⁻¹

Chiral HPLC: (AD-H, 30 min, 1 mL/min, 1% *i*-PrOH in *n*-hexane, UV 230 nm) RT: 22.81 min, 24.16 min.

6.5 Experimental Part for Chapter 5

6.5.1 General Procedure for ReactIR Monitored Rh(II)-Catalyzed C–H Functionalization

An oven-dried 25 mL 3-neck round bottom flask with stir bar fitted with a rubber septum (left neck, 14/20), ReactIRTM probe (center neck, 24/40 to 19/25 adapter, 19/25 neck), and nitrogen inlet (right neck, 14/20). The flask was then allowed to cool to room temperature under vacuum and backfilled with nitrogen. The flask was then placed in a 40 °C water bath on a stir-plate. The ReactIRTM instrument was filled with liquid nitrogen and then started. Distilled DCM (12 mL) was added to the flask by syringe and allowed to stir for 15 min to achieve temperature balance. Cyclohexane (0.1262 g, 0.162 mL, 1.50 mmol, 2.5 equiv) was then measured using a 1.00 mL

plastic syringe and added to the flask through the rubber septum under nitrogen. 2,2,2-trichloroethyl 2-(4-bromophenyl)-2-diazoacetate (0.2235 g, 0.60 mmol, 1 equiv) was then added to the reaction mixture by removing and then quickly replacing the rubber septum under nitrogen. After 15 min, the dirhodium catalyst (0.1 mol% in 1.00 mL DCM stock solution) was then added to the reaction mixture by syringe. The reaction mixture was stirred at 40 °C until complete consumption of the diazo compound (by monitoring diazo stretching frequency 2103cm^{-1}). The absorbance points and relative time at which the dirhodium catalyst was added, all the way until the end of the data collection period, was set as the diazo decomposition curve. A crude ^1H NMR spectrum was taken to analyze the rr and dr of the reaction. For some e.e. analysis, the reaction mixture was directly treated with lithium aluminum hydride solution (1.2 equiv, 1 M solution in THF) and stirred at RT for 40 minutes. Then the reaction was quenched by slow addition of $\text{Na}_2\text{SO}_4 \cdot 10\text{H}_2\text{O}$ and then stirred until bubbling stopped (about 30 minutes), filtered over Celite and eluted with DCM. Upon reaction completion, the solution was concentrated under rotovap and purified by flash column chromatography (0%, then 0%-5% Et_2O in Hexanes). The product was obtained as a colorless oil.

6.5.2 General Procedure for ReactIR Monitored Rh(II)-Catalyzed C–H Functionalization in neat condition

An oven-dried 25 mL 3-neck round bottom flask with stir bar fitted with a rubber septum (left neck, 14/20), ReactIRTM probe (center neck, 24/40 to 19/25 adapter, 19/25 neck), and nitrogen inlet (right neck, 14/20). The flask was then allowed to cool to room temperature under vacuum and backfilled with nitrogen. The flask was then placed in a 40 °C water bath on a stir-plate. The ReactIRTM instrument was filled with liquid nitrogen and then started. Cyclohexane (12 mL) was added to the flask by syringe and allowed to stir for 15 min to achieve temperature balance. 2,2,2-

trichloroethyl 2-(4-bromophenyl)-2-diazoacetate (0.2235 g, 0.60 mmol, 1.0 equiv) was added to the reaction mixture by removing and then quickly replacing the rubber septum under nitrogen. After 5 min, the dirhodium catalyst (x mol% in 0.05 mL DCM stock solution) was then added to the reaction mixture by syringe. The reaction mixture was stirred at 40 °C until complete consumption of the diazo compound (by monitoring diazo stretching frequency 2103cm^{-1}). The absorbance points and relative time at which the dirhodium catalyst was added, all the way until the end of the data collection period, was set as the diazo decomposition curve. Upon reaction completion, the solution was concentrated under rotovap and purified by flash column chromatography (0%, then 0%-5% Et₂O in Hexanes). The product was obtained as a clear oil.

6.5.3 General Procedure for ReactIR Monitored Rh(II)-Catalyzed C–H Functionalization with DCC additive

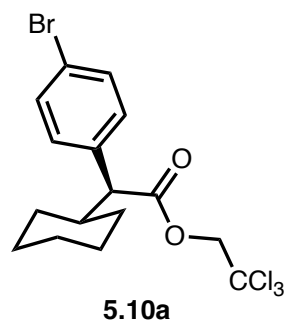
An oven-dried 25 mL 3-neck round bottom flask with stir bar fitted with a rubber septum (left neck, 14/20), ReactIRTM probe (center neck, 24/40 to 19/25 adapter, 19/25 neck), and nitrogen inlet (right neck, 14/20). The flask was then allowed to cool to room temperature under vacuum and backfilled with nitrogen. The flask was then placed in a 60 °C water bath on a stir-plate. The ReactIRTM instrument was filled with liquid nitrogen and then started. Cyclohexane (12 mL) was added to the flask by syringe and allowed to stir for 15 min to achieve temperature balance. 2,2,2-trifluoroethyl 2-diazo-2-(4-(trifluoromethyl)phenyl)acetate (0.1873 g, 0.60 mmol, 1.0 equiv) was then added to the flask by removing and then quickly replacing the rubber septum under nitrogen. Then N,N'-dicyclohexylcarbodiimide (DCC) (1 mol%, 1.238 mg in 0.05 mL DCM stock solution) was added to the flask by syringe. After 5 min, the dirhodium catalyst (0.0005 mol% in 0.05 mL DCM stock solution) was then added to the reaction mixture by syringe. The reaction mixture was stirred at 60 °C until complete consumption of the diazo compound (by monitoring diazo stretching

frequency 2098cm^{-1}). The absorbance points and relative time at which the dirhodium catalyst was added, all the way until the end of the data collection period, was set as the diazo decomposition curve. Upon reaction completion, the solution was concentrated under rotovap and purified by flash column chromatography (0%, then 0%-5% Et₂O in Hexanes). The product was obtained as a colorless oil.

6.5.4 General Procedure for Rh(II)-Catalyzed C–H Functionalization scope exploration and Characterization of the C–H Functionalization Products

A 20 mL scintillation vial equipped with a stir bar was flame dried under vacuum. After cooling down, the vial was charged with diazo compounds(1.0 equiv, 0.20 mmol) and 4Å MS (1000% wt). The vial was then flushed with nitrogen for 3 times and the nitrogen balloon was left on the septum. Substrates (4.0 mL) were injected to the vial and the mixture was heated to 60 °C and stirred at 700 rpm for 5 min. DCC(0.002 mmol, 0.41 mg, 1 mol%) was then injected in 0.05 mL DCM stock solution by syringe in one portion. After 5 min, the dirhodium catalyst Rh₂(R-TPPTTL)₄ (0.001 mol%, 0.000002 mmol, 0.00493 mg in 0.05 mL DCM stock solution) was then added to the reaction mixture by syringe. The reaction mixture was stirred at 60 °C until complete consumption of the diazo compound (monitored by TLC). Upon reaction completion, the solution was concentrated under rotovap and purified by flash column chromatography (0%, then 0%-2% Et₂O in Hexanes).

6.5.5 Characterization of the C–H Functionalization Products

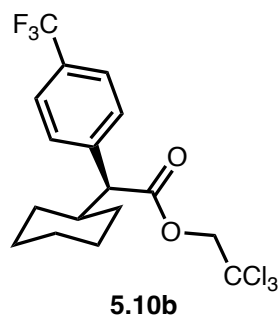


2,2,2-trichloroethyl (*S*)-2-(4-bromophenyl)-2-cyclohexylacetate

This compound was prepared according to General procedure 6.5.4 for Rh(II)-catalyzed C–H functionalization scope exploration, using cyclohexane (4.0 mL) as the substrate and solvent, 2,2,2-trichloroethyl 2-(4-bromophenyl)-2-diazoacetate (74.5 mg, 0.20 mmol, 1.0 equiv), Rh₂(*R*-TPPTTL)₄ (0.00493 mg in 0.05 mL cyclohexane stock solution, 0.000002 mmol, 0.001 mol%). After flash chromatography (0%, then 2% Et₂O in hexanes) the product was obtained as a clear oil (82.5 mg, 96% yield). The ¹H NMR data are consistent with literature values.⁵

¹H NMR (400 MHz, Chloroform-*d*) δ 7.47 – 7.34 (m, 2H), 7.24 – 7.20 (m, 2H), 4.74 (d, *J* = 12.0 Hz, 1H), 4.61 (d, *J* = 12.0 Hz, 1H), 3.33 (d, *J* = 10.7 Hz, 1H), 2.03 (qt, *J* = 11.0, 3.3 Hz, 1H), 1.95 – 1.81 (m, 1H), 1.81 – 1.68 (m, 1H), 1.62 (dd, *J* = 8.7, 3.6 Hz, 2H), 1.43 – 1.21 (m, 2H), 1.21 – 0.94 (m, 3H), 0.75 (qd, *J* = 12.1, 3.6 Hz, 1H).

Chiral HPLC: (AD-H, 30 min, 1 mL/min, 0.1 % *i*PrOH in hexanes, UV 230 nm) tR: Major: 9.0 min, Minor: 15.7 min, 93% ee.



2,2,2-trichloroethyl (*S*)-2-cyclohexyl-2-(4-(trifluoromethyl)phenyl)acetate

This compound was prepared according to General procedure 6.5.4 for Rh(II)-catalyzed C–H functionalization scope exploration, using cyclohexane (4.0 mL) as the substrate and solvent, 2,2,2-trichloroethyl 2-diazo-2-(4-(trifluoromethyl)phenyl)acetate (72.3 mg, 0.20 mmol, 1.0 equiv), Rh₂(*R*-TPPTTL)₄ (0.00493 mg in 0.05 mL cyclohexane stock solution, 0.000002 mmol,

0.001 mol%). After flash chromatography (0%, then 2% Et₂O in hexanes) the product was obtained as a clear oil (81.4 mg, 97% yield).

IR(neat) 2929, 2854, 1749, 1618, 1449, 1421, 1372, 1322, 1121, 1067, 1019, 843, 759, 718, 601, 570 cm⁻¹

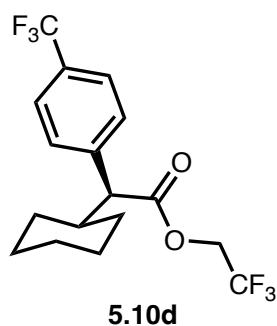
¹H NMR (400 MHz, Chloroform-d) δ 7.70 – 7.53 (m, 2H), 7.49 (d, J = 8.1 Hz, 2H), 4.77 (d, J = 12.0 Hz, 1H), 4.64 (d, J = 12.0 Hz, 1H), 3.46 (d, J = 10.6 Hz, 1H), 2.11 (qt, J = 11.0, 3.4 Hz, 1H), 1.96 – 1.82 (m, 1H), 1.77 (dtt, J = 12.5, 3.6, 1.9 Hz, 1H), 1.70 – 1.59 (m, 2H), 1.39 – 1.28 (m, 2H), 1.15 (dddd, J = 17.5, 11.0, 9.0, 4.8 Hz, 3H), 0.79 (qd, J = 12.0, 3.5 Hz, 1H).

¹³C NMR (151 MHz, Chloroform-d) δ 171.73, 141.19, 130.42, 130.21, 129.99, 129.78, 129.38, 127.02, 125.77, 125.75, 125.72, 125.70, 125.22, 123.42, 121.62, 94.94, 74.46, 58.74, 41.21, 32.07, 30.52, 26.34, 26.08, 26.03.

¹⁹F NMR (565 MHz, Chloroform-d) δ -62.57.

HR-MS:(-p APCI) calcd for [C₁₇H₁₇O₂³⁵Cl₃F₃] 415.02517 found 415.02518

Chiral HPLC: (AD-H, 30 min, 1 mL/min, 0.1 % iPrOH in hexanes, UV 230 nm) tR: Major: 7.3 min, Minor: 11.7 min, 95 % ee.



2,2,2-trifluoroethyl (*S*)-2-cyclohexyl-2-(4-(trifluoromethyl)phenyl)acetate

This compound was prepared according to General procedure 6.5.4 for Rh(II)-catalyzed C–H functionalization scope exploration, using cyclohexane (4.0 mL) as the substrate and solvent, 2,2,2-trifluoroethyl 2-diazo-2-(4-(trifluoromethyl)phenyl)acetate (62.4 mg, 0.20 mmol, 1.0 equiv),

$\text{Rh}_2(\text{R-TPPTTL})_4$ (0.00493 mg in 0.05 mL cyclohexane stock solution, 0.000002 mmol, 0.001 mol%). After flash chromatography (0%, then 2% Et_2O in hexanes) the product was obtained as a white solid (72.3 mg, 98% yield).

MP: 62-64 °C

IR(neat) 2932, 2856, 1753, 1618, 1450, 1421, 1323, 1276, 1123, 1068, 1019, 980, 832, 643, 601, 552 cm^{-1}

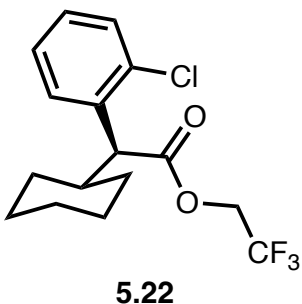
^1H NMR (600 MHz, Chloroform- d) δ 7.59 (d, $J = 8.0$ Hz, 2H), 7.45 (d, $J = 8.0$ Hz, 2H), 4.55 (dq, $J = 12.7, 8.4$ Hz, 1H), 4.34 (dq, $J = 12.6, 8.4$ Hz, 1H), 3.42 (d, $J = 10.5$ Hz, 1H), 2.06 (qt, $J = 11.1, 3.3$ Hz, 1H), 1.84 – 1.74 (m, 2H), 1.69 – 1.60 (m, 2H), 1.35 – 1.27 (m, 2H), 1.20 – 1.12 (m, 2H), 1.12 – 1.05 (m, 1H), 0.78 (qd, $J = 12.1, 3.6$ Hz, 1H).

^{13}C NMR (151 MHz, Chloroform- d) δ 171.93, 141.06, 130.49, 130.27, 130.06, 129.84, 129.22, 127.73, 127.01, 125.83, 125.81, 125.79, 125.76, 125.20, 123.99, 123.40, 122.15, 121.60, 120.32, 61.02, 60.77, 60.53, 60.29, 58.36, 41.48, 31.88, 30.52, 26.31, 26.06, 26.02.

^{19}F NMR (565 MHz, Chloroform- d) δ -62.65, -73.82.

HR-MS (-p APCI) calcd for $[\text{C}_{17}\text{H}_{17}\text{O}_2\text{F}_6]$ 367.11382 found 367.11377

Chiral HPLC (AD-H, 30 min, 1 mL/min, 0.1 % $i\text{PrOH}$ in hexanes, UV 230 nm) tR: Major: 5.4 min, Minor: 6.3 min, 97% ee



2,2,2-trifluoroethyl (S)-2-(2-chlorophenyl)-2-cyclohexylacetate

This compound was prepared according to General procedure 6.5.4 for Rh(II)-catalyzed C–H functionalization scope exploration, using cyclohexane (4.0 mL) as the substrate and solvent, 2,2,2-trifluoroethyl 2-(2-chlorophenyl)-2-diazoacetate (55.7 mg, 0.20 mmol, 1.0 equiv), Rh₂(R-TPPTTL)₄ (0.00493 mg in 0.05 mL cyclohexane stock solution, 0.000002 mmol, 0.001 mol%). After flash chromatography (0%, then 2% Et₂O in hexanes) the product was obtained as a clear oil (52.9 mg, 79% yield).

IR(neat) 2928, 2854, 1752, 1474, 1446, 1406, 1277, 1220, 1133, 1033, 979, 895, 842, 749, 643, 555, 459 cm⁻¹

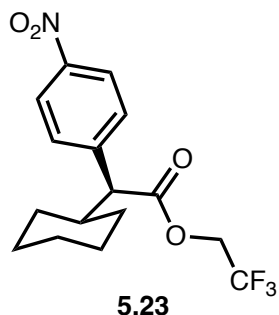
¹H NMR (400 MHz, Chloroform-d) δ 7.54 (dd, J = 7.8, 1.8 Hz, 1H), 7.40 (dd, J = 7.9, 1.5 Hz, 1H), 7.28 (td, J = 7.5, 1.5 Hz, 1H), 7.21 (td, J = 7.6, 1.8 Hz, 1H), 4.57 (dq, J = 12.7, 8.4 Hz, 1H), 4.35 (dq, J = 12.7, 8.5 Hz, 1H), 4.15 (d, J = 10.5 Hz, 1H), 2.07 (qt, J = 11.0, 3.3 Hz, 1H), 1.97 – 1.73 (m, 2H), 1.65 (dq, J = 6.1, 3.9 Hz, 2H), 1.33 (dddd, J = 20.0, 12.7, 6.4, 2.6 Hz, 2H), 1.25 – 1.08 (m, 3H), 1.00 – 0.87 (m, 1H).

¹³C NMR (151 MHz, Chloroform-d) δ 172.06, 135.10, 134.91, 129.84, 129.18, 128.73, 127.40, 125.86, 124.03, 122.19, 120.35, 60.86, 60.62, 60.38, 60.13, 52.91, 41.80, 31.82, 29.88, 26.37, 26.19, 26.15.

¹⁹F NMR (565 MHz, Chloroform-d) δ -73.54.

HR-MS (+p APCI) calcd for [C₁₆H₁₉O₂³⁵ClF₃] 335.10202 found 335.10207

Chiral HPLC: (AD-H, 60 min, 1 mL/min, 0 % iPrOH in hexanes, UV 230 nm) tR: Major: 12.9 min, Minor: 15.2 min, 91% ee



2,2,2-trifluoroethyl (*S*)-2-cyclohexyl-2-(4-nitrophenyl)acetate

This compound was prepared according to General procedure 6.5.4 for Rh(II)-catalyzed C–H functionalization scope exploration, using cyclohexane (4.0 mL) as the substrate and solvent, 2,2,2-trifluoroethyl 2-diazo-2-(4-nitrophenyl)acetate (57.8 mg, 0.20 mmol, 1.0 equiv), Rh₂(*R*-TPPTTL)₄ (0.00493 mg in 0.05 mL cyclohexane stock solution, 0.000002 mmol, 0.001 mol%). After flash chromatography (0%, then 2% Et₂O in hexanes) the product was obtained as a white solid (64.5 mg, 93% yield).

MP: 75-77 °C

IR(neat) 2930, 2854, 1751, 1714, 1606, 1522, 1449, 1407, 1345, 1273, 1220, 1164, 1142, 1124, 1060, 1039, 1016, 978, 897, 847, 831, 735, 694, 643, 553, 502, 444 cm⁻¹

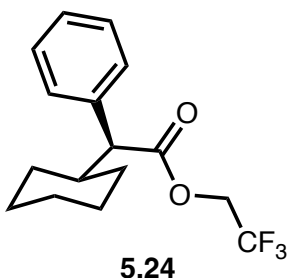
¹H NMR (600 MHz, Chloroform-*d*) δ 8.28 – 8.08 (m, 2H), 7.56 – 7.47 (m, 2H), 4.75 – 4.44 (m, 1H), 4.55 (dq, *J* = 12.7, 8.4 Hz, 1H), 4.37 (dq, *J* = 12.7, 8.4 Hz, 1H), 3.49 (d, *J* = 10.4 Hz, 1H), 2.06 (qt, *J* = 11.1, 3.4 Hz, 1H), 1.84 – 1.71 (m, 2H), 1.68 – 1.56 (m, 2H), 1.37 – 1.22 (m, 2H), 1.21 – 1.07 (m, 3H), 0.79 (qd, *J* = 12.0, 3.7 Hz, 1H).

¹³C NMR (151 MHz, Chloroform-*d*) δ 171.39, 147.68, 144.41, 129.75, 125.74, 123.95, 123.90, 122.06, 120.22, 61.05, 60.80, 60.56, 60.32, 58.23, 41.67, 31.76, 30.48, 26.17, 25.97, 25.92.

¹⁹F NMR (565 MHz, Chloroform-*d*) δ -73.77.

HR-MS (+p APCI) calcd for [C₁₆H₁₉O₄NF₃] 346.12607 found 346.12629

Chiral HPLC (AD-H, 30 min, 0.5 mL/min, 1 % iPrOH in hexanes, UV 230 nm) tR: Major: 17.9 min, Minor: 19.8 min, 97% ee



2,2,2-trifluoroethyl (*S*)-2-cyclohexyl-2-phenylacetate

This compound was prepared according to General procedure 6.5.4 for Rh(II)-catalyzed C–H functionalization scope exploration, using cyclohexane (4.0 mL) as the substrate and solvent, 2,2,2-trifluoroethyl 2-diazo-2-phenylacetate (48.8 mg, 0.20 mmol, 1.0 equiv), Rh2(R-TPPTTL)4 (0.00493 mg in 0.05 mL cyclohexane stock solution, 0.000002 mmol, 0.001 mol%). After flash chromatography (0%, then 2% Et2O in hexanes) the product was obtained as a white solid (58.7 mg, 98% yield).

MP: 78-80 °C

IR(neat) 2926, 2853, 1751, 1601, 1497, 1450, 1407, 1276, 1219, 1165, 1141, 1122, 1062, 979, 895, 842, 730, 698, 643, 553, 504 cm⁻¹

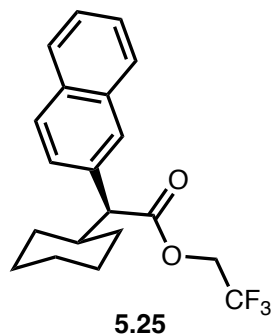
¹H NMR (400 MHz, Chloroform-d)) δ 7.33 (dddd, J = 14.4, 12.6, 6.9, 1.8 Hz, 5H), 4.77 (d, J = 12.0 Hz, 1H), 4.62 (d, J = 12.0 Hz, 1H), 3.38 (d, J = 10.7 Hz, 1H), 2.11 (dtd, J = 14.4, 11.6, 11.0, 8.1 Hz, 1H), 1.89 (d, J = 12.7 Hz, 1H), 1.75 (d, J = 13.2 Hz, 1H), 1.64 (d, J = 4.3 Hz, 2H), 1.44 – 1.28 (m, 2H), 1.22 – 1.05 (m, 3H), 0.94 – 0.64 (m, 1H).

¹³C NMR (101 MHz, Chloroform-d) δ 172.60, 137.05, 128.84, 127.78, 124.56, 121.81, 61.01, 60.65, 60.29, 59.92, 58.60, 41.27, 32.00, 30.56, 29.95, 29.91, 26.44, 26.15, 26.11.

¹⁹F NMR (376 MHz, Chloroform-d) δ -73.70.

HR-MS (-p APCI) calcd for [C₁₆H₁₈O₂F₃] 299.12644 found 299.12632

Chiral HPLC (AD-H, 30 min, 1 mL/min, 0.1 % iPrOH in hexanes, UV 230 nm) tR: Major: 5.3 min, Minor: 5.8 min, 93% ee



2,2,2-trifluoroethyl (S)-2-cyclohexyl-2-(naphthalen-2-yl)acetate

This compound was prepared according to General procedure 6.5.4 for Rh(II)-catalyzed C–H functionalization scope exploration, using cyclohexane (4.0 mL) as the substrate and solvent, 2,2,2-trifluoroethyl 2-diazo-2-(naphthalen-2-yl)acetate (58.8 mg, 0.20 mmol, 1.0 equiv), Rh₂(R-TPPTTL)₄ (0.00493 mg in 0.05 mL cyclohexane stock solution, 0.000002 mmol, 0.001 mol%). After flash chromatography (0%, then 2% Et₂O in hexanes) the product was obtained as a clear oil (68.0 mg, 97% yield).

IR(neat) 2930, 2854, 1754, 1474, 1446, 1407, 1278, 1220, 1168, 1148, 1135, 1115, 1041, 980, 750, 660, 555, 460 cm⁻¹

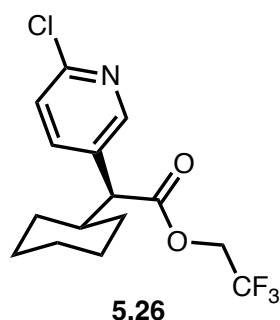
¹H NMR (400 MHz, Chloroform-d) δ 7.86 – 7.78 (m, 3H), 7.76 (d, J = 1.8 Hz, 1H), 7.54 – 7.42 (m, 3H), 4.58 (dq, J = 12.7, 8.5 Hz, 1H), 4.30 (dq, J = 12.7, 8.4 Hz, 1H), 3.51 (d, J = 10.7 Hz, 1H), 2.16 (qt, J = 11.1, 3.4 Hz, 1H), 1.89 – 1.74 (m, 2H), 1.69 – 1.58 (m, 2H), 1.34 (ddd, J = 15.9, 9.8, 6.4 Hz, 2H), 1.22 – 1.07 (m, 3H), 0.82 (qd, J = 13.0, 12.1, 9.3 Hz, 1H).

^{13}C NMR (151 MHz, Chloroform-d) δ 172.57, 134.52, 133.58, 133.05, 128.58, 128.07, 128.02, 127.88, 126.47, 126.39, 126.24, 124.10, 122.27, 60.89, 60.65, 60.41, 60.16, 58.70, 41.26, 32.06, 30.65, 29.96, 26.45, 26.17, 26.10.

^{19}F NMR (565 MHz, Chloroform-d) δ -73.67.

HR-MS:(-p APCI) calcd for $[\text{C}_{20}\text{H}_{20}\text{O}_2\text{F}_3]$ 349.14209 found 349.14218

Chiral HPLC: (Whelk, 60 min, 0.25 mL/min, 0 % iPrOH in hexanes, UV 230 nm) tR: Major: 27.8 min, Minor: 24.6 min, 83% ee



2,2,2-trifluoroethyl (*S*)-2-(6-chloropyridin-3-yl)-2-cyclohexylacetate

This compound was prepared according to General procedure 6.5.4 for Rh(II)-catalyzed C–H functionalization scope exploration, using cyclohexane (4.0 mL) as the substrate and solvent, 2,2,2-trifluoroethyl 2-(6-chloropyridin-3-yl)-2-diazoacetate (55.9 mg, 0.20 mmol, 1.0 equiv), $\text{Rh}_2(\text{R-TPPTTL})_4$ (0.00493 mg in 0.05 mL cyclohexane stock solution, 0.000002 mmol, 0.001 mol%). After flash chromatography (0%, then 2% Et_2O in hexanes) the product was obtained as a clear oil (44.6 mg, 66% yield).

IR(neat) 2929, 2854, 1752, 1584, 1564, 1462, 1409, 1391, 1277, 1167, 1143, 1123, 1106, 1023, 980, 834, 774, 742, 645, 555, 522 cm^{-1}

^1H NMR (600 MHz, Chloroform-d) δ 8.29 (d, J = 2.5 Hz, 1H), 7.71 (dd, J = 8.3, 2.5 Hz, 1H), 7.32 (d, J = 8.3 Hz, 1H), 4.55 (dq, J = 12.7, 8.4 Hz, 1H), 4.37 (dq, J = 12.7, 8.4 Hz, 1H), 3.38 (d,

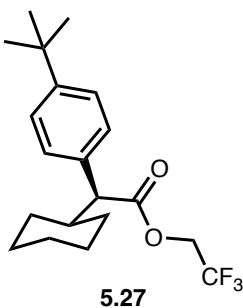
$J = 10.3$ Hz, 1H), 2.12 – 1.87 (m, 1H), 1.76 (d, $J = 3.5$ Hz, 2H), 1.68 – 1.60 (m, 2H), 1.39 – 1.26 (m, 2H), 1.19 – 1.05 (m, 3H), 0.80 (ddt, $J = 13.8, 9.8, 5.0$ Hz, 1H).

^{13}C NMR (151 MHz, Chloroform- d) δ 171.60, 151.17, 150.13, 138.69, 131.74, 125.73, 124.61, 123.90, 122.06, 120.22, 61.13, 60.89, 60.64, 60.40, 55.05, 41.51, 31.75, 30.46, 26.17, 25.98, 25.93.

^{19}F NMR (565 MHz, Chloroform- d) δ -73.68

HR-MS:(+p APCI) calcd for $[\text{C}_{15}\text{H}_{18}\text{O}_2\text{N}^{35}\text{ClF}_3]$ 336.09727 found 336.09754

Chiral HPLC: (Whelk, 30 min, 0.5 mL/min, 1% iPrOH in hexanes, UV 230 nm) tR: Major: 24.3 min, Minor: 27.7 min, 94% ee



2,2,2-trifluoroethyl (*S*)-2-(4-(tert-butyl)phenyl)-2-cyclohexylacetate

This compound was prepared according to General procedure 6.5.4 for Rh(II)-catalyzed C–H functionalization scope exploration, using cyclohexane (4.0 mL) as the substrate and solvent, 2,2,2-trifluoroethyl 2-(4-(tert-butyl)phenyl)-2-diazoacetate (60.1 mg, 0.20 mmol, 1.0 equiv), $\text{Rh}_2(\text{R-TPPTTL})_4$ (0.00493 mg in 0.05 mL cyclohexane stock solution, 0.000002 mmol, 0.001 mol%). After flash chromatography (0%, then 2% Et_2O in hexanes) the product was obtained as a clear oil (18.2 mg, 25% yield).

IR(neat) 2927, 2854, 2110, 1752, 1507, 1449, 1407, 1365, 1275, 1220, 1164, 1141, 1125, 1113, 1062, 1042, 1019, 979, 838, 826, 771, 716, 646, 565, 452 cm^{-1}

^1H NMR (600 MHz, Chloroform- d) δ 7.36 (d, $J = 8.3$ Hz, 2H), 7.34 – 7.15 (m, 2H), 4.59 (dq, $J = 12.7, 8.5$ Hz, 1H), 4.31 (dq, $J = 12.7, 8.5$ Hz, 1H), 3.35 (d, $J = 10.6$ Hz, 1H), 2.06 (qt, $J = 11.1, 3.3$

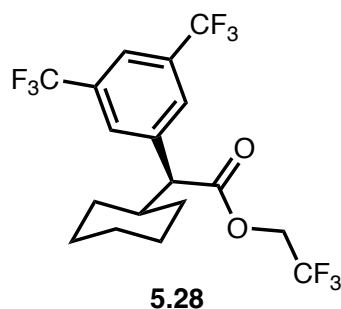
Hz, 1H), 1.86 – 1.71 (m, 2H), 1.71 – 1.61 (m, 2H), 1.46 – 1.38 (m, 1H), 1.36 (d, $J = 5.7$ Hz, 1H), 1.34 (s, 9H), 1.18 (ddd, $J = 11.9, 8.8, 2.8$ Hz, 2H), 1.15 – 1.03 (m, 1H), 0.79 (qd, $J = 12.1, 3.6$ Hz, 1H).

^{13}C NMR (151 MHz, Chloroform- d) δ 172.78, 150.63, 133.92, 128.41, 125.71, 124.17, 122.33, 60.79, 60.55, 60.31, 60.07, 58.14, 41.30, 34.70, 31.97, 31.56, 30.61, 26.48, 26.16, 26.14.

^{19}F NMR (565 MHz, Chloroform- d) δ -73.54

HR-MS:(-p APCI) calcd for $[\text{C}_{20}\text{H}_{26}\text{O}_2\text{F}_3]$ 355.18904 found 355.18949

Chiral HPLC: (Whelk, 60 min, 0.25 mL/min, 0% iPrOH in hexanes, UV 230 nm) tR: Major: 24.3 min, Minor: 27.7 min, 94% ee



2,2,2-trifluoroethyl (S)-2-(3,5-bis(trifluoromethyl)phenyl)-2-cyclohexylacetate

This compound was prepared according to General procedure 6.5.4 for Rh(II)-catalyzed C–H functionalization scope exploration, using cyclohexane (4.0 mL) as the substrate and solvent, 2,2,2-trifluoroethyl 2-(3,5-bis(trifluoromethyl)phenyl)-2-diazoacetate (76.0 mg, 0.20 mmol, 1.0 equiv), $\text{Rh}_2(\text{S-2-Cl-5-Br-TPCP})_4$ (0.00493 mg in 0.05 mL cyclohexane stock solution, 0.000002 mmol, 0.001 mol%). After flash chromatography (0%, then 2% Et_2O in hexanes) the product was obtained as a clear oil (85.6 mg, 98% yield).

IR(neat) 2934, 2857, 1755, 1451, 1408, 1374, 1274, 1165, 1123, 1062, 1042, 980, 900, 846, 705, 681, 645, 550, 459 cm^{-1}

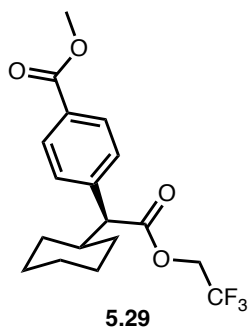
¹H NMR (400 MHz, Chloroform-d) δ 7.81 (m, 3H), 4.59 (dq, $J = 12.6, 8.4$ Hz, 1H), 4.36 (dq, $J = 12.6, 8.3$ Hz, 1H), 3.51 (d, $J = 10.4$ Hz, 1H), 2.06 (qt, $J = 11.1, 3.3$ Hz, 1H), 1.80 (tt, $J = 6.7, 3.2$ Hz, 2H), 1.74 – 1.59 (m, 2H), 1.43 – 1.26 (m, 2H), 1.26 – 1.04 (m, 3H), 0.91 – 0.74 (m, 1H).

¹³C NMR (151 MHz, Chloroform-d) δ 171.30, 139.6, 132.6, 132.4, 132.13, 131.91, 129.10, 129.08, 129.05, 129.03, 126.16, 125.74, 124.35, 123.91, 122.54, 122.07, 122.04, 122.02, 121.99, 121.97, 120.73, 120.23, 61.21, 60.96, 60.72, 60.48, 58.23, 41.79, 31.75, 30.57, 26.18, 25.98, 25.92.

¹⁹F NMR (565 MHz Chloroform-d) δ -62.90, -73.83.

HR-MS:(-p APCI) calcd for [C₁₈H₁₆O₂F₃] 435.10121 found 435.10108

Chiral HPLC: (Whelk, 30 min, 0.25 mL/min, 0% iPrOH in hexanes, UV 230 nm) tR: Major: 18.9 min, Minor: 20.4 min, 83% ee



methyl (S)-4-(1-cyclohexyl-2-oxo-2-(2,2,2-trifluoroethoxy)ethyl)benzoate

This compound was prepared according to General procedure 6.5.4 for Rh(II)-catalyzed C–H functionalization scope exploration, using cyclohexane (4.0 mL) as the substrate and solvent, methyl 4-(1-diazo-2-oxo-2-(2,2,2-trifluoroethoxy)ethyl)benzoate (60.4 mg, 0.20 mmol, 1.0 equiv), Rh₂(R-TPPTTL)₄ (0.00493 mg in 0.05 mL cyclohexane stock solution, 0.000002 mmol, 0.001 mol%). After flash chromatography (0%, then 2% Et₂O in hexanes) the product was obtained as a clear oil (66.0 mg, 92% yield).

IR(neat) 2931, 2853, 1754, 1725, 1611, 1436, 1281, 1168, 1144, 1113, 1021, 980, 745, 550, 491 cm⁻¹

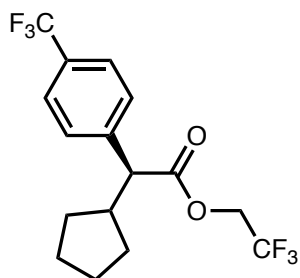
¹H NMR (600 MHz, Chloroform-d) δ 8.07 – 7.93 (m, 2H), 7.46 – 7.33 (m, 2H), 4.54 (dq, $J = 12.8$, 8.4 Hz, 1H), 4.34 (dq, $J = 12.7$, 8.4 Hz, 1H), 3.91 (s, 3H), 3.41 (d, $J = 10.5$ Hz, 1H), 2.10 – 2.02 (m, 1H), 1.82 – 1.73 (m, 2H), 1.67 – 1.59 (m, 2H), 1.34 – 1.27 (m, 2H), 1.18 – 1.07 (m, 3H), 0.77 (qd, $J = 12.1$, 3.6 Hz, 1H).

¹³C NMR (151 MHz, Chloroform-d) δ 171.96, 167.04, 142.20, 130.13, 129.77, 128.89, 125.84, 124.00, 122.16, 120.33, 60.97, 60.73, 60.49, 60.24, 58.54, 52.38, 41.41, 31.92, 30.53, 26.33, 26.09, 26.03.

¹⁹F NMR (565 MHz, Chloroform-d) -73.72.

HR-MS:(+p APCI) calcd for [C₁₈H₂₂O₄F₃] 359.14647 found 359.14664

Chiral HPLC: (ADH, 60 min, 0.5 mL/min, 0.5 % iPrOH in hexanes, UV 230 nm) tR: Major: 25.5 min, Minor: 33.7 min, 86% ee



5.30

2,2,2-trifluoroethyl (*S*)-2-cyclopentyl-2-(4-(trifluoromethyl)phenyl)acetate

This compound was prepared according to General procedure 6.5.4 for Rh(II)-catalyzed C–H functionalization scope exploration, using cyclopentane (4.0 mL) as the substrate and solvent, 2,2,2-trifluoroethyl 2-diazo-2-(4-(trifluoromethyl)phenyl)acetate (62.4 mg, 0.20 mmol, 1.0 equiv), Rh₂(*R*-TPPTTL)₄ (0.00493 mg in 0.05 mL cyclopentane stock solution, 0.000002 mmol, 0.001 mol%). After flash chromatography (0%, then 2% Et₂O in hexanes) the product was obtained as a clear oil (68.8 mg, 97% yield).

IR(neat) 2925, 2855, 1757, 1619, 1455, 1421, 1326, 1285, 1167, 1131, 1069, 1019, 981, 833 cm^{-1}

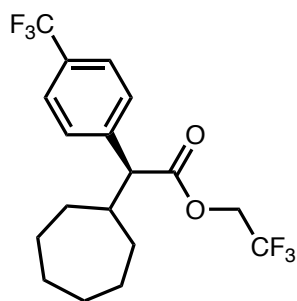
^1H NMR (400 MHz, Chloroform- d) δ 7.59 (d, J = 8.2 Hz, 2H), 7.47 (d, J = 8.1 Hz, 2H), 4.54 (dq, J = 12.7, 8.4 Hz, 1H), 4.36 (dq, J = 12.7, 8.4 Hz, 1H), 3.46 (d, J = 11.1 Hz, 1H), 2.58 (dddd, J = 12.7, 8.9, 6.5, 4.5 Hz, 1H), 2.00 – 1.87 (m, 1H), 1.76 – 1.66 (m, 1H), 1.66 – 1.56 (m, 2H), 1.46 (dddd, J = 22.9, 10.9, 6.6, 3.7 Hz, 2H), 1.06 – 0.96 (m, 1H), 0.92 – 0.81 (m, 2H).

^{13}C NMR (151 MHz, Chloroform- d) δ 171.97, 142.06, 130.25, 130.04, 128.89, 125.88, 125.86, 125.83, 125.81, 125.20, 123.99, 123.39, 122.15, 61.03, 60.79, 60.54, 60.30, 57.37, 43.73, 31.52, 30.99, 25.34, 25.03.

^{19}F NMR (565 MHz, Chloroform- d) δ -62.57, -73.77.

HR-MS:(-p APCI) calcd for $[\text{C}_{16}\text{H}_{15}\text{O}_2\text{F}_6]$ 353.09817 found 353.09863

Chiral HPLC: (ADH, 30 min, 0.5 mL/min, 0 % iPrOH in hexanes, UV 230 nm) tR: Major: 16.3 min, Minor: 19.7 min, 97% ee



5.31

2,2,2-trifluoroethyl (*S*)-2-cycloheptyl-2-(4-(trifluoromethyl)phenyl)acetate

This compound was prepared according to General procedure 6.5.4 for Rh(II)-catalyzed C–H functionalization scope exploration, using cycloheptane (4.0 mL) as the substrate and solvent, 2,2,2-trifluoroethyl 2-diazo-2-(4-(trifluoromethyl)phenyl)acetate (62.4 mg, 0.20 mmol, 1.0 equiv), $\text{Rh}_2(\text{R-TPPTTL})_4$ (0.00493 mg in 0.05 mL cycloheptane stock solution, 0.000002 mmol, 0.001

mol%). After flash chromatography (0%, then 2% Et₂O in hexanes) the product was obtained as a clear oil (72.0 mg, 94% yield).

IR(neat) 2930, 2857, 1754, 1618, 1421, 1326, 1284, 1166, 1129, 1069, 1019, 979, 831 cm⁻¹

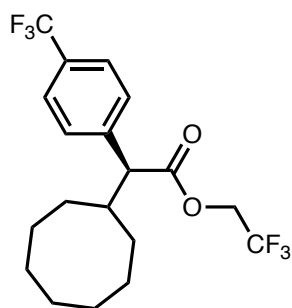
¹H NMR (400 MHz, Chloroform-d) δ 7.59 (d, J = 8.1 Hz, 2H), 7.46 (d, J = 8.1 Hz, 2H), 4.53 (dq, J = 12.7, 8.4 Hz, 1H), 4.34 (dq, J = 12.7, 8.4 Hz, 1H), 3.50 (d, J = 10.8 Hz, 1H), 2.30 (ddq, J = 10.8, 9.5, 4.8, 3.8 Hz, 1H), 1.82 – 1.73 (m, 1H), 1.70 (qd, J = 7.0, 4.0 Hz, 1H), 1.65 – 1.55 (m, 2H), 1.51 (d, J = 3.6 Hz, 4H), 1.40 – 1.28 (m, 3H), 1.07 – 0.95 (m, 1H).

¹³C NMR (151 MHz, Chloroform-d) δ 172.11, 141.57, 130.48, 130.26, 130.05, 129.83, 129.29, 127.00, 125.88, 125.85, 125.83, 125.80, 125.20, 124.00, 123.39, 122.16, 121.59, 120.32, 61.03, 60.79, 60.54, 60.30, 58.51, 42.55, 33.13, 31.51, 28.44, 28.34, 26.41, 26.31.

¹⁹F NMR (565 MHz, Chloroform-d) -62.65, -73.59.

HR-MS:(-p APCI) calcd for [C₁₈H₁₉O₂F₆] 381.12947found 381.12915

Chiral HPLC: (ADH, 30 min, 1 mL/min, 0.1 % iPrOH in hexanes, UV 230 nm) tR: Major: 6.0 min, Minor: 7.4 min, 88% ee



5.32

2,2,2-trifluoroethyl (S)-2-cyclooctyl-2-(4-(trifluoromethyl)phenyl)acetate

This compound was prepared according to General procedure 6.5.4 for Rh(II)-catalyzed C–H functionalization scope exploration, using cyclooctane (4.0 mL) as the substrate and solvent, 2,2,2-trifluoroethyl 2-diazo-2-(4-(trifluoromethyl)phenyl)acetate (62.4 mg, 0.20 mmol, 1.0 equiv),

$\text{Rh}_2(\text{R-TPPTTL})_4$ (0.00493 mg in 0.05 mL cyclooctane stock solution, 0.000002 mmol, 0.001 mol%). After flash chromatography (0%, then 2% Et_2O in hexanes) the product was obtained as a clear oil (76.2 mg, 96% yield).

IR(neat) 2923, 2855, 1754, 1618, 1447, 1421, 1324, 1274, 1163, 1124, 1068, 1019, 979, 836, 757, 721, 643, 600 cm^{-1}

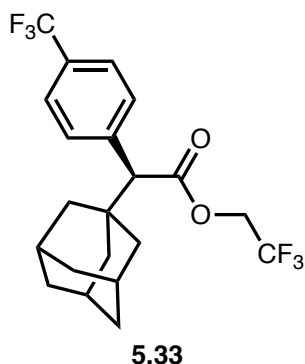
^1H NMR (400 MHz, Chloroform- d) δ 7.61 (d, $J = 8.1$ Hz, 2H), 7.49 (d, $J = 8.1$ Hz, 2H), 4.56 (dq, $J = 12.7, 8.4$ Hz, 1H), 4.36 (dq, $J = 12.7, 8.4$ Hz, 1H), 3.52 (d, $J = 11.1$ Hz, 1H), 2.52 – 2.22 (m, 1H), 1.83 – 1.61 (m, 4H), 1.57 – 1.42 (m, 6H), 1.37 – 1.29 (m, 2H), 1.12 (ddd, $J = 15.3, 8.6, 2.1$ Hz, 1H), 0.93 – 0.84 (m, 1H).

^{13}C NMR (151 MHz, Chloroform- d) δ 172.20, 141.61, 130.27, 130.06, 129.84, 129.31, 125.88, 125.86, 125.83, 125.81, 125.20, 124.00, 123.39, 122.16, 61.04, 60.80, 60.55, 60.31, 58.67, 40.73, 31.11, 29.38, 27.08, 26.58, 25.57, 25.19.

^{19}F NMR (565 MHz, Chloroform- d) δ -62.50, -73.82.

HR-MS:(-p APCI) calcd for $[\text{C}_{19}\text{H}_{21}\text{O}_2\text{F}_6]$ 395.14512 found 395.14476

Chiral HPLC: (ADH, 30 min, 1 mL/min, 0.1% iPrOH in hexanes, UV 230 nm) tR: Major: 6.5 min, Minor: 8.8 min, 92% ee



2,2,2-trifluoroethyl (2S)-2-((1S,3R)-adamantan-1-yl)-2-(4-(trifluoromethyl)phenyl)acetate

This compound was prepared according to General procedure 6.5.4 for Rh(II)-catalyzed C–H functionalization scope exploration, using adamantane (272.5 mg, 2.0 mmol, 10 equiv) as the substrate and CHCl_3 (4.0 mL) as solvent, 2,2,2-trifluoroethyl 2-diazo-2-(4-(trifluoromethyl)phenyl)acetate (62.4 mg, 0.20 mmol, 1.0 equiv), $\text{Rh}_2(\text{R-TPPTTL})_4$ (0.00493 mg in 0.05 mL CHCl_3 stock solution, 0.000002 mmol, 0.001 mol%). After flash chromatography (0%, then 2% Et_2O in hexanes) the product was obtained as a clear oil (80.1 mg, 95% yield).

IR(neat) 2909, 2851, 1753, 1618, 1423, 1325, 1278, 1166, 1129, 1070, 1020, 975, 847, 657, 604 cm^{-1}

^1H NMR (600 MHz, Chloroform- d) δ 7.57 (d, J = 8.1 Hz, 2H), 7.50 (d, J = 8.2 Hz, 2H), 4.59 (dq, J = 12.7, 8.5 Hz, 1H), 4.31 (dq, J = 12.7, 8.4 Hz, 1H), 3.46 (s, 1H), 1.98 (p, J = 3.2 Hz, 3H), 1.68 (ddt, J = 13.5, 11.1, 2.7 Hz, 6H), 1.58 (q, J = 2.3 Hz, 3H), 1.52 (dq, J = 12.3, 2.7 Hz, 3H).

^{13}C NMR (151 MHz, Chloroform- d) δ 170.70, 138.15, 130.65, 130.08, 129.86, 125.31, 125.01, 124.98, 124.96, 124.93, 124.10, 123.50, 122.26, 62.64, 60.76, 60.52, 60.28, 60.04, 39.97, 37.06, 36.75, 28.73.

^{19}F NMR (565 MHz, Chloroform- d) δ -62.54, -73.47.

HR-MS:(-p APCI) calcd for $[\text{C}_{21}\text{H}_{21}\text{O}_2\text{F}_6]$ 419.14512 found 419.14493

Chiral HPLC: (ODH, 30 min, 0.25 mL/min, 0% $i\text{PrOH}$ in hexanes, UV 230 nm) tR: Major: 20.1 min, Minor: 23.2 min, 83% ee

Reference

1. Godula, K.; Sames, D. C–H Bond Functionalization in Complex Organic Synthesis. *Science* **2006**, *312*, 67-72.
2. Scott, L. T.; DeCicco, G. J. Intermolecular carbon-hydrogen insertion of copper carbenoids. *J. Am. Chem. Soc.* **1974**, *96*, 322-323.
3. Gutekunst, W. R.; Baran, P. S. C–H functionalization logic in total synthesis. *Chem. Soc. Rev.* **2011**, *40*, 1976-1991.
4. Brückl, T.; Baxter, R. D.; Ishihara, Y.; Baran, P. S. Innate and Guided C–H Functionalization Logic. *Acc. Chem. Res.* **2012**, *45*, 826-839.
5. Abrams, D. J.; Provencher, P. A.; Sorensen, E. J. Recent applications of C–H functionalization in complex natural product synthesis. *Chem. Soc. Rev.* **2018**, *47*, 8925-8967.
6. Bergman, R. G. C–H activation. *Nature* **2007**, *446*, 391-394.
7. McMurray, L.; O'Hara, F.; Gaunt, M. J. Recent developments in natural product synthesis using metal-catalysed C–H bond functionalisation. *Chem. Soc. Rev.* **2011**, *40*, 1885-1898.
8. Newhouse, T.; Baran, P. S. If C–H bonds could talk: selective C–H bond oxidation. *Angew. Chem. Int. Ed.* **2011**, *50*, 3362-3374.
9. Chen, D. Y.; Youn, S. W. C–H activation: a complementary tool in the total synthesis of complex natural products. *Chem. Eur. J.* **2012**, *18*, 9452-9474.
10. Yamaguchi, J.; Yamaguchi, A. D.; Itami, K. C–H bond functionalization: emerging synthetic tools for natural products and pharmaceuticals. *Angew. Chem. Int. Ed.* **2012**, *51*, 8960-9009.
11. Schönherr, H.; Cernak, T. Profound methyl effects in drug discovery and a call for new C–H methylation reactions. *Angew. Chem. Int. Ed.* **2013**, *52*, 12256-12267.
12. Wencel-Delord, J.; Glorius, F. C–H bond activation enables the rapid construction and late-stage diversification of functional molecules. *Nat. Chem.* **2013**, *5*, 369-375.
13. Davies, H. M. L. Recent Advances in Catalytic Enantioselective Intermolecular C–H Functionalization. *Angew. Chem. Int. Ed.* **2006**, *45*, 6422-6425.
14. Davies, H. M. L.; Antoulinakis, E. G. Intermolecular metal-catalyzed carbenoid cyclopropanations. *Org. React.* **2004**, *57*, 1-326.
15. Kennedy, M.; McKervey, M. A.; Maguire, A. R.; Roos, G. H. P. Asymmetric synthesis in carbon-carbon bond forming reactions of α -diazoketones catalysed by homochiral rhodium(II) carboxylates. *J. Chem. Soc., Chem. Commun.*, **1990**, 361-362.

16. Doyle, M. P. Catalytic Methods for Metal Carbene Transformations. *Chem. Rev.* **1986**, *86*, 919-939.
17. Nakamura, E.; Yoshikai, N.; Yamanaka, M. Mechanism of C–H Bond Activation: C–C Bond Formation Reaction between Diazo Compound and Alkane Catalyzed by Dirhodium Tetracarboxylate. *J. Am. Chem. Soc.* **2002**, *124*, 7181-7192.
18. Yoshikai, N.; Nakamura, E. Theoretical Studies on Diastereo- and Enantioselective Rhodium-Catalyzed Cyclization of Diazo Compound via Intramolecular C–H Bond Insertion. *Adv. Synth. Catal.* **2003**, *345*, 1159-1171.
19. Wong, F. M.; Wang, J.; Hengge, A. C.; Wu, W. Mechanism of Rhodium-Catalyzed Carbene Formation from Diazo Compounds. *Org. Lett.* **2007**, *9*, 1663-1665.
20. Trindade, A. F.; Coelho, J. A. S.; Afonso, C. A. M.; Veiros, L. F.; Gois, P. M. P. Fine Tuning of Dirhodium(II) Complexes: Exploring the Axial Modification. *ACS Catal.* **2012**, *2*, 370-383.
21. Berry, J. F. Metal–metal multiple bonded intermediates in catalysis. *J. Chem. Sci.* **2015**, *127*, 209-214.
22. Padwa, A.; Zou, Y. Solvent and ligand effects associated with the Rh(II)-catalyzed reactions of alpha-diazo-substituted amido esters. *J. Org. Chem.* **2015**, *80*, 1802-1808.
23. Werle, C.; Goddard, R.; Furstner, A. The First Crystal Structure of a Reactive Dirhodium Carbene Complex and a Versatile Method for the Preparation of Gold Carbenes by Rhodium-to-Gold Transmetalation. *Angew. Chem. Int. Ed.* **2015**, *54*, 15452-6.
24. Liu, H.; Duan, J.-X.; Qu, D.; Guo, L.-P.; Xie, Z.-Z. Mechanistic Insights into Asymmetric C–H Insertion Cooperatively Catalyzed by a Dirhodium(II) Complex and Chiral Phosphoric Acid. *Organometallics* **2016**, *35*, 2003-2009.
25. Qi, X.; Li, Y.; Bai, R.; Lan, Y. Mechanism of Rhodium-Catalyzed C–H Functionalization: Advances in Theoretical Investigation. *Acc. Chem. Res.* **2017**, *50*, 2799-2808.
26. Kornecki, K. P.; Briones, J. F.; Boyarskikh, V.; Felicia Fullilove; Autschbach, J.; Schrote, K. E.; Lancaster, K. M.; Davies, H. M. L.; Berry, J. F. Direct Spectroscopic Characterization of a Transitory Dirhodium Donor-Acceptor Carbene Complex. *Science* **2013**, *342*, 351-354.
27. Berry, J. F. The role of three-center/four-electron bonds in superelectrophilic dirhodium carbene and nitrene catalytic intermediates. *Dalton Trans.* **2012**, *41*, 700-713.

28. Morton, D.; Blakey, S. B. Expanding the Carbene C–H Insertion Toolbox. *Chem. Cat. Chem.* **2015**, *7*, 577-578.
29. Hansen, J.; Autschbach, J.; Davies, H. M. Computational study on the selectivity of donor/acceptor-substituted rhodium carbenoids. *J. Org. Chem.* **2009**, *74*, 6555-6563.
30. Davies, H. M. L.; Huby, N. J. S.; Cantrell, W. R.; Olive, J. L. α -Hydroxy esters as chiral auxiliaries in asymmetric cyclopropanations by rhodium(II)-stabilized vinylcarbenoids. *J. Am. Chem. Soc.* **1993**, *115*, 9468-9479.
31. Davies, H. M. L.; Cantrell, W. R. α -hydroxy esters as inexpensive chiral auxiliaries in rhodium(II)-catalyzed cyclopropanations with vinyl diazomethanes. *Tetrahedron Lett.* **1991**, *32*, 6509-6512.
32. Davies, H. M. L.; Bruzinski, P. R.; Fall, M. J. Effect of diazoalkane structure on the stereoselectivity of rhodium(II) (S)-N-(arylsulfonyl)prolinate catalyzed cyclopropanations. *Tetrahedron Lett.* **1996**, *37*, 4133-4136.
33. Reddy, R. P.; Lee, G. H.; Davies, H. M. L. Dirhodium Tetracarboxylate Derived from Adamantylglycine as a Chiral Catalyst for Carbenoid Reactions. *Org. Lett.* **2006**, *8*, 3437-3440.
34. Hashimoto, S.-i.; Watanabe, N.; Sato, T.; Shiro, M.; Ikegami, S. Enhancement of Enantioselectivity in Intramolecular C–H Insertion Reactions of α -Diazo (β -Keto Esters Catalyzed by Chiral Dirhodium(II) Carboxylates. *Tetrahedron Lett.* **1993**, *34*, 5109-5112.
35. DeAngelis, A.; Dmitrenko, O.; Yap, G. P. A.; Fox, J. M. Chiral Crown Conformation of Rh₂(S-PTTL)₄- Enantioselective Cyclopropanation with α -Alkyl- α -diazoesters. *J. Am. Chem. Soc.* **2009**, *131*, 7230-7231.
36. DeAngelis, A.; Boruta, D. T.; Lubin, J. B.; Plampin, J. N., 3rd; Yap, G. P.; Fox, J. M. The chiral crown conformation in paddlewheel complexes. *Chem. Commun.* **2010**, *46*, 4541-4543.
37. Lindsay, V. N. G.; Lin, W.; Charette, A. B. Experimental Evidence for the All-Up Reactive Conformation of Chiral Rhodium(II) Carboxylate Catalysts- Enantioselective Synthesis of cis-Cyclopropane α -Amino Acids. *J. Am. Chem. Soc.* **2009**, *131*, 16383-16385.
38. Davies, H. M. L.; Morton, D. D. Guiding principles for site selective and stereoselective intermolecular C–H functionalization by donor/acceptor rhodium carbenes. *Chem. Soc. Rev.* **2011**, *40*, 1857-1869.
39. Fu, J.; Ren, Z.; Bacsa, J.; Musaev, D. G.; Davies, H. M. L. Desymmetrization of cyclohexanes by site- and stereoselective C–H functionalization. *Nature* **2018**, *564*, 395-399.

40. Denton, J. R.; Davies, H. M. L. Enantioselective reactions of donor/acceptor carbenoids derived from alpha-aryl-alpha-diazoketones. *Org. Lett.* **2009**, *11*, 787-790.
41. Nagashima, T.; Davies, H. M. L. Catalytic Asymmetric Cyclopropanation Using Bridged Dirhodium Tetraprolineates on Solid Support. *Org. Lett.* **2002**, *4*, 1989-1992.
42. Davies, H. M. L.; Venkataramani, C. Dirhodium tetraproline-catalyzed asymmetric cyclopropanations with high turnover numbers. *Org. Lett.* **2003**, *5*, 1403-1406.
43. Pelphrey, P.; Hansen, J.; Davies, H. M. L. Solvent-free catalytic enantioselective C–C bond forming reactions with very high catalyst turnover numbers. *Chem. Sci.* **2010**, *1*, 254-257.
44. Davies, H. M. L.; Beckwith, R. E. J.; Antoulinakis, E. G.; Jin, Q. New Strategic Reactions for Organic Synthesis: Catalytic Asymmetric C–H Activation α to Oxygen as a Surrogate to the Aldol Reaction. *J. Org. Chem.* **2003**, *68*, 6126-6132.
45. Davies, H. M. L.; Yang, J.; Nikolai, J. Asymmetric C–H insertion of Rh(II) stabilized carbenoids into acetals: A C–H activation protocol as a Claisen condensation equivalent. *J. Organomet. Chem.* **2005**, *690*, 6111-6124.
46. Davies, H. M. L.; Venkataramani, C.; Hansen, T.; Hopper, D. W. New Strategic Reactions for Organic Synthesis: Catalytic Asymmetric C–H Activation α to Nitrogen as a Surrogate for the Mannich Reaction. *J. Am. Chem. Soc.* **2003**, *125*, 6462-6468.
47. Davies, H. M. L. Finding Opportunities from Surprises and Failures. Development of Rhodium-Stabilized Donor/Acceptor Carbenes and Their Application to Catalyst-Controlled C–H Functionalization. *J. Org. Chem.* **2019**, *84*, 12722-12745.
48. Bess, E. N.; Guptill, D. M.; Davies, H. M. L.; Sigman, M. S. Using IR vibrations to quantitatively describe and predict site-selectivity in multivariate Rh-catalyzed C–H functionalization. *Chem. Sci.* **2015**, *6*, 3057-3062.
49. Qin, C.; Davies, H. M. L. Role of sterically demanding chiral dirhodium catalysts in site-selective C–H functionalization of activated primary C–H bonds. *J. Am. Chem. Soc.* **2014**, *136*, 9792-9796.
50. Adly, F. On the Structure of Chiral Dirhodium(II) Carboxylate Catalysts: Stereoselectivity Relevance and Insights. *Catalysts* **2017**, *7*.
51. Collins, L. R.; van Gastel, M.; Neese, F.; Furstner, A. Enhanced Electrophilicity of Heterobimetallic Bi-Rh Paddlewheel Carbene Complexes: A Combined Experimental, Spectroscopic, and Computational Study. *J. Am. Chem. Soc.* **2018**, *140*, 13042-13055.

52. McLarney, B. D.; Hanna, S.; Musaev, D. G.; France, S. Predictive Model for the [Rh2(esp)2]-Catalyzed Intermolecular C(sp³)-H Bond Insertion of β -Carbonyl Ester Carbenes: Interplay between Theory and Experiment. *ACS Catal.* **2019**, *9*, 4526-4538.
53. Szabo, M.; Kleineisel, M.; Nemeth, K.; Domjan, A.; Vass, E.; Szilvagy, G. Twisted paddlewheel rhodium complexes: Contribution of central and axial chirality to ECD, VCD, and NMR spectra. *Chirality* **2020**, *32*, 446-456.
54. Zhou, M.; Springborg, M. Theoretical study of the mechanism behind the site- and enantioselectivity of C-H functionalization catalysed by chiral dirhodium catalyst. *Phys. Chem. Chem. Phys.* **2020**, *22*, 9561-9572.
55. Davies, H. M. L.; Liao, K. Dirhodium tetracarboxylates as catalysts for selective intermolecular C-H functionalization. *Nat. Rev. Chem.* **2019**, *3*, 347-360.
56. Qin, C.; Boyarskikh, V.; Hansen, J. H.; Hardcastle, K. I.; Musaev, D. G.; Davies, H. M. L. D₂-symmetric dirhodium catalyst derived from a 1,2,2-triarylcyclopropanecarboxylate ligand: design, synthesis and application. *J. Am. Chem. Soc.* **2011**, *133*, 19198-19204.
57. Liao, K.; Negretti, S.; Musaev, D. G.; Bacsa, J.; Davies, H. M. L. Site-selective and stereoselective functionalization of unactivated C-H bonds. *Nature* **2016**, *533*, 230-234.
58. Liao, K.; Liu, W.; Niemeyer, Z. L.; Ren, Z.; Bacsa, J.; Musaev, D. G.; Sigman, M. S.; Davies, H. M. L. Site-Selective Carbene-Induced C-H Functionalization Catalyzed by Dirhodium Tetrakis(triarylcyclopropanecarboxylate) Complexes. *ACS Catal.* **2017**, *8*, 678-682.
59. Liao, K.; Pickel, T. C.; Boyarskikh, V.; Bacsa, J.; Musaev, D. G.; Davies, H. M. L. Site-selective and stereoselective functionalization of non-activated tertiary C-H bonds. *Nature* **2017**, *551*, 609-613.
60. Wertz, B.; Ren, Z.; Bacsa, J.; Musaev, D. G.; Davies, H. M. L. Comparison of 1,2-Diarylcyclopropanecarboxylates with 1,2,2-Triarylcyclopropanecarboxylates as Chiral Ligands for Dirhodium-Catalyzed Cyclopropanation and C-H Functionalization. *J. Org. Chem.* **2020**, *85*, 12199-12211.
61. Ren, Z.; Musaev, D. G.; Davies, H. M. L. Influence of Aryl Substituents on the Alignment of Ligands in the Dirhodium Tetrakis(1,2,2-Triarylcyclopropane-carboxylate) Catalysts. *Chem. Cat. Chem.* **2021**, *13*, 174-179.

62. Liao, K.; Yang, Y. F.; Li, Y.; Sanders, J. N.; Houk, K. N.; Musaev, D. G.; Davies, H. M. L. Design of catalysts for site-selective and enantioselective functionalization of non-activated primary C–H bonds. *Nat. Chem.* **2018**, *10*, 1048-1055.
63. Liu, W.; Ren, Z.; Bosse, A. T.; Liao, K.; Goldstein, E. L.; Bacsa, J.; Musaev, D. G.; Stoltz, B. M.; Davies, H. M. L. Catalyst-Controlled Selective Functionalization of Unactivated C–H Bonds in the Presence of Electronically Activated C–H Bonds. *J. Am. Chem. Soc.* **2018**, *140*, 12247-12255.
64. Garlets, Z. J.; Wertz, B. D.; Liu, W.; Voight, E. A.; Davies, H. M. L. Regio- and Stereoselective Rhodium(II)-Catalyzed C–H Functionalization of Cyclobutanes. *Chem* **2020**, *6*, 304-313.
65. Liu, W.; Babl, T.; Rother, A.; Reiser, O.; Davies, H. M. L. Functionalization of Piperidine Derivatives for the Site-Selective and Stereoselective Synthesis of Positional Analogues of Methylphenidate. *Chem. Eur. J.* **2020**, *26*, 4236-4241.
66. Wei, B.; Sharland, J. C.; Lin, P.; Wilkerson-Hill, S. M.; Fullilove, F. A.; McKinnon, S.; Blackmond, D. G.; Davies, H. M. L. In Situ Kinetic Studies of Rh(II)-Catalyzed Asymmetric Cyclopropanation with Low Catalyst Loadings. *ACS Catal.* **2020**, *10*, 1161-1170.
67. Green, S. P.; Wheelhouse, K. M.; Payne, A. D.; Hallett, J. P.; Miller, P. W.; Bull, J. A. Thermal Stability and Explosive Hazard Assessment of Diazo Compounds and Diazo Transfer Reagents. *Org. Process Res. Dev.* **2020**, *24*, 67-84.
68. Ye, Q.-S.; Li, X.-N.; Jin, Y.; Yu, J.; Chang, Q.-W.; Jiang, J.; Yan, C.-X.; Li, J.; Liu, W.-P. Synthesis, crystal structures and catalytic activity of tetrakis(acetato)dirhodium(II) complexes with axial picoline ligands. *Inorganica Chim. Acta* **2015**, *434*, 113-120.
69. Nelson, T. D.; Song, Z. J.; Thompson, A. S.; Zhao, M.; DeMarco, A.; Reamer, R. A.; Huntington, M. F.; Grabowski, E. J. J.; Reider, P. J. Rhodium-carbenoid-mediated intermolecular O–H insertion reactions: a dramatic additive effect. Application in the synthesis of an ascomycin derivative. *Tetrahedron Lett.* **2000**, *41*, 1877-1881.
70. Davies, H. M. L.; Townsend, R. J. Catalytic Asymmetric Cyclopropanation of Heteroaryldiazoacetates. *J. Org. Chem.* **2001**, *66*, 6595-6603.
71. Davies, H. M. L.; Manning, J. R. Catalytic C–H functionalization by metal carbenoid and nitrenoid insertion. *Nature* **2008**, *451*, 417-424.

72. Davies, H. M. L.; Panaro, S. A. Novel dirhodium tetraproline catalysts containing bridging proline ligands for asymmetric carbenoid reactions. *Tetrahedron Lett.* **1999**, *40*, 5287-5290.
73. Negretti, S.; Cohen, C. M.; Chang, J. J.; Guptill, D. M.; Davies, H. M. L. Enantioselective Dirhodium(II)-Catalyzed Cyclopropanations with Trimethylsilylethyl and Trichloroethyl Aryldiazoacetates. *Tetrahedron* **2015**, *71*, 7415-7420.
74. Guptill, D. M.; Davies, H. M. L. 2,2,2-Trichloroethyl aryldiazoacetates as robust reagents for the enantioselective C–H functionalization of methyl ethers. *J. Am. Chem. Soc.* **2014**, *136*, 17718-17721.
75. Davies, H. M. L.; Pelphrey, P. M. Intermolecular C–H insertions of carbenoids. *Org. React.* **2011**, *75*, 75-211.
76. Pirrung, M. C.; Morehead, A. T. Electronic Effects in Dirhodium(II) Carboxylates. Linear Free Energy Relationships in Catalyzed Decompositions of Diazo Compounds and CO and Isonitrile Complexation. *J. Am. Chem. Soc.* **1994**, *116*, 8991-9000.
77. Pirrung, M. C.; Morehead, A. T. Saturation kinetics in dirhodium(II) carboxylate-catalyzed decompositions of diazo compounds. *J. Am. Chem. Soc.* **1996**, *118*, 8162-8163.
78. Pirrung, M. C.; Liu, H.; Morehead, A. T. Rhodium chemzymes: Michaelis-Menten kinetics in dirhodium(II) carboxylate-catalyzed carbenoid reactions. *J. Am. Chem. Soc.* **2002**, *124*, 1014-1023.
79. Davies, H. M. L.; Bruzinski, P. R.; Lake, D. H.; Kong, N.; Fall, M. J. Asymmetric Cyclopropanations by Rhodium(II) N-(Arylsulfonyl)proline Catalyzed Decomposition of Vinyl diazomethanes in the Presence of Alkenes. Practical Enantioselective Synthesis of the Four Stereoisomers of 2-Phenylcyclopropan-1-amino Acid. *J. Am. Chem. Soc.* **1996**, *118*, 6897-6907.
80. Nielsen, C. D.; Bures, J. Visual kinetic analysis. *Chem. Sci.* **2019**, *10*, 348-353.
81. Blackmond, D. G. Kinetic Profiling of Catalytic Organic Reactions as a Mechanistic Tool. *J. Am. Chem. Soc.* **2015**, *137*, 10852-10866.
82. Chiappini, N. D.; Mack, J. B. C.; Du Bois, J. Intermolecular C(sp³)—H Amination of Complex Molecules. *Angew. Chem. Int. Ed.* **2018**, *57*, 4956-4959.
83. Miao, X.; Fischmeister, C.; Bruneau, C.; Dixneuf, P. H. Dimethyl carbonate: an eco-friendly solvent in ruthenium-catalyzed olefin metathesis transformations. *ChemSusChem* **2008**, *1*, 813-816.

84. Byrne, F. P.; Jin, S.; Paggiola, G.; Petchey, T. H. M.; Clark, J. H.; Farmer, T. J.; Hunt, A. J.; Robert McElroy, C.; Sherwood, J. Tools and techniques for solvent selection: green solvent selection guides. *Sustain. Chem. Process* **2016**, *4*.
85. Fu, L.; Hoang, K.; Tortoreto, C.; Liu, W.; Davies, H. M. L. Formation of Tertiary Alcohols from the Rhodium-Catalyzed Reactions of Donor/Acceptor Carbenes with Esters. *Org. Lett.* **2018**, *20*, 2399-2402.
86. Lehner, V.; Davies, H. M. L.; Reiser, O. Rh(II)-Catalyzed Cyclopropanation of Furans and Its Application to the Total Synthesis of Natural Product Derivatives. *Org. Lett.* **2017**, *19*, 4722-4725.
87. Bien, J.; Davulcu, A.; DelMonte, A. J.; Fraunhoffer, K. J.; Gao, Z.; Hang, C.; Hsiao, Y.; Hu, W.; Katipally, K.; Littke, A.; Pedro, A.; Qiu, Y.; Sandoval, M.; Schild, R.; Soltani, M.; Tedesco, A.; Vanyo, D.; Vemishetti, P.; Waltermire, R. E. The First Kilogram Synthesis of Beclabuvir, an HCV NS5B Polymerase Inhibitor. *Org. Process Res. Dev.* **2018**, *22*, 1393-1408.
88. Mix, K. A.; Aronoff, M. R.; Raines, R. T. Diazo Compounds: Versatile Tools for Chemical Biology. *ACS Chem. Biol.* **2016**, *11*, 3233-3244.
89. Ciszewski, L. W.; Rybicka-Jasinska, K.; Gryko, D. Recent Developments in Photochemical Reactions of Diazo Compounds. *Org. Biomol. Chem.* **2019**, *17*, 432-448.
90. Deng, Y.; Jing, C.; Doyle, M. P. Dinitrogen Extrusion from Enoldiazo Compounds Under Thermal Conditions: Synthesis of Donor-Acceptor Cyclopropenes. *Chem. Commun.* **2015**, *51*, 12924-12927.
91. Li, P.; Zhao, J.; Shi, L.; Wang, J.; Shi, X.; Li, F. Iodine-Catalyzed Diazo Activation to Access Radical Reactivity. *Nat. Commun.* **2018**, *9*, 1972.
92. Damiano, C.; Sonzini, P.; Gallo, E. Iron catalysts with N-ligands for carbene transfer of diazo reagents. *Chem. Soc. Rev.* **2020**, *49*, 4867-4905.
93. Nam, D.; Steck, V.; Potenzino, R. J.; Fasan, R. A Diverse Library of Chiral Cyclopropane Scaffolds via Chemoenzymatic Assembly and Diversification of Cyclopropyl Ketones. *J. Am. Chem. Soc.* **2021**, *143*, 2221-2231.
94. Briones, J. F.; Davies, H. M. L. Rh₂(S-PTAD)₄-Catalyzed Asymmetric Cyclopropanation of Aryl Alkynes. *Tetrahedron* **2011**, *67*, 4313-4317.

- 95.Chen, L.; Leslie, D.; Coleman, M. G.; Mack, J. Recyclable Heterogeneous Metal Foil-Catalyzed Cyclopropenation of Alkynes and Diazoacetates Under Solvent-Free Mechanochemical Reaction Conditions. *Chem. Sci.* **2018**, *9*, 4650-4661.
- 96.Diaz-Requejo, M. M.; Belderrain, T. R.; Nicasio, M. C.; Perez, P. J. The Carbene Insertion Methodology for the Catalytic Functionalization of Unreactive Hydrocarbons: No Classical C–H Activation, but Efficient C–H Functionalization. *Dalton Trans.* **2006**, 5559-5566.
- 97.Davies, H. M. L.; Hansen, T.; Churchill, M. R. Catalytic Asymmetric C–H Activation of Alkanes and Tetrahydrofuran. *J. Am. Chem. Soc.* **2000**, *122*, 3063-3070.
- 98.Bergstrom, B. D.; Nickerson, L. A.; Shaw, J. T.; Souza, L. W. Transition Metal Catalyzed Insertion Reactions with Donor/Donor Carbenes. *Angew. Chem. Int. Ed.* **2020**, *132*, 2-17.
- 99.Doyle, M. P.; Tamblyn, W. H.; Bagheri, V. Highly Effective Catalytic Methods for Ylide Generation From Diazo Compounds. Mechanism of the Rhodium- and Copper-Catalyzed Reactions with Allylic Compounds. *J. Org. Chem.* **1981**, *46*, 5094-5102.
- 100.Jana, S.; Guo, Y.; Koenigs, R. M. Recent Perspectives on Rearrangement Reactions of Ylides via Carbene Transfer Reactions. *Chem. Eur. J.* **2021**, *27*, 1270-1281.
- 101.Jones, A. C.; May, J. A.; Sarpong, R.; Stoltz, B. M. Toward a Symphony of Reactivity: Cascades Involving Catalysis and Sigmatropic Rearrangements. *Angew. Chem. Int. Ed.* **2014**, *53*, 2556-2591.
- 102.Ford, A.; Miel, H.; Ring, A.; Slattery, C. N.; Maguire, A. R.; McKervey, M. A. Modern Organic Synthesis with Alpha-Diazocarbonyl Compounds. *Chem. Rev.* **2015**, *115*, 9981-10080.
- 103.Bajaj, P.; Sreenilayam, G.; Tyagi, V.; Fasan, R. Gram-Scale Synthesis of Chiral Cyclopropane-Containing Drugs and Drug Precursors with Engineered Myoglobin Catalysts Featuring Complementary Stereoselectivity. *Angew. Chem. Int. Ed.* **2016**, *55*, 16110-16114.
- 104.Gage, J. R.; Chen, F.; Dong, C.; Gonzalez, M. A.; Jiang, Y.; Luo, Y.; McLaws, M. D.; Tao, J. Semicontinuous Process for GMP Manufacture of a Carbapenem Intermediate via Carbene Insertion Using an Immobilized Rhodium Catalyst. *Org. Process Res. Dev.* **2020**, *24*, 2025-2033.
- 105.Sheeran, J. W.; Campbell, K.; Breen, C. P.; Hummel, G.; Huang, C.; Datta, A.; Boyer, S. H.; Hecker, S. J.; Bio, M. M.; Fang, Y.-Q.; Ford, D. D.; Russell, M. G. Scalable On-Demand Production of Purified Diazomethane Suitable for Sensitive Catalytic Reactions. *Org. Process Res. Dev.* **2020**, *25*, 522-528.

106. Anthes, R.; Bello, O.; Benoit, S.; Chen, C. K.; Corbett, E.; Corbett, R. M.; DelMonte, A. J.; Gingras, S.; Livingston, R.; Sausker, J.; Soumeillant, M. Kilogram Synthesis of a Selective Serotonin Reuptake Inhibitor. *Org. Process Res. Dev.* **2008**, *12*, 168-177.
107. Yu, T.; Ding, Z.; Nie, W.; Jiao, J.; Zhang, H.; Zhang, Q.; Xue, C.; Duan, X.; Yamada, Y. M. A.; Li, P. Recent Advances in Continuous-Flow Enantioselective Catalysis. *Chem. Eur. J.* **2020**, *26*, 5729-5747.
108. Hock, K. J.; Koenigs, R. M. The Generation of Diazo Compounds in Continuous-Flow. *Chem. Eur. J.* **2018**, *24*, 10571-10583.
109. Tran, D. N.; Battilocchio, C.; Lou, S. B.; Hawkins, J. M.; Ley, S. V. Flow Chemistry as a Discovery Tool to Access sp(2)-sp(3) Cross-Coupling Reactions via Diazo Compounds. *Chem. Sci.* **2015**, *6*, 1120-1125.
110. Bogdan, A. R.; Dombrowski, A. W. Emerging Trends in Flow Chemistry and Applications to the Pharmaceutical Industry. *J. Med. Chem.* **2019**, *62*, 6422-6468.
111. Akwi, F. M.; Watts, P. Continuous Flow Chemistry: Where Are We Now? Recent Applications, Challenges and Limitations. *Chem. Commun.* **2018**, *54*, 13894-13928.
112. Audubert, C.; Gamboa Marin, O. J.; Lebel, H. Batch and Continuous-Flow One-Pot Processes using Amine Diazotization to Produce Silylated Diazo Reagents. *Angew. Chem. Int. Ed.* **2017**, *56*, 6294-6297.
113. Yu, Z.; Dong, H.; Xie, X.; Liu, J.; Su, W. Continuous-Flow Diazotization for Efficient Synthesis of Methyl 2-(Chlorosulfonyl)benzoate: An Example of Inhibiting Parallel Side Reactions. *Org. Process Res. Dev.* **2016**, *20*, 2116-2123.
114. Roda, N. M.; Tran, D. N.; Battilocchio, C.; Labes, R.; Ingham, R. J.; Hawkins, J. M.; Ley, S. V. Cyclopropanation Using Flow-Generated Diazo Compounds. *Org. Biomol. Chem.* **2015**, *13*, 2550-2554.
115. Yoo, C. J.; Rackl, D.; Liu, W.; Hoyt, C. B.; Pimentel, B.; Lively, R. P.; Davies, H. M. L.; Jones, C. W. An Immobilized-Dirhodium Hollow-Fiber Flow Reactor for Scalable and Sustainable C-H Functionalization in Continuous Flow. *Angew. Chem. Int. Ed.* **2018**, *57*, 10923-10927.
116. Fuse, S.; Otake, Y.; Nakamura, H. Integrated Micro-Flow Synthesis Based on Photochemical Wolff Rearrangement. *Eur. J. Org. Chem.* **2017**, *2017*, 6466-6473.

117. Muller, S. T.; Murat, A.; Maillos, D.; Lesimple, P.; Hellier, P.; Wirth, T. Rapid Generation and Safe Use of Carbenes Enabled by a Novel Flow Protocol with In-line IR spectroscopy. *Chem. Eur. J.* **2015**, *21*, 7016-7020.
118. Poh, J. S.; Tran, D. N.; Battilocchio, C.; Hawkins, J. M.; Ley, S. V. A Versatile Room-Temperature Route to Di- and Trisubstituted Allenes Using Flow-Generated Diazo Compounds. *Angew. Chem. Int. Ed.* **2015**, *54*, 7920-7923.
119. Rackl, D.; Yoo, C. J.; Jones, C. W.; Davies, H. M. L. Synthesis of Donor/Acceptor-Substituted Diazo Compounds in Flow and Their Application in Enantioselective Dirhodium-Catalyzed Cyclopropanation and C–H Functionalization. *Org. Lett.* **2017**, *19*, 3055-3058.
120. Baum, J. S.; Shook, D. A.; Davies, H. M. L.; Smith, H. D. Diazotransfer Reactions with p-Acetamidobenzenesulfonyl Azide. *Synth. Commun.* **1987**, *17*, 1709-1716.
121. Sullivan, R. J.; Freure, G. P. R.; Newman, S. G. Overcoming Scope Limitations in Cross-Coupling of Diazo Nucleophiles by Manipulating Catalyst Speciation and Using Flow Diazo Generation. *ACS Catal.* **2019**, *9*, 5623-5630.
122. Deadman, B. J.; O'Mahony, R. M.; Lynch, D.; Crowley, D. C.; Collins, S. G.; Maguire, A. R. Taming Tosyl Azide: the Development of a Scalable Continuous Diazo Transfer Process. *Org. Biomol. Chem.* **2016**, *14*, 3423-3431.
123. Pieber, B.; Kappe, C. O. Generation and Synthetic Application of Trifluoromethyl Diazomethane Utilizing Continuous Flow Technologies. *Org. Lett.* **2016**, *18*, 1076-1079.
124. Lehmann, H. A Scalable and Safe Continuous Flow Procedure for In-line Generation of Diazomethane and Its Precursor MNU. *Green Chem.* **2017**, *19*, 1449-1453.
125. Levesque, E.; Laporte, S. T.; Charette, A. B. Continuous Flow Synthesis and Purification of Aryldiazomethanes through Hydrazone Fragmentation. *Angew. Chem. Int. Ed.* **2017**, *56*, 837-841.
126. Maurya, R. A.; Park, C. P.; Lee, J. H.; Kim, D. P. Continuous In Situ Generation, Separation, and Reaction of Diazomethane in a Dual-Channel Microreactor. *Angew. Chem. Int. Ed.* **2011**, *50*, 5952-5955.
127. Mastronardi, F. G., B.; Kappe, C. O. Continuous Flow Generation and Reactions of Anhydrous Diazomethane Using a Teflon AF-2400 Tube-in-Tube Reactor. *Org. Lett.* **2013**, *15*, 5590-5593.

128. Wernik, M.; Poechlauer, P.; Schmoelzer, C.; Dallinger, D.; Kappe, C. O. Design and Optimization of a Continuous Stirred Tank Reactor Cascade for Membrane-Based Diazomethane Production: Synthesis of α -Chloroketones. *Org. Process Res. Dev.* **2019**, *23*, 1359-1368.
129. Liu, W.; Twilton, J.; Wei, B.; Lee, M.; Hopkins, M. N.; Bacsa, J.; Stahl, S. S.; Davies, H. M. L. Copper-Catalyzed Oxidation of Hydrazones to Diazo Compounds Using Oxygen as the Terminal Oxidant. *ACS Catal.* **2021**, *11*, 2676-2683.
130. Sharland, J. C.; Wei, B.; Hardee, D. J.; Hodges, T. R.; Gong, W.; Voight, E. A.; Davies, H. M. L. Asymmetric synthesis of pharmaceutically relevant 1-aryl-2-heteroaryl- and 1,2-diheteroarylcyclopropane-1-carboxylates. *Chem. Sci.* **2021**, *12*, 11181-11190.
131. Lindsay, V. N.; Nicolas, C.; Charette, A. B. Asymmetric Rh(II)-Catalyzed Cyclopropanation of Alkenes with Diaceptor Diazo Compounds: p-Methoxyphenyl Ketone as a General Stereoselectivity Controlling Group. *J. Am. Chem. Soc.* **2011**, *133*, 8972-8981.
132. Dumitrescu, L.; Azzouzi-Zriba, K.; Bonnet-Deplon, D.; Crousse, B. Nonmetal Catalyzed Insertion Reactions of Diazocarbonyls to Acid Derivatives in Fluorinated Alcohols. *Org. Lett.* **2011**, *13*, 692-695.
133. Azzouzi-Zriba, K.; Bonnet-Delpon, D.; Crousse, B. Transition Metal-Catalyzed Cyclopropanation of Alkenes in Fluorinated Alcohols. *J. Fluor. Chem.* **2011**, *132*, 811-814.
134. Hatridge, T. A.; Wei, B.; Davies, H. M. L.; Jones, C. W. Copper-Catalyzed, Aerobic Oxidation of Hydrazone in a Three-Phase Packed Bed Reactor. *Org. Process Res. Dev.* **2021**, *25*, 1911-1922.
135. Gagnon, A.; Duplessis, M.; Fader, L. Arylcyclopropanes: Properties, Synthesis and Use in Medicinal Chemistry. *Org. Prep. Proced. Int.* **2010**, *42*, 1-69.
136. Talele, T. T. The "Cyclopropyl Fragment" is a Versatile Player that Frequently Appears in Preclinical/Clinical Drug Molecules. *J. Med. Chem.* **2016**, *59*, 8712-8756.
137. Taylor, R. D.; MacCoss, M.; Lawson, A. D. G. Rings in Drugs. *J. Med. Chem.* **2014**, *57*, 5845-5859.
138. Salaün, J.; Bairtr, M. Biologically active cyclopropanes and cyclopropenes. *J. Curr. Med. Chem.* **1995**, *2*, 511-542.
139. Sala, M. A.; Jain, M. Tezacaftor for the treatment of cystic fibrosis. *Expert Rev. Respir. Med.* **2018**, *12*, 725-732.

- 140.Loo, T. W.; Bartlett, M. C.; Clarke, D. M. Corrector VX-809 stabilizes the first transmembrane domain of CFTR. *Biochem. Pharmacol.* **2013**, *86*, 612-619.
- 141.Jiang, Y.; Andrews, S. W.; Condroski, K. R.; Buckman, B.; Serebryany, V.; Wenglowisky, S.; Kennedy, A. L.; Madduru, M. R.; Wang, B.; Lyon, M. Discovery of danoprevir (ITMN-191/R7227), a highly selective and potent inhibitor of hepatitis C virus (HCV) NS3/4A protease. *J. Med. Chem.* **2014**, *57*, 1753-1769.
- 142.Shen, G.; Zheng, F.; Ren, D.; Du, F.; Dong, Q.; Wang, Z.; Zhao, F.; Ahmad, R.; Zhao, J. Anlotinib: a novel multi-targeting tyrosine kinase inhibitor in clinical development. *Am. J. Hematol.* **2018**, *11*, 1-11.
- 143.Link, J. O.; Taylor, J. G.; Xu, L.; Mitchell, M.; Guo, H.; Liu, H.; Kato, D.; Kirschberg, T.; Sun, J.; Squires, N. Discovery of ledipasvir (GS-5885): a potent, once-daily oral NS5A inhibitor for the treatment of hepatitis C virus infection. *J. Med. Chem.* **2014**, *57*, 2033-2046.
- 144.Köllmann, C.; Wiechert, S. M.; Jones, P. G.; Pietschmann, T.; Werz, D. B. Synthesis of 4' /5' -Spirocyclopropanated Uridine and d-Xylouridine Derivatives and Their Activity against the Human Respiratory Syncytial Virus. *Org. Lett.* **2019**, *21*, 6966-6971.
- 145.Chepiga, K. M.; Qin, C.; Alford, J. S.; Chennamadhavuni, S.; Gregg, T. M.; Olson, J. P.; Davies, H. M. L. Guide to enantioselective dirhodium(II)-catalyzed cyclopropanation with aryldiazoacetates. *Tetrahedron* **2013**, *69*, 5765-5771.
- 146.Yu, Z.; Mendoza, A. Enantioselective Assembly of Congested Cyclopropanes using Redox-Active Aryldiazoacetates. *ACS Catal.* **2019**, *9*, 7870-7875.
- 147.Singha, S.; Buchsteiner, M.; Bistoni, G.; Goddard, R.; Furstner, A. A New Ligand Design Based on London Dispersion Empowers Chiral Bismuth–Rhodium Paddlewheel Catalysts. *J. Am. Chem. Soc.* **2021**, 5666–5673.
- 148.Fu, L.; Mighion, J. D.; Voight, E. A.; Davies, H. M. Synthesis of 2, 2, 2, - Trichloroethyl Aryl - and Vinyl diazoacetates by Palladium - Catalyzed Cross - Coupling. *Chem. Eur. J.* **2017**, *23*, 3272-3275.
- 149.Calmes, M.; Daunis, J.; Jacquier, R.; Natt, F. Synthesis of (S)-(+)- Pantolactone. *Org. Prep. Proced. Int.* **1995**, *27*, 107-108.
- 150.Vaitla, J.; Boni, Y. T.; Davies, H. M. L. Distal Allylic/Benzylic C–H Functionalization of Silyl Ethers Using Donor/Acceptor Rhodium(II) Carbenes. *Angew. Chem. Int. Ed.* **2020**, *59*, 7397-7402.

151. Lebel, H.; Piras, H.; Bartholoméüs, J. Rhodium-Catalyzed Stereoselective Amination of Thioethers with N-Mesyloxycarbamates: DMAP and Bis(DMAP)CH₂Cl₂ as Key Additives. *Angew. Chem. Int. Ed.* **2014**, *53*, 7300-7304.
152. Kim, M.; Lee, J.; Lee, H.-Y.; Chang, S. Significant Self-Acceleration Effects of Nitrile Additives in the Rhodium-Catalyzed Conversion of Aldoximes to Amides: A New Mechanistic Aspect. *Adv. Synth. Catal.* **2009**, *351*, 1807-1812.
153. Anderson, B. G.; Cressy, D.; Patel, J. J.; Harris, C. F.; Yap, G. P. A.; Berry, J. F.; Darko, A. Synthesis and Catalytic Properties of Dirhodium Paddlewheel Complexes with Tethered, Axially Coordinating Thioether Ligands. *Inorg. Chem.* **2019**, *58*, 1728-1732.
154. Simpson, J. H.; Godfrey, J.; Fox, R.; Kotnis, A.; Kacsur, D.; Hamm, J.; Totelben, M.; Rosso, V.; Mueller, R.; Delaney, E. A pilot-scale synthesis of (1R)-trans-2-(2,3-dihydro-4-benzofuranyl) cyclopropanecarboxylic acid: a practical application of asymmetric cyclopropanation using a styrene as a limiting reagent. *Tetrahedron Asymmetry* **2003**, *14*, 3569-3574.
155. Marcin, L. R.; Denhart, D. J.; Mattson, R. J. Catalytic asymmetric diazoacetate cyclopropanation of 1-tosyl-3-vinylindoles. A route to conformationally restricted homotryptamines. *Org. Lett.* **2005**, *7*, 2651-2654.
156. Trindade, A. F.; Gois, P. M.; Veiros, L. F.; André, V.; Duarte, M. T.; Afonso, C. A.; Caddick, S.; Cloke, F. G. N. Axial coordination of NHC ligands on dirhodium (II) complexes: Generation of a new family of catalysts. *J. Org. Chem.* **2008**, *73*, 4076-4086.
157. Marcoux, D.; Azzi, S.; Charette, A. B. TfNH₂ as achiral hydrogen-bond donor additive to enhance the selectivity of a transition metal catalyzed reaction. Highly enantio- and diastereoselective rhodium-catalyzed cyclopropanation of alkenes using α -cyano diazoacetamide. *J. Am. Chem. Soc.* **2009**, *131*, 6970-6972.
158. Marcoux, D.; Lindsay, V. N.; Charette, A. B. Use of achiral additives to increase the stereoselectivity in Rh(II)-catalyzed cyclopropanations. *ChemComm* **2010**, *46*, 910-912.
159. Wei, B.; Hatridge, T. A.; Jones, C. W.; Davies, H. M. L. Copper(II) Acetate-Induced Oxidation of Hydrazones to Diazo Compounds under Flow Conditions Followed by Dirhodium-Catalyzed Enantioselective Cyclopropanation Reactions. *Org. Lett.* **2021**, *23*, 5363-5367.
160. Khaksar, S. Fluorinated alcohols: A magic medium for the synthesis of heterocyclic compounds. *J. Fluor. Chem.* **2015**, *172*, 51-61.

161. Berkessel, A.; Adrio, J. A.; Hüttenhain, D.; Neudörfl, J. M. Unveiling the “booster effect” of fluorinated alcohol solvents: aggregation-induced conformational changes and cooperatively enhanced H-bonding. *J. Am. Chem. Soc.* **2006**, *128*, 8421-8426.
162. Colomer, I.; Chamberlain, A. E.; Haughey, M. B.; Donohoe, T. J. Hexafluoroisopropanol as a highly versatile solvent. *Nat. Rev. Chem.* **2017**, *1*, 1-12.
163. Sinha, S. K.; Bhattacharya, T.; Maiti, D. Role of hexafluoroisopropanol in C–H activation. *React. Chem. Eng.* **2019**, *4*, 244-253.
164. Pozhydaiev, V.; Power, M.; Gandon, V.; Moran, J.; Lebœuf, D. Exploiting hexafluoroisopropanol (HFIP) in Lewis and Brønsted acid-catalyzed reactions. *ChemComm* **2020**, *56*, 11548-11564.
165. Bhattacharya, T.; Ghosh, A.; Maiti, D. Hexafluoroisopropanol: the magical solvent for Pd-catalyzed C–H activation. *Chem. Sci.* **2021**, *12*, 3857-3870.
166. Gray, E. E.; Nielsen, M. K.; Choquette, K. A.; Kalow, J. A.; Graham, T. J.; Doyle, A. G. Nucleophilic (radio) fluorination of α -diazocarbonyl compounds enabled by copper-catalyzed H–F insertion. *J. Am. Chem. Soc.* **2016**, *138*, 10802-10805.
167. Jana, S.; Yang, Z.; Li, F.; Empel, C.; Ho, J.; Koenigs, R. M. Photoinduced Proton - Transfer Reactions for Mild O-H Functionalization of Unreactive Alcohols. *Angew. Chem. Int. Ed.* **2020**, *59*, 5562-5566.
168. Qu, Z.; Shi, W.; Wang, J. A Kinetic Study on the Pairwise Competition Reaction of α -Dialkyl Esters with Rhodium(II) Catalysts: Implication for the Mechanism of Rh(II)-Carbene Transfer. *J. Org. Chem.* **2001**, *66*, 8139-8144.
169. Singha, S.; Buchsteiner, M.; Bistoni, G.; Goddard, R.; Furstner, A. A New Ligand Design Based on London Dispersion Empowers Chiral Bismuth-Rhodium Paddlewheel Catalysts. *J. Am. Chem. Soc.* **2021**, 5666–5673.
170. Hansen, J.; Li, B.; Dikarev, E.; Autschbach, J.; Davies, H. M. L. Combined experimental and computational studies of heterobimetallic Bi-Rh paddlewheel carboxylates as catalysts for metal carbenoid transformations. *J. Org. Chem.* **2009**, *74*, 6564-6571.
171. Ge, J.; Wu, X.; Bao, X. Rhodium(II)-catalyzed annulation of N-sulfonyl-1,2,3-triazoles with 1,3,5-triazinanes to produce octahydro-1H-purine derivatives: a combined experimental and computational study. *Chem. Commun.* **2019**, *55*, 6090-6093.

172. Lian, Y.; Hardcastle, K. I.; Davies, H. M. L. Computationally guided stereocontrol of the combined C–H functionalization/Cope rearrangement. *Angew. Chem. Int. Ed.* **2011**, *50*, 9370-9373.
173. Davies, H. M.; Walji, A. M. Asymmetric intermolecular C–H activation, using immobilized dirhodium tetrakis((S)-N-(dodecylbenzenesulfonyl)-prolinate) as a recoverable catalyst. *Org. Lett.* **2003**, *5*, 479-482.
174. Davies, H. M. L.; Hansen, T.; Rutberg, J.; Bruzinski, P. R. Rhodium(II) (S)-N-(arylsulfonyl)prolinate catalyzed asymmetric insertions of vinyl- and phenylcarbenoids into the Si–H bond. *Tetrahedron Lett.* **1997**, *38*, 1741-1744.
175. Davies, H. M. L.; Kong, N. Synthesis and evaluation of a novel dirhodium tetraprolinate catalyst containing bridging prolinate ligands. *Tetrahedron Lett.* **1997**, *38*, 4203-4206.
176. Davies, H.; Nadeau, E.; Li, Z.; Morton, D. Rhodium Carbenoid Induced Intermolecular C–H Functionalization at Tertiary C–H Bonds. *Synlett* **2008**, *2009*, 151-154.
177. Hansen, J. H.; Parr, B. T.; Pelphrey, P.; Jin, Q.; Autschbach, J.; Davies, H. M. L. Rhodium(II)-catalyzed cross-coupling of diazo compounds. *Angew. Chem. Int. Ed.* **2011**, *50*, 2544-2548.
178. Lamb, J. R.; Brown, C. M.; Johnson, J. A. N-Heterocyclic carbene-carbodiimide (NHC-CDI) betaine adducts: synthesis, characterization, properties, and applications. *Chem. Sci.* **2021**, *12*, 2699-2715.